"Depolymerization of lignin by biocatalytic nano-composites"

Von der Fakultät für Mathematik, Informatik und Naturwissenschaften der RWTH Aachen University zur Erlangung des akademischen Grades eines Doktors der Naturwissenschaften genehmigte Dissertation

vorgelegt von

Master of Science ETH in Umweltnaturwissenschaften

Christoph Andreas Gasser

aus Zürich, Schweiz

Berichter: Universitätsprofessor Dr. rer. nat. Andreas Schäffer

Prof. Dr. Philippe F.-X. Corvini

Tag der mündlichen Prüfung: 28.04.2017

Preface

The present doctoral thesis was conducted at the Institute for Ecopreneurship (IEC) at the University of Applied Sciences and Arts Northwestern Switzerland between July 2011 and July 2016. The work was enabled by the funding of the Swiss National Science Foundation National Research Program 66, Commission for Technology and Innovation of the Swiss Federal Office for Professional Education and Technology, European Commission within the 7th Framework Program, ECOINNOVERA, and Swiss Federal Office for the Environment (FOEN) and was performed in context of five scientific projects, i.e., "Sequential treatment of lignins by advanced chemical oxidation processes and nanobiocatalysis for the production of industrially relevant oligomers and monolignols", "Laccase-nanoparticle conjugates for the elimination of micropollutants from wastewater in bioreactors (LANCE)", "Depolymerization of lignin by biocatalytic nano composites efficient for the production of oligomers and monolignols for green polymer formulation (DELICATE)", "Microorganism and enzyme immobilization: Novel techniques and approaches for upgraded remediation of underground-, wastewater and soil (MINOTAURUS)", and "Innovations for optimal use of organic side streams and waste (IPTOSS)". In the following I would like to thank all the people who were involved and/or supported the work of the present doctoral thesis.

First of all, I want to thank my doctoral adviser Prof. Dr. rer. nat. Andreas Schäffer for the possibility to conduct the doctoral thesis at the chair of Environmental Biology and Chemodynamics at the RWTH-Aachen. His comments, questions, and positive encouragement throughout the thesis provided motivation and helped shaping the thesis and gaining new perspectives on the projects.

Furthermore, I would like to express my gratitude to Prof. Dr. Philippe Corvini for the opportunity to perform the necessary work in the labs of the IEC and to participate in the different research projects. I thank him for his continued support and advice as well as his confidence in me and for giving me the necessary freedom to perform my doctoral studies. The time at the IEC was a tremendous learning experience on a scientific and personal level. In addition, I would like to thank Prof. Dr. rer. nat. Johannes Bohrmann and Prof. Dr. rer. nat. Henner Hollert for taking time out of their busy schedule to be part of the examination board.

Special thanks go to Dr. Gregor Hommes who supervised my research activities during the beginning of the thesis. I appreciated the close collaboration and exchange of ideas and profited a lot from his experience, knowledge, inventiveness, and way of working. Moreover, I am especially grateful for the support of Erik Ammann. His help throughout the thesis was indispensable whether he assisted during the experimental work or provided instructions regarding setup and use of lab equipment.

I am also thankful to Dr. Monika Čvančarová for her support regarding analytics. I valued the matter of fact discussions and pragmatic collaboration. Furthermore, I want to thank Melanie Mucha, Dr. Markus

Gude, and Peter Nastold who were part of the project team during different periods and contributed to the project results with ideas and experimental work. Especially the efforts of Melanie Mucha regarding size exclusion chromatography and gas chromatography measurements have to be acknowledged. Moreover, the help of Vesna Olivieri from the Center for Microscopy at the University of Basel for conducting the transmission electron microscopy measurements and of Hanspeter Hächler and Ann Hirt from the Institute of Geophysics at ETH Zürich for their support and guidance regarding magnetization measurements is gratefully acknowledged.

I sincerely want to thank all the students and civil servants that supported the work for my thesis, namely Daniel Streit, Ruben Wälchli, Tobias Appenzeller, Fabienne Vannay, and Chaim Howald. It was a pleasure to work with them, and I hope they profited from the experience. I wish them all the best for their careers and personal future.

Furthermore, I would like to thank my present and former colleagues at the IEC, i.e., Jonas Löwenberg, Dr. Yannick Zimmermann, Ben Ricken, Dominique Ritty, Roland Goers, Liwia Rajpert, Karen Viacava, Dr. Boris Kolvenbach, Dr. Markus Lenz, and Dr. Verena Christen for the nice and cooperative atmosphere at work as well as their suggestions and support. Especially important on a personal level were the lengthy discussions about science and more often life in general in the evenings with Jonas Löwenberg as diversion to the sometimes demanding and challenging work days.

Finally, I would like to cordially thank my parents Bruno and Elisabeth and my brother Michael who supported me throughout my life and enabled me to pursue this path of life.

Basel, October 2016, Christoph Gasser

Preliminary remarks

Parts of this dissertation have already been published in the following publications:

Ammann, E.M., Gasser, C.A., Hommes, G., Corvini, P.F.X. 2014. Immobilization of defined laccase combinations for enhanced oxidation of phenolic contaminants. Applied Microbiology and Biotechnology, 98(3), 1397-1406.

Gasser, C.A., Ammann, E.M., Schäffer, A., Shahgaldian, P., Corvini, P.F.X. 2016. Production of superparamagnetic nanobiocatalysts for green chemistry applications. Applied Microbiology and Biotechnology, 100(16), 7281-7296.

Gasser, C.A., Ammann, E.M., Shahgaldian, P., Corvini, P.F.X. 2014. Laccases to take on the challenge of emerging organic contaminants in wastewater. Applied Microbiology and Biotechnology, 98(24), 9931-9952.

Gasser, C.A., Čvančarová, M., Ammann, E.M., Schäffer, A., Shahgaldian, P., Corvini P.F.X. 2017. Sequential lignin depolymerization by combination of biocatalytic and formic acid/formate treatment steps. Applied Microbiology and Biotechnology, 101(6), 2575-2588.

Gasser, C.A., Hommes, G., Schäffer, A., Corvini, P.F.X. 2012. Multi-catalysis reactions: new prospects and challenges of biotechnology to valorize lignin. Applied Microbiology and Biotechnology, 95(5), 1115-1134.

Gasser, C.A., Yu, L., Svojitka, J., Wintgens, T., Ammann, E.M., Shahgaldian, P., Corvini, P.F.X., Hommes G. 2014. Advanced enzymatic elimination of phenolic contaminants in wastewater: a nano approach at field scale. Applied Microbiology and Biotechnology, 98(7), 3305-3316.

Hommes, G., Gasser, C.A., Ammann, E.M., Corvini, P.F.X. 2013. Determination of oxidoreductase activity using a high-throughput microplate respiratory measurement. Analytical Chemistry, 85(1), 283-291.

Hommes, G., Gasser, C.A., Howald, C.B.C., Goers, R., Schlosser, D., Shahgaldian, P., Corvini, P.F.X. 2012. Production of a robust nanobiocatalyst for municipal wastewater treatment. Bioresource Technology, 115(0), 8-15.

The specific paragraphs that are in part taken from these publications are given in Table 0.1.

Table 0.1 Paragraphs that were already published (in part or full).

Publication	**Paragraph**
Ammann et al. 2014	4.2.3; 4.3.2.3; 6.1; 6.1.2
Gasser et al. 2012	1; 2.3; 2.4; 2.5
Gasser et al. 2014a	2.4.2.4
Gasser et al. 2014b	4.3.1; 4.3.2.4; 6.1.3
Gasser et al. 2016	4.3.3; 6.2; A1
Gasser et al. 2017	1; 2.5; 3; 4.4.2.1; 4.4.2.4; 4.4.2.5; 4.4.5.1; 7.3; A4
Hommes et al. 2013	4.2.4; 4.2.5; 5
Hommes et al. 2012	4.3.2.1; 6.1.1

Several colleagues have supported the execution of experiments and the analysis presented in this thesis. A specific list of these contributions is given in Table 0.2.

Table 0.2 Contributions of co-workers to the experiments presented in this thesis

Experiment described in paragraph	**Person/company supporting or conducting to the experiment**	**Specific contribution**
4.2.1	Roland Goers	- Production of *Phoma* sp. Laccase
4.2.3	Erik M. Ammann	- All isoelectric focusing measurements - Some protein content measurements
4.2.4	Erik M. Ammann	- All SDS-PAGE measurements as well as data analysis
4.2.5.1	Erik M. Ammann	- All Clark electrode measurements
4.2.5.2.1.2	Gregor Hommes	- All HPLC and SEC measurements
4.2.5.2.3	Erik M. Ammann	- Statistical analysis
4.3.1.2	Erik M. Ammann	- All ninhydrin assays - Some zeta potential measurements
4.3.1.2	Chaim B.C. Howald	- All TGA measurements
4.3.1.3	Erik M. Ammann	- All SEM studies
4.3.1.4	Erik M. Ammann and Vesna Olivieri	- TEM measurements and determination of size-distribution
4.3.2	Ruben Wälchli	- Immobilization of glucose oxidase, DyP, and VP
	Daniel Streit	- Immobilization of HRP
4.3.2.3	Daniel Streit	- Co-immobilization of TVL and HRP
	Erik M. Ammann	- All experiments with only laccases described in the paragraph - Co-immobilization of glucose oxidase and HRP and co-immobilization of glucose oxidase and LiP
	Fabienne Vannay	- Conducting some of the immobilization experiments
4.3.3	Erik M. Ammann	- Immobilization of glucose oxidase and DyP on MP - Conducting some of the immobilization experiments and of the stability assays
	Hanspeter Hächler	- Magnetization measurements
4.4.2.1	Melanie Mucha	- Conducting some of the SEC measurements
4.4.2.3	Solvias AG	- Elemental analysis
4.4.2.4	Monika Čvančarová	- HPLC-MS measurements and identification and quantitation of products
4.4.2.6	Melanie Mucha	- All GC-MS measurements including analysis
4.4.3.2	Daniel Streit	- Conducting some of the lignin treatment experiments
4.4.3.3	Melanie Mucha	- Sample preparation for GC-MS measurements
	Ruben Wälchli	- Conducting some of the lignin treatment experiments

„As long as wood-chemical industries are unable to process lignin to commercial advantage, their position to coal and oil industries will remain that of the country butcher competing with the Chicago meat packer who exploits everything but the squeal."

– Egon Glesinger (1949, The coming age of wood)

Abstract

Lignocellulosic biomass constitutes a promising renewable feedstock for replacement of crude oil for the production of fuels and chemicals. Next to cellulose, lignin is the second most abundant biomass component making up around 25 % of the world's biomass. While processes for valorization of cellulose already exist, namely paper pulp and second generation bioethanol production, lignin is predominantly used for the production of heat and power. However, due to the aromatic structure lignin could serve as a renewable feedstock for valuable functionalized aromatic chemicals if it can be depolymerized effectively. Despite considerable research devoted to depolymerization of the biopolymer only one process, namely vanillin production from lignosulfonates has been realized on an industrial scale to date. Basidiomyceteous white-rot fungi effectively degrade lignin in nature using a mixture of extracellular enzymes. Consequently, applying these enzymes for lignin depolymerization might present an interesting alternative to the chemical options usually considered.

The present thesis explores the potential valorization of lignin through oxidative depolymerization by applying lignin modifying enzymes (LMEs). Moreover, a new high-throughput microplate respiratory assay for efficient characterization of oxygen consuming LMEs like laccases and glucose oxidases was developed. Furthermore, an enzyme immobilization method initially developed for the immobilization of laccases on fumed silica nanoparticles (fsNP) was optimized and adapted for the immobilization of several LMEs on fsNP and superparamagnetic nanoparticles (MPs) to allow enzyme reuse and enhance enzymatic stability.

The high-throughput microplate respiratory assay allows multi-parallel measurement of O_2-consumption by enzymatic reactions in 24 or 96 well plate formats. The newly developed and validated method enables the comparative quantitation of LME characteristics. Furthermore, the time it usually takes to collect respiratory data of oxygen-consuming enzymes is considerably reduced in comparison to conventional methods employed for oxygen consumption measurements, e.g., Clark electrode-based methods. Moreover, in comparison to assays based on substrate transformation measurements, it allows direct assessment of the enzymatic activity, provides information about reaction stoichiometry, and is unaffected by possible radical chain reactions or competition between different substrates. Therefore, it allows obtaining ample data on enzymes using oxygen as a substrate and has the potential to illuminate aspects of enzymatic reactions that cannot be assessed using common enzymatic assays focusing on product formation.

Enzyme immobilization on nano-composites, i.e., fsNP was performed following a previously developed immobilization method. This method was adapted and optimized while the principle process steps remained unchanged. First the particle surfaces were modified by aminopropylation using an organofunctional alkoxysilane. In a next step enzymes were added to the suspension and allowed to

adsorb on the particles. Next a cross-linker was applied to the suspension which covalently linked the enzymes and the particles. Furthermore, internal cross-linking of enzymes and cross-linking between enzymes potentially occurred as well resulting in the formation of cross-linked enzyme aggregates (CLEAs) on the particle surface. This method was first optimized for enzyme immobilization on fsNP using laccase as model enzyme regarding the consumables required. Next it was amended in order to allow immobilization of specific enzyme combinations enabling the production of defined multi-enzyme fsNP. Finally, it was further optimized in order to allow for a more efficient production of enzyme-fsNP on the kilogram-scale.

Regarding enzyme immobilization on superparamagnetic materials, the same basic reaction steps as for fsNP were performed. MPs were produced by co-precipitation of two iron salts. Subsequently, enzyme immobilization was optimized regarding specific activity and stability of the biocatalysts using response surface methodology (RSM). Results allowed formulation of biocatalysts having high specific enzymatic activity and improved stability. The biocatalysts showed considerably higher stability compared with the dissolved enzymes over a pH range from 3 to 9 and in the presence of several chemical denaturants.

Different LME and LME combinations were screened regarding their ability to degrade lignin in the presence and absence of organic co-solvents. Organic solvents were used to increase the accessibility of the hydrophobic biopolymer to the enzymes. Considerable oxidation of lignin could be achieved using oxidative LME in combination with organic solvents. Especially in mixtures containing dimethyl sulfoxide (DMSO) or methanol (MeOH) the formation of stable monomeric substances was observed. The main monomeric reaction product was identified as 2,6-dimethoxy benzoquinone (DMBQ) and was produced at a yield of up to 2.20±0.05 wt%. However, higher molecular weight reaction products were produced as well indicating the occurrence of lignin condensation and polymerization reactions. Additionally, enzyme adsorption on polymerized lignin was observed. Of the tested enzymes, laccases seem the most promising regarding application. While similar results regarding production of low molecular weight compounds were achieved with certain peroxidases, laccases have considerable advantages regarding application. Most importantly, they do not need the addition of H_2O_2 which has to be properly controlled in case of peroxidases to prevent enzyme inactivation by too high H_2O_2 concentrations. Furthermore, laccases are already produced on an industrial level which is not the case for many peroxidases.

Several redox-mediators were tested in combination with laccases to extend the reactivity of the enzymes beyond phenolic groups on lignin. Preliminary experiments indicated that artificial mediators like 1-hydroxybenzotriazole (HBT) or 2,2,6,6-tetramethylpiperidine 1-oxyl (TEMPO) might be more effective than natural phenolic mediators since the natural mediators were partially polymerized during treatment, i.e., their oxidized forms were unstable and their redox conversion was not cyclic. Consequently, lignin treatments with laccase immobilized on MP in presence of HBT, TEMPO, or

MeOH were conducted. Five different technical lignins were used as feedstock. After biocatalytic treatment the water insoluble lignin was further treated in an additional step leading to formic acid induced lignin depolymerization. The sequential treatment allowed the production of considerable amounts of lignin oligomers as well as some phenolic monomeric compounds. Yields depended on the exact treatment as well as the lignin material used. One lignin, i.e., soda lignin from wheat straw was selected for further process optimization using RSM. At optimized conditions up to 45 wt% of lignin could be solubilized either in aqueous solution after the first treatment or in ethyl acetate (EtAc) after the second (chemical) treatment. The solubilized products were mainly low molecular weight aromatic mono- and oligomers.

The developed process constitutes a promising first step towards a possible lignin valorization strategy. However, further improvements of the process as well as more detailed study of downstream processing and possible applications of reaction products are necessary before realization can be considered.

Zusammenfassung

Lignocellulose ist ein vielversprechender, erneuerbarer Rohstoff, der künftig Rohöl ersetzen und zur Herstellung von Chemikalien und Treibstoffen verwendet werden könnte. Lignin ist ein Hauptbestandteil von Lignocellulose, macht rund 25 % der Biomasse weltweit aus und wird derzeit zum größten Teil in Anwendungen geringen Werts wie der Produktion von Wärme und Strom eingesetzt. Allerdings könnte Lignin aufgrund seiner chemischen Struktur für die Produktion von wertvollen Aromaten verwendet werden, falls es gelingt das Biopolymer effizient zu depolymerisieren. Trotz umfangreicher Forschungsarbeit auf diesem Gebiet wird bis heute nur ein Prozess zur Herstellung von Vanillin aus Lignosulfonaten industriell betrieben. In der Natur wird Lignin effizient mit Hilfe extrazellulärer Enzyme von Weissfäulepilzen abgebaut. Folglich könnte ein Lignindepolymerisationsprozess basierend auf solchen Enzymen eine interessante Alternative zu den üblicherweise untersuchten, chemischen Abbauprozessen darstellen.

In der vorliegenden Arbeit wird die potentielle Valorisierung von Lignin durch einen oxidativen Depolymerisationsprozess unter Zuhilfenahme ligninmodifizierender Enzyme (LMEs) untersucht. Des Weiteren wurde eine neue Methode zur Messung der Aktivität sauerstoffzehrender Enzyme entwickelt, welche auf einem respiratorischen Zellassay basiert. Ferner wurde eine Enzymimmobilisierungsmethode weiterentwickelt, welche ursprünglich für die Immobilisierung von Laccasen an pyrogene Kieselsäurenanopartikel (fsNP) eingesetzt wurde. Die Methode wurde optimiert und angepasst, um verschiedene LMEs an fsNP sowie an superparamagnetische Nanopartikel (MPs) zu immobilisieren.

Die neue Messmethode erlaubt die parallele Messung der Sauerstoffzehrung durch enzymatische Reaktionen in 24- oder 96-Well-Platten. Dies verkürzt und vereinfacht die Charakterisierung sauerstoffzehrender Enzyme im Vergleich zu herkömmlichen Methoden zur Bestimmung von Sauerstoffzehrung, z.B., Methoden basierend auf Clark-Elektroden. Des Weiteren erlaubt sie, im Gegensatz zu Methoden die auf Substratumsatz basieren, die direkte Messung der Enzymaktivität, liefert Informationen zu der Reaktionsstöchiometrie, und wird nicht beeinflusst durch mögliche Radikalkettenreaktionen oder Konkurrenz zwischen verschiedenen Substraten. Folglich erlaubt die neuentwickelte Methode Aspekte enzymatischer Reaktionen sauerstoffzehrender Enzyme zu untersuchen, welche von herkömmlichen Enzymassays nicht erfasst werden können.

Enzymimmobilisierung an fsNP wurde aufgrund einer bereits etablierten Immobilisierungsmethode durchgeführt. Diese Methode wurde angepasst und optimiert, während die grundsätzlichen Prozessschritte beibehalten wurden. In einem ersten Schritt wurde die Oberfläche der Partikel mittels eines organofunktionellen Silans modifiziert. In einem nächsten Schritt wurden die Enzyme zur Suspension zugegeben und an die Partikeloberfläche sorbiert. Danach wurde ein Vernetzer zugegeben,

welcher die Enzyme kovalent an die Partikeloberfläche band. Zusätzlich zur Bindung an die Partikeloberfläche fand potentiell auch Vernetzung interhalb und zwischen Enzymen statt, was zur Formierung von vernetzten Enzymaggergaten führte. Diese Methode wurde optimiert für die Immobilisierung von Laccasen an fsNP hinsichtlich der benötigten Verbrauchsmaterialien. Danach wurde sie erweitert, um die Immobilisierung spezifischer Enzymkombinationen an die Partikel zu ermöglichen. Schlussendlich wurde die Methode weiter angepasst, um die Produktion der Nanobiokatalysatoren im Kilogrammmaßstab zu ermöglichen.

Immobilisierung an MPs wurde auf der Basis derselben Immobilisierungsmethode erreicht. MPs wurden mittels Kopräzipitation zweier Eisensalze hergestellt. Danach wurde die Enzymimmobilisierung hinsichtlich spezifischer enzymatischer Aktivität und Stabilität mittels Antwortflächenmethode (RSM) optimiert. Die Resultate erlaubten die Herstellung von Biokatalysatoren mit hoher spezifischer Aktivität und erhöhter Stabilität im Vergleich zu ungebundenen Enzymen. Die immobilisierten Enzyme waren deutlich stabiler über einen pH-Bereich von 3 bis 9 und in der Gegenwart verschiedener chemischer Denaturierungsmittel.

Verschiedene LME und LME-Kombinationen wurden hinsichtlich ihrer Fähigkeit Lignin zu degradieren in An- und Abwesenheit organischer Lösungsmittel untersucht. Organische Lösungsmittel wurden eingesetzt, um die Löslichkeit des Lignins zu erhöhen und dadurch den Zugang der Enzyme zu verbessern. Beträchtliche Ligninoxidation wurde auf diese Weise erreicht. Speziell in Mischung mit Dimethylsulfoxid (DMSO) und Methanol (MeOH) wurde die Formation stabiler Monomere beobachtet. Das Hauptprodukt war 2,6-Dimethoxybenzochinon und konnte mit einer Ausbeute von bis zu 2.20±0.05 wt% hergestellt werden. Allerdings wurden auch Produkte mit höherem Molekulargewicht hergestellt. Dies deutete auf das Auftreten von Verdichtungs- und Polymerisationsreaktionen hin. Zusätzlich wurde Enzymadsorption an polymerisiertes Lignin beobachtet. Ähnliche Resultate bezüglich Produktion von niedermolekularen Produkten wurden mit bestimmten Peroxidasen und Laccasen erzielt. Allerdings haben Laccasen gegenüber Peroxidasen deutliche Vorteile bezüglich Anwendung. Laccasen benötigen keine Zugabe von H_2O_2, welche korrekt kontrolliert werden muss, um die Inaktivierung der Enzyme zu verhindern. Des Weiteren werden Laccasen bereits in industriellem Maßstab produziert und sind deshalb vergleichsweise günstig.

Verschiedene Redoxmediatoren wurden in Kombination mit Laccasen getestet, um deren Reaktivität auf nicht phenolische Ligninstrukturen zu erweitern. Vorversuche deuteten an, dass künstliche Mediatoren wie 1-Hydroxybenzotriazole (HBT) oder 2,2,6,6-Tetramethylpiperidin 1-Oxyl (TEMPO) effektiver sind als natürliche, phenolische Mediatoren, da die natürlichen Mediatoren während der Behandlung teilweise polymerisierten. Dies zeigte, dass die oxidierten Formen dieser Mediatoren nicht stabil waren und deshalb die Redoxreaktionen nicht oder nur teilweise zyklisch verliefen. Folglich wurden Ligninbehandlungen mit Laccasen immobilisiert an MP in Gegenwart von HBT, TEMPO oder MeOH durchgeführt. Fünf verschiedene technische Lignine wurden als Ausgangsmaterial verwendet.

Zudem wurde das wasserunlösliche Lignin nach der enzymatischen Behandlung einem weiteren Behandlungsschritt unterzogen, der mit Hilfe von Ameisensäure weitere Lignindepolymerisation einleitete. Die sequentielle Behandlung erlaubte die Produktion erheblicher Mengen von Ligninoligomeren sowie einiger phenolischer Monomere. Die Ausbeuten hingen von dem Ausgangslignin sowie der genauen Behandlung ab. Ein Lignin (Sodalignin von Weizenstroh) wurde ausgewählt, um den Prozess weiter mittels RSM zu optimieren. Bis zu 45 wt% des Lignins konnten bei optimalen Bedingungen entweder in Wasser (nach dem ersten Behandlungsschritt) oder Ethylacetat (nach dem zweiten Behandlungsschritt) gelöst werden. Die gelösten Stoffe waren größtenteils niedermolekulare aromatische Mono- oder Oligomere.

Der entwickelte Prozess stellt einen vielversprechenden ersten Schritt in Richtung einer möglichen Strategie zur Ligninverwertung dar. Allerdings sind weitere Verbesserungen des Prozesses sowie weitere Untersuchung vor allem bezüglich Weiterbehandlung, Aufreinigung und Verwertung der Produkte nötig.

List of figures

List of tables

Abbreviations

Abbreviation	Description
2,6-DMP	2,6-dimethoxyphenol
*Aae*APO	Aromatic peroxygenase from the agaric fungus *Agrocybe aegerita*
ABTS	2,2′-azino-bis(3-ethylbenzthiazoline)-6-sulfonic acid
AP-fsNP	Aminopropylated fsNP
APTES	3-aminopropyltriethoxysilane
ANOVA	Analysis of variance
AMF	Area of the monomer fraction
BCR	Benefit cost ratio
BSA	Bovine serum albumin
BSTFA	N,O-bis(trimethylsilyl)trifluoroacetamide
CFA	Extracellular flux analyzer
CFA24	XF24-2 extracellular flux analyzer (Seahorse Bioscience)
CFA96	XF96-2 extracellular flux analyzer (Seahorse Bioscience)
CLEAs	Cross-linked enzyme aggregates
CLECs	Cross-linked enzyme crystals
CLEs	Cross-linked enzymes
CPL	Laccases of *Coriolopsis polyzona*
CPL-fsNP	CPL immobilized on fsNP
CPL-TVL-fsNP	CPL and TVL immobilized on fsNP
CUL	Laccase of *Cerrena unicolor*
CUL-fsNP	CUL immobilized on fsNP
DAD	Diode array detector
DDQ	2,3-dichloro-5,6-dicyano-1,4-benzoquinone
DMBQ	2,6-dimethoxy-1,4-benzoquinone
DMSO	Dimethyl sulfoxide
DyP	Dye-decolorizing peroxidases
EtAc	Ethyl acetate
[EMIM] [DEP]	1-ethyl-3-methylimidazolium diethyl phosphate
FAD	Flavin adenine dinucleotide
fsNP	Fumed silica nanoparticles
FTIR	Fourier transform infrared spectroscopy
G	Guaiacyl unit
GTL	Crude laccase of *Thielavia* genus
GTL-fsNP	GTL immobilized on fsNP
GTL-POL-fsNP	GTL and POL immobilized on fsNP
H	*p*-hydroxyphenyl unit
HAT	Hydrogen atom transfer
HBT	1-Hydroxybenzotriazole
HCV	Hepatitis C virus
HIV	Human immunodeficiency virus
HPLC	High-performance liquid chromatography
HRP	Horseradish peroxidase
LiP	Lignin peroxidase
LLE	Liquid-liquid extraction
LME	Lignin-modifying enzymes

Abbreviation	**Description**
LMS	Laccase mediator system
LOD	Limit of detection
LOQ	Limit of quantitation
LPS®	Lignin Precipitation System
LSC	Liquid scintillation analyzer
MALS	Multi-angle light scattering
MeOH	Methanol
MnP	Manganese peroxidase
MP	Superparamagnetic particles
MPC	McIlvain phosphate-citrate buffer
MTO	Methyltrioxorhenium
Mw	Weight average molecular mass
NMR	Nuclear magnetic resonance
OCR	Oxygen consumption rate
OL	Organosolv lignin
PB	Sörensen phosphate-buffer
POL	Laccase from *Pleurotus ostreatus*
POL-fsNP	POL immobilized on fsNP
POM	Polyoxometalate
PSL	Laccase of *Phoma* sp.
PSL-fsNP	PSL immobilized on fsNP
PTFE	Polytetrafluoroethylene
PVDF	Polyvinylidene fluoride
RI	Refractive index
RVL	Laccase from *Rhus vernicifera*
RSM	Response surface methodology
S	Syringyl unit
SDS-PAGE	Sodium dodecyl sulfate-polyacrylamide gel electrophoresis
SEC	Size exclusion chromatography
SEM	Scanning electron microscopy
S-SL	Sarkanda soda lignin obtained after LPS®
SW-SL	Soft wood soda lignin obtained after LPS®
TEM	Transmission electron microscopy
TEMPO	2,2,6,6-Tetramethyl-1-piperidinyloxy
TGA	Thermo gravimetrical analysis
Trolox	(±)-6-hydroxy-2,5,7,8-tetramethylchromane-2-carboxylic acid
TVL	Laccase from *Trametes versicolor*
TVL-fsNP	TVL immobilized on fsNP
TVL-MP	TVL immobilized on MP
Vc	Measurement volume of the CFA24 or CFA96
VP	Versatile peroxidase
W-SE	Wheat straw lignin obtained after steam-explosion pre-treatment and LPS®
W-SL	Wheat straw soda lignin obtained after LPS®

Contents

1. Introduction

The depletion of fossil carbon reserves and concern about global warming calls for substitutes of fossil fuels and petrochemicals (Marquardt et al. 2010). For power production, multiple alternatives are available, e.g., wind, sun, biomass, hydroelectricity, nuclear fission. However, biomass is the only known renewable resource that can be converted to both fuels and chemicals (Zhang 2008). Therefore, biorefineries using lignocellulosic feedstock have been proposed as alternatives to petroleum-based refineries (e.g., Wyman and Goodman 1993; Holladay et al. 2007; Kamm et al. 2007; Zhang 2008; Michels and Wagemann 2010). Recalcitrance to degradation of lignin is a major obstacle to harness lignocellulosic biomass efficiently (Mansfield et al. 1999; Achyuthan et al. 2010; Zakzeski et al. 2010a; Sanderson 2011).

Lignin, a complex three-dimensional amorphous polymer consisting of methoxylated phenylpropanoid units of various types (Achyuthan et al. 2010; Isroi et al. 2011), is the second most abundant constituent of plant biomass next to cellulose, accounting for approximately 20 % of carbon fixed in land ecosystems (Ruiz-Dueñas and Martínez 2009). About 50 million tons of technical lignin is produced worldwide mostly by the pulp and paper industry (Wertz and Bédué 2013) and typically used in commercial applications of low value, for example, as concrete additive (Doherty et al. 2011) or as low-grade fuel. However, due to its structure, it constitutes a potential renewable source for aromatic added value chemicals (Holladay et al. 2007) and numerous studies have been conducted with the goal to depolymerize lignin (Zakzeski et al. 2010a). Despite these efforts and the abundance of the resource, lignin depolymerization processes are, to date, not even conducted at pilot-scale (Xu et al. 2014). This is mostly due to challenges posed by lignin depolymerization itself and by product separation (Xu et al. 2014). However, recent advances at lab-scale showed promising results regarding lignin degradation (Rahimi et al. 2014; Lancefield et al. 2015; Luterbacher et al. 2015; Zeng et al. 2015). Specifically targeting lignin β-O-4 ether bonds applying two-step processes seems promising (Rahimi et al. 2014; Lancefield et al. 2015). In the first step these bonds were oxidized in the Cα position while the second step cleaved the oxidized linkages (Rahimi et al. 2014; Lancefield et al. 2015). However, achievable low molecular weight product yields using these processes heavily depend on the quantity of β-O-4 ether bonds of the lignin material and most biomass pretreatment methods employed today, e.g., kraft pulping or organosolv processes considerably alter the lignin structure leading to a decrease or complete loss of β-O-4 bonds (Rahimi et al. 2014).

In nature lignin is efficiently degraded by basidiomyceteous white-rot fungi by employing a mixture of extracellular enzymes (Ruiz-Dueñas and Martínez 2009). Among these certain peroxidases, i.e., manganese (MnP), lignin (LiP), and versatile peroxidases (VP), and laccases in combination with redox mediators or auxiliary enzymes like flavin adenine dinucleotide (FAD) dependent oxidases have been shown to cause lignin degradation (Leonowicz et al. 2001; Wong 2009). Applying these enzymes to

processes for oxidative lignin depolymerization might present an interesting alternative to the chemical oxidation processes that are usually operated under harsh reaction conditions, i.e., high temperatures, pressures, and extreme pH values and lead to high amounts of solid residues. While enzymatic processes work at ambient pressure and temperature they also have some drawbacks. Loss in enzymatic activity over time and separation of the enzymes from the processed lignin are complicating factors that have to be addressed. One approach to increase enzymatic stability and allow enzyme separation and reuse is immobilization of biocatalysts on solid support materials (Sheldon 2007). In this context especially immobilization on porous inexpensive inorganic materials with high specific surface areas is of interest since it allows production of biocatalysts with high enzymatic activities per carrier weight while not extensively increasing costs. Consequently, nanoparticles consisting of silica or magnetite seem suitable carrier materials since they are both cheap and meet the criteria of high surface area per weight. Magnetite provides the additional advantage that it is ferrimagnetic and can therefore be easily separated from other solids in a reaction mixture through the application of a magnetic field.

The present work investigates the biocatalytic processing of lignin making use of oxidative lignin-modifying enzymes (LME) immobilized on nanoparticles. LME are immobilized on silica as well as magnetite particles using a sorption assisted immobilization approach (Zimmermann et al. 2011). The influence of the treatments on the molecular weight distribution of lignin will be assessed and for promising treatment conditions the produced low molecular weight compounds will be identified and quantified. Furthermore, several strategies to improve the effectiveness of the treatment will be investigated. For instance, the application of radical scavengers might prevent or limit undesired condensation and polymerization reactions, while small redox-mediators might allow oxidation of lignin substructures that are not directly accessible to LME. Furthermore, extension of the treatment process with a second chemical depolymerization step potentially further improves product yields.

2. Background

2.1. Lignin structure

Lignin is a class of heterogeneous, amorphous, hydrophobic, natural polymers that exists in all terrestrial plants (Lu and Ralph 2010). Furthermore, some aquatic organisms might also contain lignin or at least lignin-like components (Delwiche et al. 1989). It is comprised of three main 4-hydroxyphenylpropanoids, i.e., coniferyl, sinapyl, and *p*-coumaryl alcohol (Figure 2.1; Achyuthan et al. 2010). Cross-linking of these alcohols leads to phenylpropanoid units in the lignin polymer that differ in the mehoxy substitution on the aromatic rings (Figure 2.1) named guaiacyl (G), syringyl (S), and *p*-hydroxyphenyl (H) units, respectively (Wong 2009). Depending on the lignin source the ratios between the different phenylpropanoid units differ. Hardwood lignin derived from angiosperms consists of similar amounts of G and S units while only containing traces of H units (G/S/H = 50:50:t), while softwood lignin derived from gymnosperms predominantly consists of G units containing only traces of S units and low levels of H units (G/S/H = 96:t:4), and lignin derived from grasses (monocots) is comprised of mostly G but also contains considerable amounts of S and H units (G/S/H = 70:25:5) (Brunow 2001; Fukushima 2001; Higuchi 2006). Some additional phenolic compounds are suspected to be lignin monomers as well, since not all structures found in lignin can be formed by coupling of the three main lignin monomers (Figure 2.2; Vanholme et al. 2008). An unambiguous definition of lignin structures is by no means straightforward. One of the more concise and comprehensive definitions has been given by Brunow et al. (1999). This definition is given in the following.

"This description is not a chemical definition of protolignins, but summarizes the main structural features based on knowledge available today. Protolignins are biopolymers consisting of phenylpropane units with an oxygen atom at the *p*-position (as OH or O–C) and with none, one or two methoxyl groups in the *o*-positions to this oxygen atom. These *o*-positions may alternatively be C-substituted or O-substituted with other substituents than methoxyl. Only a few of the aromatic units are substituted in other ring positions. A few percent of the building blocks in protolignins are not phenylpropane units. The side chain is missing or shortened, or the unit is replaced by a quinoid group. The phenylpropane units are attached to one another by a series of characteristic linkages (β–O–4, β–5, β–β, etc.) or, alternatively, exist as members of a series of characteristic end groups (e.g. cinnamaldehyde units). Practically all the types of structural elements detected in protolignins have been demonstrated to be formed on oxidation of the *p*-hydroxycinnamyl alcohols in vitro (Freudenberg and Neish 1968; Adler 1977). The structural elements in protolignins are not linked to one another in any particular order. Protolignins are not optically active. The polymer is branched and cross-linking occurs. In addition, the following facts should be noted: (1) there are strong indications of the occurrence of linkages between protolignin and carbohydrates, (2) some types of protolignins are esterified with phenolic acids (grass lignins with *p*-coumaric acid and certain other lignins, such as aspen lignin, with *p*-hydroxybenzoic

acid), and (3) scattered observations suggest that there are some units, for example, dihydroconiferyl alcohol units, that cannot be thought to have been produced on oxidation of *p*-hydroxycinnamyl alcohols." (Brunow et al. 1999)

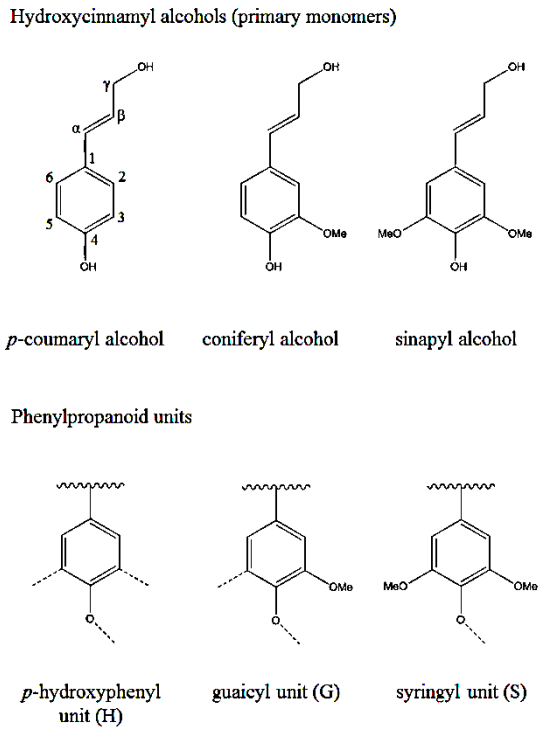

Figure 2.1 Chemical structure of the primary monomers constituting the lignin structure and of the corresponding phenylpropanoid units occurring in the lignin structure

theory suggests that lignin monomers are oxidized by oxidative enzymes like peroxidases leading to radical formation and that these radicals couple in a combinatorial way (Freudenberg 1965). The formation of lignin polymers is controlled by physical parameters like temperature, pH, ionic strength, supply of reactants, oxidative enzyme concentrations, and the matrix in general and, therefore, not truly random (Ralph et al. 2004; Vanholme et al. 2008). A newer hypothesis, however, proposes that the coupling of the lignin monomers is under complete control of proteins bearing arrays of dirigent sites (Davin and Lewis 2005). However, the dirigent model of lignin polymerization still lacks experimental demonstration while there are several observations that contradict it (Ralph et al. 2009). Since the newer hypothesis has, as of yet, not produced enough evidence in its favor lignin formation will be discussed according to the original theory.

There is some debate on the mechanisms controlling lignin formation. The original

After radical formation through oxidative enzymes, radicals can couple at various sites due to resonance delocalization (Wong et al. 2009). Various structural units are built by C-C or ether linkages (Wong et al. 2009). An overview of the most important structural units is given in Figure 2.3. Coupling of monomers to the growing polymer usually leads to the formation of β-linked structures like β-O-4 or β-5 (Wong 2009). Coupling between lignin oligo- or polymers on the other hand leads to the formation of 5-5 or 4-O-5 linked structures (Wong 2009). These two structures are branch-points in the lignin polymer (Ralph et al. 2004). The addition of a monomer to a 5-5 unit can be followed by internal trapping of the quinone methide by the other phenol thereby leading to the formation of a dibenzodioxocin unit (Karhunen et al. 1995 a, b; Kukkola et al. 2003). Most 5-5 units have been reported to form such

dibenzodioxocin structures (Ralph et al. 1999). Resinol (β-β) structures likely form through dimerization of lignin monomers (Wong 2009). While these structures seem to be not very abundant in lignin (Wong 2009), a second pathway for the formation of resinol structures has been proposed, suggesting that resinol formation occurs through a 5-coupling of a monomer to the growing lignin polymer (Zhang et al. 2003). However, it is unclear whether this reaction occurs in nature (Ralph et al. 2004). Formation of β-1 structures is rather complex but seems to occur through the coupling of a monomer with a β-O-4 phenolic end-unit (Ralph et al. 2004). Some β-1 structures have been reported to be involved in spirodienone substructures (Zhang and Gellerstedt 2001). These structures might also serve as branching points in lignins.

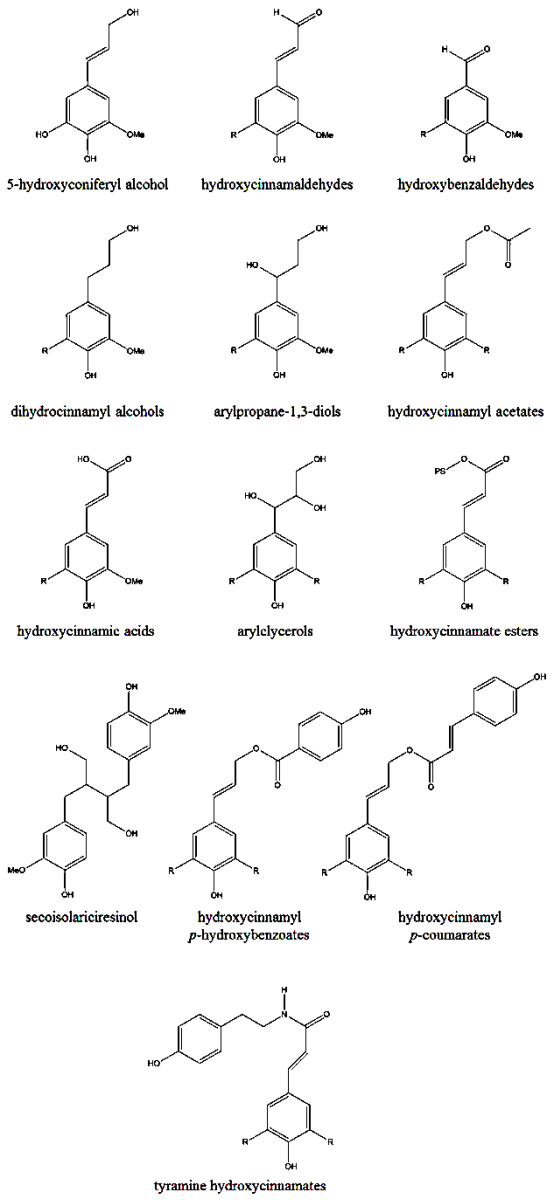

Figure 2.2 Phenolics that are suspected to be lignin monomers according to Vanholme et al. (2008). PS = polysaccharide.

Frequency of the different lignin sub-structures in the respective lignin macromolecules depends on the relative abundance of the different lignin monomers. Certain linkages can or cannot be formed depending on the disposition of methoxy substitutions on the aromatic ring of the respective 4-hydroxyphenylpropanoid. For example, while coupling of a coniferyl alcohol to a G unit of a growing lignin polymer allows the formation of G-β-O-4-G as well as G-β-5-G, the coupling of a coniferyl alcohol to a S unit only leads to the formation of β-O-4-S, but not G-β-5-S, because S has a methoxy group at the 5 position (Wong et al. 2009). The same is the case for linkages between S and G units.

While S-4-O-5-G bonds are formed 5-5 linkages will not occur (Wong et al. 2009). Furthermore, no bonds will be formed between two S units (Wong et al. 2009). Consequently, in hardwoods (containing similar amounts of S and G units) around 80 % of the phenylpropanoid units are involved in β-O-4 structures, while in softwoods (containing predominantly G units) around 50 % of the phenylpropanoid units are involved in β-O-4

structures (Alder 1977). Other structures common in softwoods are β-5, 5-5, and 4-O-5 accounting for around 10 %, 25 %, and 4 %, respectively (Brunow 2001), while around 2 % of phenylpropanoid units in softwood are involved in β-1 structures (Alder 1977). However, all these numbers likely vary between actual lignins and are just estimations of the ratios in which the different linkages occur. In fact, the sheer number of possible lignin isomers resulting from coupling of the lignin monomers suggests that virtually no two lignin macromolecules are identical (Ralph et al. 2004). Still some schematic representations on how lignin structures of soft and hardwood might look are shown in Figure 2.4.

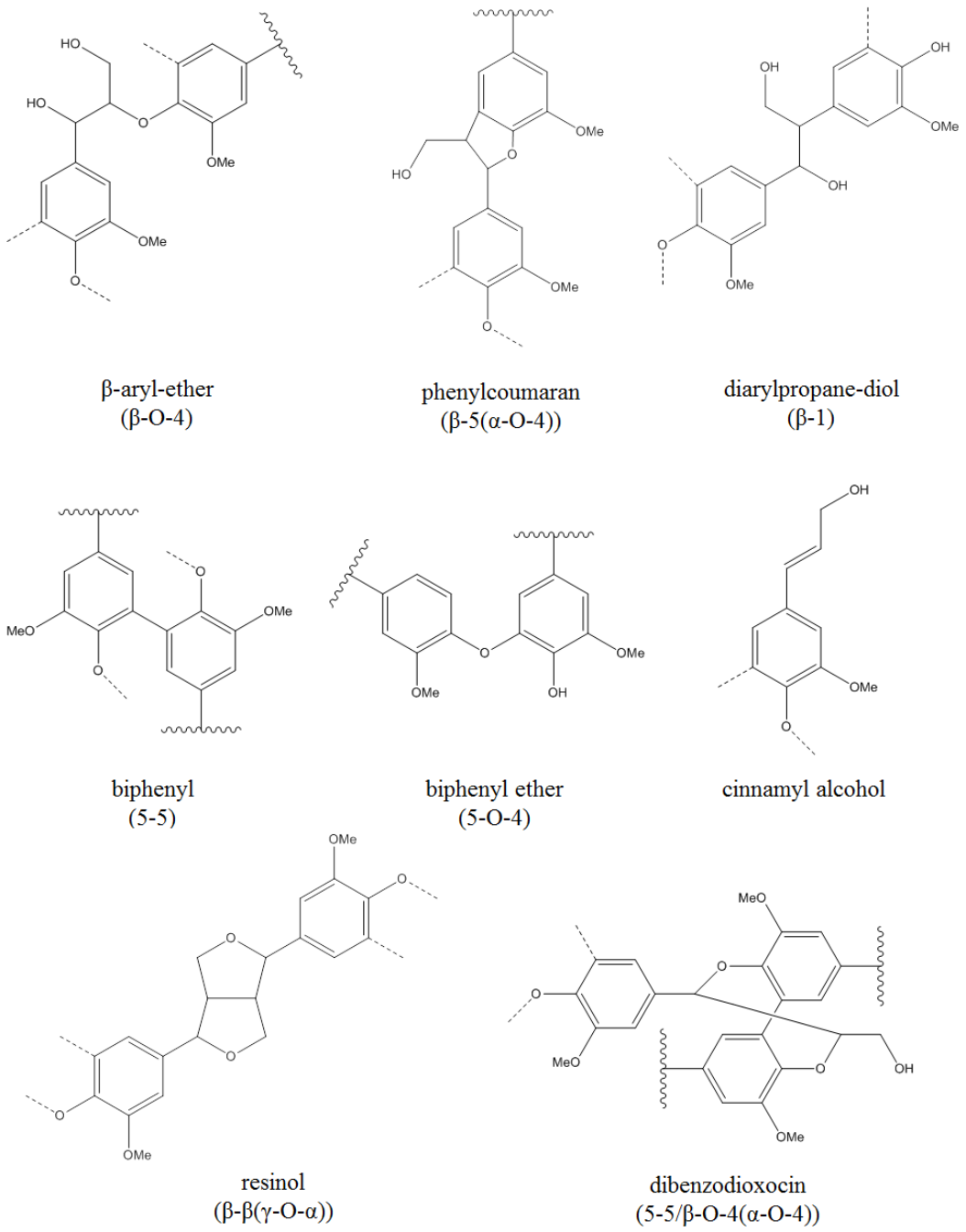

Figure 2.3 Major structural units of lignins

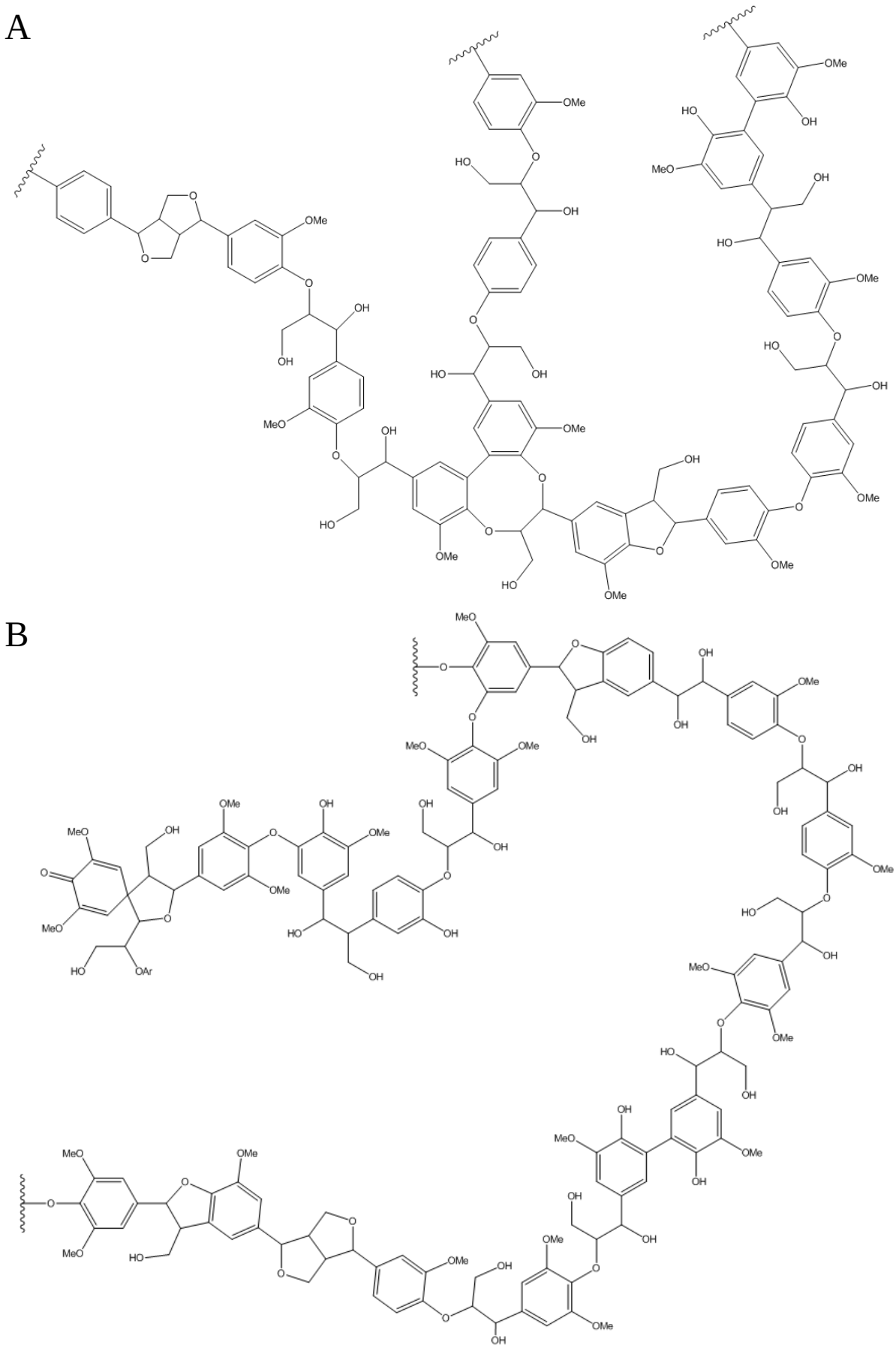

Figure 2.4 Schematic representation of softwood (A) and hardwood (B) lignin structures based on structures presented by Zakzeski et al. (2010a).

The structures of lignins obtained from lignocellulose after separation from cellulose and hemicellulose, however, varies from the structure of natural lignin depending on the method applied for separation and the botanical origin (Lora 2008). Therefore, the most prominent separation techniques and their influence on the natural lignin structure will be discussed in the next section.

2.2. Lignin pretreatment

In order to obtain lignin as feedstock for valorization from lignocellulose a pretreatment step is necessary to isolate the lignin fraction. So far, the lignin polymer could not be isolated exhaustively due to its molecular association and potential covalent bonds with polysaccharides (Holtman et al. 2007). Depending on the pretreatment method used, undesired chemical transformations like the incorporation of sulfur can occur. Furthermore, the molecular weight of lignin can be reduced and the chemical bond linkages can be altered (Gluckstein et al. 2010). Various physical and chemical lignocellulose pretreatment processes exist often with the goal to gain lignin free cellulose and hemicellulose (Bozell et al. 2007; Kamm et al. 2007; da Costa Sousa et al. 2009; Lu and Ralph 2010).

On an industrial scale lignin arises in the pulp and paper industries in which kraft lignin or lignosulfonates are produced as by-product. In the future it can be expected that lignin will also originate from biorefineries as by-product of the production of second generation biofules. Solvent based pretreatments, so called organosolv processes solubilizing lignin and parts of hemicellulose leaving a relatively pure insoluble cellulose fraction are applied in several pilot-scale biorefineries (Gosselink 2011). Furthermore, steam explosion pretreatments are discussed as promising alternative in biorefinery schemes (Sun and Cheng 2002) and already applied in a demonstration scale cellulose ethanol facility of the Iogen Corporation in Canada (Zheng et al. 2009). Soda or soda-anthraquinone pulping processes are also widely applied for non-wood feedstocks like straw, sugar cane bagasse, flax etc. yielding sulfur free soda lignins (Lora and Glasser 2002). Therefore, lignins derived from steam explosion, organosolv processes, and soda pulping can be considered to be additional interesting feedstocks due to the expected increase in availability in the future. Consequently, the five process types, i.e., kraft lignin, lignosulfonate, organosolv, steam explosion, and soda pulping process and their effects on the lignin structure will be discussed in this section.

2.2.1. Kraft lignin process

Chemical pulping processes in the pulp and paper industry are applied in order to separate enough lignin from cellulosic fibers to produce a pulp suitable for paper production. The kraft lignin process is the most prominent chemical pulping technique in industry. It is a simple, rapid process leading to high quality pulp with high mechanical strength (Gierer 1980). The kraft process employs high pH values through the application of sodium hydroxide and sodium sulfide while cooking wood chips for 1 to 2 h at 170 °C (Gierer 1980). This leads to the breakdown of the lignin structure due to reactions of the hydroxide and hydrosulfide anions with lignin producing smaller water/alkali-soluble molecules (Chakar and Ragauskas 2004). The breakdown of lignin proceeds through the cleavage of α-O-4 and β-

O-4 bonds leading to an increase in phenolic hydroxyl groups (Toven and Gellerstedt 1999) while all other linkages between the phenylpropane units like C-C and 4-O-5 remain unaffected (Gierer 1980). Even though large quantities of sulfides are used only small amounts of sulfur get introduced into kraft lignin through the formation of thiol groups (Zakzeski et al. 2010a). Furthermore, some additional functional groups and bonds are formed during the process like stilbenes (Littiä et al. 2003). Next to fragmentation, condensation reactions of lignin occur during cooking leading to the formation of stable C-C bonds of the diaryl methane type (Chakar and Ragauskas 2004). Consequently, kraft lignin contains a high amount of stable C-C bonds which are either unaffected by or get formed during the pulping process thereby leading to macromolecules that are very hard to depolymerize by chemical or biological processes (Werhan 2013). A schematic representation of the kraft lignin structure is given in Figure 2.5 A.

In the kraft pulping process cellulose is separated from the dissolved lignin through filtration after cooking. The remaining so-called “black liquor” is subsequently concentrated through evaporation and used as fuel in recovery boilers to provide energy for the pulping process (Werhan 2013). Energetic improvements of the kraft pulping process have led to the situation that many kraft pulp mills are currently limited by the energy load that can be processed in the recovery boilers (Öhman 2006). Therefore, a reduction of the thermal load to the recovery boiler allows increased pulp production. Consequently, partial removal of kraft lignin from the black liquor in form of solid lignins becomes increasingly interesting since next to overcoming the limitations set by the recovery boilers it also leads to the formation of a marketable product in the form of kraft lignin (Lora 2008). Therefore, it can be expected that the supply of kraft lignin as renewable raw material and feedstock will increase in the future.

2.2.2. Lignosulfonate process

Another prominent group of pulping processes leads to the production of lignosulfonates. In these processes wood is usually cooked at 125 to 150 °C for 3 to 7 h and treated with calcium sulfite at pH 1 to 2 or with magnesium sulfite at pH 3 to 5 (Saake and Lehnen 2000). Through this process hydrophilic sulfonic acid groups are introduced at the α-carbon atoms making lignin soluble in aqueous solution (Saake and Lehnen 2000). Next to sulfonation, also hydrolysis and condensation reactions occur (Saake and Lehnen 2000). Other sulfite processes are conducted at alkaline or neutral pH (Saake and Lehnen 2000). In these processes sodium or ammonia are used as base (Saake and Lehnen 2000). In contrast to the processes performed under acidic conditions the β-O-4 bonds are less stable at neutral and alkaline conditions and depending on reaction conditions can be cleaved during these processes (Saake and Lehnen 2000). In comparison to kraft lignin, lignosulfonates have a higher average molecular weight and also a higher monomer molecular weight due to the introduction of sulfonate groups (Zakzeski et al. 2010a). A schematic representation of the structure of lignosulfonates is given in Figure 2.5 B.

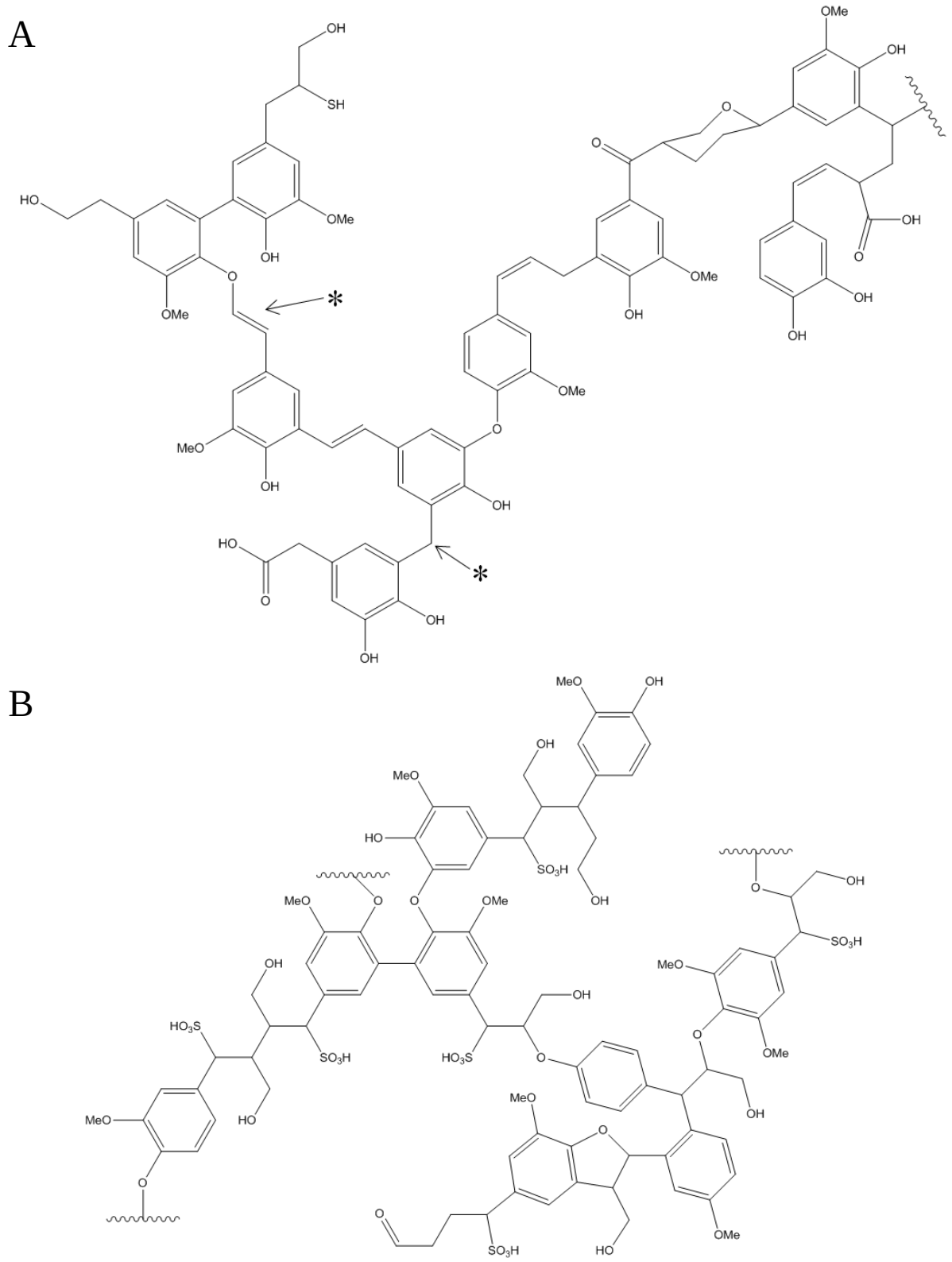

Figure 2.5 Schematic representation of kraft lignin (A) and lignosulfonate (B) lignin structures based on structures presented by Zakzeski et al. (2010a). It is unclear whether diphenyl methane or vinyl aryl ether linkages are present in kraft lignin (depicted by *) since a study found no evidence for such linkages in contrast to other reports (Littiä et al. 2003).

Lignosulfonates have been used for the commercial production of vanillin starting in 1936 originally using a technology developed by Howard (Sandborn et al. 1936). The process was further optimized and more and more pulp and paper mills adapted it. By the year 1981 Ontario Pulp and Paper produced 3.4 million kg vanillin per year which was enough to meet 60 % of the world demand at the time (Hocking 1997). However, during the production of vanillin from lignosulfonates large amounts of caustic liquids (160 kg per kg vanillin produced) were formed (Hocking 1997). The need to safely dispose of all this material was one of the main reasons why all of the plants producing vanillin from lignin in North America are now closed (Hocking 1997). However, Borregaard Industries (Sarpsborg, Norway) is still producing vanillin from lignosulfonates (Borges da Silva et al. 2009).

2.2.3. Soda lignin process

The soda process is a further pulping process mostly applied to non-wood biomass like straw, bagasse, or flax but also to some extent to hardwoods (González-García et al. 2010; Rodríguez et al. 2010). The biomass is cooked in NaOH prior to precipitation, liquid solid separation, and drying (Lora and Glasser 2002). In comparison to kraft and sulfite pulping the process works in the absence of sulfur. Therefore, the resulting lignin is sulfur free and its chemical structure is closer to native lignin (Nadif et al. 2002; Wörmeyer et al. 2011). However, the pulping liquors often contain high amounts of silica which is difficult to separate from lignin and often co-precipitates (Lora and Glasser 2002). Consequently, soda lignins are often of low purity. This drawback can be overcome by the Lignin Precipitation System (LPS®, Abächerli and Doppenberg 1998) which is used commercially for the production of high purity lignin from annual fibers such as wheat straw. Lignin is separated by first acidifying the alkaline liquor. This is followed by a maturation step which depends on the type of liquor that is processed (Lora and Glasser 2002). During this maturation step slurry is formed and the lignin can be separated subsequently by filtration and drying (Lora and Glasser 2002). Resulting lignins are of high purity (>90 %) and contain low amounts of ash (<2 %; http://www.bio-based.eu/iBIB/pdf/47.pdf, accessed: 19.4.2016).

2.2.4. Organosolv processes

Organosolv processes employ organic solvents or their aqueous solutions in order to extract lignin from lignocellulosic feedstocks. These processes allow the separation of the different lignocellulose components into three fractions: a relatively pure cellulose fraction, an aqueous hemicellulose fraction, and a dry lignin fraction (Duff and Murray 1996). This makes these pretreatment processes attractive for biorefineries targeting the use of all biomass components since the resulting hemicellulose and cellulose fractions can be easily hydrolyzed enzymatically to biofuels like ethanol after delignification and the lignin fraction is also available for further processing. Furthermore, they are considered to be more environmentally friendly compared to the kraft and lignosulfonate processes since they employ less harsh reaction conditions and do not use sulfides leading usually to purer lignin fractions with lower sulfur contents (Zakzeski et al. 2010a).

One of the major cost factors of the organosolv process is the cost of organic solvent used (Zhao et al. 2009). Therefore, organosolv processes employing expensive organic solvents or solvents that are not easy to recover like high boiling point alcohols, dioxane (Gajzago et al. 1973), phenol (Zacchi et al. 1988), *N*-methyl-morpholine-*N*-oxide (Katrib et al. 1988), or ethylendiamine (Thompson et al. 1992) seem to be unattractive for use at large scale production even though the enzymatic hydrolysis of the pretreated biomass could be improved by these processes (Zhao et al. 2009). Organic acids like formic acid or acetic acid have also been used for the pretreatment of biomass (Muurinen 2000). However, these solvents do not swell carbohydrates (Young and Davis 1986) while causing severe corrosion and are therefore also of minor interest for lignocellulose pretreatment (Zhao et al. 2009). While pretreatment or pre-pretreatment of biomass with peracetic acid could considerably increase the enzymatic digestibility of cellulose (Taniguchi et al. 1982; Mohamed et al. 1983; Ando et al. 1988; Teixeira et al. 1999a, b) this process is most likely too expensive as well due to the use of valuable chemicals that are consumed during pretreatment (Zhao et al. 2009). More feasible alternatives seem to be pretreatment methods employing low boiling point alcohols like methanol (MeOH) or ethanol or methods using acetone as solvent since recovery of these solvents can be easily performed by distillation and they are not very expensive.

In treatments using MeOH or ethanol lignocellulose is cooked at temperatures of 150 °C to 200 °C in aqueous solutions of the corresponding solvent in the presence or absence of a catalyst like sulfuric, phosphoric, or hydrochloric acid. In the presence of an acid catalyst lower hydrolysis temperatures can be employed compared to uncatalyzed systems. During the process lignin and hemicellulose and to lower extent cellulose are dissolved leaving cellulosic fibers with varying amounts of undissolved hemicellulose and lignin. During the process mainly α-O-4 and to a much smaller degree β-O-4 bonds of lignin are hydrolyzed. Furthermore, ether and ester linkages between hemicellulose and the α-carbons of lignin are broken. Removal of the volatile solvent after cooking leads to precipitation of the lignin fraction which might also contain some lipophilic extractives of the original lignocellulose feedstock. Separation of the solid lignin fraction from the dissolved hemicellulose sugars through filtration allows separation of all three major lignocellulose components. (Chum et al. 1985)

2.2.5. Steam explosion process

During the steam explosion process chipped lignocellulose material is exposed to high pressure saturated stream at temperatures of 160-210 °C corresponding to pressures of 0.69-4.83 MPa for several seconds to few minutes (Sun and Cheng 2002). Subsequently, the pressure is rapidly reduced to atmospheric pressure, thereby inducing explosive decompression of the lignocellulose material. Due to the high temperatures hemicellulose is degraded in the process and lignin is transformed (Sun and Cheng 2002). Consequently, cellulose hydrolysis is enhanced (Grous et al. 1986) while the biomass particle structure is opened going along with a reduction in particle size and an increase in pore volume (Michalowicz et

al. 1991). There are several alternative procedures with and without the application of chemical catalysts like sulfuric acid, sulfur dioxide, sodium hydroxide, or ammonia (da Costa Sousa et al. 2009).

Steam treatment of wood goes along with hydrolysis of acetyl groups in hemicellulose. Consequently, reaction conditions become acidic. In these conditions carbonimu ions in the lignin structure are formed. In β-O-4 lignin structures these ions react further on the one hand leading to the cleavage of the β-ether linkage and the formation of a Hibbert ketone together with a new phenolic end-group. On the other hand, formation of stable C-C bonds between the Cα and a nearby electron rich carbon like a C-2/C-6 present in a guaiacyl or syringyl ring occurs, leading to polymerization. Due to these reactions an overall decrease in molecular weight of the lignin fraction as well as a decrease of β-O-4 lignin structures is usually observed going along with an increase in polydispersity and phenolic group content. (Li et al. 2007, 2009)

2.3. Inorganic catalysis

Depolymerization of lignin and lignin model compounds through inorganic catalysts has been attempted in a plethora of studies. Inorganic catalysts were usually used under harsh reaction conditions. The variation between the lignin feedstocks used in the various studies on lignin transformation impedes the comparison of their performances because a benchmark substrate is lacking. Furthermore, comparability is complicated by the fact that different methods are used for product recovery and also because many studies solely dealt with lignin model compounds.

Chemical lignin transformation reactions can be divided into lignin cracking, hydrolysis, catalytic reduction, and catalytic oxidation reactions. Lignin catalytic cracking processes are adapted from petroleum refineries and work at harsh reaction conditions, especially high temperatures, usually above 300 °C. They can cleave lignin β-O-4 ether bonds as well as relatively unstable carbon–carbon bonds (Thring and Breau 1996) such as Cα–Cβ bonds. Lignin fragmentation by hydrolysis is also achieved at high temperatures, usually above 270 °C. Pandey and Kim (2011) reviewed the thermochemical depolymerization and conversion of lignin, including catalytic cracking and hydrolysis processes. These high-temperature processes lead to tar or char formation, volatile components, and complex mixtures of compounds (van Haveren et al. 2008; Zakzeski et al. 2010a; Pandey and Kim 2011).

Paralleling the emerging concept of green chemistry, more and more new chemical catalysts are designed to work in aqueous environments at milder reaction conditions (Hailes et al. 2007; Sheldon 2008). The following section is restricted to a few selected studies where mild reaction conditions were used or that were published just recently.

2.3.1. Lignin reduction

Reductive lignin depolymerization usually removes alcohol, aldehyde, ether, and acid moieties. Therefore, it has the potential to produce simpler bulk aromatic compounds like benzene, toluene, and xylene (B, T, X) as well as phenol (van Haveren et al. 2008), which could be directly used by

conventional petrochemical processes (Holladay et al. 2007). Furthermore, the removal of oxygen from lignin makes it a better working fuel (Sanderson 2011). Hydrogenation or hydrodeoxygenation of lignin and lignin model compounds with heterogeneous catalysts, performed at high temperatures and pressures, not only cleaved ether bonds but also hydrogenated aromatic rings, thereby producing an inefficient mixture of compounds (Sergeev and Hartwig 2011). Selective cleavage of lignin model compounds through electrocatalytic hydrogenation at relatively low temperatures (50 °C) was reported (Mahdavi et al. 1997; Dabo et al. 1999; Cyr et al. 2000). Few studies used homogenous catalysts to reduce lignin or lignin model compounds (e.g., Hu et al. 1997; Plasseraud and Süss-Fink 1997; Schulz et al. 2000). A nickel catalyst was employed for hydrogenolysis of dimeric 4-O-5, α-O-4, and β-O-4 lignin model compounds and several alkyl–aryl and diaryl ethers at temperatures between 80 and 120 °C and pressure of 1 bar of hydrogen (Sergeev and Hartwig 2011). The aromatic C–O bonds of the ethers were selectively cleaved and produced exclusively alcohols and arenes. Furthermore, the ether linkages of the lignin model compounds were broken. Degradation of the α-O-4 model compound yielded 99 % 3,4-dimethoxytoluene and 2-methoxyphenol. Hydrogenation of the β-O-4 model yielded 89 % guaiacol. Thereby, it was demonstrated that the aromatic C–O bonds could be selectively cleaved in the presence of other C–O bonds, while leaving the arene units intact (Sergeev and Hartwig 2011). Whereas these results look promising, the effectiveness of the catalyst on different lignin feedstocks, not just lignin model compounds, has still to be demonstrated. A further issue is the soluble form of the catalyst, which makes separation from products difficult (Sanderson 2011).

2.3.2. Lignin oxidation

Oxidative lignin depolymerization requires catalysts that selectively disrupt the linkages in lignin in order to form specific aromatic alcohols, aldehydes, acids, or other specially functionalized aromatics like vanillin, syringaldehyde, or vanillic acid (Holladay et al. 2007; Zakzeski et al. 2010a). Many of the resulting chemicals might be used as platform chemicals for subsequent organic synthesis or are target fine chemicals (Zakzeski et al. 2010a). The oxidation of lignin and lignin model compounds was also briefly discussed in a recent review on biomass oxidation (Collinson and Thielemans 2010). Heterogeneous catalysts, more specifically, TiO_2 and Pt/TiO_2, have been used for photocatalytic oxidation to process lignin from wastewater streams of the paper industry (Portjanskaja and Preis 2007; Ma et al. 2008; Portjanskaja et al. 2009). These processes were applied at relatively mild temperatures (~20 °C), but products and percentages of conversion were not specified.

Methyltrioxorhenium (MTO) has been used as a catalyst in the presence of H_2O_2 at 60 °C to cleave the CC double bond of isoeugenol and trans-ferulic acid, thereby producing vanillin (Herrmann et al. 2000). Further authors used the catalytic MTO/H_2O_2 system (homogeneous as well as heterogeneous) to oxidize technical lignins and lignin model compounds at 25 °C (Crestini et al. 2005, 2006). Phenolic, non-phenolic, and dimeric lignin model compounds were oxidized to a large extent. The oxidation of

18.2 g L^{-1} sugar cane, red spruce kraft, and hardwood organosolv lignin at room temperature led to high degrees of degradation and produced lignin fragments of increased solubility.

Various studies investigated the electrochemical oxidation of lignin using different electrodes (e.g., Pardini et al. 1992; Parpot et al. 2000; El-Ashtoukhy et al. 2009). Dominguez-Ramos et al. (2008, 2010a, b) used boron-doped diamond electrodes for the oxidation of lignosulfonates. They were able to oxidize approximately 90 % of the total organic carbon in a lignosulfonate solution. However, the structure of the degradation products was not elucidated. For the electrochemical oxidation of kraft lignin, different IrO_2-based electrodes were used (Tolba et al. 2010). Vanillin and vanillic acid were formed as primary intermediates. Apparent degradation rate constants were determined for temperatures ranging from 2 to 60 °C and were highest at 60 °C.

As mentioned in paragraph 2.2.2 one commercial process for the oxidation of lignosulfonates exists (Faith et al. 1965). Lignosulfonates are produced through sulfite pulping in the pulp and paper industries. Their oxidation produces vanillin in a yield of 10–20 % (w/w based on the dry weight of lignosulfonates). The spent acid sulfite pulping liquors are oxidized with air at 160–170 °C at alkaline pH. After oxidation, the products are extracted using organic solvents and further purified (Hocking 1997; Ramachandra Rao and Ravishankar 2000).

Due to economic and environmental reasons, production of vanillin from lignosulfonates is a declining process (Sixta 2006). Therefore, Rudolf von Rohr and co-workers investigated an alternative process using kraft lignin as feedstock (Voitl and Rudolf von Rohr 2008; 2010; Voitl et al. 2010; Werhan et al. 2011). Kraft lignin is a by-product of the kraft process, which is presently the most prominent pulping process (Auhorn and Niemela 2007).

$H_3PMo_{12}O_{40}$ was used as homogeneous catalyst in an 80 % (v/v) MeOH/water solvent at acidic pH at 170°C under an atmosphere of 10.8 bar of oxygen containing 8.9 g L^{-1} dry kraft lignin at the start of the oxidation process (Voitl and Rudolf von Rohr 2010). Monomeric products were extracted with chloroform. The process yielded 3.5 % (w/w) vanillin and 3.5 % (w/w) methyl vanillate. A total of 10 % (w/w) of monomers could be extracted, including further products like acetovanillone and methylparaben. Additionally, approximately 60 % (w/w) of oligomeric products with significantly lower molecular weight than kraft lignin were found in the extract (Voitl and Rudolf von Rohr 2010).

In a more recent study, different metal salt catalysts were tested as replacement for $H_3PMo_{12}O_{40}$ (Werhan et al. 2011). For all studied salts ($CuSO_4$, $CoCl_2$, $FeCl_3$, and $CuCl_2$), higher maximal vanillin concentrations were found than in the presence of $H_3PMo_{12}O_{40}$ or without catalyst. However, only experiments using $CoCl_2$ and $CuSO_4$ as catalyst reached similar concentrations of the valuable methyl vanillate as experiments using $H_3PMo_{12}O_{40}$. The average molecular weight of the product mixture was considerably lower in experiments using metal salts as catalysts compared to experiments using

$H_3PMo_{12}O_{40}$. The treatment with $FeCl_3$ or $CuCl_2$ as catalyst led to the lowest average molecular weight (Werhan et al. 2011).

The oxidation of Alcell lignin, soda lignin, and several lignin model compounds was investigated using oxygen with $CoCl_2 \cdot 6H_2O$ as homogenous catalyst dissolved in an ionic liquid (1-ethyl-3-methylimidazolium diethyl phosphate, [EMIM] [DEP]) at 80 °C (Zakzeski et al. 2010b). Ionic liquids (ILs) are mixtures of cations and anions melting below 100 °C. Ethyl acetate (EtAc) extraction after lignin oxidation yielded no monomeric products. However, the difference between the attenuated total reflectance infrared spectra after various reaction times suggested a selective oxidation of the dissolved lignin (Zakzeski et al. 2010b). Treatment of lignin model compounds with the catalyst did not disrupt β-O-4, 5-5, and other linkages. Phenolic functional groups remained unchanged as well. However, alcohol moieties were oxidized to form aldehydes or, at high oxygen pressures or substrate loadings, to form acids (Zakzeski et al. 2010b). In a more recent study, the cobalt-catalyzed oxidation of lignin model compounds in [EMIM] [DEP] was further investigated (Zakzeski et al. 2011).

Further studies for the oxidation of lignin and lignin model compounds conducted at mild reaction conditions with homogeneous catalysts used metalloporphyrin, metallosalen, metallo-TAML, -DTNE, -TACN, polyoxometalate (POM) based, simple metal salt-based, and miscellaneous catalyst systems and have been reviewed (Zakzeski et al. 2010a).

Many lignin oxidation studies have been carried out and several used mild reaction conditions to depolymerize lignin. These great efforts lead to processes where about 10 to 20 wt% of technical lignins could be converted to value-added monomers (Hocking 1997; Ramachandra Rao and Ravishankar 2000). Although this constitutes a considerable accomplishment, given the complexity of the task, higher product yields from technical lignins are necessary for the processes to become economically attractive. Therefore, new approaches seem indispensable to achieve efficient lignin depolymerization.

2.4. Enzymatic catalysis

Lignin is efficiently degraded in nature by basidiomyceteous white-rot fungi through multiple enzymes (Levasseur et al. 2008; Ruiz-Dueñas and Martínez 2009; Sánchez 2009; Wong 2009; Collinson and Thielemans 2010; Hatakka and Hammel 2010). This illustrates the potential of biocatalysts for lignin depolymerization. In contrast to inorganic catalysts, biocatalysts can be much more selective and able to distinguish between functional groups (Vennestrøm et al. 2010a) but require mild reaction conditions and are often inactivated in non-aqueous solutions (Doukyu and Ogino 2010). The first part of this section covers the different enzymes involved in natural degradation processes of lignin. Application of enzymes in industrial processes is challenging since they are usually less stable than inorganic catalysts, not easily recycled, and only work in a relatively narrow temperature window. The second part of this section discusses these challenges and presents ways to improve the biocatalyst properties.

2.4.1. Lignin degradation in nature

After extensive research, the mechanisms of fungal lignin degradation become gradually clearer (reviewed by, e.g., Kersten and Cullen 2007; Hammel and Cullen 2008; Ruiz-Dueñas and Martínez 2009; Wong 2009). Enzymes potentially involved in degrading lignin are divided into lignin oxidases and lignin-degrading auxiliary enzymes, corresponding to their direct or indirect participation to lignin degradation, respectively (Table 2.1). They have been described at length in previous studies and reviews (e.g., Henriksson et al. 2000; Ozimek et al. 2005; Whittaker 2005; Mayer 2006; Joosten and van Berkel 2007; Hammel and Cullen 2008; Ruiz-Dueñas and Martínez 2009; Wong 2009; Faulds 2010; Giardina et al. 2010; Lundell et al. 2010; Singh Arora and Kumar Sharma 2010). In addition, relevant information on these enzymes is collected in general databases (e.g., http://www.brenda-enzymes.org).

2.4.1.1. Lignin oxidases

Efficient lignin mineralization in nature is only achieved by basidiomycetous white-rot fungi, which commonly inhabit forest litter and fallen trees (Kersten and Cullen 2007). Degradation of lignin is hindered by its non-phenolic aromatic nature, which prevents direct oxidation by low-redoxpotential oxidoreductases (Ruiz-Dueñas and Martínez 2009). Moreover, bulky lignin polymers are often hardly accessible to enzymes. To overcome these limitations, white-rot fungi have developed highly specialized heme-containing ligninolytic peroxidases, i.e., LiP, MnP, and VP, which use H_2O_2 as oxidant (Ruiz-Dueñas and Martínez 2009).

It is assumed that LiPs are able to oxidize the aromatic rings of lignin via long-range electron transfer (Ruiz-Dueñas and Martínez 2009). The unspecific oxidation of the aromatic rings of lignin produces unstable cation radicals, which react further and undergo different non-enzymatic reactions like scission of Cα–Cβ and 4–ether linkages (Martínez et al. 2005). The latter finally leads to the release of aromatic aldehydes, demethoxylation with subsequent MeOH release or aromatic ring cleavage prior to the formation of muconate-type structures (Martínez et al. 2005; Ruiz-Dueñas and Martínez 2009).

MnP oxidizes Mn^{2+} to Mn^{3+} (Gold et al. 1984). Mn^{3+} is subsequently stabilized by organic acids like oxalic acid, which results in Mn^{3+} chelates which act as redox mediators oxidizing phenolic lignin structures (Glenn and Gold 1985; Gold et al. 2000). Furthermore, it has been shown that lipid peroxidation by MnP might play an important role in lignin biodegradation. Mineralization of non-phenolic lignin model compounds as well as ^{14}C-labeled synthetic lignin and ^{14}C-labeled wheat straw was instigated by the presence of an unsaturated fatty acid, i.e., linoleic acid and a surfactant, i.e., Tween 20 or Tween 80 emulsifying water-insoluble components leading to a homogenous mixture of unsaturated fatty acids and water (Kapich et al. 1999a). Subsequently, it was shown that peroxidized unsaturated fatty acids are capable to oxidize non-phenolic β-O-4-linked lignin model compounds irrespective of MnP, indicating that direct contact between MnP and lignin is not necessary but, rather, that the formed peroxyl radicals act as agents for lignin degradation (Kapich et al. 1999b). In nature, lipid substances might be produced by the fungus (Enoki et al. 1999) and are also already present in

wood (Hofrichter et al. 2001). VP represents a hybrid of LiP and MnP and is able to directly oxidize non-phenolic lignin units as well as Mn^{2+} (Ruiz-Dueñas et al. 2009).

There are several white-rot fungi that exclusively produce MnP as extracellular peroxidase e.g., *Ceriporiopsis subvermispora* (Lobos et al. 1994), *Dichomitus squalens* (Périé et al. 1996), *Lentinula (Lentinus) edodes* (Leatham 1986), *Phanerochaete sordida* (Rüttimann-Johnson et al. 1994), and *Pleurotus ostreatus* (Giardina et al. 2000), indicating that MnP might be essential for lignin biodegradation. Other white-rot basidiomycetes produce LiP alongside MnP, e.g., *Phanerochaete chryosporium* (Hatakka 1994), *Phlebia radiate* (Vares et al. 1995), and *Trametes versicolor* (Johansson and Nyman 1993), while VPs have been detected in *Pleurotus* (Camarero et al. 1999) and *Bjerkandera* (Mester and Field 1998) species.

Another group of enzymes potentially involved in the oxidation of lignin are laccases, copper-containing oxidases oxidizing phenolic rings to phenoxy radicals while using molecular oxygen as oxidant (Baldrian 2006). They usually have a low redox potential with few exceptions (Uzan et al. 2010). Therefore, they are unable to directly catalyze the oxidation of non-phenolic aromatic rings of lignin (Ruiz-Dueñas and Martínez 2009). However, they are able to degrade high-redox-potential substrates in the presence of small chemical oxidants acting as redox mediators (reviewed by, e.g., Morozova et al. 2007; Cañas and Camarero 2010; Kudanga et al. 2011). These mediators form radicals, which are able to penetrate the lignocellulose matrix (Ruiz-Dueñas and Martínez 2009). Nevertheless, the role of laccase in lignin biodegradation is still debated. While many white-rot fungi produce laccases, there are no laccase-encoding genes present in the whole genome of *P. chryosporium* (Martinez et al. 2004), a white-rot basidiomycete able to completely degrade all components of lignocellulose (Kersten and Cullen 2007). Furthermore, 17 laccase-encoding genes have been found in *Coprinopsis cinerea*, a basidiomycetous fungus unable to degrade lignin (Hatakka and Hammel 2010). Moreover, in the absence of suitable mediators, laccases oxidize the phenolic groups present in lignin, which results in polymerization (Rochefort et al. 2004). Therefore, it remains unclear if laccases play a role in natural lignin degradation processes. However, since laccases can be produced in sufficient amounts for industrial applications (Hou et al. 2004), whereas this could not be achieved for ligninolytic peroxidases so far (Singh et al. 2011), their potential application for lignin depolymerization in industrial processes in combination with suitable mediators should not be disregarded.

Table 2.1 Enzyme groups potentially involved in the degradation of lignin. The values given refer to the corresponding enzyme group as a whole and depict the temperature and pH ranges in which active enzymes of the associated group have been described. References were obtained from http://www.brenda-enzymes.org. (adapted from Gasser et al. 2012)

Family	Enzyme group	pH optimum Range	pH working Range[a]	Temperature optimum Range °C	Temperature working Range °C[b]	Reaction	References
Lignin Oxidases Family LO1	laccase (EC 1.10.3.2)	2 – 9	0.5 – 11.5	20 – 85	0 – 100	4 benzenediol + O_2 = 4 benzosemiquinone + 2 H_2O	Baldrian 2004; Dubé et al. 2008; Haibo et al. 2009; Pakhadina et al. 2009; Shao et al. 2009; Wang et al. 2010; Wu et al. 2010
	catechol oxidase (EC 1.10.3.1)	3.5 - 9	3 – 9.5	4 – 70	4 – 80	2 catechol + O_2 = 2 1,2-benzoquinone + 2 H_2O	Doğan et al. 2005; Gülçİn et al. 2005; Selinheimo et al. 2006; Sellés-Marchart et al. 2006; Kim et al. 2011
Lignin Oxidases Family LO2	versatile peroxidase (EC 1.11.1.16)	3 - 5	No entries	No entries	No entries	donor + H_2O_2 = oxidized donor + 2 H_2O	Camarero et al. 1999
	lignin peroxidase (EC 1.11.1.14)	1 - 6	1 - 7	23 – 70	10 – 80	(3,4-dimethoxyphenyl)methanol + H_2O_2 = 3,4-dimethoxybenzaldehyde + 2	Aitken and Irvine 1989; Alam et al. 2009; Gohdake et al. 2009; Gomes et al. 2009
	manganese peroxidase (EC 1.11.1.13)	2.5 – 6.8	2.5 – 11	22 – 60	10 – 75	2 Mn(II) + 2 H^+ + H_2O_2 = 2 Mn(III) + 2 H_2O	Paszczyński et al. 1988; Giardina et al. 2000; Wang et al. 2002; Cheng et al. 2007; Gomes et al. 2009
	generic peroxidases (EC 1.11.1.7)	3 – 11.7	2 – 11.7	10 - 84	0 – 90	2 phenolic donor + H_2O_2 = 2 phenoxyl radical of the donor + 2 H_2O	Shin et al. 1997; Senczuk et al. 2003; Suzuki et al. 2006; Vernwal et al. 2006; Jeoung et al. 2007
	chloroperoxidase (EC 1.11.1.10)	2.5 - 6	2 - 7	30 - 35	20 – 50	RH + chloride + H_2O_2 = RCl + 2 H_2O	Petri et al. 2004; Bayramoğlu et al. 2008; Yadav et al. 2010
Lignin Oxidases Family LO3	cellobiose dehydrogenase (EC 1.1.99.18)	2.7 - 9	2.5 - 10	20 - 75	10 – 80	cellobiose + acceptor = cellobiono-1,5-lactone + reduced acceptor	Schou et al. 1998; Baminger et al. 2001; Sigoillot et al. 2002; Zamocky et al. 2006
Lignin Degrading Auxiliary Enzymes Family-LDA1-8	aryl-alcohol oxidase (EC 1.1.3.7)	5 - 8.5	2 - 10	30 - 55	20 – 60	an aromatic primary alcohol + O_2 = an aromatic aldehyde + H_2O_2	Guillén et al. 1992; Okamoto and Yanase 2002; Ferreira et al. 2005; Kumar and Goswami 2006
	vanillyl-alcohol oxidase (EC 1.1.3.38)	7 – 10.5	6 - 12	38	No entries	vanillyl alcohol + O_2 = vanillin + H_2O_2	de Jong et al. 1992; van den Heuvel et al. 2001

Table 2.1 (continued)

Family	Enzyme group	pH optimum Range	pH working Range[a]	Temperature optimum Range °C	Temperature working Range °C[b]	Reaction	References
	glyoxylate oxidase (EC 1.2.3.5	8	6.5 -8.5	40	No entries	glyoxylate + H_2O + O_2 = oxalate + H_2O_2	Akamatsu and Shimada 1994
	pyranose oxidase (EC 1.1.3.10)	4 - 8.5	2.5 – 11	35 – 65	25 – 70	D-glucose + O_2 = 2-dehydro-D-glucose + H_2O_2	Schäfer et al. 1996; Artolozaga et al. 1997; Leitner et al. 2001; Takakura and Kuwata 2003: Odaci et al. 2010
	galactose oxidase (EC 1.1.3.9)	5.5 - 8	5 – 9	30 - 50	20 – 60	D-galactose + O_2 = D-galacto-hexodialdose + H_2O_2	Alberton et al. 2007; Isobe et al. 2007; Sasaki et al. 2010
	glucose oxidase (EC 1.1.3.4)	4 – 7	3 – 11	25 – 70	10 – 70	β-D-glucose + O_2 = D-glucono-1,5-lactone + H_2O_2	Crognale et al. 2006; Simpson et al. 2007; Altikatoglu et al. 2010; Hashemifard et al. 2010; Courjean and Mano 2011
	benzoquinone reductase (EC 1.6.5.6)	6 – 7	5 - 9	40 - 45	15 - 50	NADPH + H^+ + *p*-benzoquinone = $NADP^+$ + hydroquinone	Shimizu et al. 1988
	alcohol oxidase (EC 1.1.3.13)	3 – 9	3 - 10	30 - 65	18 – 65	a primary alcohol + O_2 = an aldehyde + H_2O_2	Couderc and Baratti 1980; Patel et al. 1981; Kumar and Goswami 2006; Jadhav et al. 2009; Gvozdev et al. 2010
Lignin Degrading Auxiliary Esterases Family EST	feruloyl esterase (EC 3.1.1.73)	3 – 9	2.6 - 11	20 – 65	5 – 75	feruloyl-polysaccharide + H_2O = ferulate + polysaccharide	Garcia-Conesa et al. 2004; Wong 2006; Aurilia et al. 2007; Moukouli et al. 2008; Hegde and Muralikrishna 2009
Others	aryl-alcohol dehydrogenase (EC 1.1.1.91)	6.1 - 8.8	5 – 9.5	30	30 – 55	an aromatic alcohol + $NADP^+$ = an aromatic aldehyde + NADPH + H	Muheim et al. 1991; Gross and Zenk 1969

PH (a) and temperature (b) ranges in which enzymes of the corresponding group have been described expressing at least 20 % of the maximal activity

2.4.1.2. Lignin degrading auxiliary enzymes

The H_2O_2 needed by the ligninolytic peroxidases and possibly laccases, is produced in situ by lignin-degrading auxiliary enzymes (LDA1-8) like, e.g., aryl–alcohol oxidase or glyoxal oxidase (Shah and Nerud 2002). It has been shown that aryl–alcohol oxidase is able to use the aromatic aldehydes produced by lignin breakdown or synthesized by fungi as substrate for H_2O_2 generation in cyclic redox reactions, which also involve aryl–alcohol dehydrogenase (Guillén et al. 2000). Furthermore, there is evidence that FAD oxidases like aryl–alcohol oxidase or glucose oxidase (Leonowicz et al. 1999) prevent the recondensation of intermediates during lignin degradation by reducing the de novo formed quinonoids and radical compounds thereby hindering repolymerization (Marzullo et al. 1995). H_2O_2 has also been shown to be produced by oxidation of lignin-derived hydroquinones through laccases and VPs (Guillén et al. 2000; Gómez-Toribio et al. 2001, 2009) or Mn^{2+} oxidation through laccases (Schlosser and Höfer 2002).

Lignin-degrading auxiliary esterases, i.e., feruloyl esterases, have been shown to hydrolyze ferulate bridges between lignin and carbohydrates in monocotyledons and dicotyledons and to disrupt the cell wall structure in combination with xylanases and might, therefore, be involved in the initial stages of lignocellulose degradation (Topakas et al. 2007; Koseki et al. 2009).

2.4.1.3. Hydroxyl radical production

Hydroxyl radicals, which are the strongest oxidants in white-rot fungi cultures (Forney et al. 1982; Backa et al. 1992), can initiate the attack on lignocellulose and presumably cause hydroxylation, demethoxylation, and depolymerization of lignin (Evans et al. 1994; Joseleau et al. 1994). They can be produced by cellobiose dehydrogenase via Fenton reaction (Henriksson et al. 2000; Ludwig et al. 2010; Harreither et al. 2011). A further path leading to hydroxyl radical production involves *p*-quinones originating from lignin decomposition. They can be used by quinone reductases, laccases, and peroxidases in redox cycle reactions to activate oxygen (Guillén et al. 1997). This in turn reduces the ferric iron present in wood either by the superoxide radicals or semi-quinone radicals to ferrous iron (Guillén et al. 2000). Subsequent re-oxidation of the ferrous iron by H_2O_2 reduction produces hydroxyl radicals (Guillén et al. 2000).

2.4.1.4. Potential additional lignin-modifying enzymes

There are some reports of additional enzymes that might have the potential to act on lignin. Chloroperoxidases might contribute to lignin degradation since they have been shown to catalyze the cleavage of the β-O-4 bond of a dimeric lignin model compound (Ortiz-Bermúdez et al. 2003). Furthermore, they might chlorinate lignin and be partly responsible for the natural production of chloroaromatics (Ortiz-Bermúdez et al. 2003).

Two dye-decolorizing peroxidases (DyP) secreted by the jelly fungus *Auricularia auricular-judae* have been shown to oxidize non-phenolic lignin model compounds and highredox-potential dyes, i.e.,

Reactive Blue 5 and Reactive Black 5 at acidic pH (activity maximum at pH 1.4), indicating the ligninolytic activity of these enzymes (Liers et al. 2010). The redox potential of five different DyPs has been calculated to be at least ~1.2 V and it has been suggested that this might be sufficient for the oxidation of non-phenolic lignin structures at low pH values between 1.5 and 3.0 (Hofrichter et al. 2010). However, not all DyPs are capable to oxidize non-phenolic lignin model compounds and whether certain DyPs can actually depolymerize lignin has still to be investigated (Hofrichter et al. 2010).

A further group of enzymes hypothesized to take part in the degradation of methoxylated compounds originating from lignin is aromatic peroxygenases (Kinne et al. 2011). Extracellular aromatic peroxygenase from the agaric fungus *Agrocybe aegerita* (*Aae*APO) has been shown to cleave non-phenolic β-O-4 lignin model compounds as well as phenolic dimers but seems to be unable to oxidize polymeric lignin (Kinne et al. 2011). Therefore, *Aae*APO seems not to be directly involved in lignin biodegradation but rather in the oxidation of compounds with low molecular masses such as lignin fragments or lignans (Kinne et al. 2011).

2.4.1.5. Lignin modification by brown rot fungi

Besides white-rot basidiomycetes, brown-rot fungi are also capable to degrade lignocellulose in nature. While lignin is not significantly mineralized by brown-rot fungi, its structure is altered, i.e., its aromatic methoxyl content is lower and its content of conjugated carbonyls and carboxyls as well as phenolic hydroxyls is higher (Yelle et al. 2008). While hydroxyl radicals seem to play a major role in lignocellulose degradation by brown-rot fungi (Hammel et al. 2002), there also appear to be hydrolytic enzymes involved in the process (Cohen et al. 2005). It has been argued that consequently some lignin degradation has to occur because otherwise these enzymes would be hindered to act on their target substrates, e.g., cellulose by the small pore sizes of intact wood (Yelle et al. 2008). Analysis of lignocellulose degraded by the brown-rot basidiomycete *Gloeophylum trabeum* via two-dimensional solution-state nuclear magnetic resonance (NMR) spectroscopy indicated degradation of lignin side chains during brown-rot (Yelle et al. 2008). However, brown-rotted lignin has been shown to be polymeric and to keep most of its aromatic residues (Jin et al. 1990). Therefore, it has been suggested that lignin is initially depolymerized by brown-rot fungi (Yelle et al. 2008). Subsequently, the content of phenolic units on lignin increases due to hydroxyl radicals reacting with the aromatic rings (Yelle et al. 2008). Thereafter, the lignin units get reconnected through radical coupling of the phenolic units (Yelle et al. 2008).

2.4.1.6. Lignin degradation by bacteria

Many bacteria have lignin-degrading ability (reviewed by Bugg et al. (2011)). They are able to solubilize lignin and modify the lignin structure (Buswell and Odier 1987; Ball et al. 1989; Godden et al. 1992). However, they do not mineralize lignin to a large extent (Buswell and Odier 1987). These bacteria produce several extracellular enzymes that are involved in the degradation of lignocellulosic biomass like peroxidases, cellulases, and esterases (Santhanam et al. 2012). However, at present, the enzymology

of bacterial lignin degradation is not well understood (Bugg et al. 2011). Nevertheless, the results suggest that similar enzyme types as in fungi might be involved. It has been reported that *Streptomyces viridosporus* T7A, a lignin-degrading actinomycete, secretes several peroxidases able to catalyze the cleavage of lignin model compounds (Ramachandra et al. 1988). Subsequently, several actinomycetes exhibiting extracellular peroxidase activity have been identified (Mercer et al. 1996). More recently, a DyP has been identified and characterized in the actinomycete *Rhodococcus jostii* sp. RHA1 able to catalyze Cα–Cβ bond cleavage of a lignin model compound (Ahmad et al. 2011). Production of laccases by bacteria has been reported as well (Miyazaki 2005; Kellner et al. 2008; Niladevi et al. 2008). This indicates that suitable enzymes produced by bacteria could potentially be used by themselves or in combination with enzymes from fungi in future conversion processes of lignin. Using bacteria instead of fungi for enzyme production would most likely reduce the practical challenges posed when working with fungi concerning protein expression and genetic manipulation.

2.4.2. Enhancement of biocatalyst properties

The performance of one-pot multi-catalytic reactions with LME can be limited by several reaction parameters, e.g., pH, temperature, and solvent. In general, pH is not a major constraint regarding activity as several LME active at rather high or low pH have been described (Table 2.1). Therefore, the right selection of enzymes allows for reaction conditions to be acidic as well as alkaline. However, enzyme stability might become an issue under extreme pH conditions, which are, e.g., associated to chemical oxidation processes. Temperature seems to be a major limitation as few enzymes are active at temperatures above 90 °C. Most LMEs show activity maxima between 20 and 70 °C. However, some overlap between the temperature ranges of LME and inorganic catalytic processes exists (Figure 2.6). Moreover, enzymes are often inactivated or denatured in the presence of organic solvents (Ogino and Ishikawa 2001), further limiting their usability for the conversion of lignin in combination with chemical catalysis.

Improving enzyme stability and activity under harsh reaction conditions would lead to a broader application range, thereby increasing the possible combinations with other bio-or inorganic catalysts. In principle, there are three ways to obtain modified enzymes with improved properties. Enzymes can be isolated from extremophiles, obtained by classical protein engineering where stabilizing mutations can be predicted on the basis of the enzyme structure, and produced through directed evolution (Eijsink et al. 2005; Turner 2009). “Directed evolution is a widely-used engineering strategy for improving the stabilities or biochemical functions of proteins by repeated rounds of mutation and selection” (Bloom and Arnold 2009). These three strategies are also often used in combination. Additionally, enzyme immobilization often leads to the enhancement of enzyme stability and sometimes even of activity (Mateo et al. 2007). Furthermore, immobilization facilitates the recovery and reuse of enzymes (Sheldon 2007). In this section, several scientific and technological advances leading to the effective improvement of LME properties are discussed.

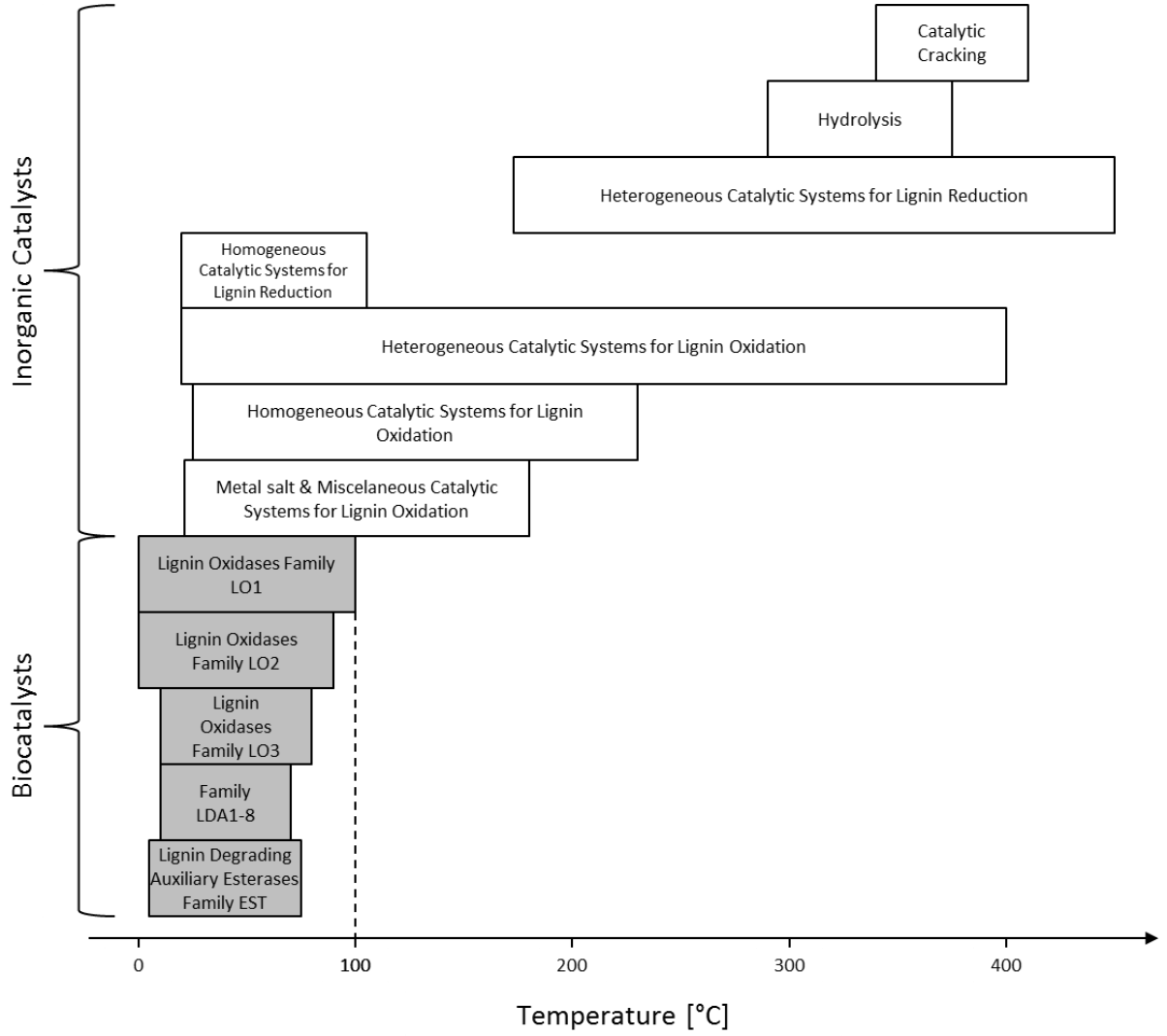

Figure 2.6 Temperature ranges of the different enzyme families (grey background; data from Table 2.1) and in which the different types of chemical catalyses of lignin and lignin model-compounds (white background) were performed (data from Zakzeski et al. 2010a). Family LDA1-8; Lignin Degrading Auxiliary Enzymes (adapted from Gasser et al. 2012)

2.4.2.1. Thermostability

Increased enzymatic thermostability often goes along with a general stability increase of the enzyme, making it more tolerant to extreme pHs, high salt concentration, the presence of organic co-solvents, etc. (Arnold 1990; Ogino and Ishikawa 2001). High process temperatures confer advantages like low levels of microbial side-contamination, improved reaction yields, increased solubility of reaction substrate, and product and time savings (Arnold 1990; Ogino and Ishikawa 2001; García-Ruiz et al. 2010).

However, increasing stability through point mutations often leads to a trade-off between stability and activity (García-Ruiz et al. 2010). Stability increases are mostly gained through mutations, which establish new interactions and thereby prevent unfolding and denaturation under harsh conditions (Reetz et al. 2006). At the opposite, activity increases are mostly achieved through destabilizing mutations that

lead to better access for the substrates to the active sites of the enzymes (Bloom and Arnold 2009). Therefore, to produce enzymes with increased stability and activity, several mutations are often necessary. Several studies reported the increase of enzyme thermostabilities of LME through mutations, also often in combination with increased activities (Reading and Aust 2000; Morawski et al. 2001; Festa et al. 2008; García-Ruiz et al. 2010). For instance, a recombinant MnP had a higher activity than the native enzyme produced by *Phanerochaete chrysosporium* but was also more readily inactivated at temperatures of 37 °C and above (Reading and Aust 2000). The recombinant enzyme was modified by the insertion of a disulfide bond, which increased the enzyme's thermostability while retaining its enhanced activity. The newly built enzyme retained most of its activity up to a temperature of 52 °C, where it was inactivated at a similar rate as the native enzyme (Reading and Aust 2000). Other studies applied directed evolution to improve the thermostability of, e.g., a horseradish peroxidase (HRP) (Morawski et al. 2001), laccase from *P. ostreatus* (Festa et al. 2008), and VP from *Pleurotus eryngii* together with high-redox-potential laccase from basidiomycete PM1 (García-Ruiz et al. 2010). The enzymes were expressed in *Saccharomyces cerevisiae* in all three studies. The half-life of the newly developed HRP was increased by a factor of 3 (Morawski et al. 2001) and that of laccase by a factor of 1.4 (Festa et al. 2008) in comparison to the native enzyme at 60°C. The study aiming to improve the thermostability of VP and high-redox-potential laccase reported that the VP retained ~30 % of its maximal activity at 65 °C (three times more than the native enzyme) and the high-redox potential laccase retained 40 % of its maximal activity at 72 °C (ten times more than the native enzyme) (García-Ruiz et al. 2010).

2.4.2.2. H_2O_2 tolerance of peroxidases

Peroxidases are inactivated by too high substrate, i.e., H_2O_2, concentrations. The oxidative damage of peroxidases has been referred to as suicide inactivation (Valderrama et al. 2002). Since H_2O_2 is needed by peroxidases to degrade lignin, either control of H_2O_2 concentrations or increased tolerance of peroxidases to higher H_2O_2 concentration levels is necessary to run continuous processes. Control of H_2O_2 concentrations could be achieved either by supplying H_2O_2 to fed batches (Mielgo et al. 2003) through electro-chemical methods (Lee and Moon 2003) or through the control of H_2O_2-producing enzymes (Lan et al. 2006). Some studies report on the operation of continuous processes with LiP from *Phanaerochaete chrysosporium* whereby the enzymatic production of H_2O_2 was used as a mean to control the concentration of the latter (Lan et al. 2006; Qiu et al. 2009). H_2O_2 was supplied by glucose oxidase from *Aspergillus niger*, which was in turn controlled through regulation of glucose concentration and pH. The effectiveness of this combination was demonstrated through the conversion of different dyes. In one study, 90.9 % of rhodamine B was converted over 1 h when H_2O_2 was produced enzymatically compared to only 41.0 % when H_2O_2 was supplied externally every 5 min (Lan et al. 2006). Total supplied H_2O_2 amounts over the course of the whole experiment were 300 µM in both cases (Lan et al. 2006). In another study, LiP and glucose oxidase were co-immobilized on nanoporous gold (Qiu et al. 2009). Some 87.2, 75.5, and 84.6 % of pyragallol red, rhodamine B, and fuchsine,

respectively, were converted over 3 h when H_2O_2 was supplied enzymatically compared to only 55.6, 44.3 and 53.5 % when LiP was immobilized as a single enzyme and 1 µM H_2O_2 was supplied externally in one pulse at the beginning of the experiment (Qiu et al. 2009).

Gil-Rodríguez et al. (2008) reported the isolation of a peroxidase from daikon radish (*Raphanus sativus L. cv. daikon*) resistant to H_2O_2, named Zo peroxidase. Future detailed study of the enzyme structure of Zo peroxidase might reveal the properties responsible for its H_2O_2 tolerance and may help in the production of further H_2O_2-resistant peroxidases (Gil-Rodríguez et al. 2008). Several studies reported achieving enhanced H_2O_2 tolerance of ligninolytic peroxidases through mutagenesis. For example, MnP from *P. chrysosporium* with nine times higher H_2O_2 stability (Miyazaki-Imamura et al. 2003) and HRP with 25-, 18-, and 12-fold increased H_2O_2 stability (Ryan and Ó'Fágáin 2007) compared to the wild type were reported. Furthermore, increased H_2O_2 tolerance of a VP from *Bjerkandera adusta* was achieved by producing crosslinked enzyme aggregates of VP in combination with glucose oxidase from *A. niger* (Taboada-Puig et al. 2011).

2.4.2.3. Stability in non-aqueous solvents

Lignin can be dissolved in some organic solvents (Muurinen 2000; Zhao et al. 2009), making it more available for catalysts. However, enzymes are usually inactivated and denatured in the presence of organic solvents (Doukyu and Ogino 2010) since they generally require water to maintain their native structure by promoting non-covalent interactions like hydrogen bonds, and van der Waals, hydrophobic, and ionic interactions (Singer 1963). Furthermore, polar solvents are able to enter the protein's interior which might induce secondary and tertiary structural changes and are abler than apolar solvents to remove protein-bound water (Serdakowski and Dordick 2008). Additionally, the higher solubility of the substrate in organic solvents constitutes a thermodynamic stabilization of the substrate in its initial state, which leads to a decrease of the observed enzymatic activity (Serdakowski and Dordick 2008). Changing solvent polarity can lead to a more stable transition state and therefore reduce the activation energy of the catalyzed reaction as shown, for example, for subtilisin-catalyzed transesterification reactions in organic solvents (Kim et al. 2000). Therefore, the addition of small amounts of water and the decrease of solvent polarity can lead to more enzymatic activity in organic solvents (Serdakowski and Dordick 2008). Another way to obtain active enzymes in non-aqueous solvents is protein engineering (Serdakowski and Dordick 2008). No LME are reported to be organic solvent tolerant by nature in a recent review on the subject (Doukyu and Ogino 2010). However, several studies successfully maintained the enzymatic activity of LME in organic solvents (e.g., Dai and Klibanov 1999; Ozawa and Klibanov 2000; van de Velde et al. 2001; Liu et al. 2006; Zumárraga et al. 2007).

Alternatively, biomass can be dissolved in ILs. Several ILs are able to dissolve lignocellulose and allow the separation and at least partial recovery of each fraction. The solubility of carbohydrates and lignin in ILs has been reviewed recently (Zakrzewska et al. 2010). The highest solubility of kraft lignin was

achieved using 1,3-dimethylimidazolium methanesulfonate ([Mmim] [CH_3OSO_3]) or 1,3-dimethylimidazolium trifluoromethanesulfonate ([Bmim] [CF_3SO_3]) as solvent (Lee et al. 2009).

Several reviews discuss enzymatic reactions and enzyme stabilization in ILs (e.g., Cantone et al. 2007; van Rantwijk and Sheldon 2007; Gorke et al. 2010; Zhao 2010). Dissolution of lignocellulose in ILs and prospects on possible future uses of ILs in biorefineries are discussed in a feature article (Sun et al. 2011). The possibility to directly dissolve lignocellulose and separate lignin from cellulose and hemicellulose might allow an exhaustive utilization thereof and has the potential to facilitate the treatment of lignin with biocatalysts (Sun et al. 2011).

2.4.2.4. Enzyme immobilization

Enzyme immobilization can improve the properties of biocatalysts by increasing their stability and activity under various conditions (e.g., extreme pHs, organic solvents, elevated temperatures) (Bommarius and Riebel-Bommarius 2004) and allows enzyme reuse and biocatalysts separation from reaction products, thereby permitting the operation of continuous processes (Polizzi et al. 2007). Immobilization techniques have been the subject of several reviews (e.g., Mateo et al. 2007; Brady and Jordaan 2009; Hartmann and Jung 2010; Jochems et al. 2011; Ba et al. 2013).

Basically, three methods can be distinguished, i.e., support or carrier binding, encapsulation or entrapment, and cross-linking (Durán et al. 2002; Sheldon 2007; Ba et al. 2013). Each method possesses specific advantages and disadvantages depending on the targeted application. Carrier binding methods such as physical adsorption and covalent or ionic binding immobilize the enzymes on a support material. Adsorption occurs via electrostatic interactions, van der Waals forces, and even hydrogen bonding between enzymes and carrier surface (Ba et al. 2013).

2.4.2.4.1. Covalent immobilization on solid support material

Stability is a crucial factor with respect to efficient enzyme use. During lignin treatment potential unfavorable conditions due to the presence of organic solvents or the application of low pH values might lead to considerable enzyme inactivation. Regarding methods like carrier binding or encapsulation, the physical bonding is generally insufficient to keep the enzyme fixed to the support or prevent enzyme leakage, while ionic binding is normally stronger (Sheldon 2007). Covalent binding leads in general to an even more stable immobilization of the biocatalysts on the carrier (Sheldon 2007).

Regarding the specific enzymatic activity that can be immobilized on carriers, the specific surface area of the support material seems to be a decisive factor. The same immobilization protocol was used for the covalent immobilization of laccase from *Coriolopsis polyzona* on spherical silica nanoparticles with a specific surface area of 17.4 $m^2\ g^{-1}$ and to fumed silica nanoparticles (fsNP) with a specific surface area of ~390 $m^2\ g^{-1}$ (Zimmermann et al. 2011). Resulting biocatalysts immobilized on fsNP had a 14.3 times higher specific enzymatic activity than biocatalysts immobilized on spherical silica nanoparticles, demonstrating the importance of a large specific surface area.

The series of reaction steps during enzyme immobilization was investigated in the context of this study as well. In a first approach, the surface of the fsNP was modified with 3-aminopropyltriethoxysilane (APTES). In a second step, the cross-linker was added and allowed to react with the amino group on the surface of the modified fsNP. Excess cross-linkers were removed before; in a third step, the enzymes were added and covalently immobilized on the particle surface. In a second approach, a sorption step was introduced in which the enzymes were allowed to adsorb to the modified particle surface prior to cross-linker addition. The first approach results in covalent immobilization of the enzymes on the particle surface, while the second approach additionally results in intramolecular cross-linking of the enzyme molecules and consequently in the formation of cross-linked enzyme aggregates (CLEAs) on the particle surface. The second approach allowed the immobilization of nearly twice as much enzymatic activity on the fsNP surface. The stability of the two biocatalysts was investigated in buffer solutions at pH 7 over 1 month. No considerable differences in stability could be observed. After 32 d, the biocatalysts retained 63.3±1.3 and 57.0±2.2 % of their initial activity for biocatalysts produced by the first and second approaches, respectively.

Immobilization increased enzymatic stability considerably since only 20.1±1.7 % of the initial activity of dissolved laccase remained after 29 d. Stability tests in WWTP effluent at pH 8.2 were conducted with biocatalysts produced with the second immobilization approach, with dissolved enzymes, and enzymes only adsorbed on fsNP. While the covalently immobilized enzymes still retained around 80% of their initial enzymatic activity after 32 d, the dissolved and the adsorbed enzymes lost most of their activity within the first 10 d (Zimmermann et al. 2011).

In an additional study, laccase from *T. versicolor* (TVL) and HRP were co-immobilized on aluminum particles by cross-linking and layer-by-layer coating with alternatively charged polyelectrolytes (Crestini et al. 2011). The resulting multi-enzyme biocatalysts had increased stability compared to the free enzymes. A total of 2 g L^{-1} milled wheat straw lignin was treated with the biocatalysts in water. Before the start of the experiment, the wheat straw lignin was completely insoluble. After treatment with the biocatalysts, 61.3 and 59.8 wt% of milled wheat straw lignin were in solution with and without addition of a chemical laccase mediator, respectively. The water-soluble material consisted of polymers with significantly lower average molecular weight than the starting material, demonstrating that lignin depolymerization outweighed lignin solubilization. Control experiments with free enzymes and singly immobilized enzymes (used alone or in mixture, with or without laccase mediator) led to less efficient lignin conversion and depolymerization (Crestini et al. 2011). Furthermore, the immobilized catalysts could be recycled more than ten times. This study gives further indication that a multicatalyst approach is expedient for lignin depolymerization and demonstrates the advantages of immobilized enzymes over free enzymes due to higher stability and recyclability.

Next to the often reported favorable effects on enzymatic stability through enzyme immobilization on solid carriers (Cabana et al. 2009; Zimmermann et al. 2011; Nair et al. 2013), there are also shortcomings

to the resulting biocatalysts. For example, reduced activity towards certain substrates in comparison to dissolved enzymes is sometimes reported and attributed to diffusional limitations of substrates (Hommes et al. 2012). Furthermore, insoluble lignin might adsorb on the carrier surfaces reducing accessibility of the active sites of the biocatalysts for the targeted compounds. In case of particles, it might also intensify aggregation and settling of support particles harboring the immobilized biocatalysts, making proper mixing more laborious. Furthermore, separation of immobilized enzymes from insoluble lignin residues after treatment might be difficult. Therefore, the application of magnetic carrier materials might be of interest allowing magnetic separation of the biocatalsysts from other insoluble material. Surface modification of magnetite particles with APTES could be successfully demonstrated (Ma et al. 2003; Yamaura et al. 2004). Consequently, this will enable enzyme immobilization on magnetic carriers applying a cross-linking agent like glutaraldehyde. Applying this concept will allow production of magnetic nanobiocatalytic materials that can be easily separated from insoluble lignin material after reactions.

2.4.2.4.2. Encapsulation

A further immobilization method, known as encapsulation (entrapment), occurs via inclusion of enzymes inside a polymer network (gel lattice) such as organic polymer, silica solgel, or a membrane device such as a hollow fiber or a microcapsule in order to preserve the enzyme's three-dimensional structure (Sheldon 2007). While there are reports on improved enzymatic stability due to encapsulation (e.g., Lloret et al. 2011) diffusion limitations leading to slower reaction kinetics are commonly reported for encapsulated enzymes (Pierre 2004). Furthermore, encapsulation induced aggregation or unfolding of proteins is a major issue in the preparation of such biocatalysts, rendering the choice of a suitable methodology particularly important (Castellanos et al. 2002).

2.4.2.4.3. CLEAs

Another immobilization approach uses protein cross-linking by covalently binding functional groups (e.g., amine groups, carboxylic groups) of different enzyme molecules using a bi- or multi-functional reagent in the absence of a carrier (Ba et al. 2013), which is the main advantage of this method. Consequently, the specific activity of the catalysts can be expected to be higher compared to catalysts immobilized on solid supports assuming that cross-linking does not severely affect the catalytic activity of the enzymes. Several protein cross-linking methods exist such as cross-linking the enzymes in solution (cross-linked enzymes, CLEs), spray-drying the biocatalysts prior to immobilization (cross-linked spray dry, CLSD), laborious cross-linking of highly pure enzyme microcrystals (cross-linked enzyme crystals, CLECs), or the formation of enzyme aggregates using raw enzymes (CLEAs) (Sheldon 2007; Ba et al. 2013). Biocatalysts such as CLEs and CLSD have generally low mechanical stability, which is not the case for CLECs and CLEAs (Sheldon 2007; Ba et al. 2013). However, production of CLECs is much more laborious than for CLEAs, leading to increased costs.

As already pointed out by others (Sheldon 2007), direct comparison of the different immobilization methods based on literature is difficult. Most studies compare the performances of immobilized/insolubilized enzymes prepared by only one technique with the free enzyme. However, every enzyme responds uniquely to an immobilization method, and for proper comparison, several parameters would have to be determined, like enzyme pH optimum, immobilization efficiency, enzyme activity, and enzyme stability (Jochems et al. 2011). Moreover, some of the changes in enzymatic stability and activity that are observed might not be due to conformational changes of the enzyme but due to differences in the vicinity of the immobilized/insolubilized biocatalyst compared to the bulk environment (De Maio et al. 2003). Since substrate oxidation to radical species takes place at the active site of the enzymes, the radical concentration in proximity of the immobilized biocatalysts might be higher than in bulk solution. Therefore, the occurrence of radical chain reactions might be increased in reactions using immobilized enzymes compared to reactions using dissolved enzymes.

2.5. Multi-catalyses reactions and chemoenzymatic combinations

The complex mechanism of lignin degradation in nature and the limited success of lignin depolymerization with single catalysts indicate that efficient lignin conversion to platform and fine chemicals might only be achieved by combining various catalysts. Making use of the unique properties of biocatalysts as well as of chemical catalysts represents a new approach (Vennestrøm et al. 2010a).

One possibility to treat lignin using chemical catalysts as well as biocatalysts would be a sequential treatment in several reactors, allowing optimal reaction conditions for each catalyst. While this might be necessary for certain reactions (especially reactions with chemical catalysts only working effectively at high temperatures), using multiple catalysts in one reactor would offer several advantages, such as process intensification, reduction of product separation and purification steps, material consumption, waste generation, and time and yield losses (Murzin and Leino 2008; Vennestrøm et al. 2010a). However, conducting such one-pot catalytic transformations is challenging. Temperature and reaction media (as already discussed in the previous chapter), pressure, compatibility, and reaction rates are key parameters to consider when combining enzymes and inorganic catalysts (Vennestrøm et al. 2010a). The highest pressure used in chemical catalysis as reported by a comprehensive review (Zakzeski et al. 2010a) was 46 MPa (Kashima et al. 1964). However, these processes were conducted at temperatures between 250 and 450 °C and are therefore unsuitable for enzymatic reactions. The highest pressure for chemical catalysis conducted at 100 °C or below as reported by the same review was 18 MPa (Borthakur 2007). Pressures in this order of magnitude seem to have only limited effects on enzyme stability as pressures of 100–200 MPa are required to dissociate oligomeric proteins (Silva and Weber 1993) and even higher pressures of 400–800 MPa are needed to denature small monomeric proteins (Heremans 1982).

Compatibility between reactants, intermediates, substrates, and bio- and inorganic catalysts that are employed in one-pot processes is more crucial and has to be ensured (Vennestrøm et al. 2010a).

Furthermore, reaction rates have to be adjusted in order to avoid the formation of undesired compounds or substrate limitation for one of the catalysts (Murzin and Leino 2008; Vennestrøm et al. 2010a). Therefore, reliable kinetic models describing the transformation processes have to be developed, which is not an easy task because a lot of parameters and variables have to be considered and integrated together in the models, e.g., catalyst–catalyst interactions, mass transfer processes, feedback inhibition, etc. (Murzin and Leino 2008). Recently, processes relying on the chemo-enzymatic conversion of biomass were discussed in a further review, which however did not mention the use of lignin as feedstock (Marr and Liu 2011).

While chemo-enzymatic combinations for lignin transformation have not been extensively explored so far, several interactions between LMEs and chemical transformation processes can be envisioned (Figure 2.7). Chemical transformation of lignin could provide compounds that can be used by laccases as mediators (Figure 2.7, a). Phenol—a compound that has been shown to act as laccase mediator for the oxidation of, e.g., polycyclic aromatic hydrocarbons like anthracene (Johannes and Majcherczyk 2000a)—has been produced by, e.g., hydrocracking of organocell lignin (Meier et al. 1994). Chemical oxidation of lignin has led to the formation of other compounds that have been reported to act as laccase mediators in a review (Cañas and Camarero 2010), e.g., vanillin (e.g., Badamali et al. 2009; Partenheimer 2009; Werhan et al. 2011) or aceto vanillone (e.g., Crestini et al. 2005, 2006; Badamali et al. 2009). Therefore, employing laccase in combination with certain chemical catalysts might lead to in situ production of laccase mediators, and consequently the addition of laccase mediators in advance might not be necessary.

Furthermore, the different oxidases can be employed for H_2O_2 production (Figure 2.7, b). This has been demonstrated previously (Vennestrøm et al. 2010b). Glucose oxidase from *A. niger* was immobilized on a titanium silicate catalyst. The H_2O_2 produced as a side-product by the glucose oxidase-catalyzed oxidation of one substrate (e.g., β- glucopyranose) was used as oxidizing agent by the chemical catalyst for the oxidation of another substrate (e.g., allyl alcohol, 2-butanol, 2-propanol, crotyl alcohol). A similar combination can be envisaged between FAD-oxidase enzymes and, for example, MTO catalysts that require H_2O_2 as primary oxidant for the oxidation of lignin (e.g., Herrmann et al. 2000; Crestini et al. 2005, 2006). The degradation of lignin or lignin model compounds by the MTO/H_2O_2 oxidation system has led to the formation of aromatic aldehydes (Herrmann et al. 2000; Crestini et al. 2005, 2006) as well as aromatic alcohols (Herrmann et al. 2000) (Figure 2.7, c). These products could be directly used by FAD-oxidases and alcohol dehydrogenases in redox cycles for the further production of H_2O_2. Moreover, repolymerization of intermediates like quinonoids and radical compounds during lignin degradation might be prevented by employing FAD-oxidases.

Chemical oxidation of lignin by, e.g., POM (Gaspar et al. 2007) or Co(salen) (Canevali et al. 2002) catalysts can result in quinones and hydroquinones that can be used by quinone reductases, laccases, and peroxidases in redox cycles for the production of superoxide radicals (Figure 2.7, d). Furthermore,

it has been shown that laccase can re-oxidize reduced POM catalysts. This has been used for the continuous delignification of eucalypt kraft pulp (Gamelas et al. 2007). The POM catalyst ($[SiW_{11}V^{V}O_{40}]^{-5}$) was employed at around 90 °C in a batch reactor for pulp delignification. TVL was applied in a separate aerated batch reactor for the reoxidation of the reduced POM catalysts at 45°C. The reoxidized chemical catalysts were separated from the enzymes via an ultrafiltration ceramic membrane and returned to the first reactor. By this continuous system, nearly 70 % of pulp delignification was obtained (Gamelas et al. 2007).

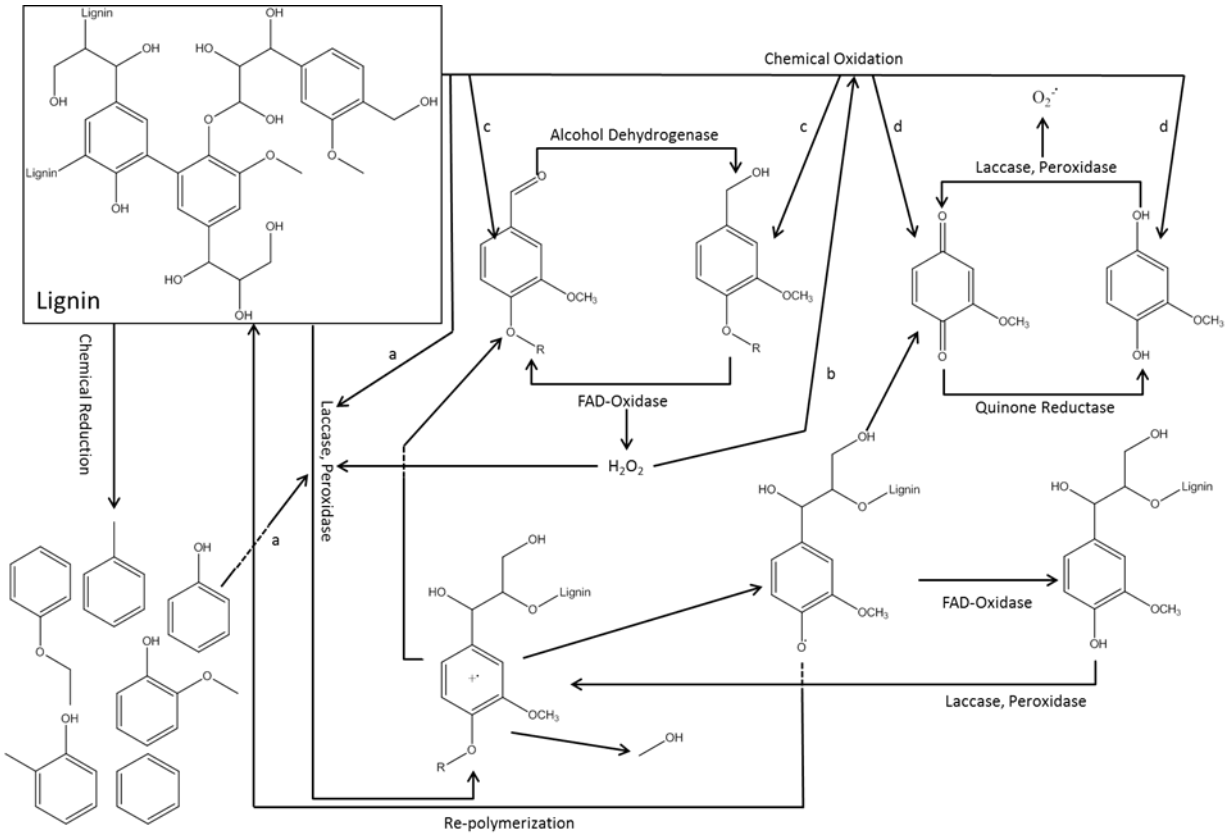

Figure 2.7 Scheme depicting possible interactions between biological and chemical lignin degradation (for explanation, see text, adapted from Gasser et al. 2012)

High lignin conversion to lower molecular weight compounds was achieved recently, by two-step processes combining an oxidation step with a second reaction step targeting oxidized β-O-4 ether bonds (Rahimi et al. 2014, Lancefield et al. 2015). In one study cellulolytic enzyme lignin, i.e., an almost native lignin from aspen was first oxidized aerobically using a 4-Acetamido-2,2,6,6-tetramethylpiperidine 1-oxyl/HNO_3/HCl catalyst system using acetonitrile as solvent (Rahimi et al. 2013). This system was shown to oxidize the side chains of lignin β-O-4 model compounds in the Cα position leading to the formation of Cα ketones (Rahimi et al. 2013). Subsequently, these oxidized side-chains were cleaved in the second reaction step by a formic acid induced depolymerization step (Rahimi et al. 2014). Samples were treated at 110 °C for 24 h. This allowed the production of 52.2 wt% of

monomeric reaction products and 9.0 wt% of di- and trimeric reaction products. These are the highest yields of low molecular weight compounds produced from lignin reported to date (Rahimi et al. 2014). Another study followed a similar approach (Lancefield et al. 2015). Birch lignin was oxidized in a first step using a 2,3-dichloro-5,6-dicyano-1,4-benzoquinone (DDQ)/tBuONO/O_2 catalytic system in 2-methoxyethanol/1,2-dimethoxyethane (2:3) at 80 °C for 14 h. As in the study described above, this led to side-chain oxidation and the formation of Cα-ketones in β-O-4 lignin bonds as demonstrated by oxidation of lignin model compounds. The oxidized β-O-4 lignin bonds were subsequently cleaved using zinc as reductant in presence of NH_4Cl. Through this process one main monomeric reaction product, i.e., 3-hydroxy-1-(4-hydroxy-3,5-dimethoxyphenyl)propan-1-one was produced at a yield of 5 wt% (Lancefield et al. 2015). While these results are promising, achievable low molecular weight product yields using these processes heavily depend on the quantity of β-O-4 ether bonds of the lignin material and most biomass pretreatment methods employed today, e.g., kraft pulping or organosolv processes considerably alter the lignin structure leading to a decrease or complete loss of β-O-4 bonds (Rahimi et al. 2014).

3. Aims and Scope

The aim of the present thesis was the development of a lignin depolymerization strategy making use of LME immobilized on nanomaterials. Enzymes of interest were identified by literature study (see paragraph 2.4.1) and comprise laccases, LiP, HRP, VP, MnP, DyP, and glucose oxidase.

For high-throughput characterization of oxygen consuming enzymes, i.e., laccases and glucose oxidase a new method was developed making use of an extracellular flux-analyzer allowing directly measuring the oxygen consumption of the enzymes in the presence of a substrate, e.g., lignin. This method allows the quantitation of enzyme characteristics (i.e., profiles of activity at various pH values) and minimizes the time it usually takes to collect respiratory data of oxygen-consuming enzymes.

Covalent enzyme immobilization on two solid carrier materials, i.e., fsNP and superparamagnetic particles (MP) using a sorption-assisted surface conjugation approach (Zimmermann et al. 2011, see paragraph 2.4.2.4.1) was explored. The goal was to study and optimize the immobilization process more in depth to gain increased understanding and allow efficient production of biocatalysts with high specific enzymatic activity and stability. Furthermore, the method was augmented to enable the immobilization of several different enzymes on the same particle, i.e., to allow the production of multi-enzyme nanobiocatalysts.

Initial lignin treatment experiments were conducted with the goal to establish reaction conditions allowing effective lignin oxidation. To that end different organic solvents were applied in order to partly solubilize lignin, thereby, increasing the accessibility for the enzymes. Subsequently, the effects of different oxidative LMEs on the molecular weight distribution of lignin were evaluated, newly formed low molecular weight compounds for most promising setups were identified and quantified, and most promising LMEs were selected for further experiments.

Thereafter, ways to improve the overall reaction regarding production of low molecular weight compounds were investigated. Results of the first experiments showed that while lignin oxidation could be achieved and stable low molecular weight compounds were formed considerable polymerization occurred as well. Therefore, reaction conditions were adapted with the objective to limit polymerization and potentially produce higher yields of low molecular weight products. The following approaches were investigated:

- Laccases were used in combination with an antioxidant and its effect on the molecular weight distribution of lignin was evaluated.
- Laccases were used in combination with redox mediators in order to extend the effectivity of the reactions towards non-phenolic lignin structures

- The enzymatic oxidation step was combined with a formic acid induced depolymerization step in order to further break down the residual oxidized lignin.

Success of the processes was evaluated by quantitation of newly formed low molecular weight products as well as by overall changes in the molecular weight distribution of lignin. Finally, based on the experimental results, two potential processes for lignin valorization were described and a preliminary economic evaluation of these processes was conducted.

4. Materials and Methods

4.1. General

The substrates 2,2′-azino-bis(3-ethylbenzthiazoline)-6-sulfonic acid (ABTS), 2,6-dimethoxyphenol (2,6-DMP), 4-hydroxy-3,5-dimethoxybenzaldehyde azine (syringaldazine), diclofenac sodium salt, hydroquinone, and additional analytical grade chemicals were purchased from Sigma-Aldrich (Switzerland) and used without further purification. FsNP (surface area: 390±40 m^2 g^{-1}; aggregates of particles with a size of 7 nm) were purchased from Sigma-Aldrich (Switzerland). Radiolabeled [phenyl acetic acid ring-U-^{14}C] diclofenac (2-[(2,6- dichlorophenyl)amino]benzeneacetic acid) sodium salt was purchased from GE Healthcare, U.K. Citric acid and dimethyl sulfoxide (DMSO, Rotisolv, ≥99,99 %, headspace grade) were purchased from Carl Roth GmbH (Switzerland). Other chemicals were of analytical grade and high purity and purchased from Sigma-Aldrich (Switzerland). Different buffer systems were used, i.e., McIlvain phosphate-citrate buffer (MPC; McIlvaine 1921), Sörensen phosphate-buffer (PB; 0.1 M), malonate buffer (0.1 M), and acetate buffer (0.1 M).

Colorimetric assays were conducted using a plate reader (Synergy™ 2 Multi-Mode Microplate Reader, BioTek Instruments Inc., Switzerland) and Gen5 1.08 Data Analysis Software (BioTek Instruments Inc., Switzerland). Design Expert 8.0.7.1 software (Stat-Ease, Inc., Minneapolis) was used for development and analysis of experimental designs.

4.2. Enzymes and enzyme characterization

4.2.1. Origin of enzymes

Commercial enzyme formulation and crude solutions of laccases obtained from filtered fermentation broths were used. Laccase from *Trametes versicolor* (Sigma; TVL), *Pleurotus ostreatus* (Sigma; POL), HRP (Sigma; type II), LiP (Sigma), VP from *Bjerkandera adusta* (Jean Bioscience), and MnP from *Nematoloma frowardii* (Jena Bioscience) were purchased as lyophilized powder, whereas the laccase from *Rhus vernicifera* (Sigma; RVL) was purchased as crude acetone powder. Crude laccase of *Thielavia* genus (Ecostone LCL45-Lot 7590; GTL) was purchased from AB Enzymes GmbH (Germany). Laccases of *Coriolopsis polyzona* (CPL) and *Cerrena unicolor* (CUL) were provided as filtered fermentation broth by Wetlands Engineering SPRL (Belgium). Glucose oxidase from *Aspergillus niger* (Affymetrix) was purchased in stabilized aqueous solution. Laccase of *Phoma* sp. *UHH 5-1-03* (PSL) was produced by fermentation according to Junghanns et al. (2008) with minor modifications (i.e. using 2,6-xylinine 0.8 mM as inducer). The culture broth was harvested by successive filtration steps. The downstream process started with 0.5 mm nylon sieve filtration for raw biomass elimination, followed by the addition of detergent (Brij 35) and the stepwise filtration using a rotating ceramic filtration systems (Novoflow AG, Germany) with 0.2 and 0.01 μm cut-off. In a final step the

obtained retentate was precipitated with acetone, dissolved in PB (pH 8) and stored at 4 °C until used for further experiments.

4.2.2. Colorimetric enzymatic activity assays

Enzymatic activities were determined by measuring absorbance changes of standard substrates or the products formed over time. Measurements were conducted in 96-well plates by applying 50 µL of enzyme containing solution to 150 µL of solution containing substrate and in some cases additional compounds necessary for the corresponding enzymatic reaction. Color changes were monitored by measuring the absorbance for 420 s at 6 s intervals. Table 4.1 summarizes the contents of the reaction solutions for each enzyme and also contains information on the measured wavelength, and the molar adsorption coefficient used for calculation of enzymatic activity. The corresponding enzymatic units were defined as the amount of enzyme transforming 1 µmol of substrate per min. Units (U) were calculated using Eq.1.

$$\frac{U}{L} = \frac{\Delta E \times V_t}{\varepsilon \times d \times V_s} \text{ (Eq.1)}$$

with ΔE being the change in extinction of light [min^{-1}], ε being the molar absorption coefficient [M^{-1} cm^{-1}], d being the layer thickness [cm], V_t being the total volume [L], and V_s being the sample volume of enzyme containing solution [L].

Table 4.1 Composition of reaction solutions of the different enzymatic assays used for determination of enzymatic activities

Enzyme	Buffer	pH	Substrate	Additional compounds	Wavelength [nm]	Molar absorption coefficient [M^{-1} cm^{-1}]
Laccase	MPC 100 mM	3	0.2 mM ABTS	-	420	30,800[a]
Peroxidases	Acetate 100 mM	4	0.2 mM ABTS	50 µM H_2O_2	412	32,400[b]
High redox potential peroxidases	MPC 100 mM	3	2.0 mM veratryl alcohol	400 µM H_2O_2	310	9,300[c]
High redox potential peroxidases	MPC 100 mM	3	32 µM azure B	100 µM H_2O_2	651	39,600
Manganese peroxidase	Malonate 50 mM	4.5	0.2 mM ABTS	100 µM H_2O_2 200 µM MnSO4	420	36,000[d]
Glucose oxidase	Acetate 100 mM	4	0.2 mM ABTS	0.33 M β-D-glucose 1,250 U L^{-1} HRP	412	32,400[b]
Catalase	PB 100 mM	7	10.3 mM H_2O_2	-	240	42.58

Molar extinction coefficients were obtained from; a) Zimmermann et al. (2011), b) Shindler et al. (1976); c) Tien and Kirk (1988) d) Hofrichter et al. (1998). Molar extinction coefficient for azure B and H_2O_2 was determined under assay conditions.

4.2.3. Various assays

Analytical isoelectric focusing was carried out using a Model 111 Mini IEF Cell (Bio-Rad) according to the instruction manual. Amersham calibration kits (low range (pH 3–10) and high range (pH 5–10.5)) for pI determinations (GE Healthcare) were used as pI marker proteins. Bio-Lyte ampholyte (3/10, 40 %) was used as carrier ampholyte for the pH gradient, and gels were stained with Coomassie brilliant blue R-250. The total protein content of enzyme working solutions was quantified by the bicinchoninic acid assay (Smith et al. 1985). Bicinchoninic acid protein assay kits (Pierce®, Thermo Scientific, Germany) were used, and assays were conducted according to the instruction manual.

4.2.4. Enzyme content quantitation

Sodium dodecyl sulfate-polyacrylamide gel electrophoresis (SDS-PAGE) was carried out according to a standard protocol (Laemmli 1970). The gels were stained with SYPRO Orange gel stain (Sigma) according to the procedure instructions of the provider. Precision Plus Protein Standards (Bio-Rad) were used as molecular markers. The calibration curve for laccase protein amount determination was obtained by applying bovine serum albumin (BSA) standards. The bands of the corresponding enzymes were selected by identifying the bands which had a molecular weight closest to the molecular weight reported in the literature. The LabImage 1D software (Kabelan, Germany) was used for the calculation of the amount of enzyme protein

4.2.5. Oxygen consumption rate measurements

For the characterization of oxygen consuming enzymes like laccases or oxidases a high throughput assay was developed for the determination of oxygen consumption rates (OCRs). For comparison OCRs of enzymes were also determined using a Clark like electrode.

4.2.5.1. Determination of oxygen consumption rates using Clark electrode

OCRs were determined using a Clark electrode (Oxytherm System, Hansatech Instruments Ltd., England) at 22 °C under atmospheric air saturation conditions (0.28 mM O_2). Eight hundred µL of Britton–Robinson buffer (pH 2–10) with 10 µL of enzyme solution/particle suspension were stirred at 30 °C with 50 rpm in a 2 mL reaction chamber. Oxygen consumption was monitored for 5 min until equilibrium was reached. Subsequently, 10 µL of the substrate 2,6-DMP (164 mM in H_2O) was added to provide a concentration of 2 mmol 2,6-DMP L^{-1} in the reaction vessel. The signal was recorded for 5 min. Data were fitted using the Oxygraph plus software provided by the manufacturer.

4.2.5.2. Determination of oxygen consumption rates using fluorimetric measurements

All O_2-detection assays based on fluorimetric measurements were performed using either an XF24-2 (CFA24) or XF96-2 (CFA96) extracellular Flux Analyzer (CFA; Seahorse Bioscience). The fluorimetric

detection of O_2 and H^+ levels via solid state probes immobilized on a sensor cartridge (see the configuration in Figure 5.2) in CFA24 (single spotted fluorophores) and CFA96 (hybrid sensor spot) allows a multiparallel measurement of 24 and 96 samples, respectively. The sensor cartridge lowers to within 200 µm of the well bottom during a measurement cycle, creating a transient micro chamber. This chamber defines the measurement volume (Vc) which is ~7 µL and ~3 µL for CFA24 and CFA96, respectively (Wu et al. 2007). The CFA provides changes in oxygen concentration with respect to Vc (pmol min^{-1} Vc^{-1}) every 12 and 16 s for the CFA24 and CFA96, respectively. Both versions of the CFA are temperature controlled, and all assays were conducted at constant temperatures of 35 °C.

After a measurement cycle, the sensor cartridge rises and the medium is re-oxygenated through mechanical mixing, thus theoretically allowing repeated measurements of O_2 and pH over time. The sensor cartridge is equipped with four reagent delivery chambers per well for injecting compounds into the wells during an assay. OCR, changes in pH, and absolute levels of O_2 and pH can be visualized in the data output. Different tests were carried out in order to evaluate the performance of the CFA and to assess their applicability for enzymatic assays. For each test conducted, the main protocol described in Figure 5.2 has been followed. The limit of detection (LOD) and the limit of quantitation (LOQ) for both CFA systems (24 and 96) were calculated as described before (Kromidas 2011).

4.2.5.2.1. Verification of fluorimetric oxygen consumption rate measurements

4.2.5.2.1.1. Single product formation: 2,6-DMP transformation using RVL

In order to assess the electron transfer rate during single product formation, CFA96 assays using 2,6-DMP and RVL were conducted following the main protocol (Figure 5.2) with some slight modifications. Wells contained 160 µL of 4 mM 2,6-DMP at pH 7. After injection of 20 µL of RVL solution and mixing oxygen, concentrations were measured for 210 s. Subsequently 20 µL of 1 M HCl solution were injected per well in order to stop the transformation reaction. After 10 s of mixing, the plate was removed and the absorbance of each well was measured at 477 nm in order to determine 2,6-DMP transformation using a molar extinction coefficient of 14,800 M^{-1} cm^{-1} (Slomczynski et al. 1995).

4.2.5.2.1.2. Cation radical chain reaction: Diclofenac transformation

With the aim to assess differences between single and multi-substrate reaction CFA96 assays using diclofenac as substrate and various amounts of GTL were conducted following the main protocol (Figure 5.2) with some slight modifications. Wells contained 180 µL of radiolabeled diclofenac (4.5 mM; 733 Bq) dissolved in MPC (pH 7). After injection of 20 µL of GTL solution and mixing, oxygen concentrations were measured for 900 s. Subsequently 20 µL of 1 M NaOH solution were injected per well in order to stop the transformation reaction. After 30 s of mixing, the plate was removed. Contents of wells treated with the same amount of laccase were pooled, and 50 µL of each resulting sample was measured in a liquid scintillation analyzer (LSC) in order to determine total sample radioactivity. Subsequently 300 and 100 µL of each sample were dried with N_2 at 37 °C. The 300 µL samples were

taken in order to quantify diclofenac and diclofenac transformation product recovery. After drying, diclofenac and acetonitrile soluble diclofenac transformation products were extracted with acetonitrile and measured by LSC. Remaining residues were dissolved in H_2O and measured by LSC. The 100 µL-samples were taken for high-performance liquid chromatography (HPLC) analysis. After drying, diclofenac and acetonitrile soluble diclofenac transformation products were extracted with acetonitrile and measured by HPLC. HPLC analyses were carried out using an Agilent Technology HPLC 1200 series coupled to a radioisotope detector, Ramona Star (Raytest, Germany). A Nucleodur C18 Pyramid column (150 mm × 4 mm, 3 µm particle size, Macherey and Nagel) was thermostated at 40 °C, and the flow-rate was set at 0.8 mL min^{-1}. Aliquots of 25 µL were injected in the HPLC. Elution was performed using a water/acetonitrile gradient starting from 55:45 (v/v) to 0.2:99.8 (v/v) in 17 min. All elution solvents were acidified with formic acid to a final concentration of 0.1 %. For analysis of reaction products samples containing 3.9 mM diclofenac (2.6 × 106 dpm mL^{-1}) and 1.2 mg mL^{-1} GTL were incubated for 20 h at 25 °C and pH 7. Controls without laccase or without diclofenac were incubated as well. Samples were lyophilized and afterward dissolved in DMSO. Subsequently they were analyzed by size exclusion chromatography (SEC). For this purpose, an HPLC column cascade consisting of two polargel M columns (300 mm × 7.5 mm, 8 Å Phenomenex, Torrance) and a column guard was used. The eluent DMSO with 0.1 % LiBr was used in isocratic mode. Analysis was performed with a flow rate of 0.6 mL min^{-1} and an oven temperature of 50 °C.

4.2.5.2.2. Assessment of sensor interferences of the extracellular flux analyzers

4.2.5.2.2.1. Formation of colored product: Syringaldazine transformation

In order to evaluate possible interferences of the fluorimetric sensor caused by a colored reaction solution, the CFA96 assays using syringaldazine as substrate and GTL as laccase were conducted as described above with some slight modifications. Wells contained 180 µL of syringaldazine at various concentrations (ranging from 0.03 mM to 0.1 mM) dissolved in 60 % (v/v) ethanol and 40 % (v/v) MPC (pH 5). After injection of 20 µL of GTL solution and mixing, oxygen concentrations were measured for 210 s. Subsequently 20 µL of 1 M NaOH solution was injected per well in order to stop the transformation reaction. After 10 s of mixing, the plate was removed and the absorbance of each well was measured at 525 nm in order to determine syringaldazine transformation.

4.2.5.2.2.2. Direct sensor oxidation: Hydrogen peroxide reduction

CFA24 assays using H_2O_2 and HRP were conducted as described above. Wells contained 200 µL reaction mixtures consisting of 0.07 mM H_2O_2 and 1.3 mM ABTS in acetate buffer (pH 4.4) or pure water.

4.2.5.2.3. Data treatment of the results from the extracellular flux analyzers

CFA OCR raw data was transformed using the “Level(Direct)Akos” algorithm that is a component of the Seahorse CFA software package and has been fully described before (Gerencer et al. 2009). The

algorithm accounts for the O_2 flow into the measurement volume through the atmosphere and the walls of the microplate (Gerencer et al. 2009).

The statistical criteria for the reproducibility of the CFA assay was assessed by testing the data set on its normal distribution (Shapiro-Wilk normality test, chosen significance level $p<0.1$) and equal variances (Bartlett test of homogeneity of variances, chosen significance level $p<0.1$). Parametric data were evaluated using analysis of variances (chosen significance level $p<0.1$) and Tukey's honestly significant test (standard significance level $p<0.05$), respectively. For nonparametric data, the one-way analysis of means (not assuming equal variances, chosen significance level $p<0.1$) and one-way analysis of variance by ranks (Kruskal−Wallis, chosen significance level $p<0.1$) was chosen. Outlier exclusion was performed using the Chi-squared test for outliers.

4.2.5.2.4. Oxygen consumption rate measurements in the presence of lignin

For the characterization of oxygen consuming enzymes, i.e., different laccases in the presence of lignin the assay described under 4.2.5 using the CFA96 was used. Experiments were conducted in PB pH 5 using 50 or 250 U g^{-1} lignin. Furthermore, CFA 96 experiments with varying lignin concentrations from 0.4 to 3 g lignin µmol^{-1} laccase, i.e., 0.13 to 1.00 g lignin L^{-1} were conducted using GTL and OL.

4.3. Enzyme immobilization

4.3.1. Particle characterization

4.3.1.1. Rheological measurements

Rheological responses of particle suspensions of different particle densities and with different surface modifications were determined using a plate-and-plate geometry (plate diameter 40 mm and plate-to-plate gap 0.15 mm) on a Bohlin Gemini advanced rheometer (Malvern Instruments, UK). The particle suspensions were directly applied to the plate and experiments were conducted at a constant temperature of 40 °C. The data was fitted with the Ostwald–de Waele relationship (Ostwald 1925):

$$\tau = K\left(\frac{\partial u}{\partial y}\right)^n \quad \text{(Eq. 2)}$$

with τ being the dynamic viscosity, K the flow consistency index, i.e., the dynamic viscosity at a shear rate of 1 s^{-1}, $\partial u/\partial y$ the shear rate or the velocity gradient perpendicular to the plane of shear in s^{-1}, and n the flow behavior index.

4.3.1.2. Evaluation of surface functionalization

The efficiency of aminopropylation was determined following a ninhydrin assay described before (Sun et al. 2006). Briefly, a solution was prepared by dissolving ninhydrin in DMSO at a concentration of 172 mM under a stream of nitrogen gas. Next, 25 mL of sodium acetate buffer (4 M, pH 6.0) were added to 75 mL of ninhydrin containing DMSO solution. The resulting mixture was aerated with nitrogen gas

for 10 min. Next, 1 mL of particle containing solution was added to 1 mL of ninhydrin solution and incubated at 100 °C for 15 min. Subsequently, the reaction mixture was cooled in an ice-bath to room temperature before 5 mL of a 50 % (v/v) ethanol solution was added. After thorough mixing for 15 s the absorbance was measured at 570 nm.

Changes of the surface charge due to functionalization of the particles were determined by means of zeta potential measurement by electrophoretic mobility measurements on particle suspensions in pure water using a Zetasizer nano-ZS (Malvern Insturments UK). The pH of the suspension was adjusted to pH 7 prior to measurement using 0.01 M HCl. Additionally, mass increases of the particles after aminopropylation and after immobilization of the enzymes were measured by means of thermo gravimetrical analysis (TGA) using a Thermobalance (Mettler TC 15 TA controller equipped with a Mettler TG 50). An aliquot of 10 mg lyophilized particles were heated from 50 to 700 °C at a heating rate of 10 °C min^{-1} under aerobic environment.

Fourier transform infrared spectroscopy (FTIR) measurements of dried MPs and MPs modified with APTES were performed using a BioRad FTS 3000MX Excalibur spectrometer equipped with a Golden Gate™ Diamond ATR Top-plate. Direct transmittance was measured at a resolution of 8 cm^{-1} from 600 to 4000 cm^{-1}, and 32 scans were taken per sample.

4.3.1.3. Scanning electron microscopy studies

10 µL of particle suspensions were spread on freshly cleaved mica surfaces and dried. Subsequently, sputter coating of particles with Au-Pd was performed before scanning electron microscopy (SEM) studies were conducted using a Supra 40 V system (Carl Zeiss, Switzerland) with accelerating voltages of 15 and 20 kV.

4.3.1.4. Transmission electron microscopy

Particle size and morphology of MPs and MP-laccase conjugates were evaluated using transmission electron microscopy (TEM; 80 kV; FEI Morgagni 179 268D). The samples were dispersed in water and drop casted onto carbon-coated copper grid and allowed to dry completely at room temperature. The size distribution was determined by measuring the diameter of at least 300 particles using ImageJ software (version 1.48v).

4.3.1.5. Magnetization measurements

The magnetic properties of the MPs, MPs after surface modification with APTES, and MP-laccase conjugates were studied with a Princeton Measurement Corporation vibrating sample magnetometer (MicroMagVSM, model 3900). Magnetization curves were measured at room temperature using a varying sample interval between 398 A m^{-1} in low fields to 7958 A m^{-1} in high fields, and an averaging time of 100 ms. The magnetization was normalized with sample mass.

4.3.2. Enzyme immobilization on fsNP

4.3.2.1. Optimization of consumable consumption

Optimization started on the basis of fsNP–laccase conjugates preparation by means of a sorption assisted immobilization method previously described (Zimmermann et al. 2011). Thereby, the influence of different parameters, i.e., amount of laccase, APTES, and glutaraldehyde were tested to optimize the immobilization procedure in terms of minimizing the applied resources (Table 4.2).

Table 4.2 Amounts of laccase, APTES and glutaraldehyde used for production of fsNP-laccase conjugates (adapted from Hommes et al. 2012)

Laccase	Applied laccase [U mg^{-1} fsNP]	APTES [µmol mg^{-1} fsNP]	Glutaraldehyde [µmol mg^{-1} fsNP]
PSL	4	0	0
	4	0, 0.08, 4	10
	4	0.8	0.1, 1, 10
CPL	4	0	0
	4	0, 0.08, 4	10
	4	0.8	0.1, 1, 10
GTL	0.5, 1.0, 2, 3, 4	0.8	1
	4	0	0
	4	0, 0.08, 4	10
	4	0.8	0.1, 10

4.3.2.2. Resulting method after optimization of consumable consumption

Coating of the fsNP with APTES was performed by incubation with 0.8 mmol APTES per gram fsNP for 20 h in PB buffer at pH 7.5 under stirring at room temperature. Subsequently, the fsNP-APTES conjugates were washed several times with PB buffer in order to remove excess APTES. Afterwards the conjugates were usually suspended in PB buffer at pH 7.5 except for the immobilization of HRP where conjugates were suspended in 0.1 M carbonate-bicarbonate buffer at pH 9.5. In a second step 0.07 g protein per gram fsNP of the enzymes were added to the fsNP-APTES conjugates. Next, the suspensions were stirred for 2 h at 4 °C. Afterwards 1.0 mmol glutaraldehyde per gram fsNP was added dropwise and the suspensions were stirred for an additional 20 h at 4 °C. Finally, fsNP-enzyme conjugates were washed repeatedly with PB buffer in order to remove excess enzymes and glutaraldehyde.

4.3.2.3. Immobilization of multiple enzymes on the same carrier

Co-immobilization of two and simultaneous immobilization of up to five enzymes was conducted in similar fashion as described under 4.3.2.2. Enzymes to be immobilized were applied simultaneously and it was assured that the total protein amount used corresponded to the optimal protein load.

In order to prove the suitability of the applied method for immobilization of multiple enzymes on the same carrier, control experiments were conducted in some cases, immobilizing the respective enzymes separately. For each enzyme, the protein amount applied for the production of single enzyme-fsNP conjugate was equal to the protein amount of the corresponding enzyme applied for co-immobilization. In case of the simultaneous immobilization of five enzymes, four separate control experiments were

conducted. The number of laccases to be immobilized was increased in each experiment from one to four. For each enzyme, the protein amount applied in control experiments was equal to the protein amount of the corresponding enzyme applied for the simultaneous immobilization of five enzymes.

4.3.2.4. Enzyme immobilization at kilogram-scale

Immobilization at kilogram-scale was carried out according to the principle described under 4.3.2.2. A suspension of 100 g fsNP L^{-1} was prepared using PB at pH 7. The suspension was homogenized with a magnetic stirrer (RCT basic IKAMAG® or RET basic IKAMAG®, IKA®, Germany) at 700 rpm and 0.8 mmol APTES g^{-1} fsNP was added during stirring. The thixotropic sample was shaken until it became liquid and placed on an overhead shaker (Reax 2, Heidolph, Germany) for 24 h at 20 °C. The excess APTES was washed away by two successive centrifugation/resuspension steps [2,900×g for 15 min on a MSE Mistral 3000E centrifuge (MSE, England)]. 0.07 g protein g^{-1} fsNP was added before the suspension was placed on an overhead shaker and treated for 2 h at 4 °C. Afterwards, the suspension was stirred at 1,200 rpm and 1.0 mmol glutaraldehyde g^{-1} fsNP was added dropwise. The suspension was again treated on an overhead shaker for 24 h at 4 °C. Subsequently, the excess enzymes and glutaraldehyde were washed away by two centrifugation resuspension steps at 2,900×g for 15 min.

4.3.3. Enzyme immobilization on MP

4.3.3.1. Particle synthesis

MPs were synthesized by co-precipitation of $FeCl_2$ and $FeCl_3$. Prior to particle synthesis, all solutions used were purged with N_2 in order to remove oxygen. An aqueous solution of $FeCl_2$ (1 M), $FeCl_3$ (2 M), and $NaNO_3$ (1 M) was prepared. Subsequently, 0.48 mL of 2 M NaOH solution was added in one batch per milliliter of iron-containing solution. After shaking the solution for 5 min, the particles were separated magnetically from the supernatant and suspended in pure water repeatedly until pH 7 was reached.

4.3.3.2. Immobilization procedure

Coating of MPs with APTES was performed by incubating different amounts of APTES with 12.25 g L^{-1} MP suspended in 0.1 M phosphate buffer (PB) at pH 7.5 at 80 °C for 20 h on an incubation shaker (IKA KS 4000 ic, HuberLab, Switzerland) shaking at 250 rpm. After, surface modification particles were washed twice with PB at pH 5 prior to the addition of 114 mg TVL protein g^{-1} MP, and the mixture was shaken for 2 h at 4 °C. Subsequently, 2 mmol g^{-1} MP glutaraldehyde were added to the particles and they were shaken for an additional 20 h at 4 °C. Finally, particles were washed seven times with PB (pH 7.5).

4.3.3.3. Stability tests

Stability tests were conducted by shaking 1 g L^{-1} conjugate of TVL and MP (TVL-MP) at 250 rpm on a compact shaker (KS 15 A, Edmund Bühler GmbH, Germany) at room temperature. Organic solvents

were applied at 30 % (v/v) in PB at pH 7. H_2O_2 and NaN_3 were applied at 1 mM and 100 µM, respectively in PB at pH 7. Enzymatic activities were measured at different time points.

4.3.3.4. Optimization of reaction times, pH, enzyme, and cross-linker amount

4.3.3.4.1. Optimization regarding specific activity

Enzymes were immobilized on MP following the principle steps described in paragraph 4.3.3.2 using 18 mmol APTES g^{-1} MP. Response surface methodology (RSM) was used to optimize the immobilization procedure in terms of highest specific enzymatic activity. Specific enzymatic activity was defined as enzymatic activity per particle weight. The influence of five factors, i.e., protein amount, glutaraldehyde amount, time for enzyme adsorption, time for incubation with glutaraldehyde, and pH was investigated. A third-degree polynomial model was fitted to the results using Design Expert 8.0.7.1 software. The model was subsequently reduced to only contain significant factors ($p \leq 0.05$) and factors necessary to maintain model hierarchy using the step-wise automatic model regression of the software. Confirmation experiments were conducted at predicted optimal conditions, i.e., conditions predicted to yield highest specific enzymatic activities. More detailed information on the experimental design, conducted experiments, and the resulting model are shown in the appendix A1.1 (Table A. 1, Table A. 2, and Table A. 3).

Protein contents of washing solutions of certain selected samples were determined. All washing solutions of one experiment were combined. Proteins of washing solutions were precipitated on ice in −20 °C cold 80 % acetone for 3 h. After precipitation samples were centrifuged (5,000×*g*, 15 min) and supernatants removed. Subsequently, proteins were dissolved in pure water and measured by the bicinchoninic acid assay.

4.3.3.4.2. Optimization regarding stability

Stability experiments were conducted at eight different conditions. The influence of pH on biocatalyst stability was evaluated at pH 3, 5, 7, and 9, the effect of two organic solvents, i.e., MeOH and acetone was tested, and the impact of H_2O_2 and the laccase inhibitor NaN_3 on the residual activity was assessed. Residual activity (defined as the percentage of the initial enzymatic activity remaining) of the biocatalysts was determined at three different time points, i.e., 1, 7, and 14 d for every condition.

A second-degree polynomial model was fitted to the results of each time point for every tested condition using Design Expert 8.0.7.1 software. The influence of five factors on the residual enzymatic stability was evaluated, i.e., protein amount, glutaraldehyde amount, protein adsorption time, glutaraldehyde reaction time, and pH used during enzyme immobilization. Transformation of the results was conducted prior to fitting whenever recommended by the software. The models were subsequently reduced to only contain significant factors ($p \leq 0.05$) and factors necessary to maintain model hierarchy using the step-wise automatic model regression of the software.

The three models obtained (one for each tested time point) for every tested condition, i.e., for every pH value, every solvent, NaN_3, and H_2O_2 were compared based on the model F values of the analysis of variance (ANOVA). The model F value compares the model variance with the residual (error) variance and is calculated by dividing the model mean square by the residual mean square. Consequently, a higher model F value indicates that more of the observed variability of the response can be explained by the investigated factors. Therefore, for every condition tested, the model with the highest F value was selected to evaluate the influence of the different factors on the biocatalyst stability for the corresponding condition. Conducted experiments and selected models are shown in the appendix A1.2 (Table A. 4-Table A. 12, and Table A. 14).

To determine the formulation predicted to yield particles with best properties regarding stability in all tested conditions, a multiple response method was used (Myers et al. 2009). Briefly, an objective function, i.e., the desirability function (D) was devised (Eq. 3).

$$D = \left(\prod_{i=1}^{n} d_i \right)^{\frac{1}{n}} \quad \text{(Eq. 3)}$$

In this function, d_i are the desirability ranges for each response and n is the number of responses. The desirable ranges go from zero to one for the least to the most desirable outcome, respectively. In case of the stability experiments, least and most desirable outcome has been defined as 0 and 100 % residual activity, respectively. In the present case, eight desirability ranges (one for every tested condition) were included in the desirability function. The respective time point to consider for every tested condition was based on the model selection described above.

To find the optimal formulation regarding biocatalyst stability a second-degree polynomial model was fitted to the obtained D values and subsequently reduced to only contain significant factors ($p \leq 0.05$) and factors necessary to maintain model hierarchy using the step-wise automatic model regression of the software. The resulting model is shown in the appendix A1.2 (Table A. 13 and Table A. 14).

4.3.3.5. Biocatalyst characterization

Kinetic constants towards substrates listed in Table 6.8 were determined by mixing 50 µL laccase containing solution with 150 µL substrate containing solution at various substrate concentrations in 96-well plates. Concentrations of laccase solutions were 1.58 mg L^{-1} except for 2,6-DMP, ABTS, and 3-amino-4-hydroxybenzensulfonic acid. For these three substrates, laccase concentrations were 0.16 mg L^{-1}. Changes in the extinction of light at the corresponding wavelength given in Table 6.8 were measured and enzymatic activities expressed as micromoles of substrate transformed per enzyme molecule per second were calculated using the extinction coefficients given in Table 6.8. Kinetic constants were calculated by means of nonlinear regression assuming Michaelis-Menten kinetics using GraphPad Prism (GraphPad Software, Inc., version 6.05).

4.3.3.6. Dye production

To demonstrate the suitability of the immobilized enzymes for biocatalytic processes, the TVL-MPs were used for the production of a phenoxazinone dye; 0.25 mM of the precursor (3-amino-4-hydroxybenzensulfonic acid) were stirred at 500 rpm in PB at pH 5 in presence of 1 kU L^{-1} TVL-MP for 15 min.

Ten production cycles were conducted successively, and TVL-MPs were separated magnetically after each cycle for 5 min using a nickel plated neodymium magnet (25.4 × 25.4 × 12.7 mm, 1.26-1.29 T, supermagnete, Switzerland). Enzymatic activities in supernatants were measured before and after centrifugation (16,100×*g*, 5 min) to determine how much activity was lost due to ineffective particle separation. Formation of the dye, i.e., 2-amino-3-oxo-3H-phenoxazine-8-sulfonic acid was monitored by measuring the absorbance after each cycle at 420 nm after separation of particles (first magnetically and then by centrifugation as described above). Enzymatic activity remaining in the reaction vessel was determined before each cycle prior to addition of new precursor.

4.4. Lignin

4.4.1. Lignin sources

Organosolv lignin (OL) was provided by Huntsman advanced materials and originated from a mix of hardwood species, i.e. maple, birch, and aspen. Soda lignins obtained after LPS® (see 2.2.3) were provided by GreenValue SA (Switzerland). Soda lignins originated from wheat straw (W-SL), sarkanda (S-SL), and soft wood (SW-SL). A further lignin was also provided by GreenValue SA and obtained from wheat straw after steam-explosion pre-treatment and LPS® (W-SE).

4.4.2. Analytical methods

4.4.2.1. Size exclusion chromatography

Prior to SEC analysis all samples were lyophilized, filtered through 0.45 µm polyvinylidene fluoride (PVDF) filters and subsequently dissolved in DMSO. Size distributions of treated and untreated lignin of the screening experiments described in paragraph 4.4.3 and 4.4.4 were evaluated using an Agilent 1200 HPLC system connected to a diode array detector (DAD, Agilent Technologies, Germany). Chromatographic separation was achieved up to a molecular weight of 700,000 Da with a column cascade (polar gel M pre column, 50 × 7.5 mm, and two polar gel M columns 300 × 7.5 mm 8 Å, Agilent Technologies). DMSO with 0.1 % LiBr (w/w) was used as eluent and the DAD recorded adsorption spectra between 240 and 470 nm. Analysis was performed with a flow rate of 1 mL min^{-1} and an oven temperature of 50 °C.

Size distribution of treated and untreated lignin samples of all other experiments were evaluated using an Agilent 1260 infinity GPC/SEC system connected to a DAD (Agilent Technologies), refractive index (RI) detector (Agilent Technologies), a multi-angle light scattering (MALS, Dawn8^{+}, Wyatt

Technologies, Germany) detector, and a viscosimeter (Visco Star II, Wyatt Technologies). Chromatic separation was achieved using the same column cascade and eluent as described above. Analysis was performed with a flow rate of 0.9 mL min^{-1} and an oven temperature of 50 °C. Poly(methyl methacrylate) analytical standards, (±)-6-hydroxy-2,5,7,8-tetramethylchromane-2-carboxylic acid, and syringaldehyde were used for calibration. Fitting was done by a third order polynomial.

4.4.2.2. Determination of phenolic groups

Phenolic group content of insoluble lignin residues was measured using an assay described previously (Zhou et al. 2013). Briefly, residues were dissolved in 1 mL MeOH. Subsequently, 100 µL of the MeOH lignin solution were mixed with 150 µL Folin Ciocalteau's phenol reagent (2 N) and 1.5 mL nanopure water and stirred for 8 min. Afterwards, 750 µL of nanopure water containing 100 mg Na_2CO_3 was added and solutions were mixed for an additional 2 h before absorbance at 760 nm was measured. Calibration was conducted using vanillin containing samples. Vanillin and lignin free controls were used as reference.

4.4.2.3. Elemental analysis

Elemental analysis of water insoluble residues for the determination of C, H, N, and S contents was performed by combustion-thermal conductivity detection. An accurately weighed amount of test substance (usually between 1 and 2 mg) was placed in a sample capsule and inserted into an elemental analyzer (Eurovector-Hekatech EA 3000 CHNS). The lignin samples were combusted at 1,000-1,200 °C in the presence of oxygen. The total contents of C, H, N, and S were quantitatively converted to CO_2, H_2O, N_2, and SO_2. After separation the gaseous components were quantified by measurement of their thermal conductivity.

4.4.2.4. HPLC-MS analysis of low molecular weight reaction products

Low molecular weight aromatic compounds were identified and quantified using HPLC-MS. Prior to SEC analysis all samples were filtered through 0.45 µm PVDF filters. Samples were analyzed by HPLC using an Agilent 1200 Series system (Agilent Technologies, Germany) and MS using an Agilent 6320 Ion Trap Mass spectrometer with ESI electrospray ionization (Agilent Technologies). The samples were separated on a Zorbax SB C18 column (150 × 3.0 mm; particle size 3.5 µm, Agilent Technologies). The temperature of the column was set to 20 ˚C, the flow rate to 0.8 mL min^{-1} and the injection volume was 10 µl. Separation was achieved with a gradient program, using (A) MeOH : acetonitrile (1:1; v/v) and (B) 0.1 % formic acid. The elution program started with 95 % (B) and was followed by gradient to 55 % (B) in 20 min. The PDA detector for HPLC was set to 280 nm. Calibration curves were measured in the concentration range of 1 to 50 µg mL^{-1}.

To support metabolite identification, HPLC-MS analyses were performed using an Agilent 1200 Series LC system and an Agilent 6320 Ion Trap Mass spectrometer with ESI electrospray ionization (Agilent Technologies). The samples were separated on a Zorbax SB C18 column (150 × 3.0 mm; particle size

3.5 µm, Agilent Technologies). The temperature of the column was set to 20 ˚C, the flow rate to 0.5 mL min^{-1} and the injection volume was 10 µL. Separation was achieved with a gradient program, using (A) MeOH : acetonitrile (1:1; v/v) and (B) 15 mM ammonium formate. The elution program started with 95 % (B) and was followed by gradient to 55 % (B) in 20 min.

ESI operated either in positive or negative mode and scanned the mass range from 50 to 300 u with maximum accumulation time 200 ms. Production scan mode (HPLC–MS/MS) was used in order to monitor the fragmentation pattern. Target metabolite was isolated and fragmented either in positive or negative mode with amplitude 0.7. Product ion mass spectra and retention times were compared to respective standards. Instrumental parameters were as follows: Capillary spray voltage ±2233 V, nebulizer 60 psi, drying gas 12 L min^{-1}, drying temperature 340 ˚C.

4.4.2.5. Fourier transform infrared spectroscopy analysis

FTIR measurements of dried lignin samples were performed on a BioRad FTS 3000MX Excalibur spectrometer equipped with a Golden Gate™ Diamond ATR Top-plate. Direct transmittance as well as absorbance was measured. All the spectra were measured at a resolution of 4 cm^{-1} from 400 cm^{-1} to 4000 cm^{-1} and 32 scans were taken per sample. Spectra were normalized setting the peak typical for lignin at 1512 cm^{-1} (Pandey and Pitman 2003) to 1. Data was baseline corrected and normalized at 1510 cm^{-1} as suggested by Lin and Dence (1992). Peak height and areas were calculated as described by Pandey and Pitman (2003).

4.4.2.6. GC-MS measurements

Injections (1 µL) of samples into the GC-MS system (Agilent 7890A GC, 5975C MSD) were done using a temperature programmable vaporizer, using the following temperature program: 100 °C, held for 0.1 min, heated with 600 °C min^{-1} to 300 °C and held for 1.5 min. The GC system was equipped with a DB-5ms column (30 m × 250 µm × 0.25 µm). The carrier gas was He (flow of 1 mL min^{-1}). The temperature program was as follows: 65 °C for 1 min, followed by heating by 4 °C min^{-1} to 180 °C, then heating by 10 °C min^{-1} to 250 °C, and finally heating by 15 °C min^{-1} to 320 °C the final temperature was kept for 5 min. The mass spectrometer was operated in electron ionization mode; spectra were recorded in the range of 50–1,000 Da. Compounds were identified using the National Institute of Standards and Technology (NIST) library.

4.4.3. Experiments in organic solvent-buffer mixtures with oxidative enzymes

4.4.3.1. Screening of organic solvents and enzymes

A D-optimal design was compiled in order to test the influence of five categoric factors, i.e., solvent, LiP, HRP, MnP, and laccase (shown in Table A. 18). The organic solvents tested were DMSO, 2-propanol, 2-methoxyethanol, and MeOH. They were applied at a concentration of 30 % (v/v) in MPC at pH 5. In experiments where MnP was used, reaction mixtures additionally contained 1 mmol oxalate and 3 µmol $MnSO_4$. Readjustment of pH to 5 was done after oxalate addition.

Enzymatic treatment of OL was conducted as follows. OL was suspended at a concentration of 0.5 g L^{-1} in 10 mL of the respective solvent. A multi-channel tubing pump (ISMATEC, IP 16) was used to deliver two separate solutions to the reaction solution. One solution contained the respective enzyme mixture in MPC buffer at pH 5. The other solution contained 2.4 mM H_2O_2 in 60 % (v/v) of the respective organic solvent and 40 % (v/v) MPC buffer at pH 5. Reaction mixtures were stirred at room temperature and the two solutions were added at 0.54 mL h^{-1}. After 20 h 1 mL samples were taken from the reaction mixture and measured by SEC.

4.4.3.2. Optimization of enzymatic activities and pH in DMSO-buffer mixtures

The most promising enzyme and solvent combinations for treatment of OL were optimized with regard to applied enzymatic activities and pH. The different setups run are shown in Table A. 19. In order to increase throughput, experiments were conducted with an infinite® 200 pro plate reader (Tecan group Ltd., Switzerland) using 24-well plates. The reader was equipped with an injector module and a syringe pump (XE-1000, Tecan group Ltd, Switzerland) allowing to inject solutions into the wells during experiments.

Prior to insertion of the plate into the plate reader, wells were filled with 300 µL DMSO containing 263 µg OL and 700 µL of MPC buffer of the respective pH containing the respective mixture of enzymes. Subsequently, 220 cycles were run each lasting 5 min and 30 s amounting to a total duration of the experiment of 20 h and 10 min. In each cycle the following tasks were performed by the plate reader. First the plate was shaken for 10 s, next 5 µL of a solution containing 1.7 mM H_2O_2, 30 % (v/v) DMSO, and 70 % (v/v) pure water was injected in each well and finally the plate was shaken for an additional 20 s. After the experiment 1 mL samples were taken from each well and measured by SEC.

4.4.3.3. Determination of reaction products after treatment in DMSO

For the determination of low molecular weight reaction products 40 mg OL was suspended in 45 mL DMSO and 105 mL PB at pH 5.62 applying 900 U TVL. Samples were stirred with magnetic stirrers at 300 rpm. A multi-channel tubing pump (ISMATEC, ISM444B) was used to deliver a solution containing 1.7 mM H_2O_2 in 30 % (v/v) and 70 % (v/v) phosphate buffer at a rate of 8.25 mL h^{-1}. Reaction was stopped after 20 h by the addition of 1.40 g ascorbic acid and 60 g NaCl. 20 µL of a 7.6 mM solution of 2,6-dimethylphenol-D9 was added as internal standard. Afterwards, reaction mixtures were centrifuged (20,000×*g*, 20 min), the supernatant was taken to extract reaction products using successively 70, 50, and 50 mL EtAc. The EtAc phases were combined and dried with Na_2SO_4. Subsequently, the EtAc extract was filtered over silanized glass wool and concentrated using a rotary evaporator (Rotavapor EL131, Büchi, Switzerland) at 60 °C and 105 mbar down to 4 mbar. The concentrate was dissolved in 200 µL acetonitrile/EtAc (50/50) (v/v) and derivatized with 15 µL N,O-bis(trimethylsilyl)trifluoroacetamide (BSTFA) and 5 µL pyridine for 30 min at 70 °C. The derivatized samples were subsequently analyzed by GC-MS.

The pellets were washed several times with pure water in order to remove all water soluble components and freeze dried afterwards. The dried pellet was weighed and used for determination of the phenolic group content of the insoluble residues as described under 4.4.2.2. Elemental analysis of water insoluble residues for the determination of C, H, N, and S contents was performed by combustion-thermal conductivity detection as described under 4.4.2.3.

4.4.3.4. Long term experiment

The production of low molecular weight compounds was monitored during OL treatment with TVL in 30 % (v/v) MeOH over 15 d. OL was dissolved in MeOH prior to the addition of buffer, enzymes, and other substances for 1 h. 9.9 mg OL was suspended in 23.1 mL PB at pH 5.62 and 9.9 mL MeOH applying 59.1 U TVL. Samples were stirred with magnetic stirrers at 300 rpm. After 5 and 13 d 36.6 U TVL were added additionally. Samples were taken at different time points and analyzed by HPLC-MS. Furthermore, enzymatic activities were determined.

4.4.3.5. Treatment using an antioxidant

OL was treated in the presence of an antioxidant, i.e., (±)-6-hydroxy-2,5,7,8-tetramethylchromane-2-carboxylic acid (Trolox). Experiments were conducted with 0.3 g L^{-1} OL with 2 kU L^{-1} TVL in 30 % (v/v) MeOH mixed with 70 % (v/v) PB at pH 5.62. OL was dissolved in MeOH prior to the addition of buffer, enzymes, and other substances for 1 h. Samples were stirred with magnetic stirrers at 300 rpm. Different samples were taken at various time-points of the treatments. 2.5 mL samples were taken for further HPLC analysis. These samples were acidified with 100 µL 1 M HCl to stop the enzymatic reaction and to precipitate high-molecular weight lignin. After waiting two h for precipitates to form the samples were analyzed by HPLC. Additionally, 1 mL samples were taken for subsequent SEC analysis. Furthermore, 10 mL samples were taken for the further analysis of water insoluble lignin residues. Samples were acidified with 400 µL HCl and after waiting two h for precipitates to form they were washed extensively with water. Subsequently, they were weighed prior to SEC analysis.

4.4.3.6. Preliminary experiments using enzymes immobilized on fsNP

Preliminary experiments for OL treatment in 30 % (v/v) DMSO using enzymes immobilized on fsNP (as described in paragraph 4.3.2.2) were conducted as described in paragraph 4.4.3.2. A central composite design was conducted investigating the influence of enzymatic starting activities and pH on the molecular weight distribution of lignin. The different setups run are shown in Table A. 23.

4.4.3.7. Preliminary experiments using enzymes immobilized on MP

OL treatment with 2 kU L^{-1} TVL-MP was conducted in 30 % (v/v) MeOH mixed with 70 % (v/v) PB at pH 5.62 for 20 h. Two OL concentrations, i.e., 3 and 10 g L^{-1} were tested. Treatments were conducted as described in paragraph 4.4.3.5 with a few modifications. Samples were shaken on an incubation shaker (IKA KS 4000 ic, HuberLab, Switzerland) at 150 rpm. Furthermore, TVL-MPs were

magnetically separated from all samples prior to further processing using a neodymium magnet (25.4 x 25.4 x 12.7 mm, 1.26-1.29 T, supermagnete, Switzerland).

4.4.4. Preliminary test with laccase mediator systems

The effect of different laccase mediator systems (LMS) on the molecular weight distribution of OL was evaluated. The mediators were 2,2,6,6-tetramethyl-1-piperidinyloxy (TEMPO), 1-hydroxybenzotriazole (HBT), 4-hydroxybenzoic acid, syringaldehyde, acetosyringone, and *p*-coumaric acid. GTL and GTL immobilized on fsNP were used as biocatalyst.

A D-optimal design was used testing different mediator combinations and laccase activities in batch reactions in acetate buffer at pH 5 lasting 20 h. The design is shown in Table 4.3. Mediator concentrations varied from 0.0 to 15.0 mM and laccase activities varied from 100 to 1,000 U L^{-1}. OL concentration was 4 g L^{-1}. Additional experiments using syringaldehyde, acetosyringone, and *p*-coumaric acid as mediators were conducted. Setups of these experiments are also included in Table 4.3. Furthermore, control experiments without lignin and without enzymes were performed. Samples were freeze dried after treatment and subsequently dissolved in DMSO at a concentration of 1 g L^{-1} for SEC analysis.

Table 4.3 Experimental setups of batch experiments to evaluate the effect of different LMS on the molecular weight distribution of OL. OL concentration was 4 g L^{-1}. Experiments were conducted at pH 5 lasting 20 h.

GTL	**GTL fsNP**	**HBT**	**TEMPO**	**4-Hydroxybenzoic acid**	***p*-coumaric acid**	**Syringaldehyde**	**Acetosyringone**
[U L^{-1}]	**[U L^{-1}]**	**[mM]**	**[mM]**	**[mM]**	**[mM]**	**[mM]**	**[mM]**
955	-	6.2	0.4	8.4	-	-	-
550	-	-	7.5	-	-	-	-
100	-	-	-	-	-	-	-
1,000	-	-	7.3	7.7	-	-	-
685	-	7.5	-	-	-	-	-
1,000	-	-	15	-	-	-	-
100	-	-	-	-	-	-	-
100	-	6.8	8.2	-	-	-	-
1,000	-	7.8	7.2	-	-	-	-
1,000	-	-	-	15	-	-	-
550	-	-	-	-	7.5	-	-
100	-	0.2	-	6.6	8.1	-	-
100	-	7.6	-	-	7.4	-	-
537	-	-	-	2.0	13.0	-	-
1,000	-	-	-	-	-	-	-
100	-	-	-	15.0	-	-	-
280	-	-	-	7.5	-	-	-
955	-	-	-	7.7	7.3	-	-
190	-	6.9	-	8.1	-	-	-
100	-	7.6	-	-	7.4	-	-
100	-	-	5.2	-	5.0	-	-
685	-	7.5	-	-	-	-	-
100	-	-	-	-	15.0	-	-
1,000	-	15.0	-	-	-	-	-
1,000	-	-	-	-	15.0	-	-
1,000	-	2.0	9.4	-	3.6	-	-
1,000	-	-	7.3	7.7	-	-	-
100	-	-	15.0	-	-	-	-
280	-	-	-	7.5	-	-	-
100	-	15.0	-	-	-	-	-
1,000	-	-	-	-	1.0	-	-
1,000	-	-	-	-	10.0	-	-
1,000	-	-	-	-	-	1.0	-
1,000	-	-	-	-	-	10.0	-
1,000	-	-	-	-	-	-	1.0
1,000	-	-	-	-	-	-	10.0
-	1,000	-	-	-	1.0	-	-
-	1,000	-	-	-	10.0	-	-
-	1,000	-	-	-	-	1.0	-
-	1,000	-	-	-	-	10.0	-
-	1,000	-	-	-	-	-	1.0
-	1,000	-	-	-	-	-	10.0

4.4.5. Sequential lignin treatment: combining laccase mediator systems with formic acid induced depolymerization

4.4.5.1. General treatment procedure

The general procedure for lignin treatment and analysis is depicted in Figure 7.17. Lignin was treated at a concentration of 3.0 g L^{-1} in 0.1 M phosphate buffer (PB) by means of TVL magnetic particle conjugates (TVL-MP) and in presence of 30 % (v/v) MeOH, HBT, or TEMPO. Various enzymatic activities, mediator concentrations, pH values and treatment durations were applied. Reaction suspensions were shaken at 150 rpm on a compact shaker (KS 15 A, Edmund Bühler GmbH, Germany). After treatment TVL-MPs were separated using a nickel plated neodymium magnet (25.4 x 25.4 x 12.7 mm, 1.26-1.29 T, supermagnete, Switzerland), washed with water three times and then lyophilized. Subsequently, lignin samples were acidified to pH 2 with 1 M HCl. After 2 h in the acidified conditions the insoluble material was separated by centrifugation (15 min, 4,500xg). Thereafter, samples were taken from the supernatant for HPLC and SEC analyses.

Insoluble material obtained after enzymatic treatment was combined with the lignin-containing suspensions obtained from washing of TVL-MP. Subsequently, they were washed with water (pH adjusted to 2 with HCl) before they were lyophilized. After freeze-drying lignin residues were weighed and samples for GPC measurements were taken prior to formic acid/formate treatment. Treatment was performed at a concentration of 7 g L^{-1} in 80 % formic acid in microwave reaction vials (2-5 mL, Biotage, Sweden) under magnetic stirring. Varying amounts of sodium formate were added before samples were sealed, heated to 110 °C under stirring at 1,500 rpm. After treatment samples for HPLC, and GPC were taken before formic acid was evaporated. 1.5 mL aliquots of the residues were extracted with EtAc (three times, 1.5 mL). EtAc extracts were dried and weighed before they were measured on SEC.

4.4.5.2. Optimization of lignin treatment

Lignin was treated sequentially according to the general procedure described above (4.4.5.1). RSM was used in order to study the effect of six influencing factors on the lignin reaction products, i.e., enzymatic activity, HBT concentration, enzymatic treatment time, initial pH of enzymatic treatment, formic acid/formate reaction time, and sodium formate concentration. A IV-optimal design was chosen consisting of 28 model points, 5 experiments to estimate lack of fit, and 3 replicates. The experimental matrix is shown in the appendix (Table A. 26). Subsequently, second-degree polynomial models were fitted to different experimental results, i.e., lignin solubility in aqueous solution at pH 2 after enzymatic treatment, weight average molecular mass (Mw) of insoluble material after enzymatic treatment, Mw of lignin after formic acid/formate treatment, lignin solubility in EtAc after formic acid/formate treatment, Mw of EtAc soluble fraction after formic acid/formate treatment, total yield of identified monomers after formic acid/formate treatment, and total lignin solubility (either in aqueous solution after enzymatic treatment or in EtAc after formic acid/formate treatment). Results were transformed prior to model

fitting whenever recommended by the Design Expert software and resulting models were reduced to only contain significant factors ($p \leq 0.05$) and factors necessary to maintain model hierarchy using the step-wise automatic model regression of the software. All models as well as the corresponding ANOVA are shown in the appendix (Table A. 25-Table A. 33). Optimal conditions regarding total lignin solubility predicted by the associated model were tested and results compared to model predictions of all the different models.

4.4.5.3. Formic acid/formate treatment with carbocation scavenger

OL was subjected only to the formic acid/formate treatment as described in paragraph 4.4.5.1. Treatments were conducted with OL alone and in presence of 0.7 g L^{-1} 2-naphtol.

4.4.5.4. Lignin treatment over several reaction cycles

W-SL was treated following the general procedure described in paragraph 4.4.5.1 over five consecutive reaction cycles. 15 kU TVL-MP were applied initially. Treatments were conducted with 7.38 mM HBT at pH 5 for 48 h. After each cycle separated TVL-MP were reused for treatment of a new batch of W-SL. Between cycles separated TVL-MP were not washed in order to retain as much enzymatic activity as possible. Therefore, some insoluble products were transferred from one cycle to the next. Extensive washing of the particles was only conducted after the last cycle.

5. Development of a high-throughput microplate respiratory assay for the characterization of oxygen consuming enzymes

Among the LME of interest for lignin treatment there are certain enzymes, e.g., laccases and oxidases which consume oxygen during their catalytic cycle (general information on the different enzymes used is listed in Table 5.1). For simplicity and sensitivity reasons, the determination of activity (in vivo or in vitro) of these enzymes is mostly performed by means of photometrical tests using phenolic substrates, whereby the colored oxidation products are monitored (Johannes and Majcherczyk 2000b). In case of oxidases the use of an additional enzyme, i.e. a peroxidase is necessary which uses the produced H_2O_2 for oxidation of the substrate (Sun et al. 2002). These tests are commonly based on the transformation of substrates like guaiacol, 2,6-DMP (Prillinger and Esser 1977), syringaldazine (Harkin and Obst 1973), or ABTS (Childs and Bardsley 1975). For high-throughput characterization of oxygen consuming enzymes a microplate respiratory assay was developed

A model to describe the laccase-catalyzed oxidation of phenol was developed by Kurniawati and Nicell (2009). To generalize the catalytic cycle, this model can be extended as described in Figure 5.1. According to the proposed catalytic cycle of laccase (Figure 5.1, A), the native enzyme (E) is oxidized by oxygen (O_2) to produce an oxidized enzyme species (E^*) that subsequently reacts with molecules of substrate (S) resulting in the production of free radicals ($S^\bullet$) that combine either with other radicals or through cross-coupling with different substances (X) to create products (P). These products might react as new substrates (S_2) that will again undergo the reaction cycle and compete with the original substrate (S_1). Also shown are side reactions including laccase inactivation (E_{inact}).

The occurring reactions in photometrical tests in the case of oxidases are even more complex (Figure 5.1, B). The oxidase (E) is oxidized by oxygen (O_2) to produce an oxidized enzyme species (E*) and H_2O_2. The oxidized enzyme species reacts with a substrate (OS) while H_2O_2 oxidizes a peroxidase (E_2) to an oxidized peroxidase species (E_2^*) that subsequently reacts with molecules of the substrate (S) which subsequently undergo similar reactions as in case of laccase.

Given the possibility of multiple oxidation steps of a substrate, the understanding of the enzymatic reaction requires precise analytical tools. The simple assessment of substrate depletion or the dynamic of product formation does not allow a satisfying determination of the contribution of the oxygen consuming enzyme to substrate transformation. Actually some oxidation reactions can be overlooked if, for instance, the formed products have the ability to act as new substrates ($S_{2, 3, 4}$...) or if the described reaction of $S^\bullet$ to P is a free radical chain reaction.

Table 5.1 Characteristics of the different enzymes (extended and adapted from Ammann et al. 2014 and Hommes et al. 2012)

Enzyme	Specific activity [U mg^{-1} protein]	Molecular weight [kDa][a]	[kDa][b]	Isoelectric point [pH]
Laccases				
Genus *Thielavia*	14.2±0.3	75.6	80	4.2 – 7.6
Coriolopsis polyzona	22.1±1.0	59.8	59	3.9
Cerrena unicolor	6.0±0.1	58.1	57	3.8
Pleurotus ostreatus	7.9±0.1	58.3	59	<3.0
Trametes versicolor	12.5±0.3	61.6	63	<3.0
Phoma sp.	11±3 - 26±4[c]	-	-	-
Peroxidases				
Horseradish peroxidase (from *Amoracia rusticana*)	137.9±1.0	-	44[d]	3.0 - 9.0[d]
Lignin peroxidase	0.9±0.0	-	-	-
Manganese peroxidase (from *Nematoloma frowardii*)	5.9±0.2	-	-	-
Versatile peroxidase (from *Bjerkandera adusta*)	0.5±0.0	-	-	-
DyP	0.88±0.05	-	-	-
Oxidases				
Glucose oxidase (from *Aspergillus niger*)	26.5±1.9-127.0±1.4[e]	-	160	4.2[f]
Additional enzymes				
Catalase (from bovine liver)	1,786.0±21	-	250[d]	5.4[d]

a) Molecular weight (kDa) was determined in triplicates by SDS-PAGE

b) Molecular weight (kDa) as reported in the literature or as given by the supplier (Genus *Thielavia*, Paloheimo et al. 2006; *Coriolopsis polyzona*, Hüner 2007; *Cerrena unicolor*, Michniewicz et al. 2006; *Pleurotus ostreatus*, Morozova et al. 2007; *Trametes versicolor*, Collins et al. 1996; Glucose oxidase, Tsuge et al. 1975).

c) Different batches of *Phoma* sp. were used after processing of the fermentation broth. Specific activities varied between batches.

d) Value given by supplier

e) Different batches of glucose oxidase were used.

f) According to Pazur and Kleppe (1964)

For simplicity and sensitivity reasons, the determination of laccase activity (in vivo or in vitro) is mostly performed by means of photometrical tests using phenolic substrates, whereby the colored oxidation products are monitored (Johannes and Majchercyk 2000b). These tests are commonly based on the transformation of substrates like guaiacol, 2,6-DMP (Prillinger and Esser 1977), syringaldazine (Harkin and Obst 1973), or ABTS (Childs and Bardsley 1975).

However, measuring changes in oxygen concentrations, caused by the laccase catalyzed reduction of oxygen (reaction rate constant k_1, Figure 5.1), enables a direct quantitation of electrons transferred to the substrate. Thus, issues posed by mere product or substrate quantitation are avoided.

In recent years, methodologies have been developed to allow for more efficient and high-throughput measurements of OCR in cell respiration assays. These methods have several drawbacks like sensor drift, electrode fouling, detection limit, and difficulties in sensor positioning (Molter et al. 2009).

Aiming at this approach, the CFAs (i.e., XF24 and XF96 Analyzer, Seahorse Biosciences) were developed to assay cultured cells in a conventional 24- or 96-well microtiter plate format.13 This represented a significant advance in the high-throughput assessment of physiological parameters in cell monolayers compared to conventional investigations using Clark electrode-based methods and cell suspensions.

In this chapter a new method for high-throughput screening of catalysts using oxygen as a substrate with the CFA-24 and -96 is described. The focus is on the development of an enzymatic assay using laccase as model enzyme for the development of protocols that allow for the measurement of enzymatic oxygen consumption with a minimum of biocatalyst per well in a multiwell format. The goal of the proposed approach was to acquire a high quantity of information and minimize the time it takes to collect respiratory data from samples containing oxygen-consuming enzymes.

5.1. Validation of the CFA based enzymatic activity assay

The protocol for the developed assay for the determination of enzymatic activity of oxygen consuming enzymes is shown in Figure 5.2. With the objectives to ensure robust signal, minimal noise, and keeping OCR values within the linear range of response, within the dynamic range of the instrument, and within the signal range of the algorithms employed to calculate respiration rates, the determination of optimal quantities of biocatalysts per well was carried out. Figure 5.2 shows an example of an OCR measurement and the linearity of the OCR response to different concentrations of laccase protein for POL using 2,6-DMP as the substrate at pH 6. The linear range lies between 2 and 6 mg L^{-1} laccase protein ($R^2 = 0.998$). The linear range depends on the pH, substrate, and enzyme. Therefore, a suitable enzyme concentration has to be identified anew whenever one of these parameters is changed in order to obtain a linear range of response. The CFA system consists mainly of two parts, the light detection apparatus and the sensor cartridges. In combination both parts were tested in terms of measurement performance.

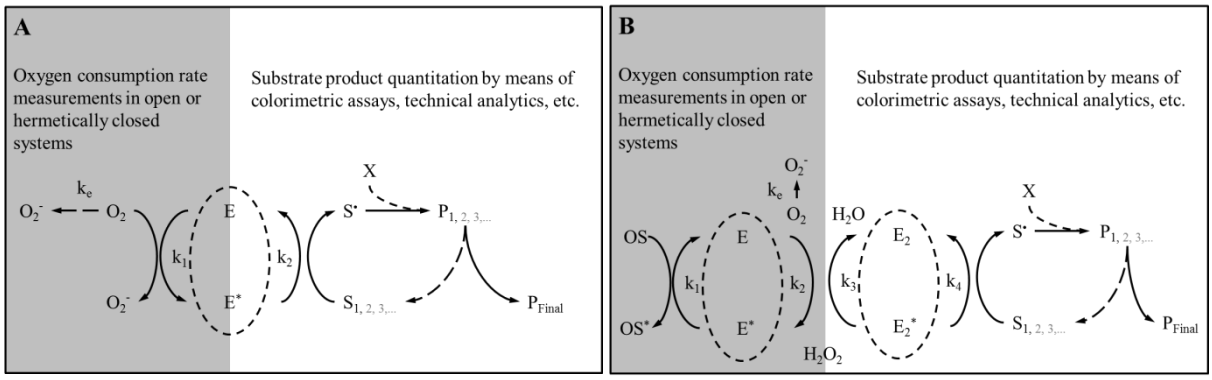

Figure 5.1 A) Catalytic cycle of native laccase (E) oxidized by oxygen (O_2) with formation of an oxidized species (E*) that subsequently reacts with substrate molecules ($S_{1,2,3...}$), leading to free radicals (S•) that create products ($P_{1,2,3,..}$) either by reacting with other free radicals or with different substances (X). Depending on the molecular structure of the substrate, this results in the production of an end product (P_{final}) or a substrate ($S_{1,2,3,..}$) that can subsequently again be converted. k_1 and k_2 (M^{-1} s^{-1}) are the apparent second-order rate constants for the reaction representing the sequence of binding of oxygen and oxidation of the enzyme as a single step (k_1) and the reaction between E^* and substrates ($S_{1,2,3,...}$) (k_2), respectively; k_e (s^{-1}) is the first-order rate constant for the consumption of oxygen by the electrode. The figure was adopted from Kurniawati and Nicell (2009) and extended with possible free radical chain reactions described by Zhang et al. (2002) depending on the type of substrate (adapted from Hommes et al. 2013).

B) Catalytic cycle of oxidase enzyme (E) oxidized by oxygen (O_2) with formation of oxidized species (E^*) and H_2O_2. E^* subsequently reacts with oxidase substrate OS while H_2O_2 oxidizes an additional peroxidase enzyme E_2 that subsequently reacts with substrate molecules ($S_{1,2,3,...}$), leading to free radicals (S•) that create products ($P_{1,2,3,..}$) either by reacting with other free radicals or with different substances (X). Depending on the molecular structure of the substrate, this results in the production of an end product (P_{final}) or a substrate ($S_{1,2,3,..}$) that can subsequently again be converted. k_1 and k_2 (M^{-1} s^{-1}) are the apparent second-order rate constants for the reaction representing the sequence of binding of oxygen and oxidation of the oxidase enzyme as a single step (k_1) and the reaction between E^* and substrates (OS), respectively; k_3 and k_4 (M^{-1} s^{-1}) are the apparent second-order rate constants for the reaction representing the oxidation of the peroxidase enzyme with H_2O_2 as a single step (k_3) and the reaction between E_2* and substrates ($S_{1,2,3,...}$) (k_4), respectively; k_e (s^{-1}) is the first-order rate constant for the consumption of oxygen by the electrode.

5.1.1. Limit of detection and quantitation

One major parameter evaluated for the validation of the CFA based laccase activity assay was the LOD and LOQ, determined by measuring substrate-free (i.e., with enzymes, without substrate) and enzyme-free (i.e., without enzymes, with substrate) control samples simultaneously with every assay (Figure 3A). The CFA24 control measurements reveal larger variations (enzyme-free, −10.7±49.1 pmol min^{-1} Vc^{-1}; substrate-free, 3.6±44.8 pmol min^{-1} Vc^{-1}) compared to the CFA96 system (enzyme-free, 0.3±9.5 pmol min^{-1} Vc^{-1}; substrate-free, 1.1±10.7 pmol min^{-1} Vc^{-1}). Consequently, LOD and LOQ values for the CFA24 (LOD=56.6±15.4 pmol min^{-1} Vc^{-1}, LOQ=150.7±38.6 pmol min^{-1} Vc^{-1}) were higher than for the CFA96 (LOD=26.3±5.5 pmol min^{-1} Vc^{-1}, LOQ=87.6±18.4 pmol min^{-1} Vc^{-1}).

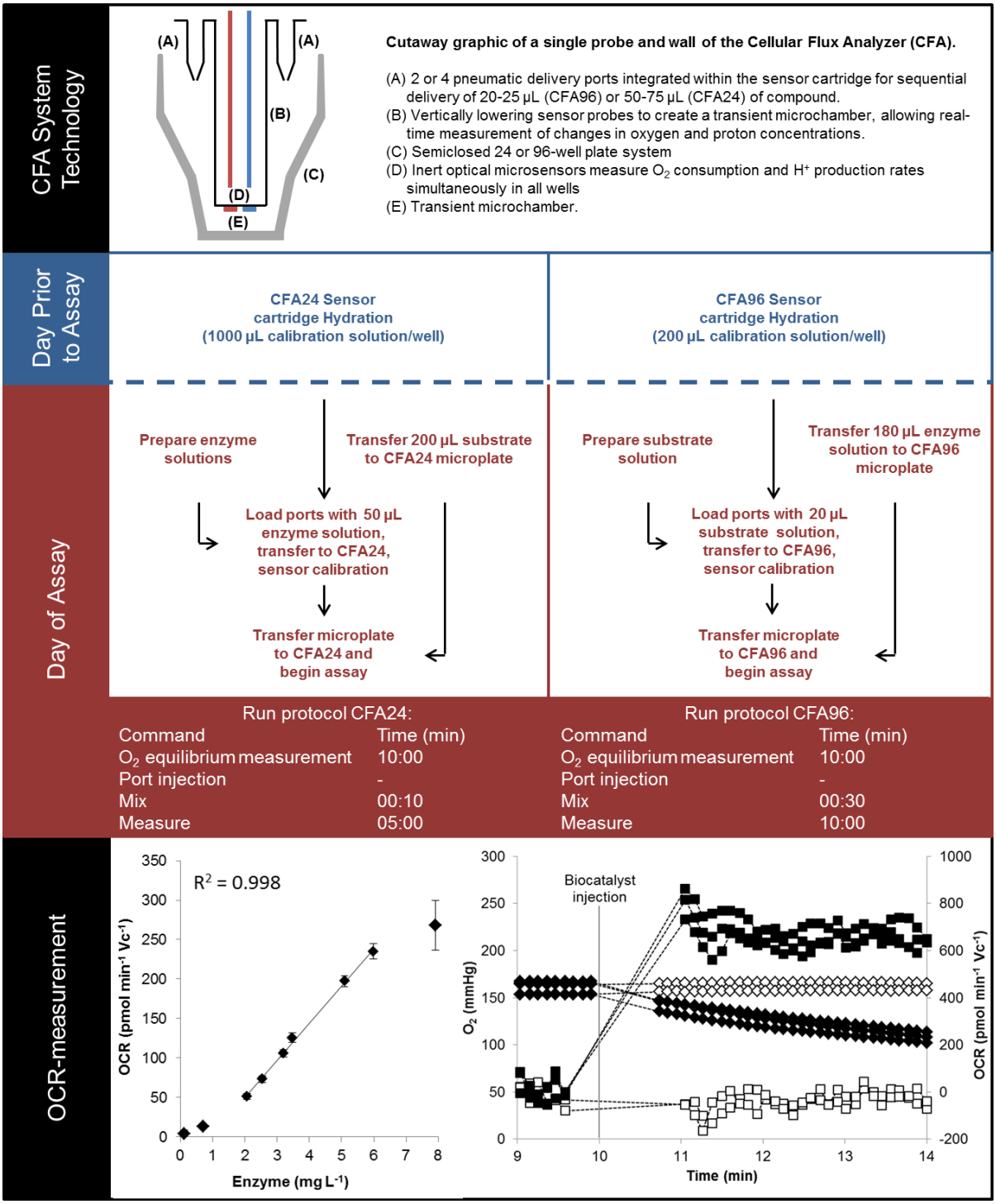

Figure 5.2 Cutaway graphic of a single probe and well of the CFA24 system and a schematic diagram of the novel assay for multi-parallel laccase activity quantitation via OCR measurements using the CFA (CFA24 or 96) including the run protocol. The lower graph (left) shows OCR values for different POL concentrations at pH 6 using 2,6-DMP (2 mM) as the substrate (n=4). The lower graph (right) shows examples of CFA measurements using 2,6-DMP as substrate (2 mM, pH 5, n=3) with POL as the biocatalyst (filled markers) and control measurements (substrate-free and enzyme-free control; empty markers). Data are displayed as change in oxygen tension (mmHg of O_2; diamonds) and as OCR (pmol min^{-1} Vc^{-1}, squares; adapted from Hommes et al. 2013).

5.1.2. Injection efficiency and uniformity

In order to quantify possible losses due to protein sorption in the injection ports of the CFA96, the injection efficiency of both ports (A and D) of the analyzer was tested by injecting GTL. GTL concentrations were quantified after injection through optical density measurements of each well at 330 nm. In total, 83.9±2.8 % and 81.4±3.8 % of laccase were recovered after injection via ports A and D, respectively. These results show that enzymes were injected evenly over the whole plate. However, approximately 17 % of the enzymes were lost during injection most likely due to sorption of the proteins on the plate material in the injection ports. This shows that losses of enzymes due to sorption in the injection ports of the CFA96 can be significant and therefore have to be accounted for, if the experimental setup requires injection of enzyme solutions. Protein sorption is a complex process that is dependent among other factors on the specific protein mixture applied (Nakanishi et al. 2001). Therefore, sorption losses in the injection ports will likely be different for every enzyme solution applied. Testing the enzymatic activity of the substrate free controls after the experiment would be an uncomplicated way to quantitate these losses provided the enzymes are stable over the course of the measurement.

5.1.3. Reproducibility

In order to evaluate the reproducibility of the CFA assay, the pH activity range (pH 3−7) of free laccases of POL (Figure 5.3, B) and GTL (GTL; Figure 5.3, C) using 2,6-DMP as substrate was examined for both systems (CFA24 and CFA96) by running the same assay three times using different cartridges (CFA24, n=3 and CFA96, n=7 for each cartridge and pH value). Regarding the CFA24 assay, both analysis of variances and Tukey's honestly significant test, respectively, showed no significant difference of the OCR measured under the same conditions between the cartridges, with two exceptions. Measured OCRs for GTL at pH 5 and 6 were significantly higher in one cartridge compared to the other two. However, measurements of this cartridge resulted in higher OCR values over the whole investigated pH range (pH 3−7) compared to the other two. This might have been due to a slight variation in the sensor response of the cartridge measuring higher values. Regarding the CFA96 assay, there were two statistically significant differences between OCRs obtained by the different cartridges. OCR at pH 6 using GTL was significantly higher and OCR at pH 3 using POL was significantly lower in one cartridge compared to the other two. Furthermore, the POL data set at pH 7 was not evaluated as the measured OCRs were below the LOD. The difference in OCR values obtained by the two CFA systems (CFA24 and CFA96) (Figure 5.3, B, C) might be explained by a difference in the experimental setup (Figure 5.2). During the CFA96 assay the substrate is injected, while the laccase is dissolved in buffer solution and applied manually to the reaction well. Conducting the CFA24 assay on the other hand, wells were prefilled with substrate solution, while the laccase was dissolved in physiological water (0.9 % NaCl (w/v)) before being injected during the assay. Consequently, the laccase tested in the CFA96 assay was well adapted to ambient pH, whereas the injected laccase might still have been in an adaptation process during the early measurement phase

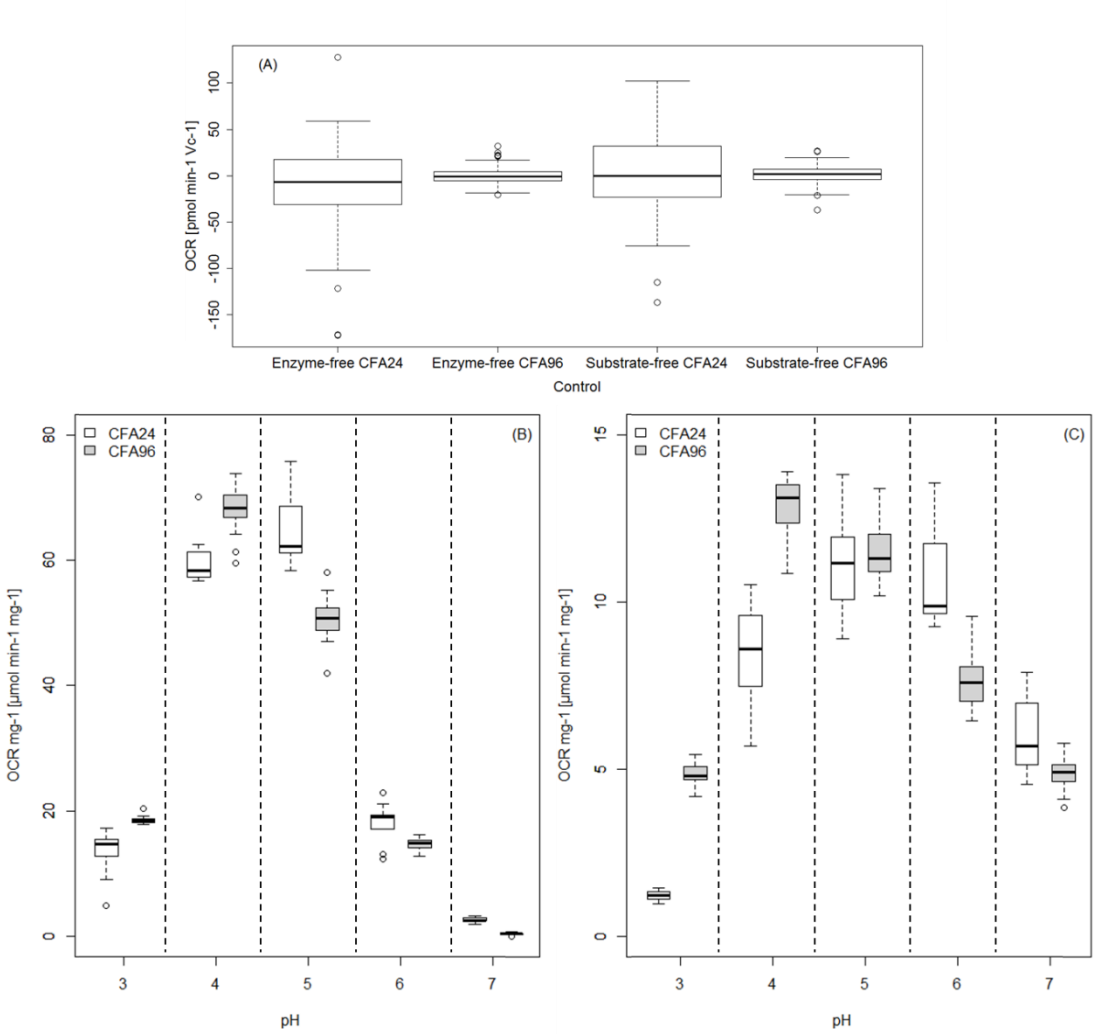

Figure 5.3 CFA assay reproducibility and system quality check: CFA assay control measurements (A); enzyme-free (n=75) and substrate-free (n=75) control measurements regarding the CFA24 system, enzyme-free (n=122) and substrate-free (n=73) control measurements regarding the CFA96 system. Comparison between the CFA24 (n=9) and CFA96 (n=21) system regarding the pH activity range of free laccases of *Pleurotus ostreatus* (POL) (B) and genus *Thielavia* laccase (GTL) (C) using 2,6-DMP as a substrate (2 mM) in MPC buffer in the respective pH (3-7). Each boxplot represents the median value as a line dissecting the box, upper (75 %) and lower (25 %) quartiles at the top and bottom box edges, the non-outlier minimum and maximum values as whiskers outside the box (1.5 x the interquartile range), and outlier values (beyond the whiskers) as open circles (adapted from Hommes et al. 2013).

using the CFA24 assay. This might explain the lower OCRs measured at pH 3 and 4 for POL (Figure 5.3, C) with the CFA24 compared to the CFA96. By closer examination of Figure 5.3B, C it becomes apparent that at each pH (with the exception of pH 5) the CFA measuring a higher OCR for GTL also measures a higher OCR for POL compared to the other CFA. Therefore, the differences might come from distinctions between the two measurement systems using different sensor designs. The CFA24 measures pH and O_2 with two separate sensors per well, while the CFA96 measures pH and O_2 with one hybrid sensor per well. The combination of both sensors causes pH to influence the measured pO_2 signal,

due to pH-dependent polarity of the sensor polymer (Schröder et al. 2007). This necessitates a different treatment of the measured raw data (Schröder et al. 2007). Both aspects, i.e., enzyme adaptation and sensor design might explain the differences between the obtained OCR values from the two systems depending on the pH. Because of the possibility of multi-parallel OCR measurements, vast data sets can be assessed and intensively analyzed by means of statistical models. This enables reliable comparative studies on oxygen consuming enzymes.

5.1.4. Comparison of OCR-measurement devices (Clark-like electrode, CFA24, and CFA96) for laccase activity determination

In a next step, the OCR of laccases obtained by transforming 2,6-DMP (2 mM) using the CFA based laccase assay were compared to the OCR performed with a classical Clark-type electrode under identical conditions (Table 5.2). Both measurement devices produced similar results independently of pH and laccase genera investigated, showing the accuracy of the CFA system.

Table 5.2 Comparison of OCR obtained by the different oxygen measurement systems using the same experimental conditions (Substrate: 2,6-DMP (2 mM); adapted from Hommes et al. 2013)

		OCR [µmol min^{-1} mg^{-1} Laccase]	
Laccase	**pH**	**CFA 24**	**Clark**
Cerrena unicolor	3	6.2±0.6	5.1±0.4
Genus *Thielavia*	4	9.0±1.8	6.1±0.6
Cerrena unicolor	5	24.7±2.9	24.0±2.2
Trametes versicolor	6	14.3±1.4	13.5±0.7

5.2. Correlation of OCR/substrate transformation/product generation

To further validate the accuracy of the CFA system, assays were conducted in order to investigate laccase catalyzed reactions, where products were formed in a defined ratio to the oxygen consumption.

5.2.1. Single product formation: 2,6-DMP transformation using RVL

Transformation of 2,6-DMP with fungal laccases from *Pycnoporus coccineus* has been shown to produce several C−O, C−C dimers and 2,6-DMP oligomers (Wan et al. 2008a). Transformation of 2,6-DMP by RVL (a low redox potential laccase) on the other hand has been reported to transform 2,6-DMP to only one product: 3,3′,5,5′-tetramethoxy-1,1′-biphenyl-4,4′-diol (Wan et al. 2008a, b). Since no consecutive reaction occurs when RVL is used as a biocatalyst, the amount of electrons transferred should be equal to the amount of 2,6-DMP molecules transformed, since the recombination of 2 mol of para-radicals produces 1 mol of 3,3′,5,5′-tetramethoxy-1,1′-biphenyl-4,4′-diol (Wan et al. 2008a). Consequently, a comparison of the transformation rate of 2,6-DMP (calculated based on colorimetric measurements of the formed 2,6-DMP dimers after the experiment) and the electron transfer rate

(calculated based on OCR measurements by the CFA system) allows validation of the suitability of the developed CFA assay. The fact that the obtained electron transfer rates (39.1±7.3 μM min^{-1}; n=13) correspond well to the 2,6- DMP transformation rates (33.5±1.1 μM min^{-1}; n=13) shows that the developed assay is suitable to correlate enzymatic OCR with the rate of product formation (in case of single product formation).

5.2.2. Free radical chain reactions

In order to assess laccase activity during a multi-substrate reaction, transformation of ^{14}C-labeled diclofenac, a nonsteroidal anti-inflammatory drug, by GTL was studied. It is already known that filamentous fungi transform diclofenac into 4′-hydroxy diclofenac and small amounts of 3′-hydroxy and 5-hydroxy diclofenac (Webster et al. 1998). More recent findings are the conversion of diclofenac to 4′-hydroxy diclofenac using *Aae*APO (Kinne et al. 2011) and the production of 4′,5- hydroxyl-diclofenac by the bacterium *Actinoplanes sp*. Degradation of diclofenac was studied recently using *Trametes versicolor* pellets (Marco-Urrea et al. 2010). After 4.5 h, the reaction mixture showed a brown color possibly due to the accumulation of an identified diclofenac metabolite 4-(2,6-dichlorophenylamino)-1,3-benzenedimethanol. Full diclofenac degradation after 24 h was reported, and no metabolites were found after that time indicating that diclofenac was either mineralized or transformed into products that could not be detected (Kunamneni et al. 2007). Since, all samples in these experiments were filtered through 0.22 and 0.45 μm filters before HPLC and NMR analysis, respectively; higher molecular polymerization products could most likely not be detected.

Our results showed additional aspects of laccase-driven diclofenac transformation (Table 5.3). While the presence of GTL leads to diclofenac transformation, electron transfer rates are substantially lower than diclofenac transformation rates, indicating that electron transfer to oxygen by GTL is only partly responsible for diclofenac transformation. Transformation products might react further by free radical chain reactions leading to further diclofenac transformation.

Table 5.3 Comparison of diclofenac transformation determined by LSC and HPLC measurements (n=1) and electron transfer rates determined by CFA measurements at different genus *Thielavia* (GTL) amounts per well (n=8; adapted from Hommes et al. 2013)

GTL per well [μg]	Radioactivity recovered [%]	Diclofenac transformation [%]	Diclofenac transformation rate [μmol min^{-1} mg^{-1} GTL]	Electron transfer rate [μmol min^{-1} mg^{-1} GTL]
0	105.2	0		
8	97.7	64.0	4.26	0.71 (± 0.17)
15	99.7	67.7	2.41	0.52 (± 0.10)
44	100.6	75.5	0.92	0.27 (± 0.04)
83	101.1	83.7	0.54	0.21 (± 0.02)
151	94.4	91.0	0.32	0.16 (± 0.01)

In order to check if losses through filtration might have occurred, GTL treated samples (^{14}C-diclofenac) were filtered through 0.45 µm polytetrafluoroethylene (PTFE) membrane filters. Comparison of radioactivity before and after filtration showed that only 17.8 % of radioactivity remained in the filtered fraction indicating that the remaining 82.2 % were retained by the filter strongly suggesting that losses of transformation products through filtration was the main reason why no higher molecular transformation products could be detected in the aforementioned study. Furthermore, the fact that virtually all the radioactivity was recovered shows that mineralization of diclofenac did not play a significant role in diclofenac transformation by GTL.

In order to verify if higher molecular diclofenac transformation products were formed during diclofenac transformation, SEC measurements of samples treated with GTL were performed. SEC chromatograms of GTL treated samples, controls, and different markers, i.e., Vitamin B12 (Figure 5.4, II), tannic acid (Figure 5.4, III), and two poly(4-vinylphenol) polymers (Figure 5.4, IV and V), are shown in Figure 5.4. Diclofenac can clearly be identified at 290 nm as well as through the radioactive signal after 20.5 mL elution volume. The chromatogram of the GTL treated sample only shows a small peak at 290 nm around 20.5 mL elution volume indicating that most of the diclofenac has been transformed. The predominant amount of the radioactive and 290 nm signal is measured between 16 and 19 mL elution volume. Eight peaks can be identified overall. They appear after 9.5, 10.7, 13.2, 16.7, 17.8, 18.8, 19.5, and 20.7 mL. The peaks at 19.5 mL (Figure 5.4, a) and 18.8 mL (Figure 5.4, b) elution volume are most likely due to diclofenac dimers (~600 Da) and trimers (~900 Da), respectively. Since the peak at 17.8 mL (Figure 5.4, c) appears before the Vitamin B12 marker, which has a molar mass of 1,355 g mol^{-1}, this peak is most likely due to diclofenac pentamers (~1,500 Da) and the peak of the diclofenac tetramers (~1,200 Da) might be superimposed. The peak at 16.7 mL (Figure 5.4, d) appears shortly before the tannic acid marker (1,702 Da) and might therefore be due to diclofenac hexamers (~1,800 Da).

Overall, the results from SEC measurements clearly show that diclofenac is transformed into higher molecular polymerization products when treated with GTL. Therefore, diclofenac transformation is no direct measure of enzymatic activity, since the intermediate radicals seem to react further without additional involvement of the enzymes. Hence, mere substrate and/or product quantitation is insufficient in such reactions to describe enzymatic activity. Additional OCR measurements give a more accurate picture of the actual contribution of the enzymes during the transformation reactions.

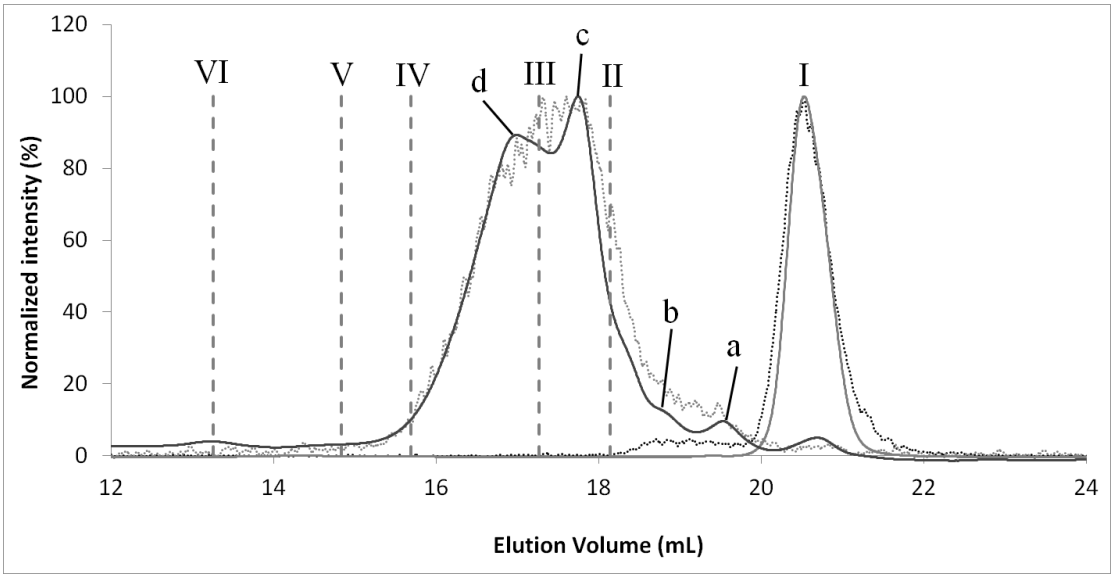

Figure 5.4 SEC chromatograms of (I) diclofenac (^{14}C signal: black dotted line, signal at 290 nm: dark grey solid line), (II) vitamin B_{12} (retention volume 18.2 mL, Mw = 1,579.58 Da), (III) tannic acid (retention volume 17.3 mL, Mw = 1,701.20 Da), (IV) Poly(4-vinylphenol) (retention volume 15.7 mL, average Mw ~11,000 Da, (V) Poly(4-vinylphenol) (retention volume 14.8 mL, average Mw ~25,000 Da), (VI) GTL control (retention volume 13.3 mL, 75.6 kDa) and GTL treated sample (^{14}C signal: dark grey dotted line, signal at 290 nm: black line; a-d: polymers detected after laccase treatment). Signals have been normalized (100 % has been defined as the highest measured signal of the corresponding run). Background radioactivity has been subtracted from the ^{14}C signals. It was calculated from the average radioactivity of the first 12 mL of the corresponding run (adapted from Hommes et al. 2013).

5.3. Assessment of sensor interferences

5.3.1. H_2O_2 sensitivity

CFA24 assays were performed applying an enzyme (HRP) that uses a strong oxidizer (H_2O_2) as substrate. HRP was tested in the presence of H_2O_2 and ABTS in order to clarify if any reaction products or initial substances, even strong oxidizers, impede with the O_2 measurement system (i.e., fluorophores). Obtained OCR over all tested HRP, H_2O_2, and ABTS combinations were 3.4±28.5 pmol min^{-1} Vc^{-1} (n=16) and thus below LOD. Therefore, it seems like the presence of HRP and H_2O_2 has no impact on O_2 measurements and that activity of laccases within mixtures of peroxidases and laccases might be analyzed in CFA assays while both enzymes catalyze the oxidation of the same substrate. This is not possible using standard colorimetric assays where only the extent of total substrate oxidation can be monitored.

5.3.2. Formation of colored product: Syringaldazine transformation

The CFA system measures oxygen concentrations and pH via highly sensitive photo detectors and a fiber-optic waveguide, which delivers light at different excitation wavelengths (oxygen, 532 nm; pH,

470 nm) and transmits a fluorescent signal through optical filters to the photo detectors. Therefore, we expected that the formation of reaction products absorbing light at these wavelengths can interfere with the measurements. The laccase-catalyzed oxidation of syringaldazine to tetramethoxy-azo-bis-methylen quinone constitutes a reaction where electron transfer rates should be proportional to substrate transformation rates, since two electrons per substrate molecule are transferred to molecular oxygen during the reaction (Sanchez-Amat and Solano 1997). Additionally, syringaldazine transformation leads to an increase in absorbance at 525 nm, i.e., close to the wavelength where the CFA system measures oxygen concentration. Therefore, this constitutes a reaction where inaccurate oxygen concentration measurements by the CFA system can be expected. Assays using syringaldazine and GTL were conducted in eight identical parallel assays and led to the measurement of negative OCR. Colorimetric measurements on the other hand showed a clear increase in tetramethoxy-azo-bis-methylen quinone (the syringaldazine transformation product) concentration. Hence, the results of the CFA system were inaccurate, as expected, showing that it is unsuitable for oxygen measurements when changes in optical density at 532 nm occur during the investigated reactions.

5.4. Oxygen consumption by laccases in the presence of lignin

OCR of laccase enzymes in the presence of OL in aqueous buffer solutions at pH 5 have been measured using the CFA 96 to evaluate whether lignin oxidation under these conditions occurs. Laccases from five different sources were tested applying 250 U g^{-1} lignin. Higher activities led to too fast oxygen consumption making calculation of meaningful OCRs impossible. OCRs are presented in Table 5.4. Increasing laccase activities led to increasing OCR for all laccases indicating that lignin acted as laccase substrate and was oxidized by the enzymes. Further experiments were conducted with GTL and varying concentrations of OL (Figure 5.5). Increasing OL concentrations led to increasing OCR further supporting the finding that OL is oxidized by laccases in aqueous solutions. A linear increase in OCR was observed with increasing OL concentrations over the whole tested range ($R^2 = 0.99$) indicating that the enzyme even at the highest liginin concentration tested, i.e., 1.0 g L^{-1} was not working at its maximum velocity.

Table 5.4 OCR for different laccases in the presence of OL at pH 5. Applied activity was 250 U g^{-1} OL.

Laccase source	**OCR**	
	[µmol min^{-1} g^{-1} OL]	**[mol min^{-1} mol^{-1} laccase]**
Trametes versicolor	0.07	6
Thielavia arenaria	2.75	36
Coriolopsis polyzona	4.15	432
Cerrena unicolor	4.07	117
Pleurotus ostreatus	2.14	139

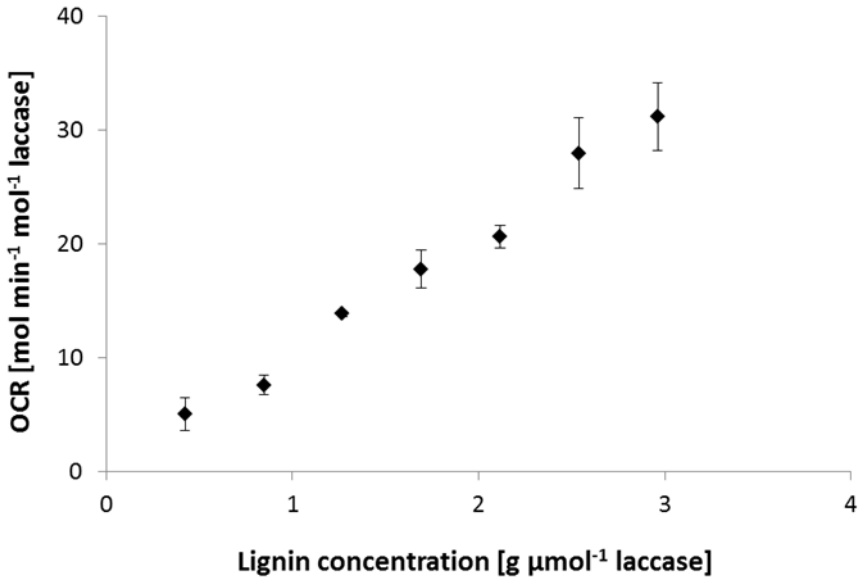

Figure 5.5 OCR for GTL at different OL concentrations at pH 5. Error bars show standard deviations (n=4).

5.5. Concluding remarks

The method described by this work allows high-throughput screening of oxygen consuming catalysts. A literature search for comparative data showed that there is a considerable lack thereof and that the majority of the values were obtained by photometric tests which are rarely conducted in the exact same way between different studies further impeding comparability. The introduced assay presents a new approach which allows high-throughput measurements and produces comparative data. Since it is based on OCR rather than substrate transformation measurements, it allows direct assessment of the enzymatic activity, provides information about reaction stoichiometry, and is unaffected by possible radical chain reactions or competition between different substrates. Therefore, it allows obtaining ample data on enzymes using oxygen as a substrate and has the potential to illuminate aspects of enzymatic reactions that cannot be assessed using common enzymatic assays focusing on product formation. However, the method might rather be suitable for the identification of potential substrates for oxygen consuming enzymes. Regarding lignin treatment there is little information to be gained in addition to verifying whether lignin is oxidized by the enzymes.

6. Enzyme immobilization

6.1. Immobilization on fumed silica nanoparticles

The economy of biocatalytic processes can be improved by enzyme reuse and increase of enzyme stability by means of immobilization technologies. Implementing the capacity of enzyme retention or recovery in existing processes enables biocatalyst separation from products; thereby allowing continuous processes and preventing carry-through of biocatalysts to subsequent process steps (Polizzi et al. 2007). The improvement of enzyme performance, such as activity and stability under application relevant conditions can be achieved by enzyme immobilization on solid surfaces, such as fsNP (Zimmermann et al. 2011). Moreover, immobilization of the biocatalyst can reduce the enzyme loss and facilitate their use in continuous processes, such as bioreactors using membrane filtration technology to retain the immobilized enzymes (Sheldon 2007; Hu et al. 2009; Corvini and Shahgaldian 2010).

In this chapter a previously published immobilization method for enzyme immobilization on fsNP (Zimmermann et al. 2011) was developed further while the principle process steps remained unchanged. First the surface of the fsNP was modified by aminopropylation using an organofunctional alkoxysilane, i.e., APTES. In this process the hydroxyl groups of the fsNP attack and displace the alkoxy groups on APTES and covalent Si-O-Si bonds are formed. Consequently, the modified fsNP display multiple amino groups on the surface. In a next step excess APTES is removed and enzymes are added to the suspension and allowed to adsorb for 2 h on the surface modified fsNP. Next a cross-linker, i.e. glutaraldehyde is added to the suspension. Glutaraldehyde reacts with the amine groups displayed on the enzymes as well as on the modified fsNP thereby covalently binding the enzymes to the fsNP and to other enzymes. The suspension is stirred for 24 h in order to give the reaction sufficient time to occur. In a last step unbound enzymes and glutaraldehyde are removed by several washing steps.

This method was first optimized regarding the consumables required. Next it was amended in order to allow immobilization of specific enzyme combinations enabling the production of defined multi-enzyme fsNP. Finally, it was further optimized in order to allow for a more efficient production of enzyme-fsNP on kilogram-scale.

6.1.1. Optimization of consumables consumption

Improvement of the sorption assisted immobilization method started with optimization of aminopropylation of fsNP using APTES. Subsequently, the effect of glutaraldehyde concentration per enzymatic activity [µmol U^{-1}] was tested in order to minimize the amount of cross-linker per amount fsNP [µmol mg^{-1} fsNP] during the immobilization. Furthermore, the quantity of enzyme per amount fsNP [U mg^{-1} fsNP] applied was tested in order to minimize washing losses and maximize immobilization yield.

6.1.1.1. Improvement of fsNP functionalization

With the aim of reducing costs and resource consumption, APTES concentration for aminopropylation of fsNP (4 µmol APTES mg^{-1} fsNP used by Zimmermann et al. (2011)) was gradually decreased. Producing fsNP–enzyme conjugates by applying constant cross-linker concentrations and enzymatic activity led to different results depending on the applied enzyme as shown in Table 6.1.

In case of PSL immobilization decreasing APTES concentration led to increasing washing losses. Virtually all enzyme activity was lost during washing using 0.08 µmol mg^{-1} fsNP. Enzyme activity of PSL dropped during incubation indicating inactivation of the laccase due to coupling reagents or conditions, since laccase activity in a control with only PSL in PB (pH 7) remained stable (97.4 % of initial activity remained). Losses in enzyme activity during incubation were 66±7 %, 13±5 %, and 39±4 % for 0.08, 0.8, and 4 µmol APTES mg^{-1} fsNP, respectively. Consequently, immobilization yield and enzyme load were highest for 0.8 µmol APTES mg^{-1} fsNP since enzyme activity losses during incubation were lowest at this APTES concentration.

Enzyme immobilization of CPL was virtually not affected by decreasing APTES concentration from 4 to 0.8 µmol mg^{-1} fsNP. Washing loss was close to 0% for both concentrations. However, washing losses rose to 74.6±4.6 % when fsNP treated with 0.08 µmol APTES mg^{-1} fsNP were used. Zeta potential at pH 7 was -21.9±1.7, -17.7±0.9, 3.5±0.4, and 4.8±0.7 mV for fsNP treated with 0, 0.08, 0.8, and 4 µmol APTES mg^{-1} fsNP, respectively. Apparently 0.08 µmol APTES mg^{-1} fsNP did not change the overall surface charge of the fsNP to an extent that could positively influence the sorption and therefore the immobilization of the enzyme. This might explain the low immobilization yield and enzyme load and the high washing loss when using 0.08 µmol APTES mg^{-1} fsNP suspended in MPC at pH 7 for the immobilization of CPL. For protein adsorption to occur, the surface charges of both protein and silica support material must be complementary (Deere et al. 2002). At pH 7 CPL which has an isoelectric point of 3.9 is net negatively charged and, consequently, repelled by fsNP treated with 0.08 µmol APTES which provided an overall negative surface charge of -17.7±0.9 mV at pH 7.

For immobilizing GTL, which showed multiple isoelectric points between 4.2 and 7.6, immobilization yield and enzyme load increased while washing loss decreased with decreasing APTES concentration, indicating that APTES modification might not be needed for GLT sorption and its immobilization onto fsNP.

Since the application of 0.8 µmol APTES mg^{-1} fsNP showed the best results considering immobilization yield and enzyme load for PSL and CPL and 0.08 µmol APTES mg^{-1} fsNP was too little modification agent to change the surface charge of the fsNPs, further experiments for optimization were conducted with 0.8 µmol APTES mg^{-1} fsNP. This allowed saving 80 % of APTES, resulting in cost savings of approximately 208 € kg^{-1} fsNP compared to the immobilization procedure used by Zimmermann et al. (2011), in which APTES modified fsNP were produced for approximately 260 € kg^{-1} fsNP.

Table 6.1 Comparison of fsNP-laccase conjugates produced with different APTES amounts (adapted from Hommes et al. 2012)

Laccase	Protein amount [mg protein mg^{-1} fsNP]	APTES [µmol mg^{-1} fsNP]	Washing loss[a] [%]	Immobilization yield[b] [%]	Enzyme load[c] [U mg^{-1} fsNP]
Phoma sp.	0.15	0.08	98.9 ± 0.1	0.4 ± 0.1	0.013 ± 0.01
UHH 5-1-03[d]	0.15	0.80	62.2 ± 0.2	32.8 ± 1.8	1.13 ± 0.03
	0.15	4.00	51.7 ± 3.8	29.5 ± 2.5	1.03 ± 0.05
Coriolopsis	0.18	0.08	74.6 ± 4.6	27.9 ± 4.3	1.20 ± 0.27
polyzona	0.18	0.80	6.1 ± 6.7	88.7 ± 6.0	4.77 ± 0.24
	0.18	4.00	0.7 ± 0.6	80.7 ± 3.2	4.56 ± 0.26
Genus	0.28	0.08	44.4 ± 4.1	74.0 ± 6.7	2.69 ± 0.05
Thielavia	0.28	0.80	60.5 ± 3.9	60.8 ± 4.8	2.30 ± 0.24
	0.28	4.00	72.2 ± 1.5	41.0 ± 5.1	1.47 ± 0.15

Test performed with constant laccase units (4 U mg^{-1} fsNP) and cross-linker concentration (10 µmol glutaraldehyde mg^{-1} fsNP). Samples (n=3) were incubated at 4 °C for 24 h.

[a] Washing loss was defined as 100% minus apparent (measured) laccase activity bound to fsNP after exhaustive washing in % relative to apparent laccase activity before washing (100 %), i.e. after incubation.

[b] Immobilization yield was defined as apparent laccase activity of the fsNP suspensions in % after exhaustive washing relative to the initially applied laccase activity (100 %).

[c] Enzyme load was defined as apparent laccase activity (in U) per mg fsNP applied remaining after exhaustive washing.

[d] Specific activity of *Phoma* sp. laccase fermentation broth used was 26±4 U mg^{-1} Protein.

6.1.1.2. Optimization of cross-linking

In order to further reduce chemical consumption of the immobilization procedure cross-coupling was optimized. The effect of cross-linker concentrations (glutaraldehyde) on both free and immobilized laccases was investigated.

Glutaraldehyde strongly affected the enzyme activity of PSL during incubation. Without glutaraldehyde this laccase kept 97.4 % of the initial applied activity, but incubation with 0.25 and 2.5 µmol glutaraldehyde U^{-1} showed a decrease in apparent laccase activity after incubation relative to the applied laccase activity (100 %) down to 72.4 % and 40.9 %, respectively, indicating enzyme inactivation through glutaraldehyde.

CPL and GTL were stable in the presence of the cross-linker. Enzyme activity of GTL was even increased considerably in the presence of glutaraldehyde, i.e., apparent laccase activity after incubation relative to applied laccase activity (100 %) being 102.8 %, 152.5 %, 164.2 %, and 142.8 % for 0, 0.025, 0.25, and 2:5 µmol glutaraldehyde U^{-1}, respectively. Enhanced enzyme activity for cross-linked laccases compared to their native forms has been reported before (Durán et al., 2002).

Producing fsNP–enzyme conjugates by applying 4 U mg^{-1} fsNP modified with 0.8 µmol APTES mg^{-1} fsNP using different glutaraldehyde amounts per mg fsNP led to different results depending on the laccase originally applied as shown in Table 6.2. The immobilization method used was not suitable for

PSL since its activity was lost in presence of glutaraldehyde. Consequently, the immobilization procedure showed low immobilization yield and led to PSL immobilized on fsNP (PSL-fsNP) with low enzyme load compared to CPL immobilized on fsNP (CPL-fsNP) and GTL immobilized on fsNP (GTL-fsNP). Therefore, further experiments were only conducted with GTL and CPL. CPL was almost entirely immobilized using 1 and 10 µmol glutaraldehyde mg^{-1} fsNP. Concerning the immobilization of GTL, decreasing glutaraldehyde from 10 to 1 µmol mg^{-1} fsNP led to a decrease in washing loss and an increase in immobilization yield and enzyme load. Reducing glutaraldehyde further to 0.1 µmol mg^{-1} fsNP led to an increase in washing losses for all three laccases indicating that cross-linker concentration was too low.

For further experiments 1 µmol glutaraldehyde mg^{-1} fsNP was used since the highest values for immobilization yield and enzyme load for GTL-fsNP were obtained and CPL was almost entirely bound to the fsNP at this glutaraldehyde amount per mg fsNP. This allowed saving 90% of glutaraldehyde, known to be environmentally dangerous, compared to the immobilization procedure used by Zimmermann et al. (2011) and therefore represents a considerable environmental relief. Furthermore, this optimization led to additional cost savings of approximately 40 € kg^{-1} fsNP.

6.1.1.3. Optimization of applied protein amount

According to Zimmermann et al. (2011) a binding efficiency of 93.9±4.6 % using 4 U CPL mg^{-1} fsNP could be achieved. This was in accordance with the obtained washing loss of 4.3±1.7 % using CPL showing that nearly all enzymes were bound to the fsNP (Table 6.2).

However, washing loss using GTL was 49.9±4.2 % showing that not all enzyme molecules were bound to the fsNP. This discrepancy between the two protein mixtures can be explained by the different specific activities of CPL and GTL. As shown in Table 5.1 specific activity was considerably higher for CPL compared to GTL. Therefore, approximately twice as many proteins were applied in the immobilization procedures with GTL compared to CPL leading to excess proteins. Therefore, further optimization of applied laccase amount of GTL was necessary.

As can be seen in Table 6.3, washing loss decreased with decreasing applied protein amounts. At 0.07 mg protein mg^{-1} fsNP the enzyme was almost entirely bound to the fsNP. The immobilization yield increased with decreasing protein amounts as well and reached 161.5±9.6 % applying 0.07 mg protein mg^{-1} fsNP. This demonstrated at the same time that immobilization of GTL led to an increase of enzymatic activity. A further decrease to 0.035 mg protein mg^{-1} fsNP led to similar values for washing loss and immobilization yield and consequently enzyme load was approximately divided by two. Accordingly, 0.07 mg protein mg^{-1} fsNP was applied in further experiments.

Table 6.2 Comparison of fsNP-laccase conjugates produced with different glutaraldehyde amounts (adapted from Hommes et al. 2012)

Laccase	Protein amount [mg protein mg-1 fsNP]	Glutaraldehyde [µmol mg^{-1} fsNP]	Washing loss[a] [%]	Immobilization yield[b] [%]	Enzyme load[c] [U mg^{-1} fsNP]
Phoma sp.	0.36	0.1	94.4 ± 0.4	7.6 ± 0.9	0.21 ± 0.01
UHH 5-1-03[d]	0.36	1.0	78.3 ± 3.0	26.6 ± 5.4	0.77 ± 0.12
	0.36	10.0	74.7 ± 2.0	17.9 ± 1.1	0.53 ± 0.03
Coriolopsis	0.18	0.1	16.8 ± 2.5	87.5 ± 7.3	3.85 ± 0.30
polyzona	0.18	1.0	4.3 ± 1.7	82.7 ± 3.4	3.61 ± 1.20
	0.18	10.0	6.1 ± 6.7	88.7 ± 6.0	4.77 ± 0.24
Genus	0.28	0.1	69.3 ± 3.1	53.4 ± 4.8	2.05 ± 0.15
Thielavia	0.28	1.0	49.9 ± 4.2	72.8 ± 1.5	2.70 ± 0.05
	0.28	10.0	60.5 ± 3.9	60.8 ± 4.8	2.30 ± 0.24

Test performed with constant laccase units (4 U mg^{-1} fsNP) and APTES concentration (0.8 µmol mg^{-1} fsNP). Samples (n=3) were incubated at 4 °C for 24 h.

[a] Washing loss was defined as 100% minus apparent (measured) laccase activity bound to fsNP after exhaustive washing in % relative to apparent laccase activity before washing (100%), i.e. after incubation.

[b] Immobilization yield was defined as apparent laccase activity of the fsNP suspensions in % after exhaustive washing relative to the initially applied laccase activity (100 %).

[c] Enzyme load was defined as apparent laccase activity (in U) per mg fsNP applied remaining after exhaustive washing.

[d] Specific activity of *Phoma* sp. laccase fermentation broth used was 11±3 U mg^{-1} Protein.

Table 6.3 Comparison of fumed silica nanoparticle (fsNP)-laccase conjugates produced with different applied GTL amounts (adapted from Hommes et al. 2012)

Applied laccase		Washing loss[a]	Immobilization yield[b]	Enzyme load[c]
[U mg^{-1} fsNP]	[mg protein mg^{-1} fsNP]	[%]	[%]	[U mg^{-1} fsNP]
0.5	0.035	-1.8 ± 4.1	160.9 ± 7.1	0.75 ± 0.63
1	0.070	0.9 ± 1.9	161.5 ± 9.6	1.53 ± 0.02
2	0.140	15.2 ± 7.5	127.3 ± 8.4	2.30 ± 0.19
3	0.210	39.0 ± 2.5	94.2 ± 1.8	2.62 ± 0.07
4	0.280	49.9 ± 4.2	72.8 ± 1.5	2.70 ± 0.05

Test performed with constant cross-linker (1 µmol glutaraldehyde mg^{-1} fsNP) and APTES (0.8 µmol mg^{-1} fsNP) concentration. Samples (n=3) were incubated at 4 °C for 24 h.

[a] Washing loss was defined as 100 % minus apparent (measured) laccase activity bound to fsNP after exhaustive washing in % relative to apparent laccase activity before washing (100 %), i.e. after incubation.

[b] Immobilization yield was defined as apparent laccase activity of the fsNP suspensions in % after exhaustive washing relative to the initially applied laccase activity (100 %).

[c] Enzyme load was defined as apparent laccase activity (in U) per mg fsNP applied remaining after exhaustive washing

6.1.2. Immobilization of multiple enzymes on the same carrier

In order to verify whether the developed immobilization method is suitable for the immobilization of multiple enzymes on the same carrier, immobilization experiments using five different laccases were conducted. Furthermore, a strategy to design defined multi-enzymatic nanobiocatalyst has been investigated. Results of the immobilization experiments are summarized in Table 6.4.

6.1.2.1. Immobilization of single laccases as benchmark

Washing losses of single laccases were below 10 % for GTL, POL, and TVL, indicating that these biocatalysts were almost entirely immobilized on the support material. For CPL and CUL, washing losses were higher compared to the other three enzymes but still below 20 %. The slightly higher washing losses for CPL and CUL were most likely due to the fact that the protein loads (0.088 and 0.080 mg protein per milligram fsNP, respectively) actually used were slightly above the calculated optimal protein load (0.07 mg protein per milligram fsNP) for these two enzymes. The specific activities of the enzyme suspensions correlated nicely with the enzyme loads of the corresponding nanobiocatalysts, i.e., higher specific activities of the enzyme suspensions resulted in higher enzyme loads of the nanobiocatalysts.

The resulting enzyme loads correlated with the specific activity of the applied laccases, and the resulting washing losses correlated with the applied protein amounts, indicating that similar protein amounts were immobilized per milligram fsNP irrespective of the enzyme used. Immobilized enzymes retained a higher percentage of their maximal enzymatic activity towards 2,6-DMP compared to free enzymes over the tested pH range (except for GTL at pH 3), indicating that the enzymatic activity is enhanced due to immobilization even at unfavorable pH. Similar favorable effects of immobilization of laccases on the relative enzymatic activity at different pH values have been reported before (e.g., Yang et al. 2006). A shift of the optimum pH due to immobilization could not be observed for any of the laccases. However, since enzymatic activities were determined at discrete pH values, small shifts of the pH optimum, as reported for the immobilization of CUL (Luterek et al. 1998), might have not been detected.

Table 6.4 Comparison of different laccase-fsNP conjugates produced with different laccases and laccase mixtures (n=3; adapted from Ammann et al. 2014).

Applied laccase(s)	Washing loss [%] [a]	Washing loss [%] [b]	Immobilisation yield [c] [%]	Enzyme Load [d] [U mg^{-1} fsNP]
GTL (0.056 mg protein mg^{-1} fsNP)	4.8 ± 3.9	6.0 ± 0.5	126.1 ± 9.6	0.91 ± 0.05
CPL (0.088 mg protein mg^{-1} fsNP)	17.1 ± 1.8	15.2 ± 0.5	139.3 ± 9.5	2.42 ± 0.12
CUL (0.080 mg protein mg^{-1} fsNP)	17.6 ± 6.5	18.0 ± 0.8	161.3 ± 17.3	0.70 ± 0.07
POL (0.062 mg protein mg^{-1} fsNP)	2.1 ± 3.1	8.5 ± 1.3	228.3 ± 16.4	1.05 ± 0.06
TVL (0.050 mg protein mg^{-1} fsNP)	7.2 ± 1.8	2.9 ± 0.1	191.1 ± 8.9	1.08 ± 0.02
GTL (0.014 mg protein mg^{-1} fsNP)	7.4 ± 4.5	0.5 ± 0.0	180.0 ± 8.7	0.30 ± 0.01
GTL, CPL (0.028 mg protein mg^{-1} fsNP)	6.7 ± 2.7	0.5 ± 0.0	205.4 ± 15.4	0.78 ± 0.06
GTL, CPL, CUL (0.042 mg protein mg^{-1} fsNP)	5.5 ± 2.1	0.5 ± 0.0	204.7 ± 3.4	0.86 ± 0.04
GTL, CPL, CUL, POL (0.056 mg protein mg^{-1} fsNP)	9.1 ± 0.5	2.6 ± 0.1	201.9 ± 13.1	1.01 ± 0.02
GTL, CPL, CUL, POL, TVL (0.070 mg protein mg^{-1} fsNP)	11.8 ± 3.3	5.0 ± 0.3	190.7 ± 1.8	1.10 ± 0.03
GTL (0.035 mg protein mg^{-1} fsNP)	5.7 ± 0.6	4.3 ± 0.3	166.1 ± 3.1	0.69 ± 0.00
POL (0.035 mg protein mg^{-1} fsNP)	5.1 ± 3.5	3.4 ± 0.3	227.4 ± 3.8	0.55 ± 0.02
GTL, POL (Total 0.070 mg protein mg^{-1} fsNP)	10.0 ± 2.9	9.8 ± 0.8	155.7 ± 1.7	1.03 ± 0.02
CPL (0.035 mg protein mg^{-1} fsNP)	8.5 ± 3.1	0.5 ± 0.0	194.4 ± 6.8	0.93 ± 0.02
TVL (0.035 mg protein mg^{-1} fsNP)	9.7 ± 2.2	2.3 ± 0.2	212.0 ± 4.7	0.75 ± 0.04
CPL, TVL (Total 0.070 mg protein mg^{-1} fsNP)	9.7 ± 4.0	6.4 ± 0.1	184.0 ± 5.6	1.37 ± 0.03

Washing loss was determined in two different ways, i.e. as [a] relative difference between the apparent (measured) laccase activity bound to the fsNP after exhaustive washing and the apparent laccase activity before washing (100 %) and [b] apparent laccase activity discarded during washing relative to the apparent laccase activity before washing (100 %), i.e. the relative laccase activity discarded during washing.

[c] Immobilization yield was defined as apparent laccase activity of the completed nanobiocatalyst suspensions relative to the initially applied laccase activity (100 %).

[d] Enzyme load was defined as apparent laccase activity per mg fsNP of the completed nanobiocatalysts.

6.1.2.2. Immobilization of multiple enzymes for proof of concept

In order to test whether immobilization of all five investigated laccases onto the same particles was feasible, different experiments were conducted. The number of laccases to be immobilized was increased successively from one up to five. With each increase in the number of applied laccases, the resulting nanobiocatalysts showed an increase in total enzyme load. Herewith, it could be shown that all five laccases were successfully co-immobilized, and thereby a biocatalyst containing all five laccases (multi-fsNP) could be produced. Therefore, the suitability of the applied method to immobilize defined combinations of laccases was proven. This allowed selection of laccase combinations for immobilization on the same particle based on their capabilities in order to produce nanobiocatalysts with enhanced abilities compared to the single enzymes. One pair of laccases was selected for co-immobilization, i.e., GTL and POL to produce nanobiocatalysts that retain most of their maximal enzymatic activity over a broader pH range.

Co-immobilizations of two laccases were assessed similar to the immobilization of five laccases by running control experiments applying only one laccase. Enzyme load of GTL and POL co-immobilized on fsNP (GTL–POL–fsNP), was higher after immobilization of both laccases compared to experiments where only one laccase was immobilized, indicating successful immobilization.

Successful co-immobilization of the studied laccases on the same particles could be demonstrated by successive immobilization of the five different enzymes. The amounts of enzyme that were immobilized on the fsNP were calculated based on the assumption that crosslinking with glutaraldehyde is in general nonspecific towards different proteins and consequently towards different enzymes, since cross-linking of proteins to a carrier with glutaraldehyde usually involves non-protonated ε-amino groups of lysin residues (Weetall 1974), and proteins usually exhibit many lysine residues on their surface, due to the polarity of the amine group (Migneault et al. 2004). The experiments demonstrated that applying enzyme mixtures with total protein amounts equal or slightly below the protein amount that can be immobilized on the fsNP allows immobilizing defined combinations of enzymes.

6.1.2.3. Characterization of immobilized laccases

Figure 6.1 shows the normalized activity of the different laccases (A) and immobilized laccases (B) at different pH values in the presence of 2,6-DMP. All laccases reached their maximal activity at pH 4 with the exception of GTL, which reached its maximal activity at pH 5. Laccase activity was reduced below 20 % of the maximal activity at pH 6 for CUL, POL, and TVL. At pH 7, the measured activity for these three laccases was below the LOD. For CPL, the reduction in laccase activity at higher pH values was not as drastic and remained at approximately 31 and 16 % of the maximal activity at pH 6 and 7, respectively. GTL retained 80 % of its maximal activity at pH 6, and at pH 7, 50 % of the maximal activity remained. For all investigated laccases, the immobilization of the enzymes did not

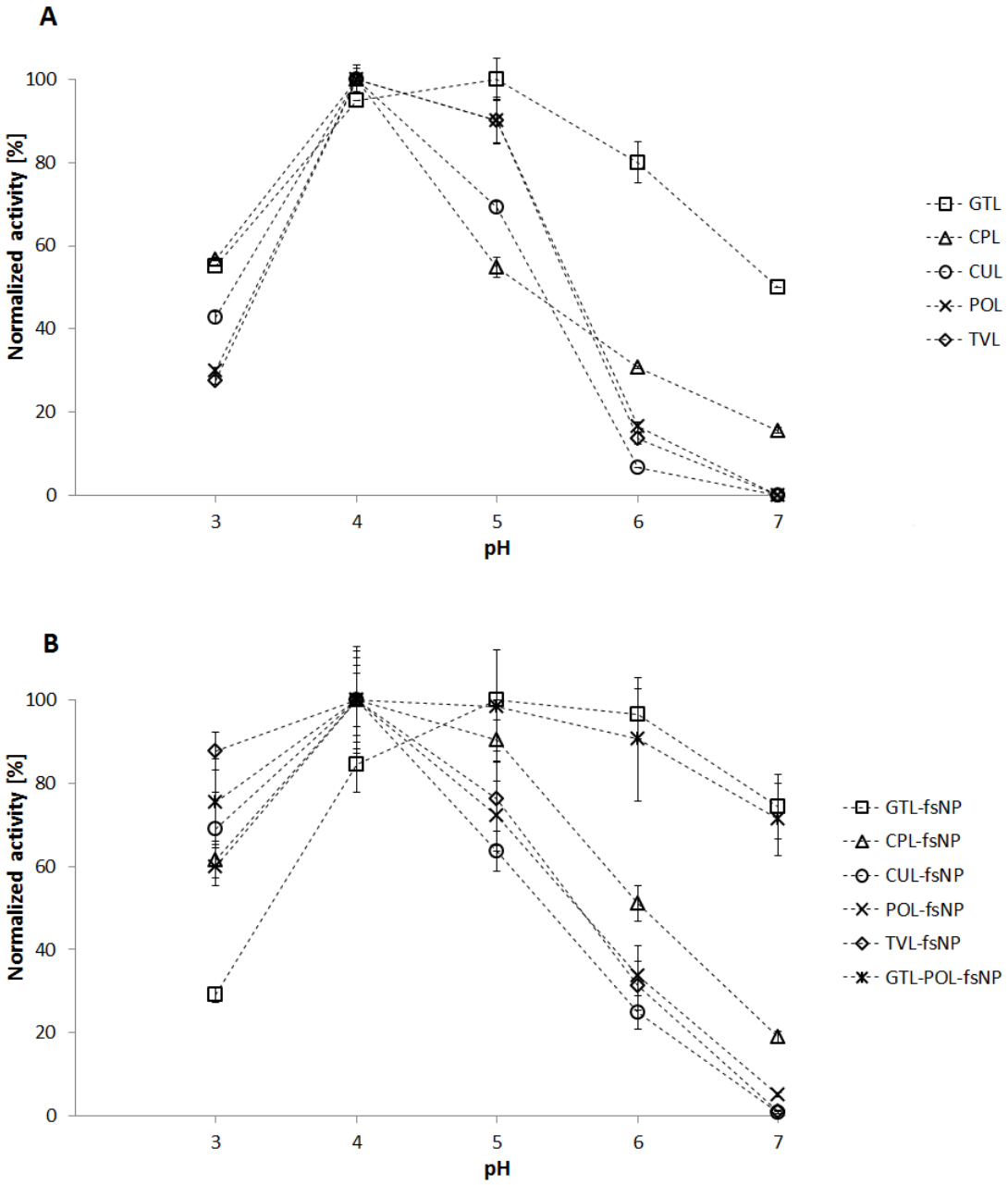

Figure 6.1 Enzymatic activity of laccases (A) and immobilized laccases (B) at different pH values during the oxidation of 2,6-DMP (2 mM). A) single laccase in its soluble form from genus *Thielavia* laccase (GTL), *Coriolopsis polyzona* (CPL), *Cerrena unicolor* (CUL), *Pleurotus ostreatus* (POL) and *Trametes versicolor* (TVL) B) single laccase-fsNP conjugates from genus *Thielavia* laccase (GTL-fsNP), *Coriolopsis polyzona* (CPL-fsNP), *Cerrena unicolor* (CUL-fsNP), *Pleurotus ostreatus* (POL-fsNP) and *Trametes versicolor* (TVL-fsNP) and two laccase-fsNP conjugates from GTL and POL (GTL-POL-fsNP). Laccase activity is normalized to the highest measured activity of the corresponding enzyme; error bars show the standard deviations (n=5; adapted from Ammann et al. 2014).

lead to an observable shift of the optimal pH regarding enzymatic activity. However, immobilized enzymes retained a higher percentage of their maximal activity compared to free enzymes at pH 6 and

7. Especially, GTL–fsNP showed little losses in activity at higher pH values compared to other immobilized laccases, retaining 97 and 74 % of maximal enzymatic activity at pH 6 and 7, respectively. At pH 3, losses in enzymatic activity compared to the maximal enzymatic activity were also smaller for all enzymes after immobilization, except for GTL. Notably, TVL retained most of its maximal enzymatic activity after immobilization at pH 3, i.e., 88 %, while it only retained 28 % in its dissolved form. The co-immobilization of GTL and POL led to the anticipated extension of the pH range, in which the nanobiocatalysts retained enzymatic activity. Enzymatic activities were always above 70 % of the activity maximum of the GTL–POL–fsNP over the tested pH range from 3 to 7. This constitutes a clear improvement at pH values above 4 compared to the nanobiocatalyst, in which POL was used as a sole enzyme and at pH 3 compared to the one-enzyme nanobiocatalyst, in which GTL was used. Furthermore, an increase in enzymatic activity towards the substrate ABTS at pH 3 was observed for all laccase genera after immobilization, as is apparent by the immobilization yields above 100 % that were achieved for all laccases and laccase combinations (Table 6.4). Enzymatic activity after immobilization also increased, when 2,6-DMP was used as a substrate for all laccases at all pH values investigated. One enzyme nanobiocatalysts showed increased enzymatic activity towards 2,6-DMP between 3.5- (pH 5, TVL immobilized on fsNP; TVL–fsNP) and 9.4- fold (pH 6, TVL–fsNP) compared to the corresponding dissolved enzymes. Enzymatic activity towards 2,6-DMP by co-immobilized enzymes increased between 4.9- (pH 4, GTL–POL–fsNP) and 11.6-fold (pH 7, GTL–POL–fsNP) compared to the corresponding mixture of dissolved enzymes at the same enzyme ratio. Immobilization of five different laccases onto one carrier led to an increase in enzymatic activity towards 2,6-DMP between 10.3- (pH 3) and 15.5-fold (pH 7), in comparison to a mixture of the respective native laccases applied at the same enzyme ratio.

The co-immobilization of specifically selected laccases allowed the production of biocatalysts with a broader pH-activity range, in case of the GTL–POL–fsNP, compared to the corresponding singly immobilized laccases. This indicates that the characteristics of single laccases regarding pH activity profile complemented one another after co-immobilization.

6.1.2.4. Immobilization of multiple LMEs on fumed silica nanoparticle

Several LMEs in addition to the five laccases were immobilized on fsNP using the immobilization method developed in section 6.1.1. Results of these experiments are summarized in Table 6.5. All enzymes were successfully immobilized. However, biocatalysts with LiP displayed low enzyme loads in comparison to the other biocatalysts. This is most likely due to the low specific enzymatic activity of LiP (see Table 5.1). Furthermore, LiP lost all activity towards the nonphenolic dye (Azure B). Therefore, these results indicate, that further improvement and/or purification of LiP might be necessary before this enzyme is of interest for application outside of basic research. However, DyP and VP retained their activity towards the nonphenolic substrate after immobilization indicating that these enzymes might be more suitable for lignin treatment after immobilization.

Table 6.5 Different LME-fsNP conjugates (n=3)

Enzyme	**Source**	**Immobilization yield [a] [%]**	**Enzyme load [b] [U mg^{-1} fsNP]**	**Enzyme load [c] [U g^{-1} fsNP]**
Glucose oxidase	*Aspergillus niger*	98.9±15.0	6.73±0.42	
VP	*Bjerkandera adusta*	49.5±1.8	0.18±0.00	0.41±0.06
LiP		70.1	0.02	0.00
DyP		93.6±9.9	0.07±0.01	0.45±0.02
HRP	*Amoracia rusticana*	1.8	0.21	
		22.8±2.2[d]	1.20±0.09[d]	

[a] Immobilization yield was defined as apparent enzymatic activity of the completed nanobiocatalyst suspensions relative to the initially applied enzymatic activity (100 %)

[b] Activity was determined by the peroxidase assay or in case of glucose oxidase by the glucose oxidase assay

[c] Activity was determined by the azure B assay.

[d] Immobilization was conducted at pH 9.5.

HRP immobilization at pH 7.5 resulted in low immobilization yields. The HRP product applied consisted of seven isoenzymes with differing isoelectric points ranging from 3 to 9 (Table 5.1). Consequently, it could be expected that at pH 7.5 some HRP isoenzymes were positively charged. The pKa of APTES is 7.6 and it was calculated based on the Henderson–Hasselbach equation that the amino groups of APTES are fully protonated below pH 6 and are neutral above pH 9.5 (Bhat and Genzer 2007). Therefore, the particles are net positively charged at pH 7.5 repelling the positively charged enzymes. Consequently, these isoenzymes do not readily adsorb and might, therefore, not be bound to the particles after addition of the cross-linker. In order to prohibit repulsion pH during immobilization was increased to 9.5. At this pH value the particles are expected to have a net neutral charge while the enzymes have a net negative charge. Preventing repulsion by increasing pH led to a considerable increase in the enzyme load of the biocatalysts, i.e., enzyme load increased from 0.21 to 1.20 U mg^{-1} fsNP for immobilizations conducted at pH 7.5 and 9.5, respectively. However, this is still not ideal because there is no electrostatic attraction between the enzymes and the particles which is reflected in the relatively low immobilization yield of only 22.8±2.2 %.

Immobilization of multiple enzymes on the same particles was conducted as well following the approach described in paragraph 6.1.2.2. Results are summarized in Table 6.6. Three different biocatalysts containing more than one enzyme type were produced for proof of concept, i.e., TVL-HRP-fsNP, LiP-glucose oxidase-fsNP, and HRP-glucose oxidase-fsNP. Results indicate that immobilization of both enzymes was successful in all three cases. Overall activity of the TVL-HRP-fsNP was higher compared to the TVL-fsNP or HRP-fsNP alone. Furthermore, LiP-glucose oxidase-fsNP and HRP-glucose oxidase-fsNP displayed both peroxidase activity and glucose oxidase activity.

Table 6.6 Comparison of different LME-fsNP conjugates produced with single enzymes and enzyme mixtures.

Enzyme(s)	Enzyme load [U mg^{-1} fsNP] [b]	[c]
TVL (0.035 mg TVL protein mg^{-1} fsNP) [d]	0.75	
HRP (0.070 mg HRP protein mg^{-1} fsNP) [d]	1.48	
HRP, TVL [d] (0.035 mg TVL protein mg^{-1} fsNP, 0.070 mg HRP protein mg^{-1} fsNP)	2.28	
LiP (0.035 mg LiP protein mg^{-1} fsNP)	0.01	
Glucose oxidase (0.035 mg glucose oxidase protein mg^{-1} fsNP)		0.80
LiP, glucose oxidase (0.035 mg protein mg^{-1} fsNP of each enzyme)	0.01	0.90
HRP (0.035 mg HRP protein mg^{-1} fsNP)	0.02	
Glucose oxidase (0.017 mg glucose oxidase protein mg^{-1} fsNP)		0.26
HRP, glucose oxidase (0.035 mg HRP protein mg^{-1} fsNP, 0.017 mg glucose oxidase protein mg^{-1} fsNP)	0.02	0.27

[a] Immobilization yield was defined as apparent enzymatic activity of the completed nanobiocatalyst suspensions relative to the initially applied enzymatic activity (100 %)

[b] Enzyme load was defined as apparent enzymatic activity per mg fsNP of the completed nanobiocatalysts (determined either by peroxidase (in all cases in which peroxidases were applied) or laccase assay)

[c] Determined by the glucose oxidase assay.

[d] Immobilization was conducted at pH 9.5.

6.1.3. Immobilization at kilogram-scale

6.1.3.1. Optimization of particle concentration

In order to increase production efficiency of nanobiocatalysts the process was further optimized regarding the particle amount per reaction volume. Finding the optimal particle concentration during the immobilization procedure, i.e., the highest particle concentration at which particle suspensions could still be stirred without using excessive energy was an essential developmental step for more cost-effective production. Therefore, the rheological characteristics of different particle suspensions (Figure 6.2) which originated from the individual immobilization process steps were investigated. With increasing particle concentration viscosity showed a rapid increase at a critical point depending on the surface modification. This critical point was reached at approximately 100 g of particles L^{-1} for fsNP. Higher concentrations led to drastically higher viscosities of the working suspensions greatly hampering treatability. Therefore, a particle concentration of 100 g fsNP L^{-1} was deemed to be optimal, and consequently, 0.08 mol APTES and 100 g fsNP L^{-1} medium were used for surface modification of the fsNP. In the subsequent coupling step, aminopropylated fsNP (AP-fsNP) were applied, which showed a slight mass increase of approximately 6 % compared to applied fsNP mass due to surface modification. The obtained amount of 106 g AP-fsNP L^{-1} was suspended and applied for enzyme immobilization. In these optimization experiments GTL was used as enzyme to be immobilized. Again, an increase of

particle mass of approximately 15 %, due to the loading of fsNP with glutaraldehyde and protein, was measured after immobilization of the enzymes and washing of the particles. Thus, starting the production with 100 g fsNP L^{-1}, the final particle concentration was 121 g L^{-1} after the whole immobilization procedure. Particle concentration was never above the critical point and treatment was not hampered by too high viscosity of the suspension since both AP-fsNP and Lac-fsNP showed a critical increase in viscosity well after 130 g particles L^{-1}.

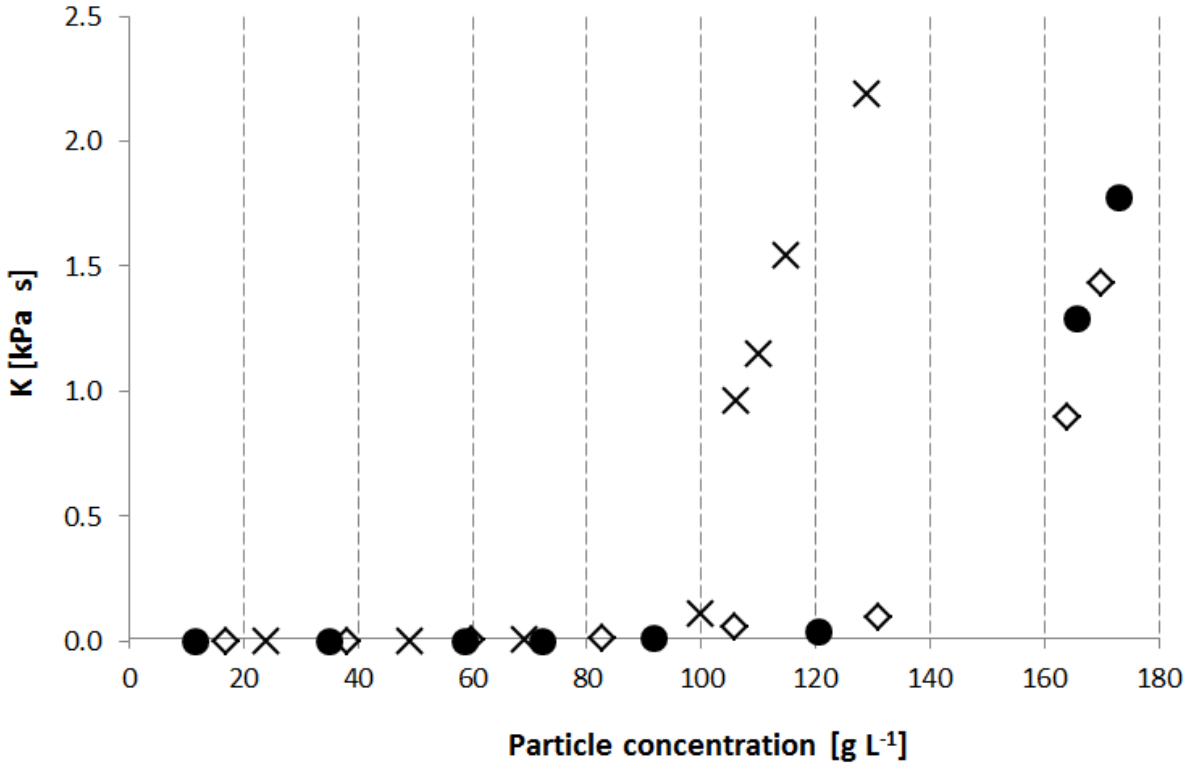

Figure 6.2 Rheological responses i.e. flow consistency indexes of fsNP (*crosses*), AP-fsNP (*diamonds*), and GTL-fsNP (*black circles*) in suspensions of different particle concentrations (adapted from Gasser et al. 2014b)

6.1.3.2. Monitoring of surface modification and enzyme immobilization

After each process step, different control measurements were performed in order to determine the efficiency of the adapted protocol. Results from amino group quantification assays and zeta-potential measurements after aminopropylation with APTES indicated successful surface modification of fsNP. The nitrogen content increased from 0.25±0.05 mg N g^{-1} fsNP for non-modified fsNP up to 16.0±0.1 mg N g^{-1} fsNP after aminopropylation and the surface charge changed drastically from −25.1±0.4 for fsNP to 6.31±0.10 mV for AP-fsNP. Those results confirmed the successful modification of the surface of the nanoparticles.

Monitoring enzymatic activity of the biocatalysts during the enzyme immobilization procedure indicated that virtually the whole enzyme load could be conjugated to the particles. Only 3.6±9.5 % of laccase

activity was lost during the washing procedure. Washing losses were determined as the relative difference of laccase activity of the suspension before (100 %) and after exhaustive washing. The residual enzymatic activity obtained after the whole production was 132.5±11.5 % of initially applied laccase activity. Thus, an enzyme load of 1.23±0.11 kU g^{-1} fsNP was achieved.

Almost the same amount of laccase activity could be immobilized using higher particle concentrations compared to particles produced on lab scale which had an activity of 1.53±0.02 kU g^{-1} fsNP. Therefore, the undertaken changes in the immobilization procedure to increase production efficiency had no considerable repercussions for the end product.

6.1.4. Concluding remarks

In summary, results showed that the developed immobilization method is suitable for immobilization of several different enzymes. Enzyme loads of biocatalysts are closely related to specific activities of applied enzymes. However, results also indicate that immobilization of enzymes with isoelectric points around or above 9 might be inefficient using the applied method since no or only small electrostatic attraction between particles and such enzymes occurs (even if pH values are adjusted) since particle surfaces have a neutral charge above pH 9.5. Consequently, the adsorption step does not lead to the desired proximity of such enzymes to the particle surface which would facilitate cross-linking.

6.2. Immobilization on superparamagnetic nanoparticles

The partial insolubility of lignins in aqueous solution as well as organic solvent buffer mixtures hinders the effective separation of heterogeneous catalysts from the reaction products after treatment. Therefore, fsNP are not the ideal enzyme carrier material for lignin treatment (see 7.1.5.1). However, carrier materials with paramagnetic or superparamagnetic properties like magnetite nanoparticles (Yamaura et al. 2004) are an attractive alternative since applying a magnetic field to otherwise stable aqueous suspensions of the particles leads to agglomeration and separation from the bulk solution. In the absence of a magnetic field, the particles can be easily re-suspended allowing their reuse. In order to conjugate the biocatalysts to the paramagnetic particles, a core-shell approach is usually applied, i.e., the magnetite core is chemically bound to an organic or polymeric shell (Ma et al. 2003; Kumar et al. 2014). Subsequently, the proteins are bound to the functional groups of the shell. The iron oxide cores are produced as nanoparticles exhibiting paramagnetic or superparamagnetic behavior (Yamaura et al. 2004). Several strategies have recently been developed to immobilize laccases on magnetic carriers (Kumar et al. 2014; Ardao et al. 2015; Kumar and Cabana 2016). Immobilization of CLEAs on magnetite particles using glutaraldehyde as cross-linker led to the production of biocatalysts with enhanced stability (Kumar et al. 2014). However, only low immobilization yields (~32 % of the applied activity) were reached after the immobilization procedure (Kumar et al. 2014). The same group reported the immobilization of CLEAs on magnetite particles using chitosan/1-ethyl-3-(3-dimethylaminopropyl)-carbodiimide hydrochloride as cross-linker (Kumar and Cabana 2016). This allowed higher immobilization yields of up to 61.4 % (Kumar and Cabana 2016).

In the present chapter, a simple and robust method for enzyme immobilization on MPs was developed and optimized based on the sorption-assisted surface conjugation method described in paragraph 6.1. TVL was used as model enzyme. The influence of different factors governing the specific enzymatic activity and stability of the biocatalysts were investigated in depth using RSM. Resulting particles were characterized by TEM, zeta potential, FTIR, and magnetization measurements. Furthermore, the enzymatic activity of resulting biocatalysts towards several laccase substrates was determined and the stability of the biocatalysts at different pH and in the presence of different chemical denaturants was assessed. In order to demonstrate the suitability of the superparamagnetic biocatalysts for green chemistry applications, a non-toxic phenoxazinone dye, i.e., 2-amino-3-oxo-3H-phenoxazine-8-sulfonic acid was produced from 3-amino-4-hydroxybenzenesulfonic acid using the immobilized enzymes. The biocatalysts were applied in ten consecutive cycles to determine the effectivity of reuse.

6.2.1. Particle synthesis and biocatalyst size distribution

MPs were produced by a co-precipitation method according to Eq. 4. Since, the goal was the development of an immobilization procedure as simple as possible particles were not produced under completely anoxic conditions. Therefore, it is possible that a part of the formed magnetite reacted further to maghemite according to Eq. 5 or that maghemite was formed directly according to Eqs. 6 and 7.

$Fe^{2+} + 2Fe^{3+} + 8OH^- \rightarrow Fe_3O_4 + 4H_2O$ (Eq. 4)

$2\ Fe_3O_4 + ½\ O_2 \rightarrow 3\ Fe_2O_3$ (Eq. 5)

$Fe^{2+} + ½\ H_2O + ¼\ O_2 \rightarrow Fe^{3+} + OH^-$ (Eq. 6)

$2\ Fe^{3+} + 6\ OH^- \rightarrow Fe_2O_3 + 3\ H_2O$ (Eq. 7)

The size distribution and morphology of the biocatalysts before and after immobilization was assessed by TEM and is shown in Figure 6.3. The particles had an average diameter of 6.0±1.3 and 13.4±4.3 nm before and after immobilization, respectively showing that the particle size clearly increased due to immobilization. Several laccase isozymes of *Trametes versicolor* have been described. They have a molecular weight of 60 to 70 kDa and dimensions of roughly 6.5× 5.5 × 4.5 nm (Bourbonnais et al. 1995; Collins et al. 1996; Bertrand et al. 2002; Piontek et al. 2002). The molecular weight of the laccases used in the present study was 63 kDa as determined by SDS-PAGE, and the enzyme purity was estimated to be 65.7±6.2 %. Consequently, the increase in particle size due to immobilization indicates that on average not more than one layer of laccase was immobilized on the particle surface.

The magnetic properties of the particles before and after surface modification and after enzyme immobilization were assessed by magnetization measurements. Magnetization curves are shown in Figure 6.4. Nanoparticles showed typical superparamagnetic behavior since the magnetization curves for all particles showed no hysteresis, were completely reversible and no remanence or coercivity was observed (Cullity and Graham 2008).

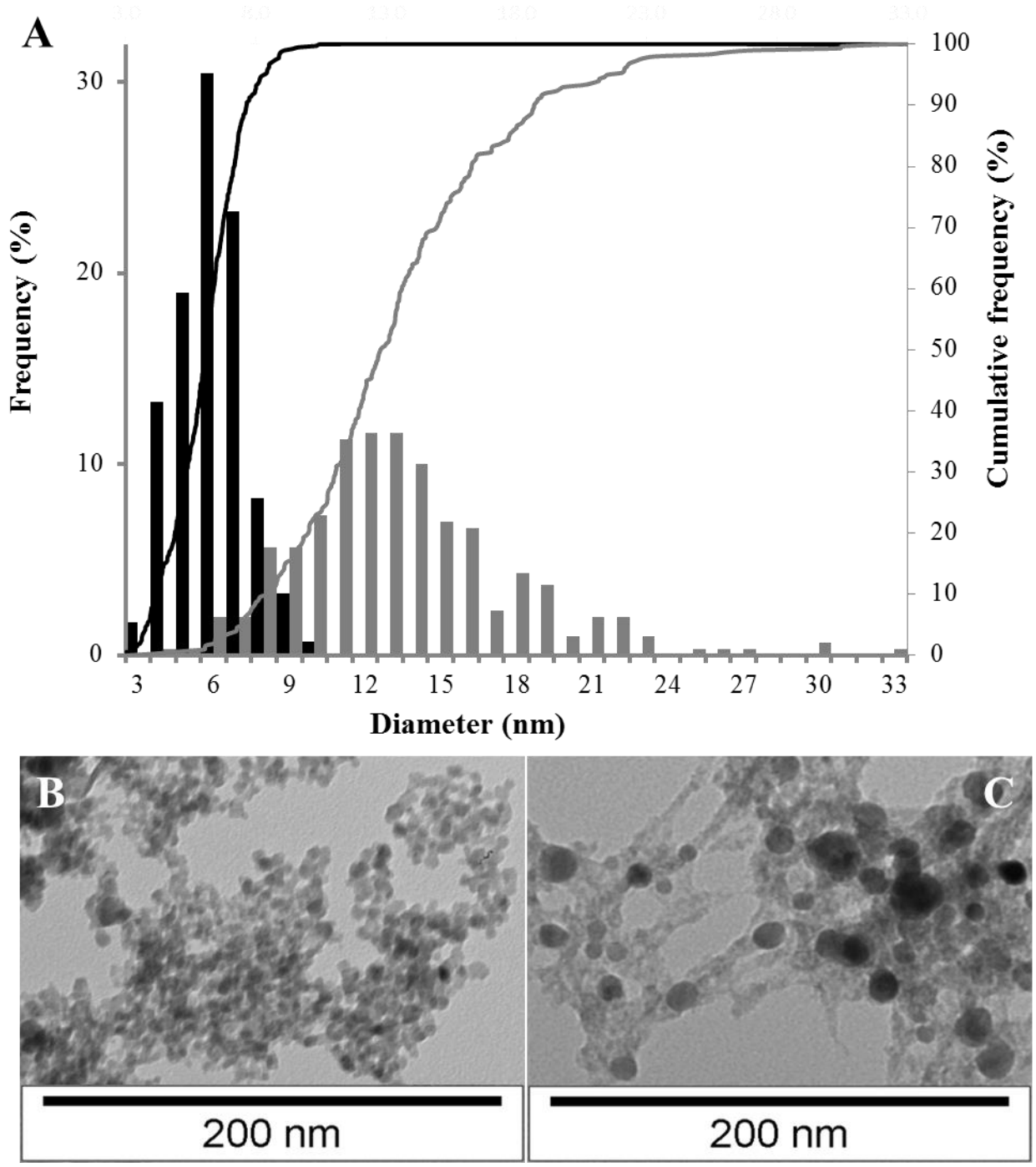

Figure 6.3 Distribution of particle diameters (A) of MP (black) and TVL-MP (grey). Bars show the frequency of particles with the corresponding diameter (rounded to 1 nm). Lines show the cumulative frequency, i.e., the percentage of particles that have at the most a diameter as displayed on the x-axis. TEM pictures of MP (B) and TVL-MP (C; adapted from Gasser et al. 2016)

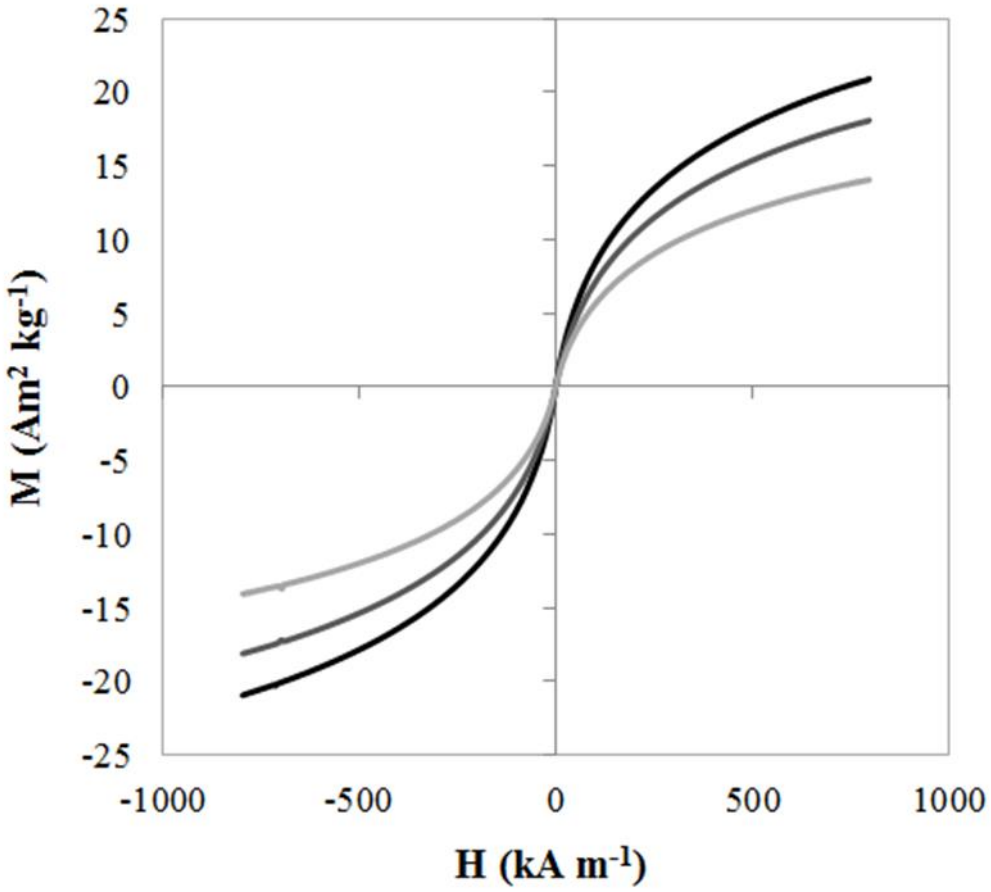

Figure 6.4 Magnetization curves of MPs (black), MPs functionalized with APTES (dark grey), and TVL-MP (light grey) measured at room temperature (adapted from Gasser et al. 2016).

6.2.2. Particle surface modification

Different specific APTES amounts were tested for surface modification of MP. Increasing amounts from 1 to 15 mmol APTES g^{-1} MP led to considerable increases in enzymatic activity of resulting biocatalysts (Figure 6.5). Increasing APTES from 15 to 18 mmol g^{-1} MP led to a slight increase in specific enzymatic activity of resulting biocatalysts while a further increase to 24 mmol APTES g^{-1} MP resulted in no further activity increase. Therefore, an APTES amount of 18 mmol g^{-1} MP was used for surface modification of MPs in all further experiments.

Zeta potential and FTIR measurements gave further evidence for successful surface modification. Zeta potential increased from 0.0 ± 1.9 to 16.2± 0.9 mV at pH 7 by modifying MPs with 18 mmol APTES g^{-1} MP indicating the presence of NH_3^+ groups on the particle surface. The obtained zeta potential of 0 mV of unmodified MP corresponds well to other studies investigating magnetite nanoparticles reporting the isoelectric point of magnetite nanoparticles to be around pH 7 (Vayssières et al. 1998; Kulak et al. 2014). FTIR spectra of MP modified with APTES showed two distinct absorption bands at 1582 and 1346 cm^{-1}, which are ascribed to NH_2 bending and Si–C stretching vibrations on the surface of the particles, respectively (Figure 6.6, McCarthy et al. 2012) which were not observed in spectra of

native MP. Furthermore, at 2920 cm^{-1}, a less pronounced band was observed in the spectra of the APTES modified MP likely due to stretching vibration of the C–H bond (Ma et al. 2003; McCarthy et al. 2012).

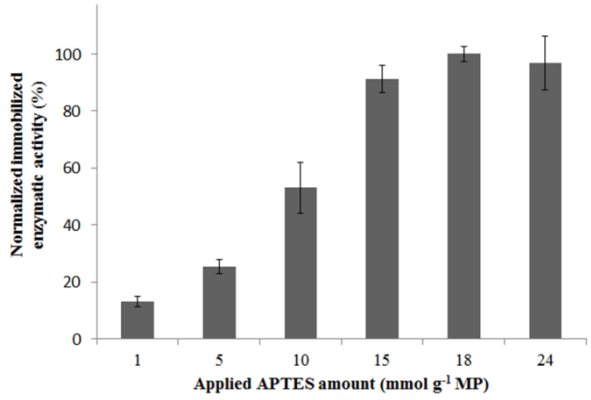

Figure 6.5 Normalized enzymatic activity of TVL-MP after surface modification with different specific APTES amounts. Error bars represent standard deviations (n=3). Average specific enzymatic activity measured at 18 mmol APTES g^{-1} MP was defined as 100 % (adapted from Gasser et al. 2016).

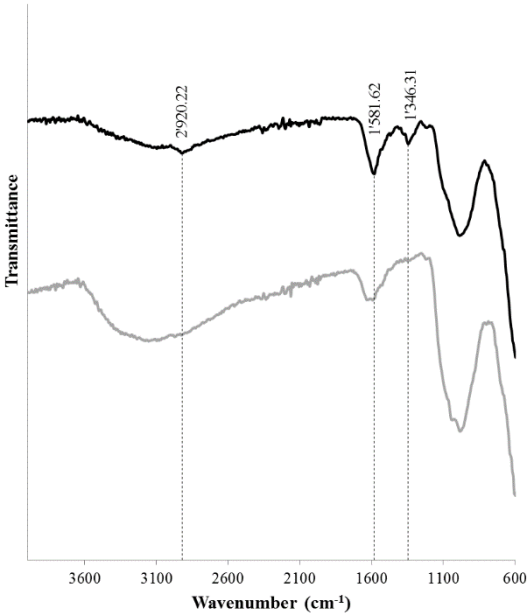

Figure 6.6 FTIR spectra of APTES coated (black) and uncoated (grey) MP (adapted from Gasser et al. 2016)

6.2.3. Optimization of immobilization procedure

6.2.3.1. Optimization regarding maximal specific enzymatic activity

The further reaction steps were optimized for maximal specific activity of the biocatalysts using RSM to gain maximum information from a given set of experiments by separating statistical deviations from statistically significant effects of the investigated parameters on the experimental results. The parameters that are actively controlled and varied between different experiments are called factors. In the present study the influence of five factors, i.e., protein amount, glutaraldehyde amount, time for enzyme adsorption, time for incubation with glutaraldehyde, and pH on the specific enzymatic activity of the resulting biocatalysts after immobilization were investigated. Factors were varied from 15 to 200 mg g^{-1} MP, 0.5 to 8.0 mmol g^{-1} MP, 0.5 to 4 h, 0.5 to 24 h, and 5 to 9 for protein amount, cross-linker amount, protein adsorption time, glutaraldehyde reaction time, and pH, respectively. A third-degree polynomial model was fitted to the results and subsequently reduced to only contain significant factors ($p \leq 0.05$) and factors necessary to maintain model hierarchy. Conducted experiments, obtained results, the ANOVA results of the response surface reduced cubic model, and the final equation in terms of the actual factors are appended in the appendix A1.1 (Table A. 1, Table A. 2, and Table A. 3).

The model predicted highest specific enzymatic activity of biocatalysts to be 4.90±0.48 kU g^{-1} MP using 94.5 mg protein g^{-1} MP, 5.21 mmol glutaraldehyde g^{-1} MP at pH 9 and conducting the protein adsorption step for 4 h and the glutaraldehyde reaction for 24 h. The corresponding experiment was conducted and biocatalysts with a specific activity of 4.60±0.27 kU g^{-1} MP were produced. The model predictions seemed to be suitable since the obtained specific activity was within one standard deviation of the specific activity predicted by the model. It was calculated that 76.0±1.5 mg proteins were immobilized per gram MP based on protein losses determined during washing. Furthermore, 69.4±5.2 % of the initially applied enzymatic activity was immobilized on the MP.

The effect of the interaction effects of the different factors included in the model are shown in Figure 6.7. Factors that are not shown were held constant at the predicted optimal conditions. Results indicate that protein amount and glutaraldehyde amount are the most essential factors influencing specific activity of the biocatalysts. Predicted optimal glutaraldehyde amount regarding maximal enzymatic activity increased from 4.25 to 6.35 mmol g^{-1} MP with increasing protein amounts from 15 to 200 mg protein g^{-1} MP while leaving the other factors at predicted optimal conditions. Increasing glutaraldehyde reaction time led to increasing specific activity while leaving the other factors at predicted optimal conditions. The effect was predicted to be more pronounced at lower glutaraldehyde amounts. Specific activity increased from 0.37±0.48 to 2.84±0.48 kU g^{-1} MP and from 2.48±0.48 to 4.14±0.48 kU g^{-1} MP when increasing glutaraldehyde reaction time from 0.5 to 24 h for glutaraldehyde amounts of 0.5 and 8.0 mmol g^{-1} MP, respectively while leaving the other factors at predicted optimal conditions.

The influences of the two-factor interaction effects of glutaraldehyde reaction times and protein adsorption time, pH and protein adsorption time, and pH and glutaraldehyde reaction time on the specific activity were predicted to be less substantial when leaving the other factors at predicted optimal conditions. Specific activities were predicted to be lowest, i.e., 2.95±0.48 kU g^{-1} MP at glutaraldehyde reaction time of 0.5 h, protein adsorption time of 4.0 h, and pH 9.

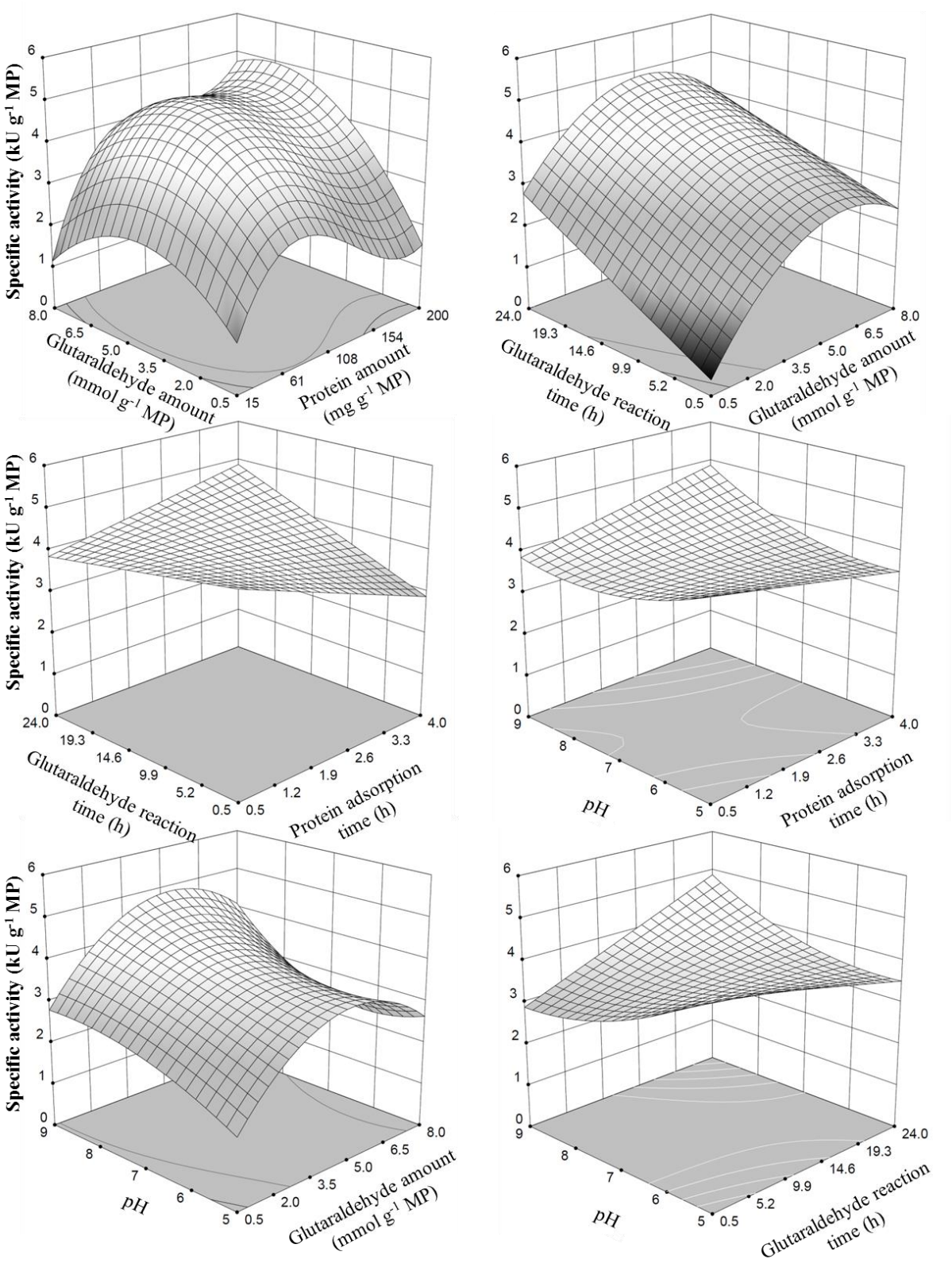

Figure 6.7 Interaction effects of the different interactions predicted by the response surface reduced third-degree polynomial model. Factors that are not shown were held constant at predicted optimal conditions, i.e., 94.5 mg protein g^{-1} MP (protein amount), 5.21 mmol glutaraldehyde g^{-1} MP (glutaraldehyde amount), 4 h (protein adsorption time), 24 h (glutaraldehyde reaction time), and 9 (pH; adapted from Gasser et al. 2016).

6.2.3.2. Optimization regarding stability

The stabilities of biocatalysts were tested under various conditions, i.e., pH 3, 5, 7, and 9 and at pH 7 in the presence of 30 % (v/v) MeOH, 30 % (v/v) acetone, 1 mM H_2O_2, or 100 µM NaN_3. The influence of the same five factors as for the optimization regarding specific enzymatic activity, i.e., protein amount, glutaraldehyde amount, time for enzyme adsorption, time for incubation with glutaraldehyde, and pH on the residual enzymatic activity of the TVL-MP was investigated using RSM. For every condition tested, a second-degree polynomial model was fitted to the results and subsequently reduced to only contain significant factors and factors necessary to maintain model hierarchy. Model results are summarized in the appendix A1.2 (Table A. 4-Table A. 14).

To determine the formulation predicted to yield particles with best properties regarding stability that takes into account the biocatalyst stability in all tested conditions, a multiple response method was applied (Myers et al. 2009). A desirability function was used (Eq. 3) which is the geometric mean of the normalized residual enzymatic activities of all tested conditions at specific time points (starting activities were defined as 1). A second-degree polynomial model was fitted to the desirabilities and subsequently reduced to only contain significant factors and factors necessary to maintain model hierarchy. Model results are summarized in the appendix A1.2 (Table A. 13 and Table A. 14). Predicted optimal biocatalyst formulations regarding biocatalyst stability for all nine models are summarized in Table A. 15. Figure 6.8 shows the predicted influence of the three significant factors, i.e., protein amount, glutaraldehyde amount, and pH and the interaction effect between protein amount and glutaraldehyde amount predicted by the model.

Glutaraldehyde is predicted to have the most pronounced effect on biocatalyst stability. Increasing glutaraldehyde amounts from 0.5 to 5.15 mmol g^{-1} MP while leaving protein amount and pH constant at 111 mg g^{-1} MP and 9, respectively, is predicted to lead to increasing biocatalyst stability (desirability increases from 0.34±0.04 to 0.59±0.04). Further increases in glutaraldehyde amounts are predicted to lead to slight decreases in biocatalyst stability. Changing protein amounts from 15 to 200 mg g^{-1} MP while leaving glutaraldehyde amounts and pH constant at 5.15 mmol g^{-1} MP and 9, respectively, is predicted to have a smaller effect on biocatalyst stability in comparison (desirability varies between 0.49±0.04 and 0.59±0.04). Stability is predicted to be highest at 111 mg g^{-1} MP. Predicted optimal glutaraldehyde amounts increased from 4.89 to 5.39 mmol g^{-1} MP with increasing protein amounts from 15 to 200 mg protein g^{-1} MP. The model predicts no interaction effect between pH and the other two significant factors. Increasing pH from 5 to 7 is predicted to lead to no considerable changes in biocatalyst stability (desirability increases by 0.01). Further increasing pH from 7 to 9 is predicted to lead to a more substantial increase in biocatalyst stability (desirability increases by 0.07).

Biocatalysts were produced according to the predicted conditions for overall optimal biocatalyst stability, i.e., with 111 mg protein g^{-1} MP, 5.15 mmol glutaraldehyde g^{-1} MP at pH 9 and conducting the protein adsorption step for 0.5 h and the glutaraldehyde reaction for 24 h. The times were chosen

based on the predictions for optimal conditions regarding biocatalyst stability by the three models predicting significant effects for protein adsorption time (MeOH) or glutaraldehyde reaction time (pH 9, NaN_3).

Magnetic biocatalysts predicted to have optimal stability were produced in triplicate and had a specific enzymatic activity of 4.31 ± 0.27 kU g^{-1} MP corresponding well to the predicted value by the response surface reduced third-degree polynomial model of 3.86± 0.48 kU g^{-1} MP. Stability of these biocatalysts and the biocatalysts produced using the formulation for maximal enzymatic activity was subsequently assessed in all eight conditions and compared with dissolved laccases.

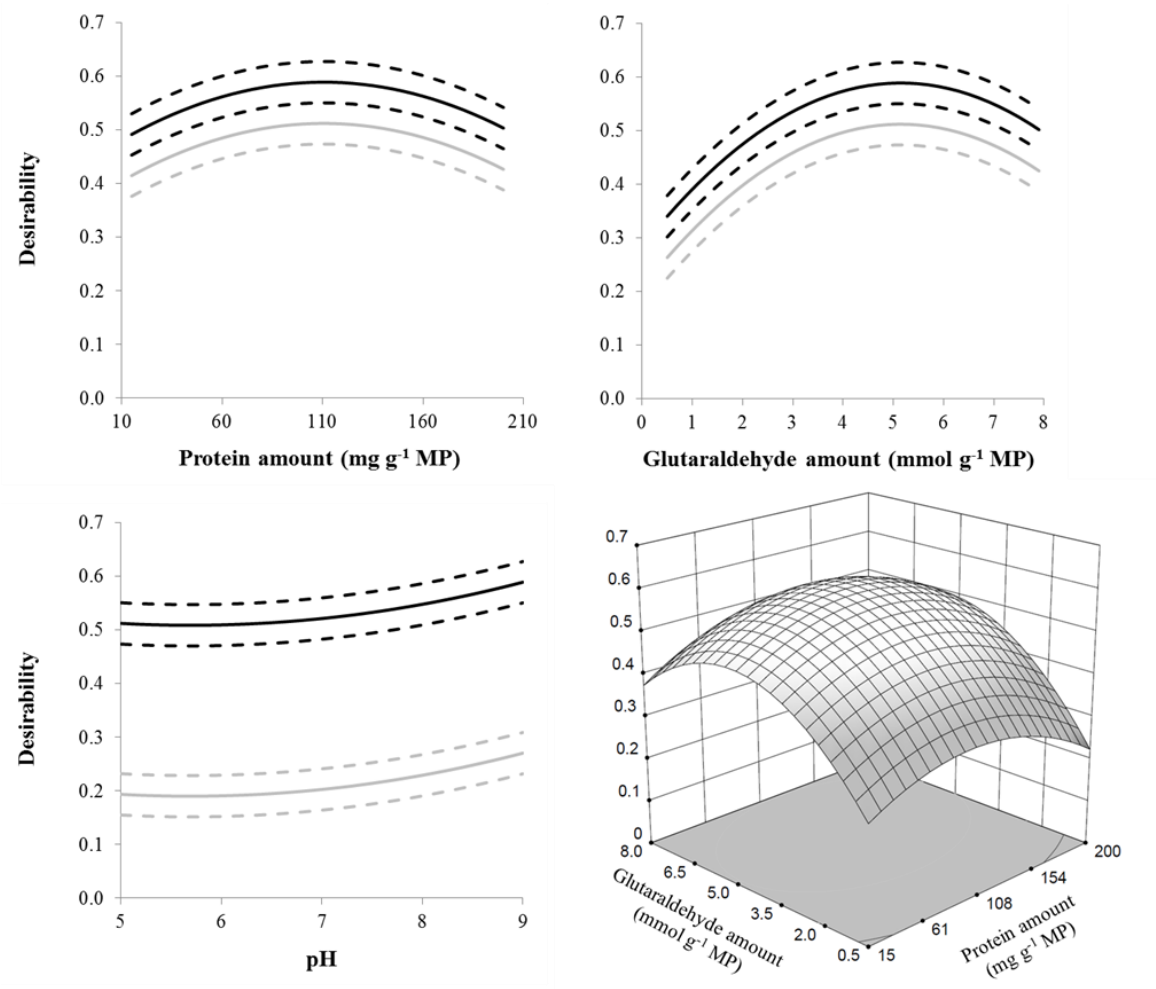

Figure 6.8 Predicted effects of the three significant factors predicted by the response surface reduced second-degree polynomial model. Dashed lines show standard deviations. For showing the effect of protein amount, glutaraldehyde amount was kept constant at 5.15 mmol g^{-1} MP and pH was 5 (grey line) and 9 (black line). For showing the effect of glutaraldehyde amount protein amount was kept constant at 111 mg g^{-1} MP and pH was 5 (grey line) and 9 (black line). For showing the effect of pH protein amount and glutaraldehyde amount was 15 mg g^{-1} MP and 0.5 mmol g^{-1} MP, respectively (grey line), and 111 mg g^{-1} and 5.15 mmol g^{-1} MP, respectively (black line). For showing the interaction between glutaraldehyde amount and protein amount, pH was kept constant at 9 (adapted from Gasser et al. 2016).

6.2.4. Biocatalyst stability and catalytic properties

6.2.4.1. Biocatalyst stability

Increased enzymatic stability is one of the main advantages of immobilized enzymes next to their facilitated reuse. Experiments evaluating the enzymatic stability at the eight different conditions used for model development were conducted with biocatalysts predicted to have optimal stability and highest specific activities, and with dissolved laccases. Changes over 63 d of incubation in all tested conditions are shown in Figure 6.9. Comparison of model predictions and measured values are shown Table 6.7.

Immobilized enzymes were considerably more stable than dissolved enzymes under all tested conditions. There were little differences regarding stability between the two tested paramagnetic biocatalysts. This was expected since formulations for biocatalyst production did not differ substantially between the two biocatalysts and predicted desirability by the model taking into account the residual stabilities measured in all eight tested conditions was also virtually the same, i.e., 0.586 and 0.589 for particles with predicted highest specific activity and predicted optimal stability, respectively.

Table 6.7 Comparison of residual activities predicted by the different response surface reduced quadratic models with measured values (±standard deviation, n=3 for measured values). TVL-MPs (max. activity) were produced according to the formulation predicted to yield maximal activity and TVL-MPs (max. stability) were produced according to the formulation predicted to yield maximal stability by the model considering overall stability of the biocatalysts. For comparison values for dissolved laccases are given as well (adapted from Gasser et al. 2016).

	Dissolved laccase	**TVL-MP (max. activity)**		**TVL-MP (max. stability)**	
	Measured	**Measured**	**Predicted**	**Measured**	**Predicted**
pH 3 (1 day)	1.7±0.4	58.9±1.8	62.6±0.1	61.6±3.7	61.6±0.1
pH 5 (14 days)	3.1±0.8	52.5±0.7	57.1±0.6	51.0±3.6	56.0±0.6
pH 7 (14 days)	34.6±1.7	84.3±1.1	94.0±7.4	88.1±4.2	94.3±7.4
pH 9 (14 days)	2.4±0.1	38.8±0.9	41.3±0.4	36.8±1.0	41.9±0.4
30% Acetone (14 days)	12.5±0.9	39.2±0.4	37.6±0.1	39.9±1.3	38.8±0.1
30% MeOH (7 days)	33.7±5.9	50.7±1.2	53.6±0.0	49.9±1.3	59.1±0.0
NaN_3 (100 µM, 14 days)	24.9±5.6	68.4±1.6	83.5±9.7	71.7±1.7	82.0±9.7
H_2O_2 (1 mM, 14 days)	33.8±1.7	80.0±3.0	84.7±7.9	83.9±6.4	86.2±7.9
Overall stability (desirability)	0.106±0.014	0.569±0.012	0.586±0.038	0.576±0.026	0.589±0.038

Immobilized enzymes remained fairly stable, i.e., did not lose more than 20 % of their initial activity at pH 7 during 14 d irrespective whether 1 mM H_2O_2 was added in the beginning of the experiment (Figure

6.9A) or not (Figure 6.9C). After 63 d residual activity was still above 60 %. For the dissolved enzymes, there were also no considerable differences in residual stabilities between the experiments conducted at pH 7 with or without H_2O_2. Therefore, no apparent enzyme inactivation due to H_2O_2 occurred. In a further experiment conducted at pH 7, the laccase inhibitor NaN_3 was added (Figure 6.9G). This yielded slightly lower residual activities for all tested biocatalysts compared with experiments conducted at pH 7 without addition of NaN_3 indicating that the enzymes were slightly inhibited by NaN_3 irrespective of immobilization. Residual activities were 82.2±0.9 and 83.8±3.0 % in the presence of NaN_3 and 91.7±1.1 and 90.6±2.1 % in the NaN_3 free samples after 1 d for the biocatalysts produced for highest specific activity and optimal stability, respectively. For the dissolved enzymes, residual activities after 1 d at pH 7 and in the presence of NaN_3 did not differ significantly (p=0.404; student's t test, two-sample equal variance, two-tailed distribution) and were 84.6±3.8 and 88.1±5.2 % for samples without and with NaN_3, respectively. However, significant differences became apparent after 4 d (p=0.003, student's t test, two-sample equal variance, two-tailed distribution). Residual activities were 76.4± 3.5 and 63.3± 0.7 % for samples without and with NaN_3, respectively. Presence of solvents also had a negative effect on enzymatic stability at pH 7. Enzymatic activity of dissolved enzymes decreased to 27.4±1.0 % during the first 3 d in 30 % acetone and then decreased more slowly to 12.5±0.9 % after 14 d (Figure 6.9E) while biocatalysts produced for highest specific activity and optimal stability retained 39.2±0.4 and 39.9±1.3 % of their initial activity, respectively after 14 d of incubation. In presence of 30 % MeOH, differences between dissolved and immobilized enzymes were least considerable for all tested conditions (Figure 6.9F). Dissolved enzymes, biocatalysts produced for highest specific activity, and optimal stability retained 28.0±0.9, 37.4±0.9, and 41.1±1.5 % of their initial activity after 14 d, respectively.

Of all tested conditions, enzymes were least stable at pH 3 (Figure 6.9A). Dissolved enzymes only retained 1.7±0.4 % of their initial activity after one day of incubation. Immobilization enhanced enzymatic stability considerably but after ten days of incubation also only 1.2±0.2 and 1.3±0.2 % of the initial activity was left for biocatalysts produced for highest specific activity and optimal stability, respectively. Dissolved enzymes were also not very stable at pH 5 (Figure 6.9B) and 9 (Figure 6.9D). After 14 d of incubation at pH 5 and 9, only 3.1±0.8 and 2.4±0.1 % of the initial enzymatic activity remained, respectively. Under these conditions, immobilization also improved the enzymatic stability substantially. At pH 5 after 14 d of incubation 52.5±0.7 and 51.0±3.6 % and after 63 d 7.7±0.4 and 7.9±0.5 % of the initial activity remained for the biocatalysts produced for highest specific activity and optimal stability, respectively. At pH 9 after 14 d of incubation 38.8±0.9 and 36.8±1.0 % and after 63 d 17.5±0.9 and 18.3±1.4 % of the initial activity remained for the biocatalysts produced for highest specific activity and optimal stability, respectively.

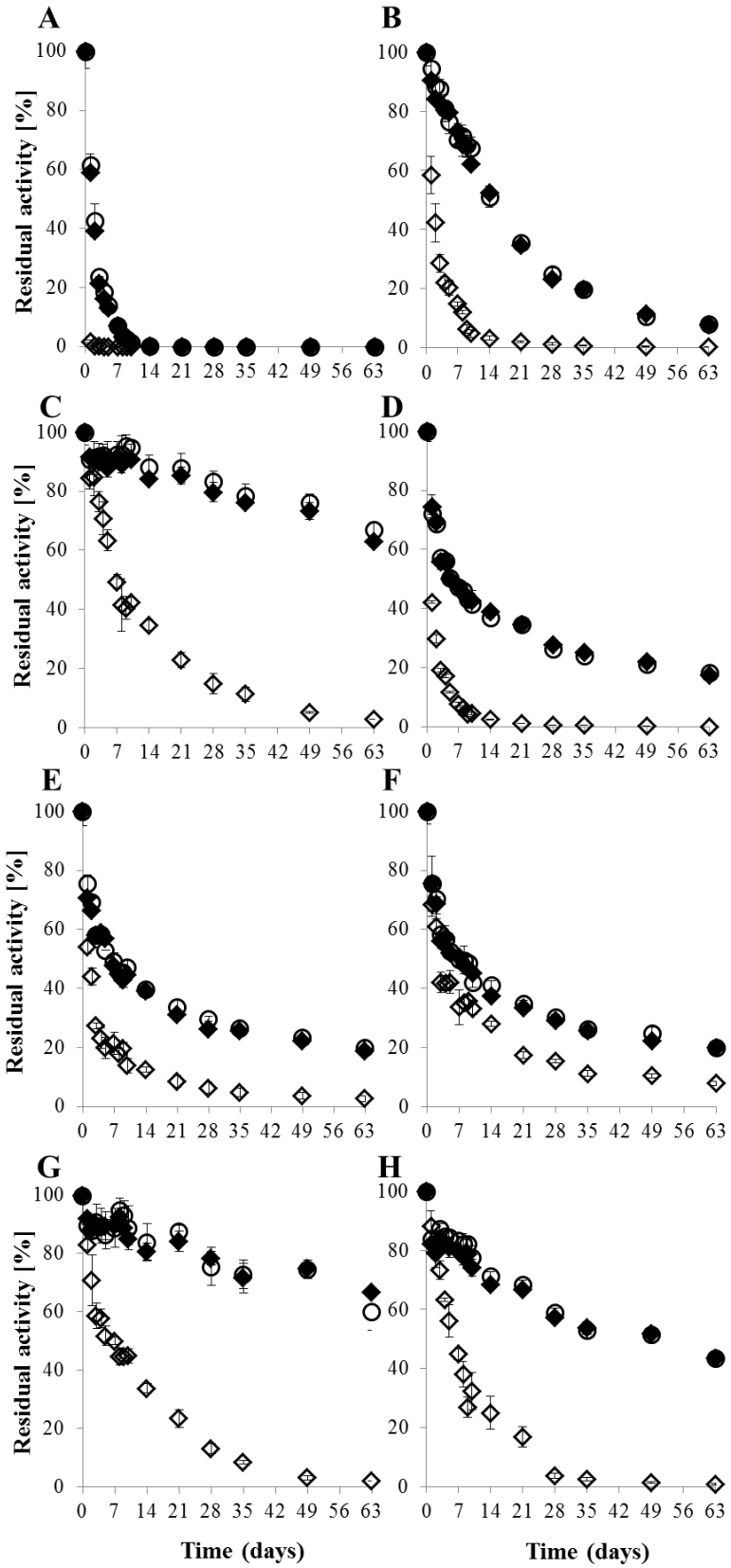

Figure 6.9 Residual activities of free laccases (empty diamond) and TVL-MPs produced using formulation for maximal specific activity (black diamonds) and stability (empty circles) incubated at pH 3 (A), pH 5 (B), pH 7 (C), pH 9 (D), and in presence of 30 % (v/v) acetone (E), 30 % (v/v) MeOH (F), 1 mM H_2O_2 (G), and 100 µM NaN_3 (H) at pH 7. Error bars show standard deviations (n=3, adapted from Gasser et al. 2016).

6.2.4.2. Assessment of biocatalyst activity towards laccase substrates

The influence of immobilization on the catalytic efficiency of the biocatalysts towards several phenolic compounds, ABTS, and the precursor used for the production of the phenoxazinone dye has been assessed by determination of the apparent k_{cat} and K_m values. The obtained values are summarized in Table 6.8. While the K_m^{app} values were higher and k_{cat}^{app} values were lower for TVL-MP than for the free enzymes for all phenolic compounds, the sequence of the catalytic efficiencies $(k_{cat}/K_m)^{app}$ of the different phenolic compounds remained the same. Regarding ABTS and 3-amino-4-hydroxybenzenesulfonic acid, K_m^{app} and k_{cat}^{app} increased due to immobilization.

Table 6.8 Apparent kinetic constants for the oxidation of various substrates at 25 °C and pH 5 by TVL-MP and TVL and extinction coefficients used for quantitation (adapted from Gasser et al. 2016).

	Extinction coefficient Wavelength (nm)	**(M^{-1} cm^{-1})[a]**	**TVL-MP k_{cat}^{app} (s^{-1})[b]**	**K_m^{app} (mM)**	**(k_{cat}/K_m)^{app} (s^{-1} mM^{-1})**	**TVL k_{cat}^{app} (s^{-1})[b]**	**K_m^{app} (mM)**	**(k_{cat}/K_m)^{app} (s^{-1} mM^{-1})**
Guaiacol	470	26,600	18.5± 1.9	0.29± 0.04	63.4±11.4	23.8± 2.4	0.25±0.03	93.8±14.1
2,6-DMP	477	14,800	39.1± 4.0	0.030± 0.004	1,300±218	45.0± 4.6	0.008± 0.001	5,620± 1,080
Vanillic acid	350	1,315	3.4± 0.4	1.03± 0.26	3.3±0.9	11.8± 1.4	0.67±0.14	17.5±4.1
Syringic acid	360	1,105	33.4± 3.6	0.42± 0.08	80.4±17.7	38.7± 3.9	0.17±0.03	227±43
Vanillin	410	807	3.8±0.5	7.3±1.5	0.5±0.1	7.2±0.8	3.0±0.6	2.4±0.5
Syringaldehyde	360	1,065	12.2± 1.3	0.082±0. 013	149±28	18.8± 1.9	0.080± 0.010	235±37
ABTS	420	35,170	34.8± 3.6	0.044± 0.007	783±143	29.0± 3.0	0.015± 0.002	1,930±320
3-amino-4-hydroxybenzen-sulfonic acid	420	8,935	51.5±5. 4	0.27±0.0 4	192±33	33.9± 3.6	0.11±0.02	298±62

[a] Extinction coefficients for guaiacol and 2,6-DMP were taken from Roy and Abraham (2006) and Hommes et al. (2013), respectively. All other values were determined at assay conditions.

[b] Errors were calculated based on the standard deviations of the kinetic constants, the applied laccase amounts, and the laccase molecular weight by means of error propagation. All experiments were conducted in triplicates.

6.2.5. Immobilization of various LMEs on superparamagnetic particles

Next to TVL, two additional LME were immobilized on MP to demonstrate the suitability of the immobilization method for immobilization of various enzymes. Selected enzymes were glucose oxidase and DyP. Chosen conditions during immobilization were the optimal conditions derived for TVL regarding maximal specific activity (6.2.3.1). Glucose oxidase was successfully immobilized. Resulting particles had an enzyme load of 14.0±0.2 kU g^{-1} MP corresponding to an immobilization yield of 69.9±3.4 %. However, DyP lost all activity during immobilization.

Preliminary experiments incubating DyP with glutaraldehyde at pH 7 and 9 were conducted for 60 h, since it was suspected that the internal cross-linking of the enzyme with glutaraldehyde might inactivate DyP. As discussed below (6.2.7) glutaraldehyde forms different polymers at acidic conditions compared

to basic conditions and glutaraldehyde polymers at basic conditions are expected to lead to enhanced cross-linking of the enzymes. Therefore, immobilization at lower pH might lead to less cross-linking allowing immobilization of active DyP. While samples incubating DyP with glutaraldehyde at pH 9 had virtually no activity left, samples at pH 7 retained 56 % of their initial activity. Glutaraldehyde free controls showed that DyP had still 65 % of the initial activity at pH 9. Therefore, a substantial part of enzyme inactivation was due to the presence of glutaraldehyde. Consequently, the immobilization of DyP was repeated at lower pH, i.e., 6.5 and yielded MP with an enzyme load of 0.06 kU g^{-1} MP corresponding to an immobilization yield of 65.8±4.4 %. The lower enzyme load of DyP-MP compared to glucose oxidase-MP and TVL-MP can be explained by the differences in specific enzymatic activities of the different enzymes, i.e., 0.88, 12.5, and 26.5 kU g^{-1} protein for DyP, TVL, and glucose oxidase, respectively. DyP-MPs were also able to transform a nonphenolic dye, i.e., Azure B as verified by the corresponding assay. DyP-MP had an enzyme load of 0.12±0.02 U g^{-1} against Azure B.

Glucose oxidase and DyP were successfully immobilized on MP showing the versatility of the developed immobilization method. Furthermore, results indicate that the formulation for enzyme immobilization has to be adapted for certain enzymes that are inactivated by glutaraldehyde at basic conditions.

6.2.6. Application example: Dye production

To demonstrate the reusability of TVL-MP they were applied for the production of a phenoxazinone dye, i.e., 2-amino-3-oxo-3H-phenoxazine-8-sulfonic acid from 3-amino-4-hydroxybenzenesulfonic acid over ten consecutive reaction cycles. Particles were separated magnetically after each cycle from the colored product. Subsequently, aqueous phase was centrifuged to remove virtually all particles from reaction solutions before the concentration of the phenoxazinone dye was determined spectrophotometrically. Enzymatic activities were determined at the beginning of each reaction cycle before 3-amino-4-hydroxybenzenesulfonic acid addition. Results are shown in Figure 6.10. Virtually, 100 % of 3-amino-4-hydroxybenzenesulfonic acid was converted to the phenoxazinone dye in all ten cycles demonstrating the reusability of the biocatalysts. However, after every cycle, some particles were lost due to inefficient separation. After ten reaction cycles, 28.4±3.7 % of the initially applied enzymatic activity remained in the reaction vessel. Losses due to inefficient separation were determined by measuring the enzymatic activities of supernatants before and after centrifugation. On average, 15.5±8.1 % of the enzymatic activity present at the beginning of a reaction cycle was lost after magnetic separation while 1.7±1.4 % remained in the supernatant after centrifugation showing that losses of enzymatic activity were predominantly due to inefficient particle separation and not due to other effects like, e.g., enzymes leaching from the particles. Calculation of the balance of the enzymatic activities over the whole experiment yielded 110.3±10.3 % of the initially applied activity indicating that enzymes remained stable during the experiment.

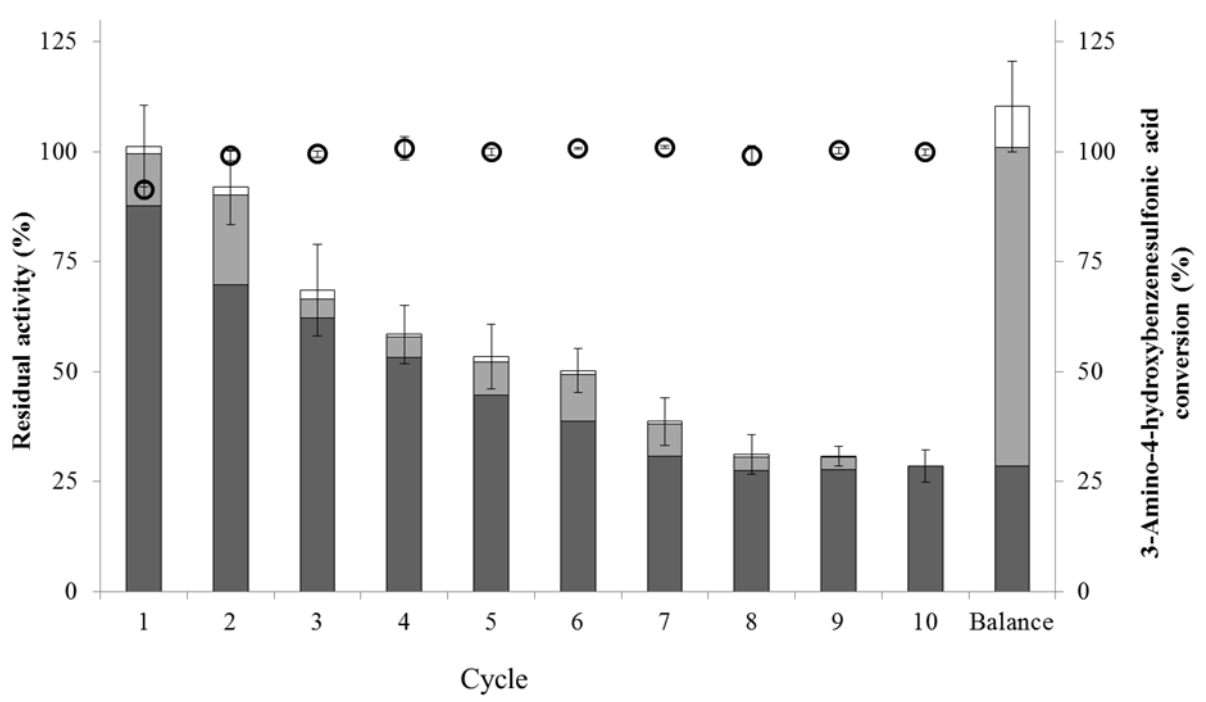

Figure 6.10 Conversion of 3-amino-4-hydroxybenzenesulfonic acid to phenoxazinone dye with TVL-MP over ten reaction cycles (empty circles). Bars show apparent enzymatic activity during treatment remaining in reaction vessels after magnetic separation (dark grey), separated by centrifugation from supernatants (light grey), and left in supernatants after centrifugation (white). A balance summing up apparent enzymatic activity remaining after ten cycles, total enzymatic activity separated from all supernatants by centrifugation, and left in supernatants after centrifugation is shown as well. Error bars of residual activities show uncertainties calculated based on the standard deviations of the different measurements (n=3) by means of error propagation. Error bars of 3-amino-4-hydroxybenzenesulfonic acid conversion show standard deviations (n= 3, adapted from Gasser et al. 2016).

6.2.7. Discussion of immobilization procedure

In the present chapter, enzymes were immobilized on MPs using the sorption-assisted surface conjugation method developed and optimized for enzyme immobilization on fsNP in chapter 6.1. The procedure is depicted schematically in Figure 6.11. Surface modification of MPs with APTES is followed by adsorption of the enzyme molecules on the particle surface. This brings the enzyme in close proximity to the MPs facilitating the subsequent cross-linking using glutaraldehyde. This general procedure was optimized in the present study regarding maximal specific enzymatic activity and optimal enzymatic stability of the resulting superparamagnetic biocatalysts.

MPs were produced by a co-precipitation of ferrous and ferric iron at alkaline conditions. Fast addition of NaOH to the iron containing solution led to immediate supersaturation due to the low solubility of iron in alkaline solution resulting in rapid nucleation of ferrite nanoparticles (Baumgartner et al. 2013). Particle size was controlled by applied ionic strength (1.0 M) and pH (11.0) during particle formation

(Vayssières et al. 1998). Obtained average particle size was 6.0±1.3 nm corresponding well to particles obtained in other studies reporting production of MPs with an average diameter of approximately 6 nm applying the same conditions regarding pH and ionic strength (Vayssières et al. 1998).

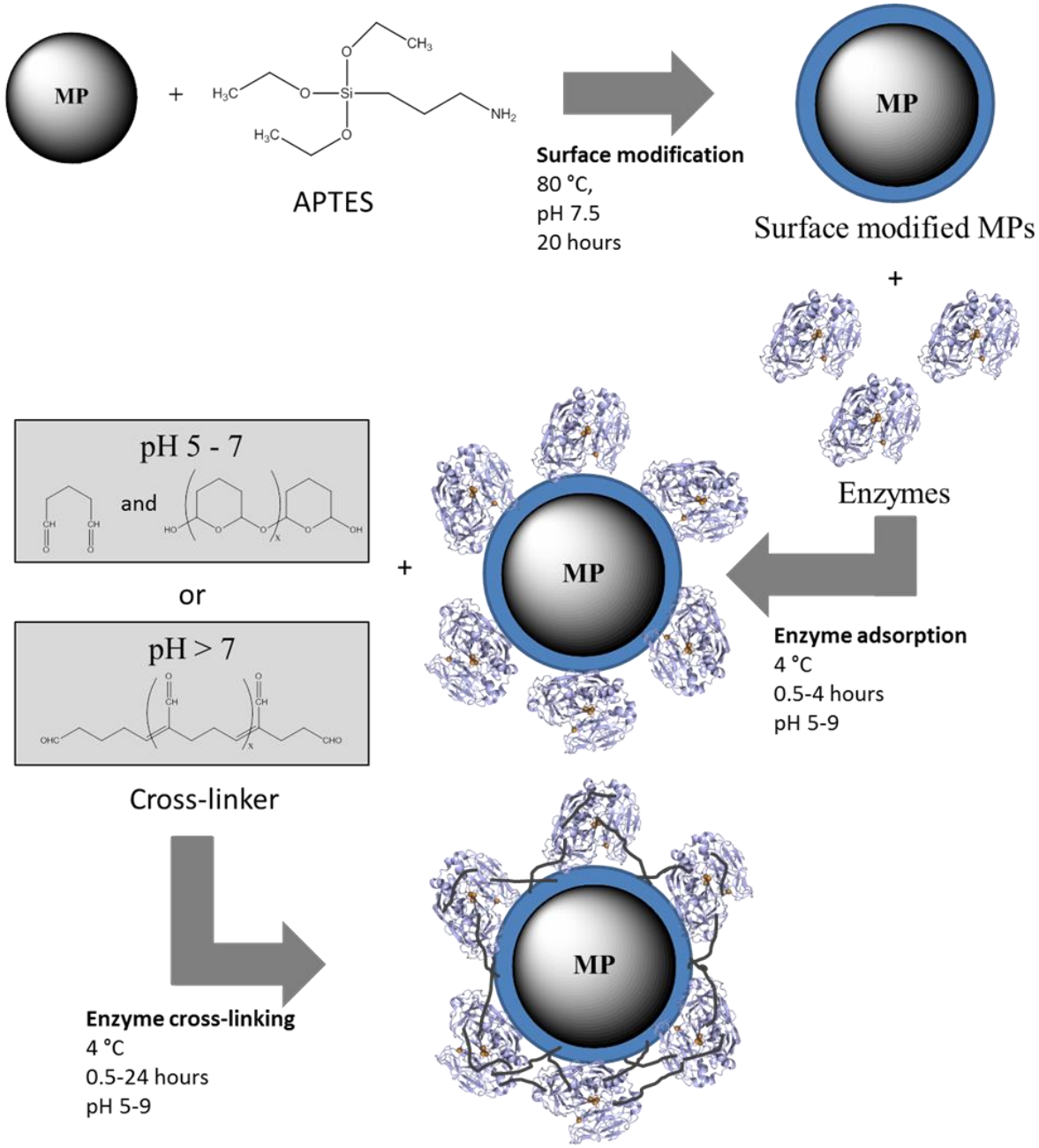

Figure 6.11 Schematic description of the sorption assisted surface conjugation method developed. Investigated ranges of reaction times and pH are stated (adapted from Gasser et al. 2016).

MPs showed typical superparamagnetic behavior usually observed for sufficiently small magnetic particles. It was calculated for magnetite particles that particles with a diameter below ~26 nm show superparamagnetic behavior at 27 °C (Cullity and Graham 2008). Since magnetization did not reach saturation but still increased asymptotically for high fields the saturation magnetization for the different

particles was calculated by fitting M vs. 1/H extrapolating the magnetization value to 1/H=0 (Liu and Zhang 2001). Saturation magnetization was estimated to be 26.7, 23.2, and 18.0 $Am^2 kg^{-1}$ for MPs, MPs functionalized with APTES, and MP-TVL, respectively. The decrease in saturation magnetization can be attributed to the coating of the particles adding nonmagnetic mass to the sample weight.

Estimated saturation magnetization values were considerably lower than the saturation magnetization of bulk magnetite (92 $Am^2 kg^{-1}$; Cullity and Graham 2008). Decreasing nanoparticle size is reported to lead to sharp decreases in saturation magnetization of ferrite nanoparticles (Yamaura et al. 2004). While the exact reasons for this decrease are still a matter of investigation, they can be ascribed to surface effects of the particles like magnetically inactive layers containing spins that are not collinear with the magnetic field (Lin et al. 1995). Furthermore, the presence of maghemite or clustering of the particles might contribute to the reduction as well.

Next the MP surface was modified with an organosilane, i.e., APTES. Nanoparticles have a large specific surface area and display many dangling bonds on the surface (Ma et al. 2003). Therefore, the atoms on the surface are suitable to adsorb ions. In case of MPs, the Fe and O atoms on the surface adsorb OH^- and H^+ ions in neutral aqueous solution, respectively leading to particles displaying many OH groups on the surface (Ma et al. 2003). These OH groups react with APTES leading to APTES coating of the particles by chemical bond (Ma et al. 2003). The successful surface modification was shown by FTIR and zeta potential measurements. Furthermore, increasing APTES amounts during the immobilization procedure from 1 to 18 mmol g^{-1} MP led to considerable increases in specific enzymatic activities of resulting biocatalysts giving further indirect evidence of effective MP surface modification.

Subsequently, the further reaction steps were optimized for maximal specific activity and optimal stability of the biocatalysts using RSM. RSM is a useful tool to optimize enzyme immobilization on solid carriers as shown previously (e.g., Demarche et al. 2012; Nair et al. 2013). Optimization for activity as well as stability was investigated since biocatalysts exhibiting high specific activity are not necessarily also most stable. For instance, internal cross-linking of the enzymes might increase their stability while it might coincidentally negatively influence their activity.

First, the enzymes were adsorbed on the surface of the particles. Interactions between the enzymes and the APTES-modified MP surface can be expected to be dominated by electrostatic attraction. The surface of the APTES-modified MPs is expected to be positively charged over the whole pH range that was tested (5 to 9) since the amino groups on the particle surface are anticipated to be protonated in this pH range. However, the degree of protonation and, therefore, the surface charge decreases with increasing pH. The pKa of APTES is 7.6, and it was calculated based on the Henderson–Hasselbach equation that the amino groups of APTES are fully protonated below pH 6 and are neutral above pH 9.5 (Bhat and Genzer 2007). The enzymes on the other hand have a net negative charge since the isoelectric points of TVL isozymes are around or below 3 (Ammann et al. 2014; Bertrand et al. 2002).

Results indicate that increasing protein adsorption time from 30 min to 4 h at pH 9 has a slightly positive effect on the maximal specific activity that can be immobilized on the MPs. Protein adsorption most likely occurs slowly since the APTES modified MPs are only slightly positively charged at this pH. Therefore, longer adsorption times lead to more enzymes in proximity of the particles facilitating cross-linking in the subsequent step. At pH 5, a slightly negative effect of prolonging adsorption time is predicted by the model. Initial adsorption of proteins on the MP surface at pH 5 should occur rapidly at this pH since all APTES amino groups are protonated. Therefore, prolonging adsorption time should not lead to a considerable increase of adsorbed enzymes. The slight decrease in enzymatic activity might be due to unfavorable conformational changes of the enzymes that occur slowly after enzyme adsorption as described for other proteins (e.g., Roach et al. 2005). However, the predicted effect is only small and further studies would be needed to confirm this.

In the next step, the cross-linking agent, i.e., glutaraldehyde was added. This leads to covalent bonds between the amino groups on the MP surface and the enzymes and to internal cross-linking of the enzymes. The internal cross-linking of the enzymes has been shown to increase their rigidity making them more resilient against denaturation (e.g., Cabana et al. 2009; Zimmermann et al. 2011; Hommes et al. 2012; Kumar et al. 2014). Predicted optimal protein amounts and glutaraldehyde amounts were similar for both biocatalyst formulations, i.e., formulations yielding TVL-MP with highest activity and stability. Further increasing protein amounts or glutaraldehyde amounts were not predicted to lead to considerable further changes or (in case of glutaraldehyde) even to particles with slightly lower specific activities. One explanation for the predicted negative effect on enzymatic activity of too high glutaraldehyde concentrations might be the occurrence of extensive enzyme cross-linking leading to losses in enzyme flexibility and, therefore, activity (Barbosa et al. 2014; Kumar et al. 2014). However, further investigations would be necessary to confirm this.

Concerning pH, best results were achieved for specific enzymatic activity and stability for the biocatalysts produced at pH 9. A possible explanation for the beneficial effect of conducting immobilization at higher pH might be the effect of pH on glutaraldehyde reactions with amino groups. Glutaraldehyde forms different polymers at acidic and neutral conditions compared with basic conditions. At acidic or neutral conditions glutaraldehyde forms hemiacetal cyclic monomers and polymers (Barbosa et al. 2014). The hydroxyl groups at each end of these compounds can react with amino groups by nucleophilic substitution (Barbosa et al. 2014). At basic conditions, glutaraldehyde builds a polymeric form of an α,β-unsaturated aldehyde (Barbosa et al. 2014). Every monomer contained in these polymers can potentially react with amino groups through the C–O double bond or the C–C double bond (Barbosa et al. 2014). The positive effect of basic conditions on the enzymatic stability of the biocatalysts might be explained by the higher amount of possible bonds that can be formed between the amino groups of the proteins and particles, and the glutaraldehyde polymers formed at basic conditions compared with the polymers formed at acidic to neutral conditions leading to enhanced

internal cross-linking of the enzymes and, therefore, increased rigidity. Furthermore, cross-linking between the enzymes and the particles might be increased at basic conditions as well leading to stronger attachment.

At optimal conditions regarding enzymatic activity, 69.4±5.2 % of the initially applied enzymatic activity was recovered. This is in a similar range as reported by another study immobilizing laccases on magnetite particles using chitosan/1-ethyl-3-(3-dimethylaminopropyl)-carbodiimide hydrochloride as the cross-linking system (Kumar and Cabana 2016) achieving an immobilization yield of 61.4 %. However, the process described in our study was not optimized regarding immobilization yield but aimed to reach optimal enzymatic activity per gram of MP. Highest immobilization yield obtained in all conducted experiments for process optimization was 153 %, yielding TVL-MP with a relatively modest specific enzymatic activity of 1.15 kU g^{-1} MP. This increase in enzymatic activity above 100 % is most likely due to the increase in k_{cat}^{app} towards ABTS for immobilized enzymes compared with dissolved enzymes (Table 6.8).

Increased enzymatic stability is one of the main advantages of immobilized enzymes next to their facilitated reuse. The increased stability of the paramagnetic biocatalysts due to immobilization was confirmed in stability experiments testing eight different conditions. Immobilized biocatalysts were considerably more stable than dissolved enzymes in all tested conditions. Other studies report similar results regarding stability increases of enzymes after immobilization using glutaraldehyde as cross-linking agent and attribute this to internal cross-linking of the enzymes as well (e.g., Cabana et al. 2009, Zimmermann et al. 2011; Nair et al. 2013; Kumar et al. 2014; Kumar and Cabana 2016). However, immobilization of the enzymes induced no apparent benefit regarding stability towards NaN_3 since immobilized enzymes and dissolved enzymes had approximately 15 and 10 % lower residual activity in the presence of NaN_3 at pH 7 compared with NaN_3 free experiments conducted at pH 7, respectively. This indicates that alteration of the catalytic site of laccase induced by azide binding (Battistuzzi et al. 2003) was occurring to a similar extent as for dissolved enzymes and was not inhibited by internal cross-linking of the enzymes. This seems consequential since the small azide should be able to bind to the catalytic site irrespective of internal cross-linking.

The influence of immobilization on the catalytic efficiency of the biocatalysts towards several phenolic compounds, ABTS, and the precursor used for the production of the phenoxazinone dye has been assessed by determination of the apparent k_{cat} and K_m values. For all phenolic compounds, a decrease in k_{cat}^{app} and an increase in K_m^{app} were observed comparing immobilized with dissolved laccases indicating lower catalytic efficiency of immobilized enzymes (Table 6.8). This decrease might be due to reduced exposure of the active sites of the enzymes, due to mass transfer limitations for the substrates, and/or due to increased rigidity of the enzymes after cross-linking which inhibits changes in the conformation of the active site to accommodate substrates (Roy and Abraham 2006; Rodrigues et al. 2013). Immobilization had no apparent influence on the specific order regarding catalytic efficiency $(k_{cat}/K_m)^{app}$

for the different phenolic substrates. Catalytic efficiency of the biocatalysts was lower towards phenolic substrates with only one methoxy group, i.e., guaiacol, vanillin, and vanillic acid compared with substrates with two methoxy groups, i.e., 2,6-DMP, syringaldehyde, and syringic acid. This is most likely due to the electron donating property of methoxy groups which reduce the redox potential of the substrates thereby facilitating laccase oxidation (Xu 1996). Substituents in the *p*-position led to an increasing K_m^{app} and decreasing k_{cat}^{app} when comparing guaicol with vanillic acid and vanillin and 2,6-DMP with syrinic acid and syringaldehyde. This decrease in catalytic efficiency is most likely due to the electron withdrawing nature of these substituents (Xu 1996). Their presence decreases the electron density at the phenoxy group, thereby making oxidation by the enzymes more difficult (Xu 1996). Regarding ABTS and the precursor, K_m^{app} increased due to immobilization. However, k_{cat}^{app} also increased. Therefore, while the reaction rate approaches V_{max} more slowly with increasing substrate concentration V_{max} is higher for immobilized enzymes. An increase in the maximum rate towards ABTS due to immobilization and/or glutaraldehyde cross-linking has been described for several different laccases including TVL previously (Hommes et al. 2012; Ammann et al. 2014; Kumar et al. 2014). The reasons for this apparent increase are not yet clear and merit further investigation. It can be speculated that cross-linking either changes the catalytic site in a way that increases substrate turnover or that the microenvironment of the enzymes is changed in a way that favors oxidation of specific substrates (Rodrigues et al. 2013; Kumar et al. 2014).

Finally, reusability of the TVL-MP was demonstrated by the production of a phenoxazinone dye, i.e., 2-amino-3-oxo-3H-phenoxazine-8-sulfonic acid over ten cycles achieving virtually 100 % of precursor conversion in each cycle. Activity losses due to incomplete separation of TVL-MP indicate that the retention of enzymatic activity can be increased considerably by application of a stronger magnetic field or by prolonging the duration of the magnetic separation step.

6.2.8. Concluding remarks

In this chapter, a simple and robust method for the efficient immobilization of enzymes on superparamagnetic nanoparticles was developed and optimized. The resulting biocatalysts are considerably more stable than dissolved enzymes and can be easily separated from reaction solutions by application of a magnetic field allowing their reuse. Therefore, application of such superparamagnetic biocatalysts in enzyme catalyzed processes has considerable potential to increase process efficiency and economics. Furthermore, the presented method has potential for the immobilization of various enzymes as shown for the immobilization of DyP and glucose oxidase and can potentially immobilize any protein displaying lysines on the surface.

7. Lignin treatment

7.1. Organic solvent buffer mixtures

An obstacle for the use of enzymes for the oxidative degradation of lignin is the hydrophobic nature and compact structure of the biopolymer which makes it insoluble in aqueous solution (Achyuthan et al. 2010) limiting the accessibility to enzymes. In nature enzymatic lignin degradation does not seem to occur in a simple aqueous environment but rather in a less polar polysaccharide gel which might cause lignin swelling and partial dissolution of lignin in the cell wall (Hammel et al. 1993). A similar effect can be achieved in vitro by partly solubilizing lignin in an organic solvent during treatment (Hammel et al. 1993).

The possibility to degrade lignin employing different LME was evaluated by screening different combinations of organic solvents and LME for their capability to produce monomeric compounds from OL. Next conditions with regard to pH and enzymatic activities for the most promising combinations were optimized and low molecular weight reaction products of three settings favorable in terms of yields were characterized.

7.1.1. Screening of organic solvents and enzymes

The influence of five different water/solvent mixtures (i.e., 30 % (v/v) DMSO, 30 % (v/v) MeOH, 30 % (v/v) 2-propanol, 30 % (v/v) 2-methoxyethanol, and 100 % MPC buffer at pH 5) and four different enzymes (i.e., MnP, LiP, HRP, and laccase) on the molecular weight distribution of OL was tested. Figure 7.1 shows two SEC chromatograms. One of a sample treated with laccase in 30 % (v/v) DMSO and one of an enzyme free control sample. A clear increase in absorbance between 19.2 and 20.2 mL elution volume (grey area) was observed. This was also the case in several other samples. As indicated by SEC measurement of low molecular weight phenolic compounds like guaiacol (19.4 mL elution volume) and isovanillin (19.1 mL elution volume), increases in the absorbance in this range of the SEC chromatogram are most likely due to the formation of monomeric aromatic compounds. Consequently, the measured areas of the peaks (from 19.2 to 20.2 mL) from the SEC chromatograms after treatment of OL were calculated for wavelengths from 284 to 308 nm and the sum of these areas has been defined as the area of the monomer fraction (AMF). A D-optimal design was used and a two-factor interaction model was fitted in order to identify the factors significantly influencing AMF. Subsequently, the two-factor interaction model was reduced to only include significant factors ($p \leq 0.05$), factors necessary to maintain hierarchy of the model, and factors that were suspected to be significant ($p \leq 0.20$).

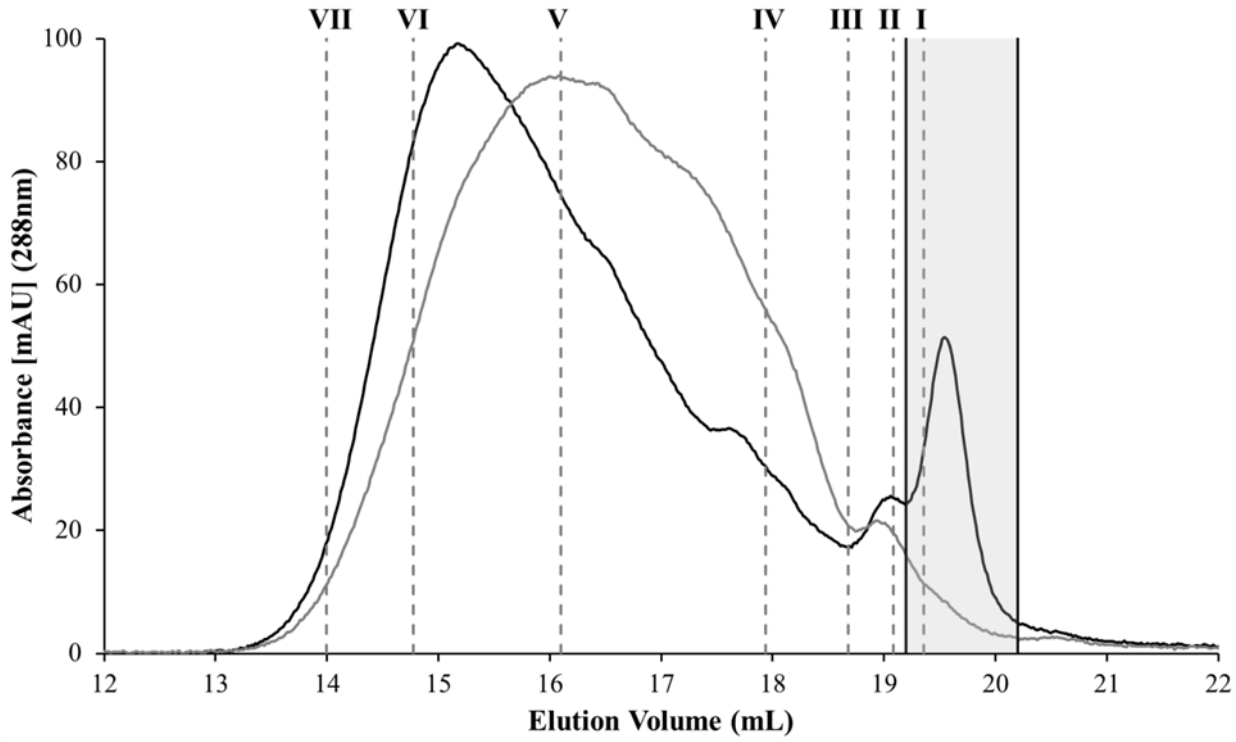

Figure 7.1 SEC chromatograms of an OL sample treated with laccase enzymes in 30 % (v/v) DMSO for 20 h (black) and an OL sample treated in 30 % (v/v) DMSO for 20 h without the addition of enzymes (grey). The grey area depicts the elution period that was considered for the calculation of AMF. The numbered grey dotted lines depict retention volumes at which the following substances eluted; guaiacol (I, MW 124.14), isovanillin (II, MW 152.15), baicalein-7-methylether (III, 284.28), riboflavin (IV, MW 376.37), tannic acid (V, MW 1,701.20), polyvinylphenol (VI, MW ~11,000), polyvinylphenol (VII, MW ~25,000).

The ANOVA results of the model are shown in Table A. 16. The following model terms were significant (i.e., had a *p*-value ≤0.05); Solvent, and Laccase. Furthermore, the factors LiP and the interaction between solvent and laccase had p-values below 0.2 which indicated that they might be significant. Consequently, the model was reduced to only contain the model terms Solvent, LiP, Laccase, and the interaction between solvent and laccase. The ANOVA results of the reduced model are shown in Table A. 17, the final equation in terms of the coded factors is given in Eq.8 and the design matrix of the screening experiment as well as the measured and calculated sums of the areas of the monomer fraction (AMF) are shown in Table A. 18.

All model terms of the reduced model were significant. The model predicts a positive effect on AMF for the model terms MeOH, DMSO, LiP, Laccase, MeOH × Laccase, and DMSO × Laccase. The positive influence of DMSO and DMSO × Laccase on AMF is considerably higher compared to MeOH and MeOH × Laccase as can be derived from Eq.8. Consequently, the experimental setup predicted by the reduced model to yield the highest AMF consists of laccase and LiP using DMSO as co-solvent. Since, the predicted influence on AMF was higher for DMSO and the interaction between DMSO and laccase compared to MeOH and the interaction between MeOH and laccase the model predicted highest

AMF when treating OL with laccase and LiP in 30 % (v/v) DMSO. However, the model clearly underestimated the AMF for three experiments, i.e., the experiment applying a combination of LiP, HRP, and MnP using DMSO as solvent, and the experiments applying solely HRP using 2-propanol or MeOH as solvent. This indicates that HRP might contribute to an increase of the monomeric fraction as well, even though this enzyme was not identified as significant by the model. Consequently, HRP was included in further optimization experiments.

$$
\begin{aligned}
&AMF\ \ [mAU] = \\
&5729 \\
&+1045 * A[MeOH] \\
&+2362 * A[DMSO] \\
&-207 * A[2-Propanol] \\
&-1002 * A[2-Methoxyethanol] \\
&+535 * C[LiP] \\
&+1129 * E[Laccase] \\
&+230 * A[MeOH] \times E[Laccase] \\
&+1662 * A[DMSO] \times E[Laccase] \\
&-915 * A[2-Propanol] \times E[Laccase] \\
&-1044 * A[2-Methoxyethanol] \times E[Laccase] \quad \text{(Eq. 8)}
\end{aligned}
$$

Dissolution of lignin in aqueous solutions containing organic solvent had a considerable impact on the accessibility of the enzymes. In the absence of an organic solvent the molecular weight distribution of lignin was virtually unchanged after enzymatic treatment. In the presence of organic solvent clear changes in the molecular weight distribution could be assigned to enzymatic treatment. Increases in the monomeric fraction could be observed when DMSO, MeOH, or 2-propanol was used as solvent and were most pronounced for DMSO. Simple alcohols like MeOH have been shown to limit condensation reactions during oxidative degradation of lignin and might also act as radical scavengers (Voitl and Rudolf von Rohr 2008). DMSO is also known to scavenge free radicals (Phillis et al. 1998) and might therefore also limit polymerization reactions of lignin oxidation intermediates. While MnP did not seem to contribute to the formation of monomers, increases in the monomeric fraction were observed in samples in which lignin was treated with LiP, HRP, or laccase or a combination of these three enzymes. Polymerization as well as depolymerization reactions occurred since both a shift towards higher molecular weight compounds and increase in monomeric fraction simultaneously occurred in several samples.

7.1.2. Optimization of enzymatic activities and pH

Based on the observations of the screening experiment described in paragraph 7.1.1, subsequent experiments testing the influence of pH and enzymatic activity were conducted with LiP, HRP, and laccase using DMSO as co-solvent. A D-optimal screening experiment was conducted and subsequently extended by a IV-optimal design. The conducted experiments are summarized in Table A. 19. Since, MnP was no longer considered in these screening experiments addition of oxalic acid to samples was no longer necessary. Therefore, additional wavelengths below 284 nm could be included in AMF calculations. The range for calculation was extended to encompass the wavelengths from 276 nm to 308 nm. A cubic model was fitted to the data and subsequently reduced to only contain significant factors ($p \leq 0.05$) and factors necessary to maintain hierarchy of the model. The ANOVA results are shown in Table A. 20 and Table A. 21 for the cubic and the reduced model, respectively.

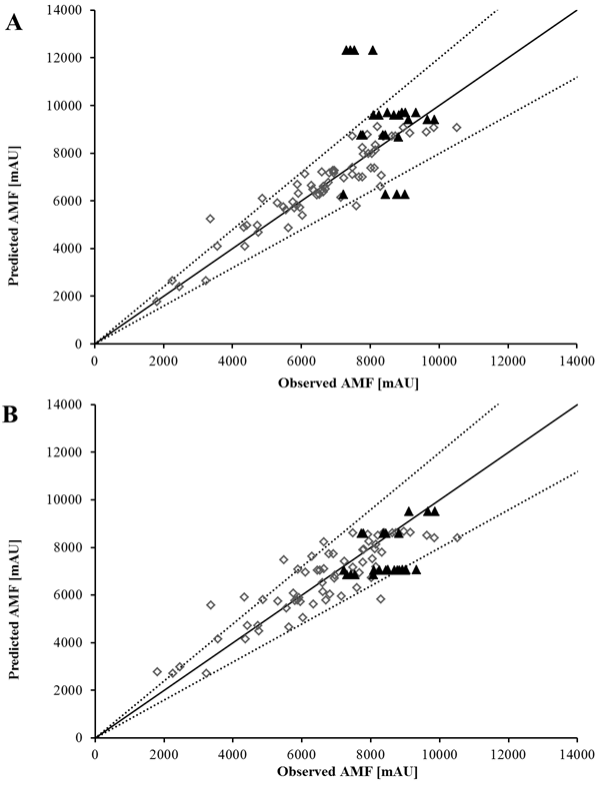

Figure 7.2 Observed areas of the monomeric fraction (AMF) in the SEC chromatograms of experiments with varying pH and enzymatic activities versus predicted AMF calculated by the cubic empirical model (A) and the reduced empirical model (B). Markers depicted by diamonds with no filling show data used for model fitting. Markers depicted by black triangles show data obtained by experiments conducted to evaluate the models. Dotted grey lines depict a deviation of ±20 % from the predicted to the observed value.

The coefficients of the final equations in terms of the actual factors of the cubic and reduced model are given in Table A. 22. Figure 7.2 shows the observed and predicted AMF calculated from SEC chromatograms (from wavelength 276 to 308 nm) of the experiments used to fit the cubic (Figure 7.2 A; diamonds) and the reduced model (Figure 7.2 B; diamonds) as well as of experiments conducted in order to evaluate the models (triangles). The cubic model clearly overestimated the AMF for experiments conducted at pH 3 applying HRP, laccase, and LiP in combination and clearly underestimated it for experiments conducted at pH 3 applying LiP and laccase in the absence of HRP.

The reduced model on the other hand predicted AMF of the control experiments reasonably well. Except for a setup using LiP and laccase at pH 3 (for which observed AMF was 22±1 % higher than predicted AMF) the model prediction never deviated more than 20 % from the observation. These deviations are most likely due to an overestimation of the influence

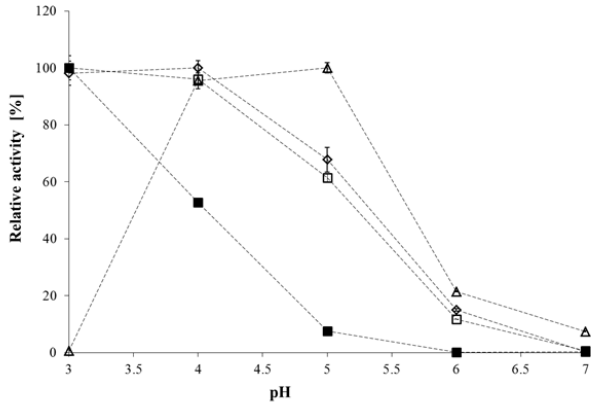

Figure 7.3 Relative activities of laccase (diamonds), HRP (triangles), and LiP (empty squares) determined by oxidation of ABTS and LiP (filled squares) determined by oxidation of veratryl alcohol. Error bars depict standard deviations of triplicates.

of HRP on AMF at pH 3. Activity tests using a standard substrate, i.e., ABTS showed that HRP is virtually inactive at this pH (see Figure 7.3).This finding is further supported by experiments at pH 3 using HRP as single enzyme which did not affect the molecular weight distribution of OL. Consequently, while the models predict an effect of HRP at pH 3 in reality there is virtually none.

The cubic model predicts highest AMF at pH 3 with enzymatic activities of 0.39, 3.48, and 4.28 U per well for LiP, HRP, and laccase, respectively.

The reduced model predicts highest AMF when applying 6 U per well HRP at pH 5.71 omitting the other enzymes. While the prediction of the reduced model fits rather well (observed AMF at highest predicted setup was 0.1±4.1 % higher than projected) the prediction of the cubic model deviates considerably from observed results (observed AMF at highest predicted setup was 37.7±2.8 % lower than projected). Next to increases in the monomeric fraction of the molecular weight distribution of lignin some samples also showed considerable increases in the higher molecular weight fraction indicating considerable polymerization of lignin

7.1.3. Characterization of reaction products

In order to characterize low molecular weight reaction products and water insoluble lignin residues one setup, i.e., using laccase at pH 5.62 in 30 % (v/v) DMSO was chosen. Overall weight, phenolic group content and elemental composition of the water insoluble residues after lignin treatment with laccase and of enzyme free controls was determined. Results are summarized in Table 7.1. Considerable increase in weight and decrease in phenolic group content was observed indicating polymerization of lignin through oxidative phenolic coupling reactions due to enzymatic treatment. Occurrence of such reactions by treatment of lignin has been proposed previously for the oxidation of wheat straw milled lignin by laccase and HRP (Crestini et al. 2011) and of lignosulfonates by HRP (Zhou et al. 2013). However, the weight increase above 100 % of the initially applied lignin cannot be entirely explained through lignin polymerization. The clear increase in nitrogen indicates that laccase proteins adsorbed on lignin and could not be washed away using water. Hydrophobic interactions have been proposed to play an important role in enzyme adsorption to lignocellulose (Palonen et al. 2004; Berlin et al. 2005a, b). In this context it has been shown that blocking of hydrophobic lignin sites using surfactants leads to a decreased adsorption of enzymes (Eriksson et al. 2002). Next to hydrophobic interactions ionic bonds

between lignin and enzymes in the presence of charged (COO^-, O^-) or partially charged (CO) functional groups have also been proposed to occur contributing to enzyme binding (Berlin et al. 2006).

The N to S ratio (w/w) of two laccases from *T. versicolor* has been calculated based on their amino acid sequences (Piontek et al. 2002; http://www.ebi.ac.uk/ena/data/view/AY049725, Accessed: 31.11.2014) to be 40.8 and 37.5. The measured N to S ratio of 4.8 of water insoluble enzymatically treated lignin is considerably lower than expected if the increase in S compared to untreated lignin would only occur due to protein adsorption. This low N to S ratio indicates that additional sulfur most likely originating from DMSO has been incorporated into lignin. DMSO, a nucleophile, might compete with the aromatic rings of lignin to react with the formed radicals and carbocations. Similar reactions have been proposed to occur between MeOH and lignin with MeOH acting as nucleophile when oxidizing kraft lignin using a POM catalyst in an acidic water MeOH mixture (Voitl et al. 2010). Occurrence of lignin polymerization was considerably reduced in reactions applying MeOH at a concentration of 80 % (v/v) compared to reactions performed only in aqueous solution, thereby demonstrating the competition between MeOH and lignin (Voitl and Rudolf von Rohr 2010).

Table 7.1 Characteristics of water insoluble residues of samples treated with laccase for 20 h at pH 5.62 in 30 % DMSO and an enzyme free control plus minus (±) standard deviations (n=8 for wt% and phenolic group content and n=3 for elemental composition).

	Enzyme free control	**OL treated with TVL**
Wt% (relative to applied lignin)	35.2±8.1	106.1±9.6
Phenolic group content [mmol g^{-1} OL]	1.97±0.21	0.22±0.05
Elemental composition		
C [%]	66.25±0.30	55.67±0.73
H [%]	5.58±0.07	5.49±0.05
N [%]	<0.3	4.09±0.08
S [%]	<0.3	0.86±0.04

Regarding low molecular weight compounds a new product, identified as 2,6-dimethoxy-1,4-benzoquinone (DMBQ) was observed at low abundances with GC-MS if no ascorbic acid was added after 20 h of treatment. When ascorbic acid was added 2,6-dimethoxy hydroquinone was identified, indicating that DMBQ was reduced to 2,6-dimethoxy hydroquinone and stabilized by the addition of the reducing agent (GC chromatograms are shown in Figure 7.4). However, high deviations of the internal standard between GC-MS measurements were observed and recoveries were low ranging from ~2 % to ~29 %. Furthermore, injected extracts of lignin repeatedly blocked the GC inlet liner indicating that further reactions took place at elevated temperatures. Furthermore, DMSO posed severe problems concerning extraction and analysis of low molecular weight products. DMSO is a polar aprotic solvent and, therefore, no clear separation of DMSO from the solvent used for extraction, i.e., EtAc (also a polar

aprotic solvent) was achieved. Furthermore, the boiling point of DMSO (189 °C) is similar to the boiling point of many phenolic compounds, e.g., phenol (182 °C), o-cresol (191 °C), syringaldehyde (192-193 °C), m-cresol (201 °C), p-cresol (202 °C), 2,6-dimethylphenol (203 °C), and guaiacol (204-206 °C). Therefore, many phenolic compounds were potentially lost during extraction and evaporation as indicated by the low recoveries of the internal standard. Consequently, DMSO might not be the solvent of choice in future applications since the production of sulfur containing products is of little interest for the chemical industry and separation of products from solvent might become laborious. Alternatively, alcohols like MeOH or 2-propanol could be used, thereby, avoiding the inclusion of sulfur while still enabling the production of monomeric compounds.

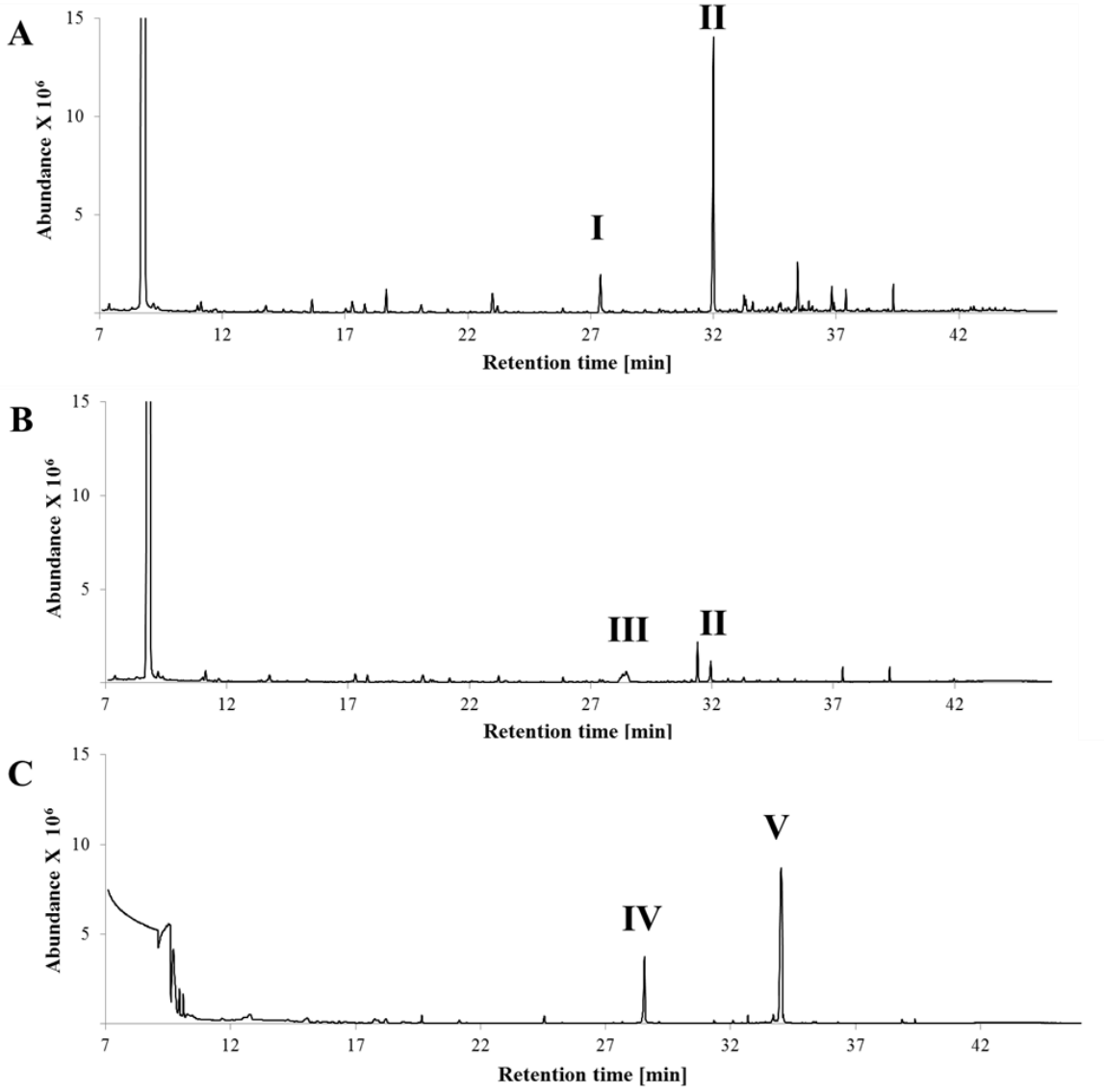

Figure 7.4 Total ion chromatogram of OL in the presence of heat inactivated laccase (A), OL treated with laccase in 30 % (v/v) DMSO at pH 5.62 for 20 h without (B) and with (C) the addition of ascorbic acid. Identified monophenolics are shown as basic substances of their TMS derivatives: Vanillin (I), syringaldehyde (II), DMBQ (not derivatized) (III), 2,6-dimethoxy hydroquinone (IV), ascorbic acid (V).

Further characterization of low molecular weight products was performed in triplicates by LC-MS measurements. Samples were treated in 30 % (v/v) MeOH at optimal pH determined by the screening experiment described above for 20 h using laccase, HRP, or a combination of LiP and laccase. Enzyme free control samples were measured as well. Yields of most prominent identified low molecular weight compounds for the different treatments are shown in Table 7.2. Several low molecular weight products were already present in the untreated sample. Some of them could be identified and quantified by the injection of standard substances. Identified compounds were syringic acid (0.052±0.002 wt%), vanillin (0.104±0.001 wt%), syringaldehyde (0.373±0.001 wt%), guaiacol (0.036±0.003 wt%), and acetosyringone (0.031±0.001 wt%). In the samples treated by enzymes a new compound, 2,6-dimethoxy hydroquinone was identified and quantified. Figure 7.5 shows the mass spectra of a standard of 2,6-dimethoxy hydroquinone standard (A) and of the metabolite (B). The mass spectra correspond very well to each other. A possible fragmentation scheme of the hydroquinone is presented in Figure 7.6. Furthermore, 2,6-dimethoxy hydroquinone eluted after the same retention time, i.e., 7.6 min as the metabolite.

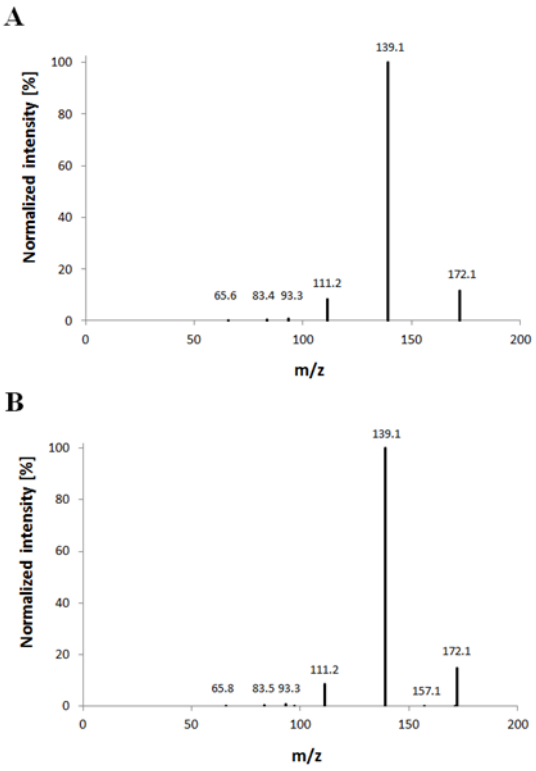

Figure 7.5 Mass spectra of 2,6-dimethoxy hydroquinone (A) and the metabolite formed by OL treatment with laccase in 30 % (v/v) MeOH (B). Intensities have been normalized with respect to the intensity of m/z 139.1 (100 %).

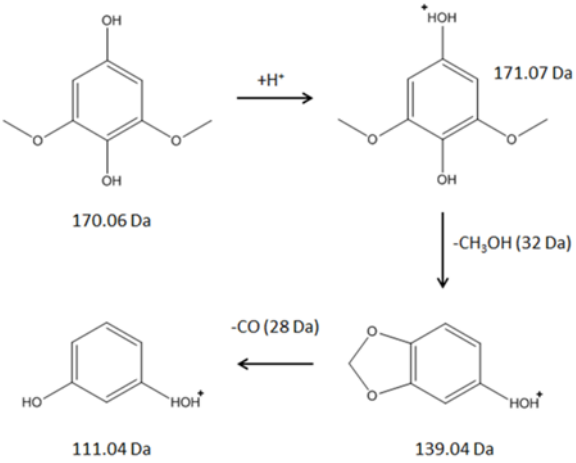

Figure 7.6 Proposed fragmentation of 2,6-dimethoxy hydroquinone leading to mass spectra presented in Figure 7.5.

Table 7.2 Yields of major low molecular weight compounds in wt% of initially applied lignin after different enzymatic treatments in 30 % (v/v) MeOH lasting 20 h (± standard deviation, n=3).

	Biocatalyst(s)			
Compound	**HRP**	**TVL**	**TVL and LiP**	**Enzyme free control**
DMBQ	1.27±0.07	1.39±0.06	0.79±0.02	-
Vanillin	-	-	0.10±0.00	0.11±0.01
Syringaldehyde	-	-	0.10±0.00	0.37±0.04

Subsequently, a long term experiment was conducted in order to evaluate maximal yields of 2,6-dimethoxy hydroquinone that can be produced from OL using the corresponding experimental setup. Samples were treated for 15 d in 30 % (v/v) MeOH and TVL was added at several time points during the experiment to ensure sufficient enzymatic activity within the samples over the whole experiment. Enzymatic activities and 2,6-dimethoxy hydroquinone yields over time are shown in Figure 7.7. Yields increased considerably during the first day of treatment reaching 1.26±0.01 wt%. Thereafter, 2,6-dimethoxy hydroquinone increased more slowly reaching 2.06±0.05 wt% after 10 d. During the next five days of treatment a less considerable increase to 2.20±0.05 wt% was observed, indicating that the maximal yield of 2,6-dimethoxy hydroquinone was virtually reached.

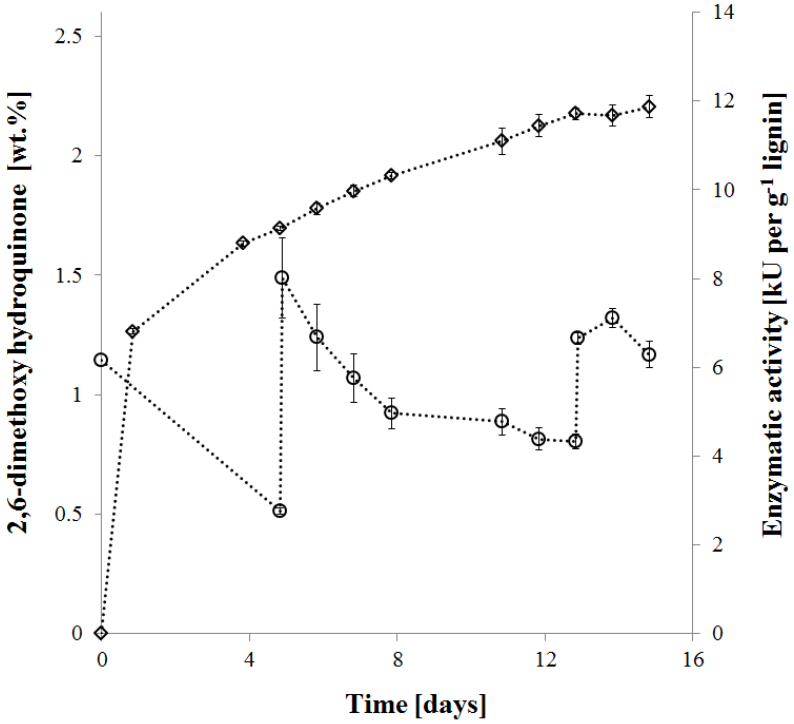

Figure 7.7 Enzymatic activities (circles) and yields of 2,6-dimethoxy hydroquinone (diamonds) during long term experiment treating OL in 30 % (v/v) MeOH with TVL at pH 5.6. Enzymes were added several times during the experiment.

The formation of 2,6-dimethoxy hydroquinone has already been achieved by oxidation of dimeric lignin model compounds by laccases (Kawai et al. 1988). A similar reaction mechanism for the formation of this compound as proposed for the dimeric lignin model compound (Kawai et al. 1988) might be occurring in real lignin (depicted in Figure 7.8). After initial oxidation of a phenolic group on a syringyl moiety, leading to the formation of a phenoxy radical, a cation intermediate is formed. Thereafter, spontaneous reactions lead to alkyl-aryl cleavage and the formation of the hydroquinone.

Next to the production of 2,6-dimethoxy hydroquinone other low molecular weight compounds, e.g., vanillin and syringaldehyde have been transformed due to laccase treatment. Both substances are known to be oxidized by laccases and are suspected to play a role in lignin degradation by white-rot fungi acting as laccase mediators (Cañas and Camarero 2010). Hence, their transformation by laccases had to be expected.

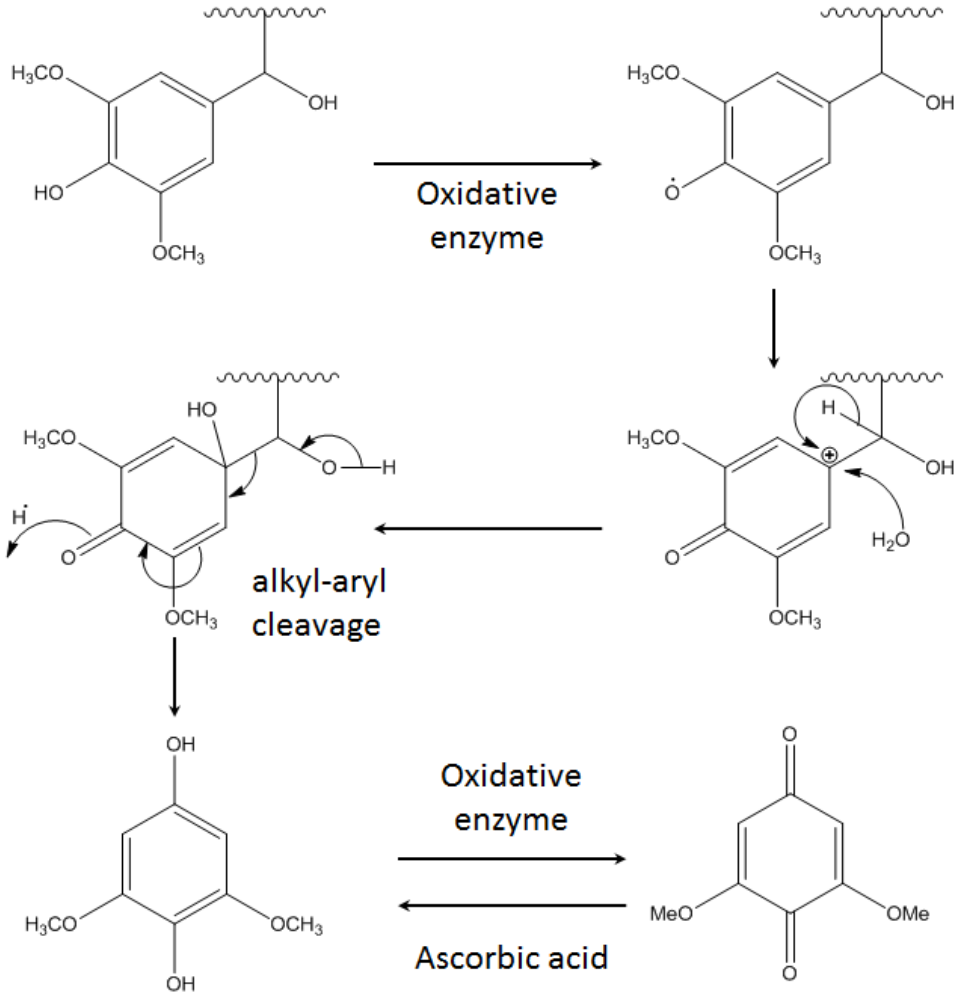

Figure 7.8 Proposed reaction mechanism for the formation of DMBQ and 2,6-dimethoxy hydroquinone from lignin through laccase oxidation based on a reaction mechanism proposed previously (Kawai et al. 1988).

7.1.4. Treatment using an antioxidant

As results from paragraph 7.1.1 and 7.1.2 showed, lignin is polymerized during enzymatic oxidation in the presence of an organic co-solvent. To prevent polymerization an antioxidant, i.e., Trolox was added during OL treatment with oxidative enzymes. Trolox is a synthetic water soluble analogue of vitamin E capable to scavenge radicals (Cadenas et al. 1989). Its presence during the enzymatic oxidation of lignin might decrease the amount of phenoxy radicals and, thereby, suppress the occurrence of polymerization reactions.

.

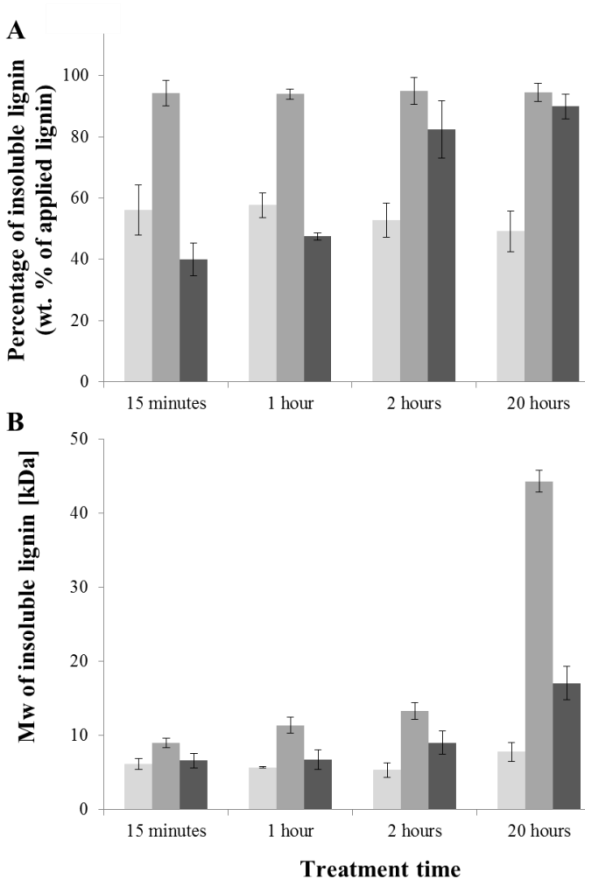

Figure 7.9 Percentage (A) and Mw (B) of insoluble lignin in 30 % (v/v) MeOH at pH 5.6 after different treatment times for control experiments (light grey), experiments with TVL (grey), and experiments with TVL and Trolox (dark grey). Error bars show standard deviations (n=3).

OL was treated with TVL at pH 5.6 in 30 % (v/v) MeOH in presence of 12 mM Trolox. Samples were taken after 15 min, 1 h, 2 h, and 20 h. Weight and Mw of the insoluble lignin was determined. Furthermore, low molecular weight products were identified and quantified. Changes in wt% and Mw of insoluble lignin are shown and compared to controls and OL only treated with TVL in Figure 7.9. Weight and Mw of insoluble material of controls did not change considerably during the experiments. The weight slightly decreased from 56.0±8.2 to 49.1±6.5 wt%. While this decrease was not statistically significant (p=0.123, students t-test, two-tailed distribution, paired samples) it might indicate that some part of OL was solubilized during the 20 h of mixing. Mw slightly increased from 6,140±760 Da to 7,780±1,285 Da. Again the difference was not statistically significant (p=0.214, students t-test, two-tailed distribution, paired samples). However, going along with the slight weight decrease this might indicate solubilization of small amounts of lower molecular weight lignin during the 20 h of mixing.

The weight of insoluble lignin of samples only treated with TVL did also not change significantly over time but was considerably higher compared to the controls, i.e., 94.4±3.0 wt% on average. Again enzyme adsorption might have considerably affected the amount of insoluble lignin as discussed above

(7.1.3). Mw clearly increased over time in these samples and was 8,960±640 and 44,300±1,460 Da after 15 min and 20 h, respectively indicating lignin polymerization.

Interestingly the weight of insoluble lignin in samples treated with TVL and Trolox was lower than in controls after 15 min of treatment, i.e., 40.0±5.0 wt%. During the 20 h of treatment the weight of insoluble lignin increased. This increase was relatively slow during the first hour, becoming more rapid during the second hour before becoming less considerable during the rest of the treatment. The weight of insoluble lignin was 47.6±1.2, 82.4±9.3, and 89.9±4.1 wt% after 1, 2, and 20 h of treatment, respectively. Mw of insoluble lignin remained virtually the same during the first hour of treatment, i.e., 6,010±200 Da before increasing to 9,030±1,550 and 17,060±2,290 Da after 2 and 20 h, respectively. These results indicate that polymerization reactions of lignin were successfully suppressed by the antioxidant during the beginning of the treatment. Furthermore, if it is assumed that some of the weight increase in lignin during the treatment is due to enzyme adsorption then this was also prevented to some extent during the first hour of the experiment. It has been shown that lignin polymerization can considerably increase the surface area of lignin (Pielhop et al. 2015). Consequently, polymerized lignin might adsorb enzymes more efficiently as proposed previously (Pielhop et al. 2015) which would explain why considerable weight increases occurred during the same time as substantial lignin polymerization set in.

The changes in identified monomer yields over time are shown in Figure 7.10. In controls syringaldehyde and vanillin concentrations stayed constant over the course of the experiment showing that these compounds were stable in the applied reaction conditions. In samples treated with TVL all vanillin and syringaldehyde was transformed already after 15 min. Furthermore, a considerable DMBQ yield of 0.94±0.01 wt% was already observed after 15 min showing that the initial production of DMBQ proceeded very fast. The DMBQ yield increased over the course of the whole experiment and reached 1.30±0.00 wt% after 20 h. In samples treated with TVL and Trolox vanillin and syringaldehyde remained stable during the first hour. Subsequently, yields started to decrease during the second hour. Finally, the two compounds were completely transformed after 20 h. Along with the decrease in vanillin and syringaldehyde the production of DMBQ started between the first and second hour of the experiment. After 20 h a DMBQ yield of 0.98±0.03 wt% was reached. The results correspond well to results of insoluble material and changes in Mw indicating that the enzymatic reaction was suppressed by Trolox during the first hour of the experiment. Subsequently, enzymatic oxidation leads to the transformation of the phenolic monomers vanillin and syringaldehyde while DMBQ starts to get produced from lignin. While it is possible that some DMBQ originates from syringaldehyde it is more likely that syringaldehyde was mostly polymerized during the reaction as shown previously (Rittstieg et al. 2002) and as our own results suggest (7.2.2). Furthermore, the produced DMBQ amount surpasses the syringaldehyde amount found in OL and still increased after complete syringaldehyde transformation indicating that most of the DMBQ originates from higher molecular weight lignin.

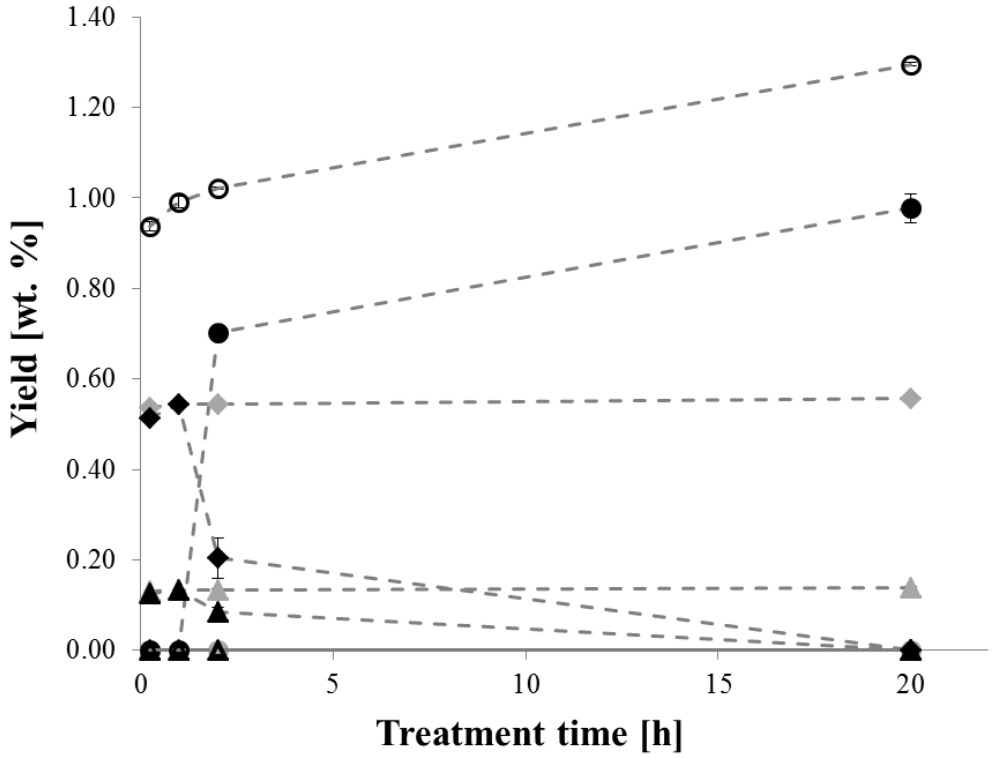

Figure 7.10 Yields of monomeric products during OL treatment in 30 % (v/v) MeOH with TVL at pH 5.6. DMBQ (circles), syringaldehyde (diamonds), and vanillin (triangles) yields are shown for controls (grey), samples treated with TVL (empty), and samples treated with TVL in the presence of Trolox (black). Error bars show standard deviations (n=3).

The application of an antioxidizing agent successfully suppressed lignin polymerization in the beginning of the experiment. However, this went along with inhibiting the formation of low molecular weight reaction products (especially DMBQ). Furthermore, the effect of Trolox decreased over time indicating that the antioxidant has to be supplied continuously during treatment or needs to be recycled by addition of a reducing agent, e.g., ascorbate (Guo and Packer 2000) to keep its effect. However, the direct enzymatic oxidation of Trolox is possible as well leading to the formation of Trolox phenoxyl radicals (Guo and Packer 2000). These radicals can potentially react further with lignin and might, thereby, be incorporated into lignin. It can be speculated that the increase in lignin solubility during the beginning of the treatment is not due to lignin depolymerization reactions but due to incorporation of Trolox into lignin adding carboxyl groups to the lignin surface and, thereby, increasing solubility of lignin in polar solvents. However, further studies would be needed to confirm this. Overall it seems questionable whether the costs added by applying Trolox can be justified, even though some lignin might have been solubilized during the start of the experiment.

7.1.5. Preliminary experiments using immobilized enzymes

7.1.5.1. Preliminary experiments using fsNP

Preliminary experiments using TVL and HRP immobilized on fsNP to treat OL were conducted using the same experimental setups as in experiments described in paragraph 7.1.2. A central composite design was chosen to assess the influence of the enzymatic activities and pH on AMF. Results are summarized in Table A. 23. Reaction conditions did not considerably influence AMF which varied between 9,064 and 10,582 mAU with the exception of the experiment conducted at pH 6.68 which had a notably lower AMF of only 7,071 mAU. Compared to enzyme free control experiments AMFs of all samples increased considerably indicating formation of low molecular weight compounds due to treatment and were in a similar range as the high values of AMF observed in experiments conducted with dissolved enzymes. Consequently, results showed that immobilized enzymes are still capable to oxidize lignin. However, separation of insoluble lignin from immobilized enzymes could not be achieved and, therefore, effects of treatment on higher molecular weight lignin was not evaluated. Consequently, fsNP were deemed unsuitable as enzyme carrier material for lignin treatment and LME immobilized on MPs were used in further experiments which considerably facilitate biocatalyst separation from reaction products.

7.1.5.2. Preliminary experiments using MP

Preliminary experiments treating OL with TVL-MP were conducted in 30 % (v/v) MeOH at pH 5.6 for 20 h. Samples were taken after 1, 2, and 20 h and low molecular weight compounds were analyzed by HPLC. As in experiments with dissolved enzymes, one main reaction product, i.e., DMBQ was produced. The DMBQ yield increased during treatment and was 0.46, 0.89, and 1.37 wt% after 1, 2, and 20 h, respectively indicating lignin oxidation by TVL-MP. DMBQ yields after 20 h were similar to yields obtained after 20 h of treatment with TVL (Table 7.2). Enzymatic activity of TVL-MPs decreased to 68.0 % of the initial activity during treatment. After treatment, TVL-MPs were separated magnetically from lignin products. Separation was monitored by measuring residual enzymatic activities in the sample. Particles could be effectively separated from the reaction suspension as evidenced by the reduction in enzymatic activity in the sample to 0.9 % of the initial activity.

7.1.5.3. Preliminary experiments at higher lignin concentrations using MP

Lignin experiments were conducted with 2 kU L^{-1} TVL-MP at two different lignin concentrations since application of higher lignin concentrations during treatment would most likely be beneficial regarding process economics as well as product separation (see chapter 8). Concentrations of 0.3 g L^{-1} used in experiments discussed up until now will most likely be too low for an efficient treatment. Therefore, OL was also treated at 3 and 10 g L^{-1} in the presence of 30 % (v/v) MeOH at pH 5.62 for 20 h. DMBQ was produced in both cases. However, yields were higher in experiments conducted at 3 g L^{-1}, i.e., they were 1.10 and 0.74 wt% for experiments conducted at 3 g L^{-1} and 10 g L^{-1}, respectively. Furthermore, Mw increased during enzymatic treatment in both cases to 11,950 and 5,860 Da for experiments conducted at 3 g L^{-1} and 10 g L^{-1}, respectively. Consequently, results show that lignin was oxidized by TVL-MP in

both experiments. However, oxidation seemed to be more efficient at 3 g L^{-1} than 10 g L^{-1} as indicated by the higher DMBQ yield and stronger increase in Mw. At 10 g L^{-1} the reaction suspension became rather dense and it might be that mixing became more difficult. Furthermore, the supply of oxygen for the enzymes might also have been reduced. However, at 3 g L^{-1} sufficient oxidation seemed to occur as shown by the DMBQ yields which were only slightly below yields obtained in experiments conducted at 0.3 g L^{-1} (1.37 wt%, see 7.1.5.2). Therefore, experiments in subchapter 7.3 were conducted at lignin concentrations of 3 g L^{-1}.

7.1.6. Concluding remarks

Considerable oxidation of OL could be achieved using oxidative LME in combination with organic solvents. Especially in mixtures containing DMSO or MeOH the formation of stable monomeric substances was observed. However, the similar boiling point of DMSO compared to many of the potential phenolic products might considerably complicate product separation from the solvent after treatment. Therefore, MeOH (boiling point 64.7 °C) seems to be a more promising solvent taking downstream processing of products into account. Furthermore, the occurrence of higher molecular weight lignin indicates that the phenoxy radicals produced react with lignin macromolecules through phenolic oxidative coupling leading to lignin condensation and polymerization. Application of an antioxidant inhibited lignin polymerization. However, the formation of low molecular weight reaction products was prevented as well indicating that the antioxidant suppressed most of the reactions initiated by enzymatic oxidation. Enzyme adsorption on lignin was observed impeding accurate analysis of higher molecular weight reaction products. Enzyme immobilization might present a possible solution for this issue. However, selection of a suitable carrier material allowing efficient biocatalyst separation seems essential in this regard. As preliminary experiments indicated, separation of fsNP from insoluble lignin might be rather laborious and necessitate separation by, e.g., filtration or density. However, insoluble lignins in aqueous suspension can form larger agglomerates that might further complicate such separation procedures. Therefore, MPs seem to be a more suitable carrier material allowing facilitated separation through application of a magnetic field.

Of the tested enzymes, laccases seem the most promising regarding application. MnP had no considerable effect on the molecular weight distribution of lignin. LiP and HRP initiated partial lignin depolymerization and polymerization. However, the differences of the observed effects on the molecular weight distribution of lignin between the peroxidases and laccases were only minor. Furthermore, all three enzymes produced mainly one monomeric product, i.e., DMBQ. Therefore, LiP and/or HRP use had no clear benefit compared to laccase. However, laccases have considerable advantages compared to peroxidases regarding application. Most importantly, they do not need the addition of H_2O_2 which has to be properly controlled in case of peroxidases to prevent enzyme inactivation by too high H_2O_2 concentrations. Furthermore, laccases are already produced on industrial levels (Hou et al. 2004) which is not the case for many peroxidases like MnP, LiP, VP, or DyP (Singh et al. 2011) and some laccases

have high specific activities which allows production of nanobiocatalysts with high enzyme loads as shown in chapter 6.

7.2. Preliminary tests with laccase mediator systems

Laccases are limited to react with phenolic lignin groups due to their relatively low redox potential (0.4-0.8 mV) (ten Have and Teunissen 2001). However, their activity can be extended towards additional functional groups common in lignin like benzyl and allyl alcohols or ethers by the application of small redox mediators (Morozova et al. 2007). A good redox mediator has to be a good laccase substrate. Furthermore, it needs to have stable oxidized and reduced forms that do not inactivate the enzyme while its redox conversion has to be cyclic (Morozova et al. 2007, Figure 7.11).

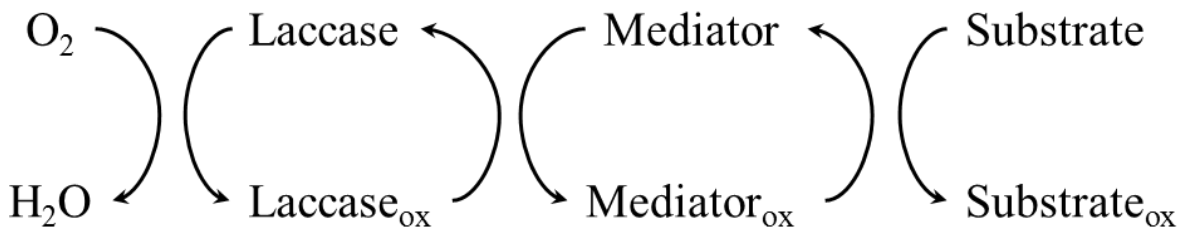

Figure 7.11 Scheme depicting a LMS cycle.

Prominent laccase mediators are of the N-OH type operating along a hydrogen atom transfer (HAT) route (Fabbrini et al. 2002, Figure 7.12). By testing different mediators of this type, HBT was identified as the most efficient (Cantarella et al. 2003). Furthermore, phenolic low molecular weight compounds like syringaldehyde or acetosyringone have been proposed as possible natural laccase mediators (Camarero et al. 2007). A further interesting laccase mediator is TEMPO which mediates the oxidation of alcohols to ketones or aldehydes along a two-electron, "ionic oxidation" type of reaction (Galli and Gentili 2004, Figure 7.13).

OL was treated by employing several potential laccase mediators. Their effect on the molecular weight of lignin was assessed in preliminary experiments in order to identify potentially promising mediators for more detailed study.

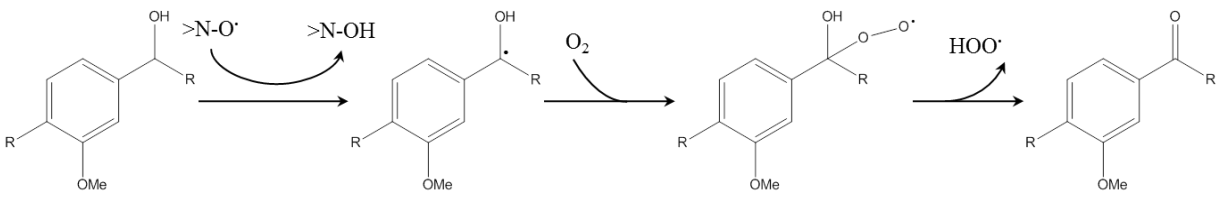

Figure 7.12 Scheme depicting the HAT pathway of laccase mediators of the NOH type.

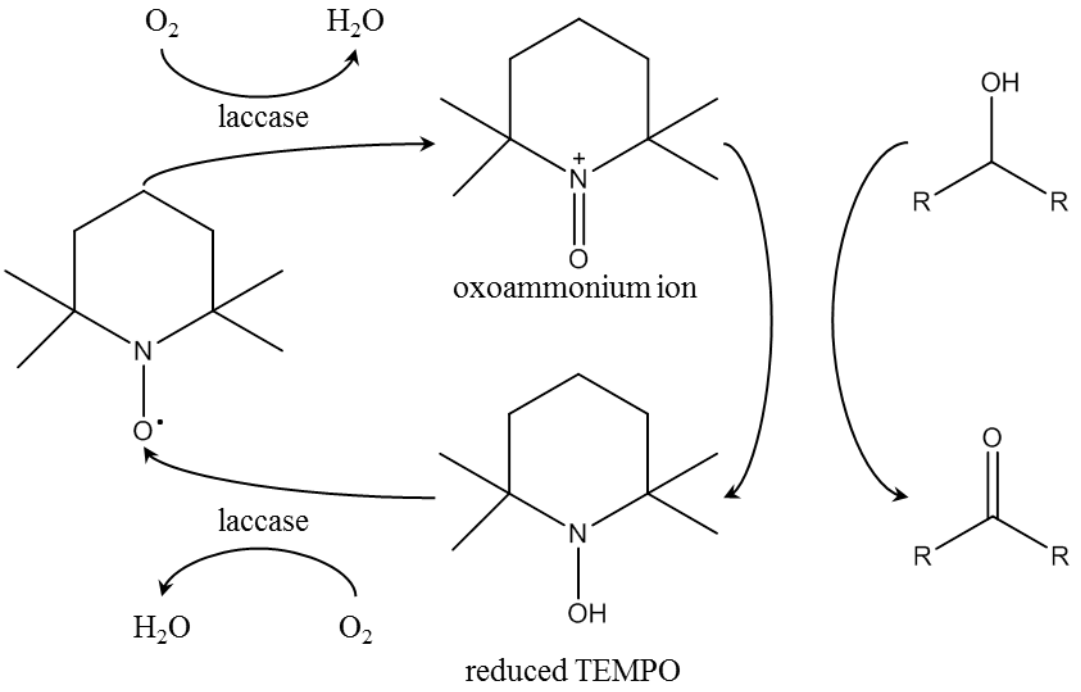

Figure 7.13 Scheme depicting the TEMPO mediated oxidation of alcohols to ketones or aldehydes.

7.2.1. Preliminary mediator screening

The effect of different LMS on the molecular weight distribution of OL was investigated. Two artificial, i.e., HBT and TEMPO and two natural, i.e., 4-hydroxybenzoic acid and *p*-coumaric acid laccase mediators were tested in different combinations following a design of experiment approach. A D-optimal design was developed testing five factors, i.e., the corresponding concentrations of the mediators and the laccase activity. Batch experiments were conducted at pH 5 for 20 h and samples were analyzed by SEC.

Figure 7.14 shows the SEC chromatograms of the different experiments in comparison to enzyme and mediator free controls. All chromatograms show a considerable decrease in absorbance at 280 nm between 13 and 17 mL elution volume (with the exception of experiment 30 in which only a slight decrease was observed). This decrease might be due to a decrease in phenolic lignin groups due to condensation or phenolic oxidative coupling reactions. Notable increases in the absorbance at 280 nm after elution volumes at which low molecular weight compounds eluted, i.e., after ~18 mL (excluding signals that were due to laccase mediators) did only occur in experiments 21, 25, 26, and 31. In all of these experiments *p*-coumaric acid was present. However, the signal of *p*-coumaric acid was reduced considerably indicating partial transformation of the mediator by laccase.

In summary, while the results of the above described screening experiment suggest that treatment with LMS led to changes in the lignin structure, there was no clear evidence for depolymerization. If new low molecular weight compounds were formed (other than the ones observed in experiments with *p*-coumaric acid) they were either unstable, superimposed by the mediator signals, or could not be detected by UV-Vis measurements between 240 and 472 nm.

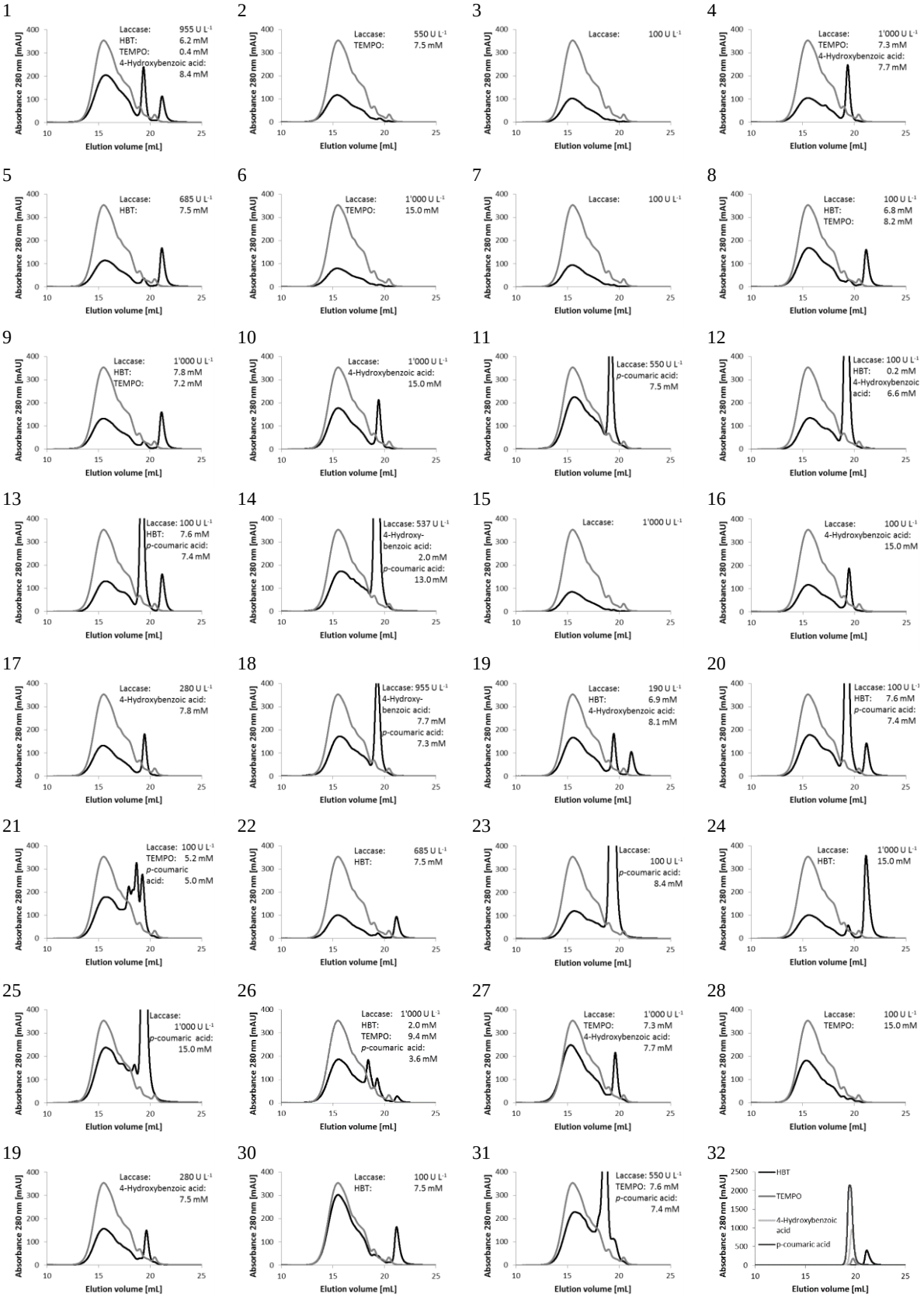

Figure 7.14 SEC chromatograms of OL treated with different LMS using GTL at pH 5 for 20 h (black) and of enzyme and mediator free controls (grey). Graph number 32 shows SEC chromatograms of applied mediators in the absence of lignin and laccase.

7.2.2. Preliminary tests of natural laccase mediators

Natural laccase mediators, i.e., *p*-coumaric acid, acetosyringone, and syringaldehyde were tested. All three of these mediators were described to induce paper pulp delignification (Camarero et al. 2007). OL was treated in batch experiments with GTL at pH 5 for 20 h. The mediators were applied at concentrations of 1 mM and 10 mM. Furthermore, control experiments in the absence of lignin were conducted applying mediators at a concentration of 10 mM. SEC chromatograms of the different experiments are shown in Figure 7.15. Applying mediators at a concentration of 1 mM only led to little changes in the molecular weight distribution of OL. Using mediators at a concentration of 10 mM led to the formation of several low molecular weight compounds. However, formation of compounds of similar size was observed in control experiments in the absence of lignin as well, indicating that polymerization reactions of the laccase mediators occurred in all three cases. Therefore, it is unclear to what extent the newly formed low molecular weight compounds derived from OL and to what extent they originated from polymerization of the mediators.

In conclusion application of natural laccase mediators led to no clear depolymerization of OL. While it cannot be ruled out that new low molecular weight compounds originating from lignin were formed during treatment, results suggest that natural mediators have to be applied at rather high concentrations (>1 mM) to have a considerable effect. Furthermore, results of lignin free controls showed that the mediators were polymerized, i.e., consumed during the reaction. Therefore, they do not fulfill the requirements of a good mediator, i.e., their oxidized forms are unstable and their redox conversion is not cyclic. Due to these reasons the application of natural laccase mediators was not studied more in depth.

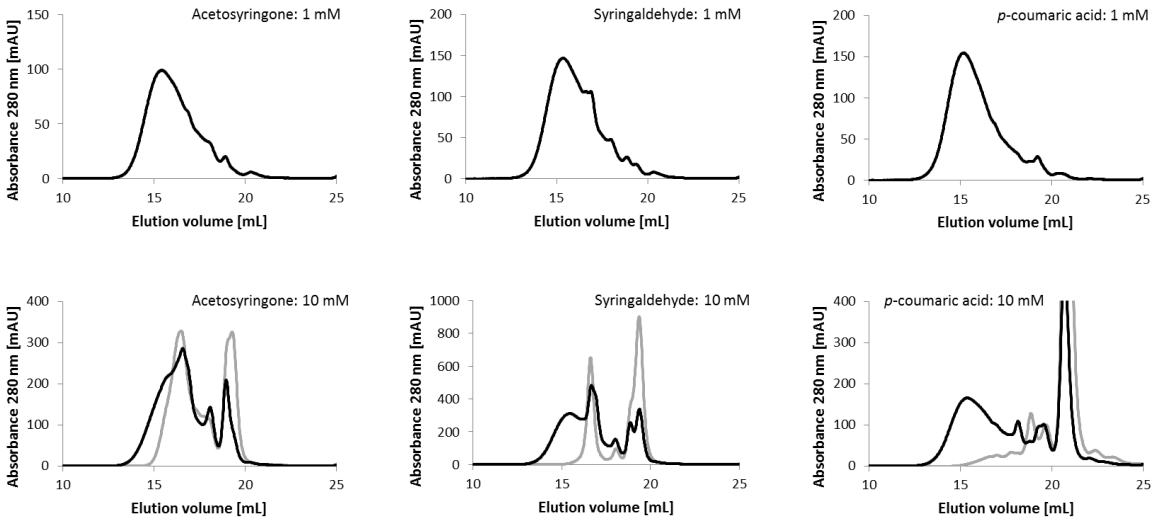

Figure 7.15 SEC chromatograms of OL treated with different natural laccase mediators using 1 kU L^{-1} GTL at pH 5 for 20 h (black) and of natural mediators treated with GTL in the absence of lignin (grey).

7.3. Sequential lignin treatment: combining laccase mediator systems with formic acid induced depolymerization

Based on the results obtained in the preliminary experiments of subchapter 7.1 and 7.2 most promising biocatalytic treatments were identified to be with TVL-MP either in the presence of the co-solvent MeOH or using an artificial redox mediator like HBT or TEMPO. In the present subchapter the suitability of the combination of these biocatalytical lignin oxidation treatments with a chemical formic acid induced lignin depolymerization step was investigated for the depolymerization of several technical lignins. The goal was to first degrade lignin during the biocatalytic oxidation step and then in a second step to cleave residual oxidized β-O-4 bonds using the chemical process step as demonstrated previously (Rahimi et al. 2014) inducing further lignin depolymerization.

Figure 7.16 summarizes the proposed reactions initiated by the sequential treatment using the LMS with HBT as example. The LMS oxidizes lignin leading to the formation of phenoxy radicals and to lignin side-chain oxidation (Crestini et al. 2003, 2011). In the absence of a mediator only phenoxy radicals are formed. Side-chain oxidation can initiate lignin depolymerization by promoting Cα-Cβ breakdown (Camarero et al. 2014) and leads to superoxide radical anion production (Crestini et al. 2003). The superoxide radical anions react further with the phenoxy radicals leading to the formation of further oxidation products like *o*-quinones, *p*-quinones, and ring-cleavage products (Crestini et al. 2003). Furthermore, phenoxy radicals can react further by disproportionation leading either to side chain oxidation in the Cα position or to the formation of *p*-quinones (Kawai et al. 1988). However, phenoxy radicals can also react with other lignin macromolecules leading to phenolic oxidative coupling and, thereby, to lignin polymerization (Crestini et al. 2003). In the second reaction step β-O-4 ether bonds are cleaved if they contain Cα ketones, i.e., if they have been oxidized during the first treatment step. The cleavage proceeds along an overall redox-neutral sequence of reaction steps leading to further lignin depolymerization (Rahimi et al. 2014).

7.3.1. Treatment of several different technical lignins

Several technical lignins were subjected to the sequential treatment. A scheme depicting the treatment is given in Figure 7.17. After the biocatalytic treatment step biocatalysts were separated magnetically before the suspension was acidified to pH 2 and insoluble lignin was separated from soluble products. Subsequently, insoluble lignin was treated by formic acid/formate treatment. Five different lignins were treated either in the presence of 30 % (v/v) MeOH, 5 mM HBT, or 5 mM TEMPO. 6 % (v/v) MeOH was added in the experiments containing TEMPO since laccases are inactivated by this mediator in the absence of simple alcohols as reported previously (Arends et al. 2006) and as observed in preliminary experiments. Most likely the oxoammonium ion formed during TEMPO oxidation (Figure 7.13) reacts with and inactivates the enzymes in the absence of a more readily available reaction partner like a simple alcohol (Arends et al. 2006). The five treated lignins were; OL (used in all experiments of subchapters 7.1 and 7.2), three different soda lignins obtained after LPS® (from

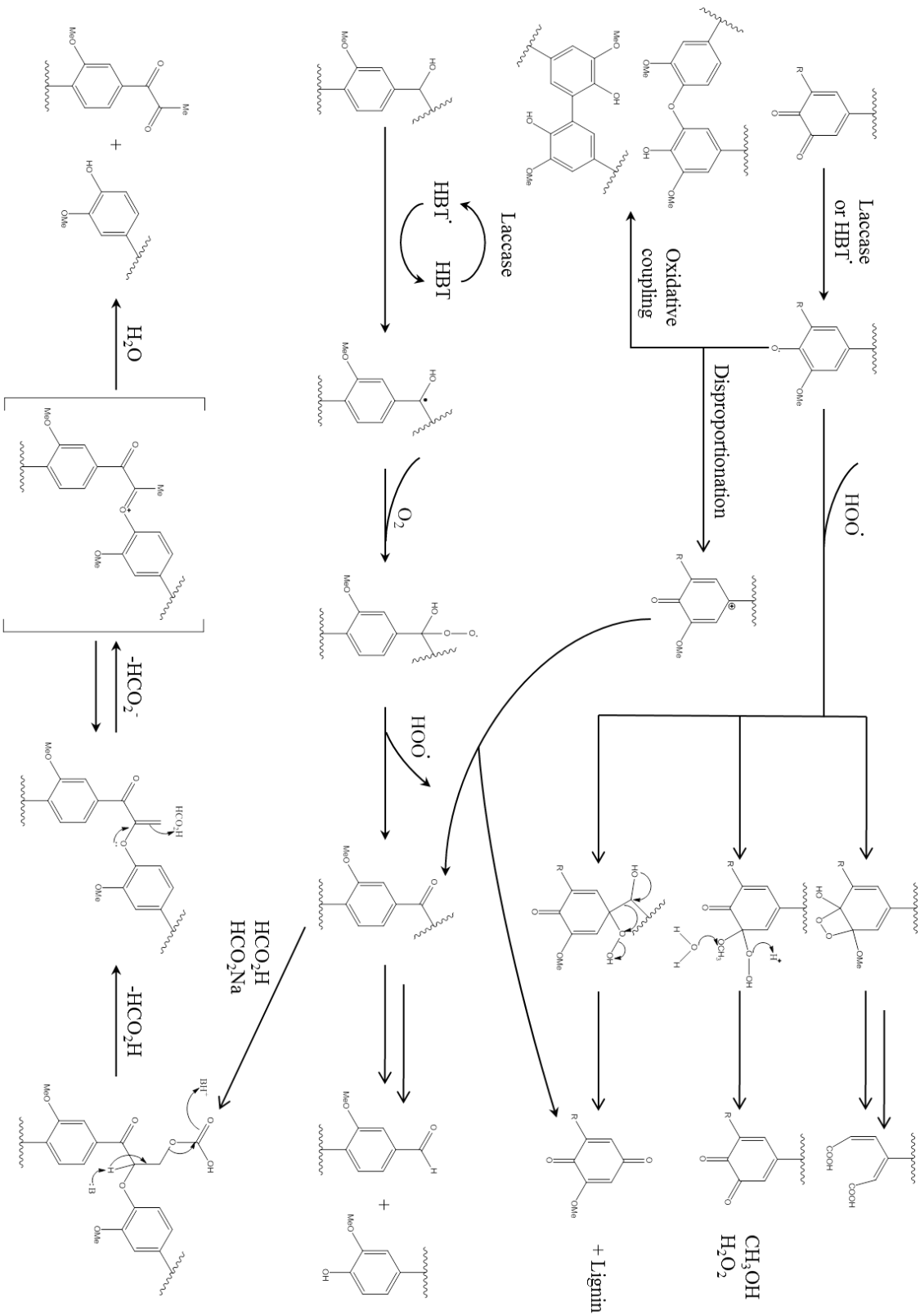

Figure 7.16 Scheme depicting the proposed reaction mechanisms induced by the sequential treatment. Proposed mechanisms are based on previous reports (Crestini et al. 2003, 2011; Kawai et al. 1988; Rahimi et al. 2014). Adapted from Gasser et al. (2017).

wheat straw (W-SL), sarkanda (S-SL), or soft wood (SW-SL)), and a lignin from wheat straw obtained after steam-explosion pre-treatment and LPS® (W-SE). Mass balances are summarized in Figure 7.18, results from SEC measurements are shown in Figure 7.19, and yields of identified low molecular weight compounds after the different treatment steps are shown in Figure 7.20 and listed in Table A. 24. The effects of the three different treatments on the lignins will be discussed in the following in separate subchapters.

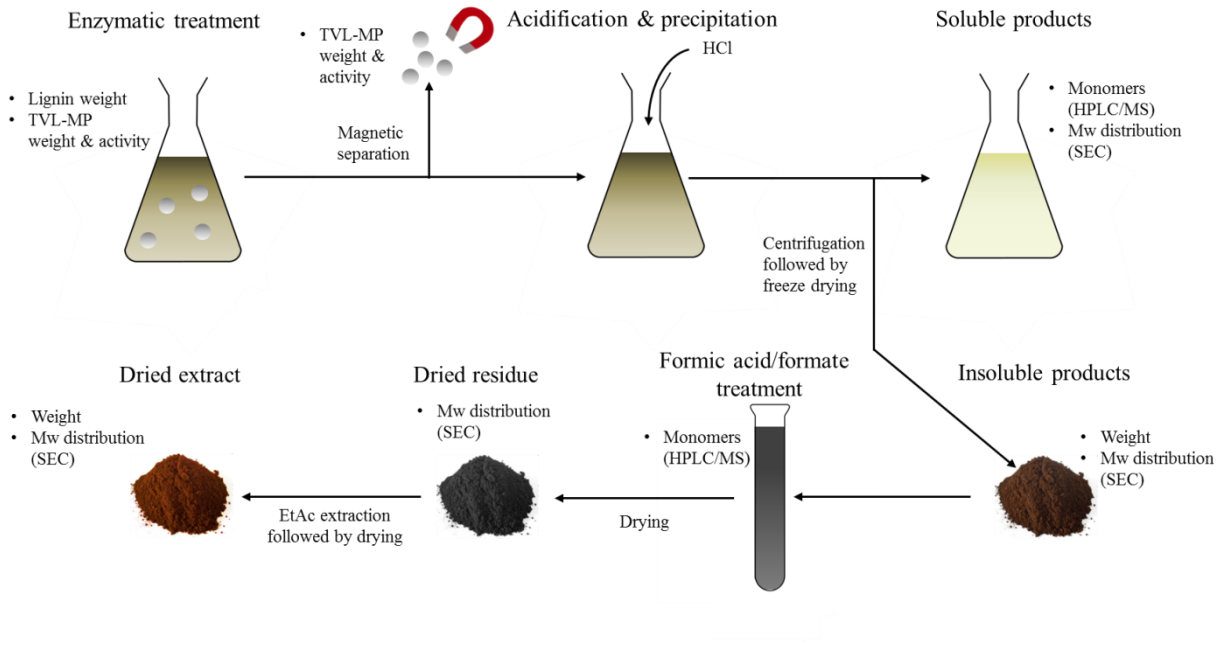

Figure 7.17 Scheme of sequential treatment and measurements conducted (adapted from Gasser et al. (2017))

7.3.1.1. Treatment in presence of organic co-solvent

Treatment of lignins with TVL-MP in 30 % (v/v) MeOH led to a reduction of soluble compounds in aqueous solution after acidification after the first treatment in case of all tested lignins (Figure 7.18). The decrease varied between the different lignins and was highest for S-SL with 18.2 wt% and lowest for W-SE with 9.8 wt%. This decrease went along with a considerable increase in Mw of the insoluble lignins after the first treatment (Figure 7.19). These results indicate that lignin treatment with TVL-MP using MeOH as co-solvent predominantly initiated polymerization reactions leading to the formation of less soluble higher molecular weight lignin macromolecules. However, the decrease in solubility might also be partly explained by lignin adsorption to the TVL-MP since between 10.4 and 15.7 wt% of lignin could not be separated magnetically from the biocatalysts.

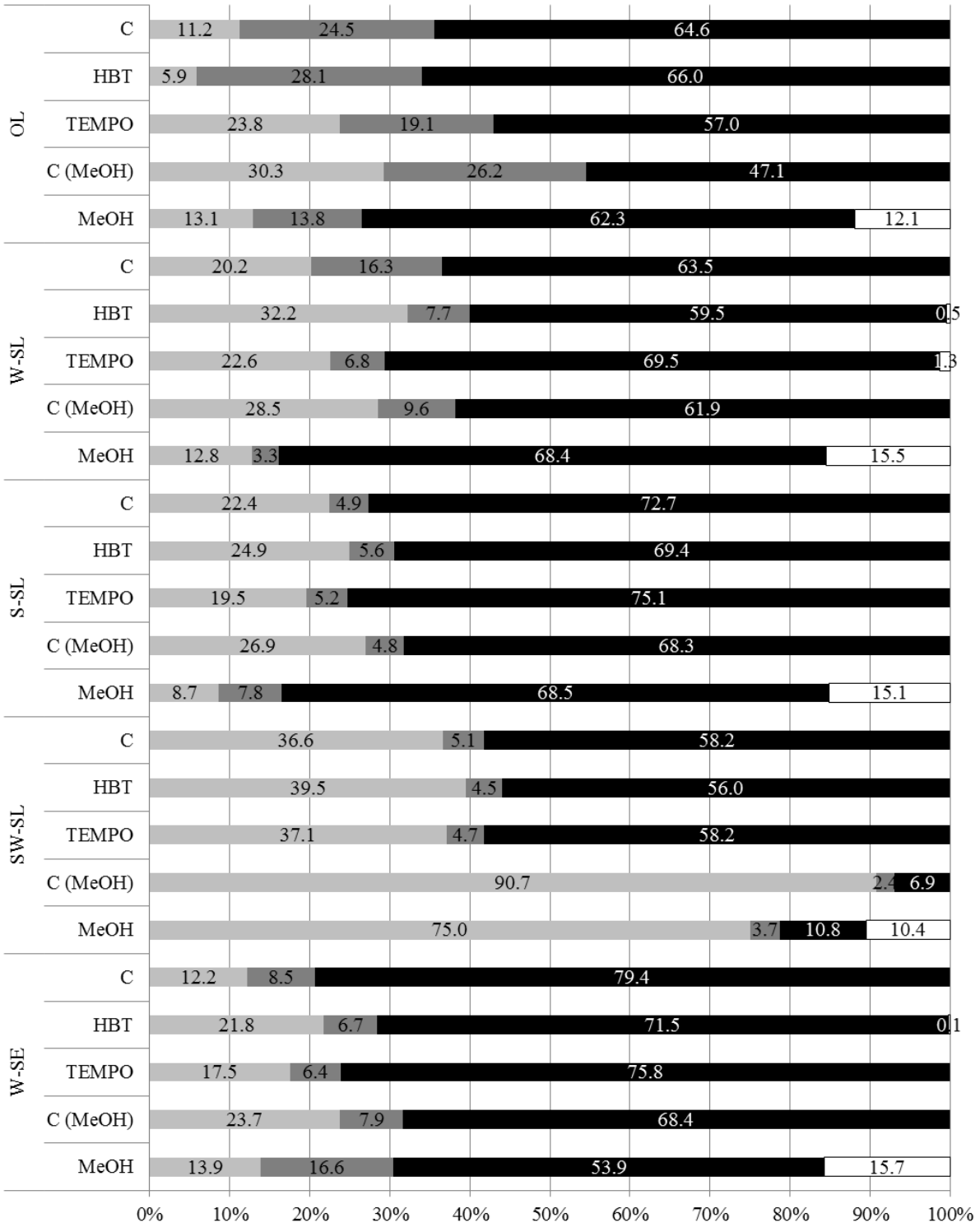

Figure 7.18 Mass balances of different lignins sequentially treated in presence of mediators as well as in presence of 30 % (v/v) MeOH. Mass balances of enzyme free controls (C) and enzyme free controls with 30 % (v/v) MeOH (C (MeOH)) are shown as well. Values are given in wt%. Light grey; aqueous soluble compounds (pH=2), dark grey; EtAc soluble compounds after formic acid/formate treatment (or in case of untreated controls after separation of water soluble (pH=2) compounds), black; residual material after treatment, white; material adsorbed on magnetite particles.

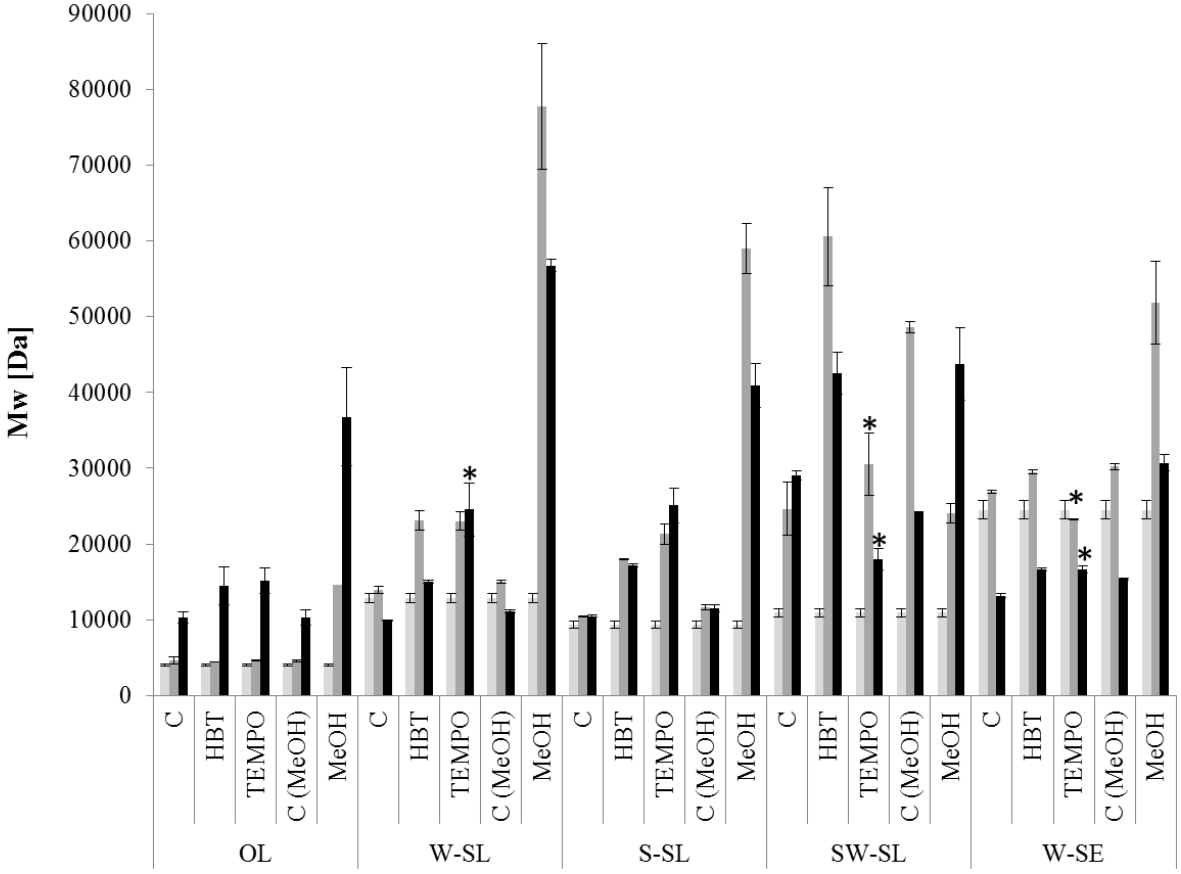

Figure 7.19 Mw of lignin starting material (light grey), insoluble residues after the first treatment step (dark grey), and after formic acid/formate treatment (black). Error bars show standard deviations (n=3). Lignins were sequentially treated with TVL-MP in presence of mediators as well as in presence of 30 % (v/v) MeOH. Results for enzyme free controls (C) and enzyme free controls with 30 % (v/v) MeOH (C (MeOH)) are shown as well. Samples not completely soluble in DMSO are designated with a *.

Regarding monomeric reaction products one main reaction product, i.e., DMBQ was formed during the first treatment step in case of all lignins with one exception, i.e., SW-SL (Figure 7.20; Table A. 24). Since, softwood lignins only contain traces of S (Higuchi 2006) it seems consequential that no DMBQ (which most likely derives from S within the lignin structure) was formed from lignin originating from softwood. DMBQ yields were similar for soda lignins derived from grasses (i.e., 0.34 and 0.31 wt% for W-SL and S-SL, respectively) and slightly lower for the lignin derived after steam explosion (i.e., 0.12 wt%). Highest yields were obtained from OL originating from hardwood lignin (1.10 wt%). This seems consequential since hardwood lignin has a higher S content compared to lignins from grasses (Brunow 2001; Fukushima 2001; Higuchi 2006). A decrease in the concentration of monomeric phenolic compounds which were present in the lignins before treatment like e.g., vanillin or syringaldehyde was observed during biocatalytic treatment of lignins irrespective of the origin indicating transformation and most likely polymerization of these compounds due to enzymatic oxidation.

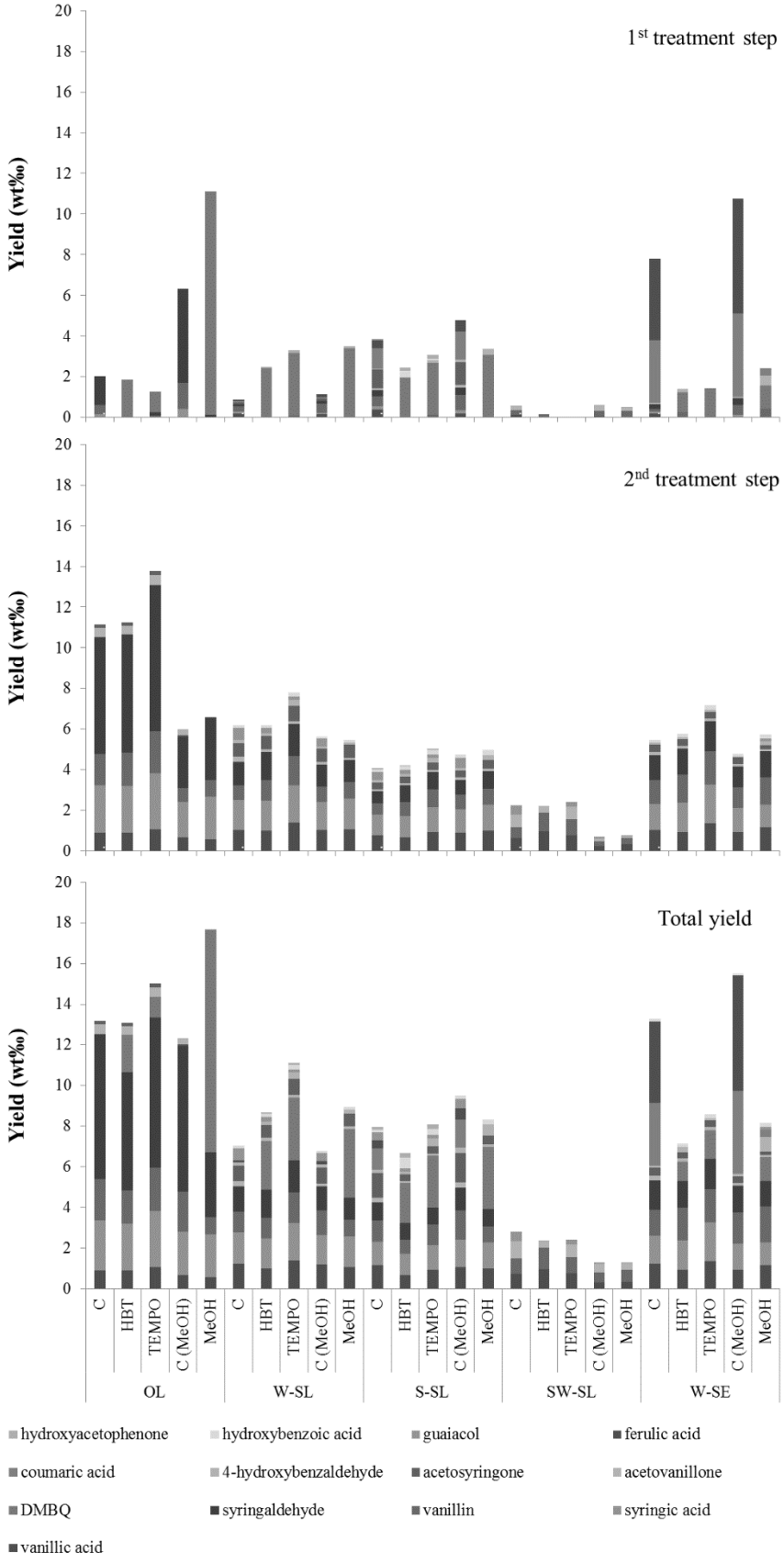

Figure 7.20 Yield of identified monomeric compounds after the different treatment steps and after the whole treatment. Lignins were sequentially treated with TVL-MP in presence of mediators as well as in presence of 30 % (v/v) MeOH. Results for enzyme free controls (C) and enzyme free controls with 30 % (v/v) MeOH (C (MeOH)) are shown as well.

Effects of the formic acid/formate reaction on Mw of lignin differed depending on the lignin. For lignins from grasses, i.e., W-SL, S-SL, and W-SE Mw decreased while for lignins from wood, i.e., OL and SW-SL Mw increased. The increase in MW for wood lignins indicates that next to the proposed cleavage of oxidized β-O-4 bonds also polymerization and condensation reactions occur. It has been proposed that in acidic media lignin carbocations are formed (Lundquist and Lundgren 1972). These carbocations react further either forming enol ether after β-proton elimination (Lundquist and Lundgren 1972) or re-polymerize with other lignin macromolecules (Sarkanen and Ludwig 1971). It might be that such polymerization reactions outweighed the depolymerization reactions in case of the lignins derived from wood. In order to test this hypothesis, OL was subjected to formic acid/formate treatment in the presence and absence of a carbocation scavenger, i.e., 2-naphtol which reacts with lignin carbocations by nucleophilic attack preventing subsequent re-polymerization reactions with other lignin macromolecules (Pielhop et al. 2015). The proposed reactions are summarized in Figure 7.21. Mw of OL increased to 6,590±110 and 12,910±600 Da in the presence and absence of 2-naphtol, respectively showing that the carbocation scavenger suppressed polymerization reactions during the formic acid/formate treatment indicating that the proposed pathway for lignin re-polymerization might indeed cause the observed increase in Mw of the wood derived lignins.

Several monomeric products were produced during the formic acid/formate reaction from all lignins treated previously with TVL-MP in presence of MeOH (Figure 7.20, Table A. 24) showing that all lignins were partially depolymerized during the second reaction step (even if the treatment led to an overall increase in Mw for lignins derived from wood). However, there were only minor differences between treated samples and controls showing that the enzymatic oxidation step had no substantial beneficial effect for the production of monomeric compounds from lignin.

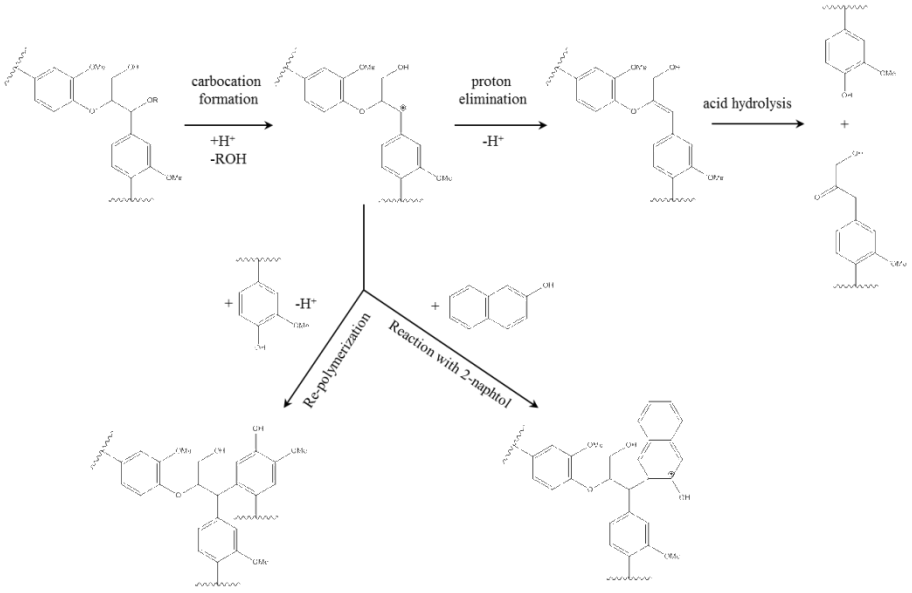

Figure 7.21 Scheme depicting proposed reactions of lignin in acidic media and the effect of 2-naphtol as carbocation scavenger (scheme is based on reaction mechanisms proposed previously by Lundquist and Lundgren (1972), Sarkanen and Ludwig (1971), and Pielhop et al. (2015)).

7.3.1.2. Treatment with redox mediator HBT

Treatment of lignins using the HBT LMS had different effects on the solubility of compounds after the first treatment depending on the lignin (Figure 7.18). An increase in soluble compounds indicating partial lignin depolymerization was observed for all lignins derived from grasses and was highest for W-SL, i.e., 12.0±4.9 wt%. For lignin from softwood there was also a slight increase in solubility of 2.9±1.9 wt% compared to controls. However, this increase was not significant (p=0.098, students t-test, two-tailed distribution, unequal variance). For OL there was even a slight decrease in solubility by 5.1±6.0 wt%. However, this decrease was also not significant (p=0.267, students t-test, two-tailed distribution, unequal variance).

Mw of insoluble lignin after the first treatment step was higher than in controls for all lignins. However, compared to insoluble lignin after treatment in 30 % (v/v) MeOH, Mw was considerably lower for all lignins with one exception, i.e., SW-SL. These results indicate that polymerization of lignins during the first treatment step was less substantial compared to treatments using MeOH. In case of W-SL and W-SE the treatment might even have led to an overall lignin depolymerization. An increase in solubility compared to controls of 12.0±4.9 and 9.7±3.7 wt% for W-SL and W-SE, respectively went along with only a modest increase in Mw of 9,210±1,370 and 2,630±390 Da for W-SL and W-SE, respectively. Therefore, the increases in Mw might be partly due to increased solubilization of lower molecular weight lignin oligomers and partly due to polymerization. It has been reported previously that in the presence of HBT, side-chain oxidation reactions predominate radical-coupling and condensation reactions (Figure 7.16, Crestini et al. 2003). This is in agreement with the observed lower amount of lignin polymerization occurring in the HBT treatments as opposed to the treatments in 30 % (v/v) MeOH.

Regarding monomeric compounds, DMBQ was obtained again as the main product after the first reaction step in all lignins except SW-SL (Figure 7.20, Table A. 24). Generally, DMBQ yields were slightly lower compared to yields obtained after treatment in 30 % (v/v) MeOH. However, in case of OL the decrease in DMBQ yield was quiet considerable and a DMBQ yield of only 0.18±0.01 wt% was obtained as opposed to 1.10±0.02 wt% after treatment in 30 % (v/v) MeOH. The lower DMBQ yields in all cases correspond well to the proposed predominance of the side-chain oxidation pathway in presence of HBT. DMBQ is most likely formed after phenoxy radical formation (Figure 7.16, Kawai et al. 1988) which would be reduced if side-chain oxidations are favored (Crestini et al. 2003). Furthermore, MeOH partly solubilizes lignin potentially increasing accessibility of phenolic groups for direct enzymatic oxidation, therefore, facilitating phenoxy radical formation. Consequently, DMBQ production as well as lignin polymerization and condensation reactions are facilitated if more lignin is dissolved. Especially in case of OL addition of the co-solvent might have considerably increased accessibility for the enzymes to phenolic groups on syringyl units which would explain the considerably higher DMBQ yield in treatments with MeOH.

Formic acid/formate reaction led to a reduction of Mw of the treated lignin for all lignins from grasses as observed after treatments with MeOH. Likewise, the Mw of OL increased. However, opposed to what was observed after treatment in MeOH, the Mw of SW-SL decreased during the formic acid/formate reaction step if the lignin was treated with the HBT LMS. It might be that lignin side-chain oxidation increased the amount of oxidized β-O-4 side-chains in this lignin, thereby, enabling subsequent cleavage during the formic acid/formate reaction (Figure 7.16). There was no significant change in solubility after the first reaction step for SW-SL while Mw increased. This indicates that no or only little Cα-Cβ cleavage after oxidation by HBT occurred in case of this lignin. Therefore, oxidized side-chains were potentially still intact prior to formic acid/format treatment which would explain the observed decrease in Mw during the second treatment step. The observed increase in Mw of controls during the formic acid/formate treatment gives further indication that the amount of cleavable bonds might have increased during treatment. However, Mw was still higher in treated samples compared to controls after the sequential treatment, i.e., Mw was 29,100±600 and 42,500±2,800 Da for controls and treated samples, respectively.

Several monomeric compounds were produced during the second treatment step from all lignins previously treated with the HBT LMS (Figure 7.20, Table A. 24). However, as in the experiments conducted in 30 % MeOH, there were only minor differences between controls and treated samples showing that the HBT LMS treatment step had no substantial beneficial effect for the production of monomeric compounds from lignin.

7.3.1.3. Treatment with redox mediator TEMPO

Treatment of lignins using the TEMPO LMS had different effects on the solubility of compounds after the first treatment depending on the lignin (Figure 7.18). No considerable change in solubility compared to controls was observed for all soda lignins. However, solubility increased by 12.6±5.2 and 5.3±2.8 wt% for OL and W-SE, respectively. No considerable difference in Mw was observed between insoluble lignins after the first treatment step between controls and treated samples for OL. Mw was 4,560±480 and 4,620±112 Da for controls and treated samples, respectively. Therefore, indicating that no considerable lignin polymerization occurred during treatment while some lignin was solubilized and therefore, potentially depolymerization reactions occurred. For the other lignins the TEMPO LMS treatment step led to an increase in Mw of insoluble lignin. In case of SW-SL and W-SE lignin even became partly insoluble in DMSO impeding correct determination of Mw by SEC. Therefore, results indicate that all lignins with the exception of OL were polymerized during the TEMPO LMS treatment.

As for the other treatments DMBQ was the main monomeric reaction product during the first treatment except for softwood lignin (Figure 7.20, Table A. 24). DMBQ yields were between yields obtained after treatments with the HBT LMS and treatments conducted in 30 % (v/v) MeOH for W-SL and S-SL. DMBQ yields were 0.85±0.20 wt% lower and 0.28±0.05 wt% higher in samples treated with TEMPO LMS compared to samples treated with HBT LMS for OL and W-SE, respectively.

Formic acid/formate reaction after TEMPO LMS treatment led to formation of black solid residues insoluble in DMSO for W-SL, SW-SL, and W-SE indicating char formation during treatment and impeding correct determination of Mw. For the other two lignins, i.e., OL and S-SL Mw increased during the second treatment step pointing towards lignin polymerization reactions. Regarding monomeric compounds the second treatment again led to the production of several compounds (Figure 7.20, Table A. 24) showing that depolymerization reactions occurred as well. Overall yields of monomeric products obtained after the second treatment were slightly higher for treatments with TEMPO compared to yields of the other treatments investigated. Compared to controls increases varied between 0.02±0.01 and 0.26±0.09 wt% for SW-SL and OL, respectively.

7.3.2. Optimization of lignin treatment for W-SL

W-SL was selected as feedstock and HBT as redox mediator for further optimization of the process. This selection was done based on the results of subchapter 7.3.1 which were promising for this setup since lignin was solubilized during the first reaction and Mw of residual lignin was reduced during the second reaction. The influences of six factors on the resulting lignin products were investigated using RSM. The factors were enzymatic activity, HBT concentration, enzymatic reaction time, pH during the enzymatic treatment, formic acid/formate treatment reaction time, and sodium formate concentration. Factors were varied from 1.5 to 15.0 kU L^{-1} (enzymatic activity), 1 to 10 mM (HBT concentration), 4 to 48 h (enzymatic reaction time), 5 to 8 (initial pH of enzymatic treatments), 4 to 48 h (formic acid/formate treatment reaction time), and 1 to 10 g L^{-1} (sodium formate concentration). The influence of these factors on several results, i.e., lignin solubility in aqueous solution at pH 2 after enzymatic treatment, Mw of water insoluble lignin after enzymatic treatment and acidification, EtAc solubility after formic acid/formate treatment, yield of identified monomers, Mw after formic acid/formate treatment, and total lignin solubility (the sum of the lignin solubilized in aqueous solution after acidification after enzymatic treatment and in EtAc after formic acid/formate treatment) were studied. Model results are given in the appendix (Table A. 25-Table A. 33). Precision of the model predictions was calculated based on the 95 % confidence intervals by means of error propagation and the obtained ranges are given in brackets after the estimated values.

7.3.2.1. Results of optimization experiments

7.3.2.1.1. Enzymatic treatment

Enzymatic treatment influenced the lignin solubility in aqueous solution after the acidification step. While 20.2±2.1 wt% of untreated lignin was solubilized, up to 29.1 wt% was solubilized during enzymatic treatments. The predicted effects of the corresponding model are depicted in Figure 7.22. Enzymatic activity was predicted to positively affect solubility. Increasing enzymatic activity from 1.5 to 15.0 kU L^{-1} was predicted to increase lignin solubility by 10.8 (6.8-14.8) wt%. The enzymatic reaction time was predicted to only have small effects on lignin solubility in the range of 3.9 (0.0-7.8) wt%. The effects of pH and HBT concentration were predicted to depend on each other. At pH 5 increasing HBT

concentration positively influenced lignin solubility (6.8 (2.5-11.1) wt%) before reaching a plateau around 6.8 mM. At pH 8 increasing HBT concentration from 1.0 to 4.0 mM led to an unsubstantial increase in solubility by 1.8 (-2.5-6.1) wt%. Further increasing HBT concentration to 10 mM leads to a more considerable decrease in solubility of 7.3 (2.8-11.7) wt%.

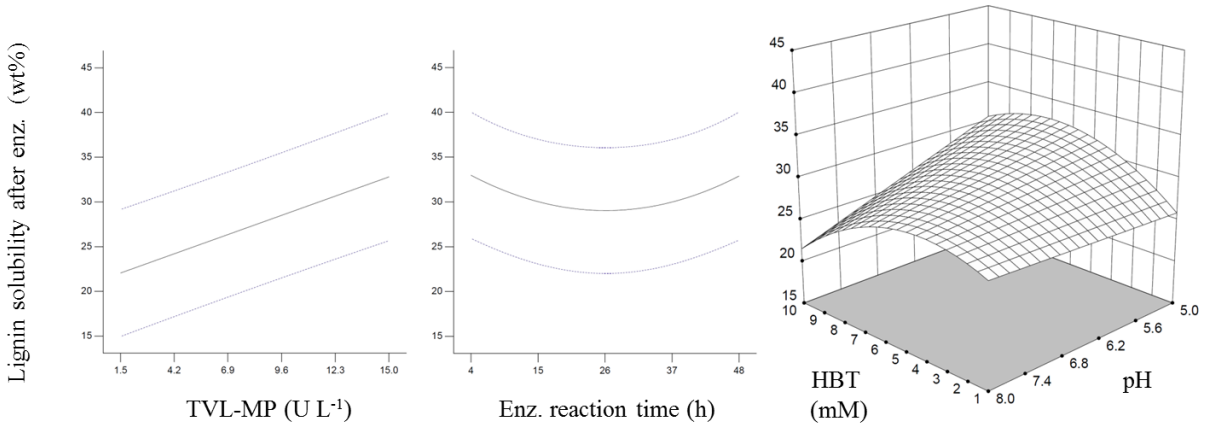

Figure 7.22 Effects of the different factors predicted by the response surface reduced second-degree polynomial model for lignin solubility after enzymatic treatment in aqueous solution (pH 2). Factors that are not shown were held constant at predicted optimal conditions concerning total lignin solubility (see text). Bands displayed show 95 % prediction intervals (adapted from Gasser et al. (2017)).

The Mw of the insoluble lignin material after enzymatic treatment was considerably affected by reaction conditions. While untreated insoluble lignin had Mw of 15,550±580 Da the Mw of insoluble lignin of different experiments ranged from 17,490 to 82,950 Da. The model predictions for the influence of the different factors are depicted in Figure 7.23. A transformation of the results was conducted prior to model fitting. Therefore, the influence of the different factors on Mw cannot be given in the same straightforward quantitative manner as for the models for which no transformation of results was necessary since the quantitative influence of changing one factor on Mw is influenced by the values of all the other factors. However, in order to still give some quantitative measures, factors that were not investigated were held constant at their center point. Increasing enzymatic activity from 1.5 to 15.0 kU L^{-1} was predicted to increase Mw by 10,990 (7,600-14,500) Da. In contrast to enzymatic activity increasing HBT concentrations were predicted to reduce Mw of insoluble materials. Increasing HBT from 1.0 to 10.0 mM was predicted to lead to a decrease of 3,950 (600-7,420) Da.

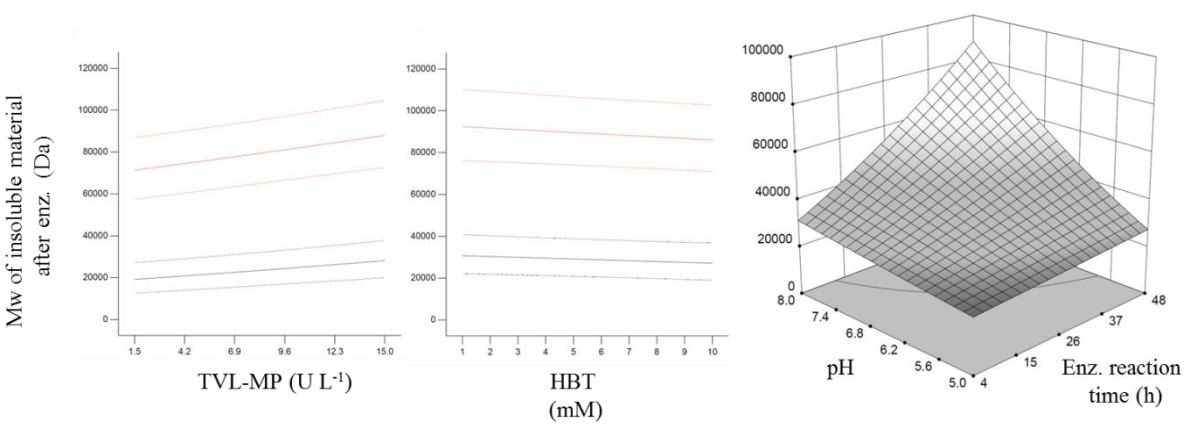

Figure 7.23 Effects of the different factors predicted by the response surface reduced second-degree polynomial model for Mw of insoluble material after enzymatic treatment. Factors that are not shown were held constant at predicted optimal conditions concerning total lignin solubility (see text). Effects for pH 5 (black lines) and pH 8 (red lines) are shown for the single factors. Bands displayed show 95 % prediction intervals (adapted from Gasser et al. (2017)).

The effects of pH and enzymatic reaction time on Mw of insoluble lignin were predicted to depend on each other. At pH 5 increasing reaction time from 4 to 48 h had only a small effect on Mw, i.e., it increases by 4,400 (350-8,740) Da. However, at pH 8 increasing reaction time from 4 to 48 h led to a considerable increase of Mw by 53,310 (45,650-61,330) Da.

Regarding monomeric compounds, the enzymatic treatment yielded one main reaction product, i.e., 2,6-dimethoxy benzoquinone (DMBQ). The yield varied between 0.00 and 0.27 wt%. No model satisfyingly describing DMBQ production could be derived (i.e., all models tested had significant lack of fit). However, it was notable that in general higher yields were obtained for longer treatment times and lower pH values. All treatments leading to yields of 0.20 wt% and more lasted at least 21 h and were conducted at pH 6.5 or lower. This indicates that DMBQ formation was rather a slow process and was facilitated by lower pH.

7.3.2.1.2. Formic acid/formate treatment

After the enzymatic treatment the insoluble lignin products were separated and subjected to formic acid/formate treatment. The Mw of lignin after this second treatment step heavily depended on the conditions applied during the first treatment step. The predicted effects of the corresponding model are depicted in Figure 7.24. Results were transformed before model fitting. As for the model discussion above, factors that are not discussed were set constant at the center point in order to give some quantitative measures. The influence of enzymatic reaction time and enzymatic activity is predicted to heavily depend on pH. While only little differences in Mw are predicted for lignin treated at pH 5 during the first reaction step, the influences of enzymatic reaction time and enzymatic activity became more substantial at higher pH. At pH 8 Mw increased by 21,400 (11,090-33,840) Da and 18,920 (9,470-33,290) Da by increasing enzymatic activity from 1.5 to 15.0 kU L^{-1} and enzymatic reaction time from

4 to 48 h, respectively. Sodium formate and HBT concentration changes only had little effects on Mw. Increasing sodium formate concentration from 1.0 to 10.0 g L^{-1} Mw increases by 5,570 (-710-13,570) Da for lignin treated with 1.5 kU $L^{-1}$and decreases by 9,240 (-1,490-17,800) Da for lignin treated with 15.0 kU L^{-1}. Changing HBT concentration during the enzymatic treatment had a lower effect on Mw after formic acid/formate treatment. Increasing HBT concentration from 1.0 mM to 5.5 mM led to a decrease of 5,470 (-1,270-11,209) Da. Further increasing HBT concentration to 10.0 mM led again to an increase of 5,560 (-140-12,250) Da. Effects of changes in formic acid/formate reaction times were more considerable. Increasing formic acid/formate reaction time from 4 to 37 h led to an increase of 11,610 (7,110-16,930) Da before reaching a plateau.

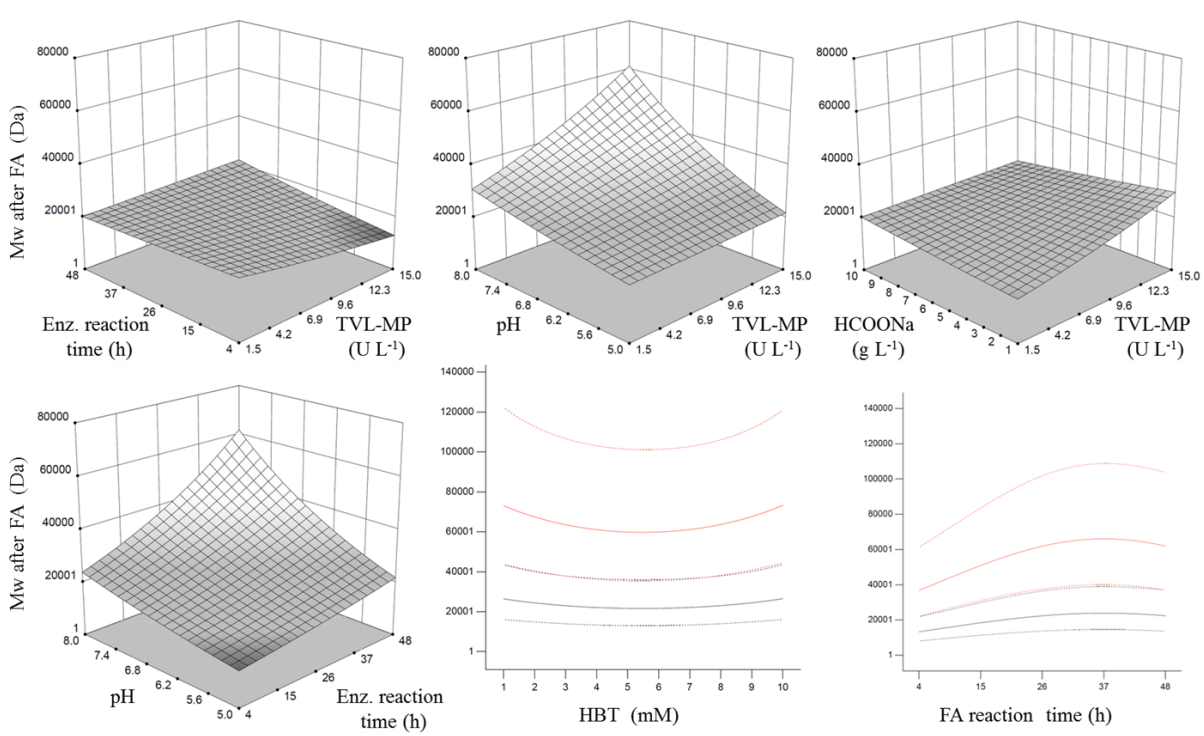

Figure 7.24 Effects of the different factors predicted by the response surface reduced second-degree polynomial model for Mw after formic acid/formate treatment. Factors that are not shown were held constant at predicted optimal conditions concerning total lignin solubility (see text). Effects for pH 5 (black lines) and pH 8 (red lines) are shown for the single factors. Bands displayed show 95 % prediction intervals (adapted from Gasser et al. (2017)).

Low molecular weight reaction products after formic acid/formate treatment were extracted in EtAc and their weight was determined after drying. The predicted effects of the corresponding model are depicted in Figure 7.25. Reaction time of the formic acid/formate treatment positively affected the amount of EtAc soluble compounds. This effect was more pronounced if the lignin was treated at lower enzymatic activities in the prior reaction step. Increasing formic acid/formate treatment time from 4 to 48 h led to an increase of 3.1 (1.6-4.6) and 0.5 (-1.1-2.0) wt% for lignin previously treated at 1.5 and 15.0 kU L^{-1}, respectively.

Increasing sodium formate concentration during the formic acid/formate treatment also positively influenced the yield of EtAc soluble compounds. This effect was more pronounced if the lignin was treated at lower pH prior to formic acid/formate treatment. Increasing sodium formate concentration from 1.0 to 10.0 g L^{-1} led to an increase of 6.7 (5.2-8.3) and 2.9 (1.4-4.4) wt% for lignin previously treated at pH 5 and 8, respectively.

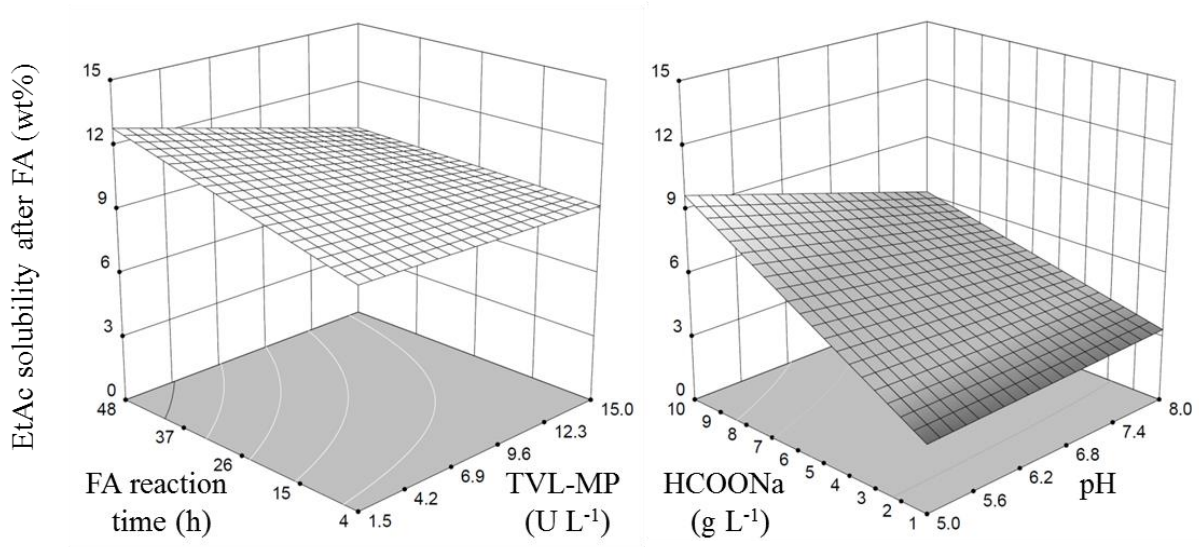

Figure 7.25 Effects of the different factors predicted by the response surface reduced second-degree polynomial model for EtAc solubility after formic acid/formate treatment in wt% (based on lignin weight initially applied for the sequential treatment). Factors that are not shown were held constant at predicted optimal conditions concerning total lignin solubility (see text; adapted from Gasser et al. (2017))

The effects of the reaction conditions on the Mw of the EtAc soluble fraction predicted by the corresponding model were also studied (Figure 7.26). Increasing sodium formate concentration and reaction time of the formic acid/formate treatment led to lower Mw of the EtAc soluble fraction. The lowest Mw was predicted for treatments lasting 48 h and using 3.9 g L^{-1} sodium formate. Further increasing sodium formate concentration to 10.0 g L^{-1} was predicted to yield EtAc fractions with slightly higher Mw (an increase of 247 (88-412) Da was predicted). However, treatments with higher sodium formate concentrations were also predicted to yield considerably higher overall amounts of EtAc soluble products (an increase of 3.3 (2.1-4.4) wt% was predicted). Therefore, the predicted increase in Mw by increasing sodium formate seems rather due to the solubilization of more oligomeric products than due to less lignin degradation. Concerning the first treatment step, increasing HBT concentration and enzymatic reaction time had a slightly negative influence on the Mw of the EtAc extractable fraction after formic acid/formate treatment leading to a decrease of 219 (3-391) and 145 (6-260) Da by increasing HBT from 1.0 mM to 10.0 mM and enzymatic reaction time from 4 to 48 h, respectively.

The effect of pH during the enzymatic treatment on the Mw of the EtAc fraction was dependent on the reaction time of the formic acid/formate treatment. At a formic acid/formate reaction time of 4 h there was little effect of pH on the Mw (a negligible increase of 12 (-207-299) Da was predicted by increasing pH from 5 to 8). However, at a formic acid/formate reaction time of 48 h a decrease of 264 (97-394) Da in Mw was predicted by increasing pH from 5 to 8. However, this decrease in Mw went along with a decrease of 1.6 (0.3-2.8) wt% in EtAc soluble products. Therefore, these results indicate that overall less low molecular weight products were produced from the lignin that was more strongly polymerized during treatment at higher pH.

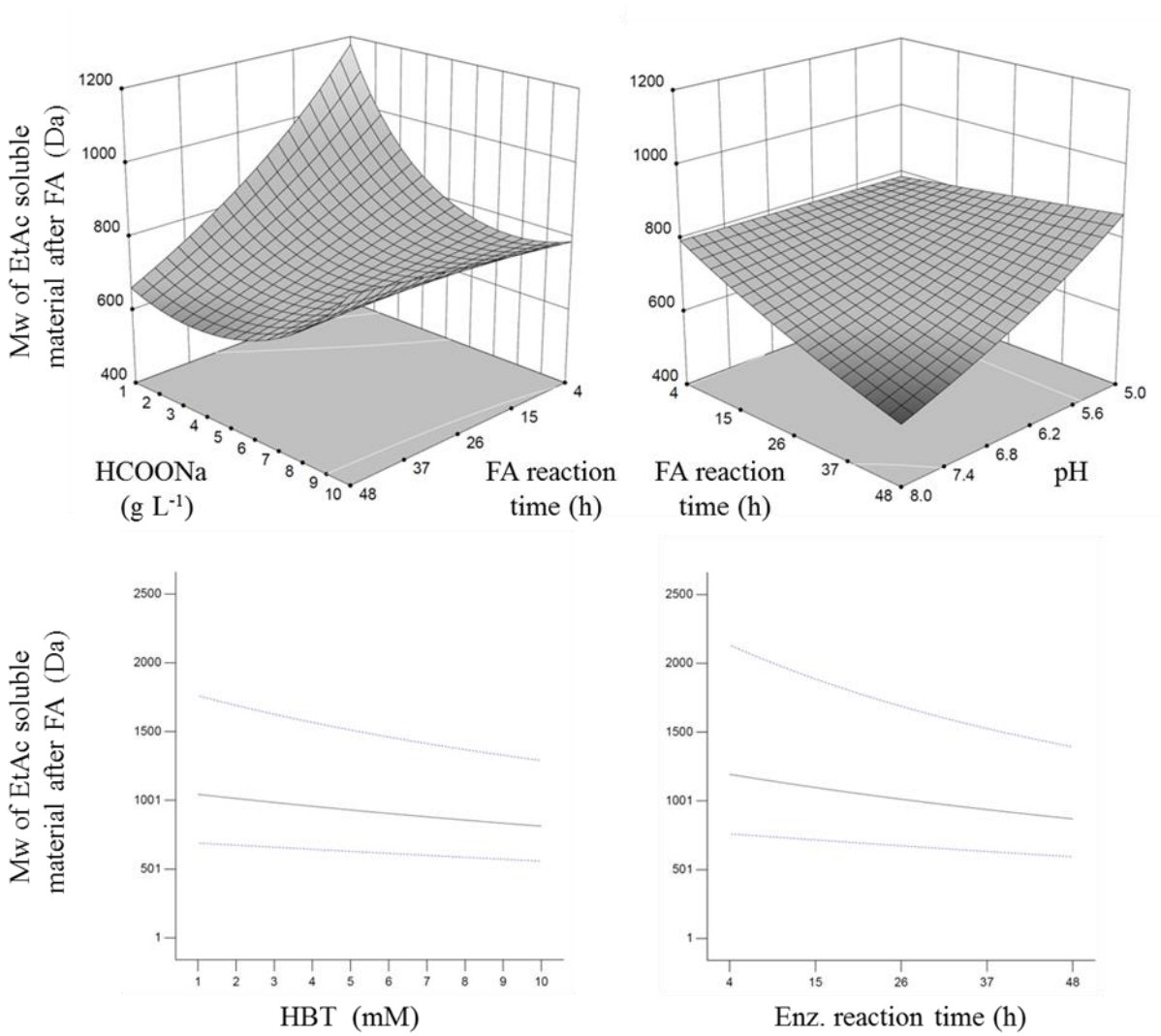

Figure 7.26 Effects of the different factors predicted by the response surface reduced second-degree polynomial model for Mw of EtAc soluble material after formic acid/formate treatment. Factors that are not shown were held constant at predicted optimal conditions concerning total lignin solubility (see text). Bands displayed show 95 % prediction intervals (adapted from Gasser et al. (2017)).

Several monomeric phenolic compounds were produced from lignin during the formic acid/formate treatment. The obtained yields of identified monomers are summarized in the appendix (Table A. 34). Total monomer yields based on the initially applied lignin weight, i.e., the lignin weight applied to the biocatalytic treatment, varied between 3.03 and 9.77 wt‰. The predicted effects of reaction conditions on the monomer yield after the second treatment step by the corresponding model are depicted in Figure 7.27. All six factors affected the monomer yields. As for the other model discussions, factors that are not discussed were set constant at the center point for quantitative discussion of the predicted effects. The effect of pH during the first treatment step depended on TVL-MP activity and the enzymatic treatment time. Monomer yield increased by 1.2 (0.6-1.9) wt‰ and decreased by 0.2 (-0.4-0.8) wt‰ at 1.5 and 15 kU L^{-1}, respectively by increasing pH from 5 to 8 and was predicted to be highest at pH 8 and 1.5 kU L^{-1}. Furthermore, monomer yield increased by 1.3 (0.7-2.0) wt‰ and decreased by 0.3 (-0.4-1.0) wt‰ at 4 and 48 h of enzymatic reaction time, respectively by increasing pH from 5 to 8 and was predicted to be highest at pH 8 and 4 h of enzymatic reaction time.

Changing sodium formate concentration during the formic acid/formate reaction was also predicted to have a modest effect on the monomer yield after the formic acid/formate treatment. The effect depended on the HBT concentration and the enzymatic reaction time. Monomer yield increased by 0.1 (-0.6-0.7) and 1.2 (0.6-1.9) wt‰ by increasing sodium formate from 1 to 10 g L^{-1} for samples treated with 1 and 10 mM HBT, respectively. Furthermore, monomer yield increased by 1.6 (0.9-2.3) wt‰ and decreased by 0.3 (-0.4-1.0) wt‰ by increasing sodium formate concentration from 1 to 10 g L^{-1} for samples treated enzymatically for 4 and 48 h, respectively.

Increasing formic acid/formate reaction time led to increasing yields of monomeric compounds indicating that lignin was depolymerized over time. The degree of increase depended on the TVL-MP activity and the HBT concentration applied during the first reaction step. Monomer yield increased by 3.9 (3.2-4.5) and 2.2 (1.5-2.9) wt‰ by increasing reaction time from 4 to 48 h for 1.5 and 15.0 kU L^{-1}, respectively, and was highest for samples treated with 1.5 kU L^{-1} for 48 h. Furthermore, monomer yield increased by 3.6 (3.0-4.3) and 2.4 (1.8-3.1) wt‰ by increasing reaction time from 4 to 48 h for 1 and 10 mM HBT, respectively and was highest for samples treated at 10 mM HBT for 42.19 h.

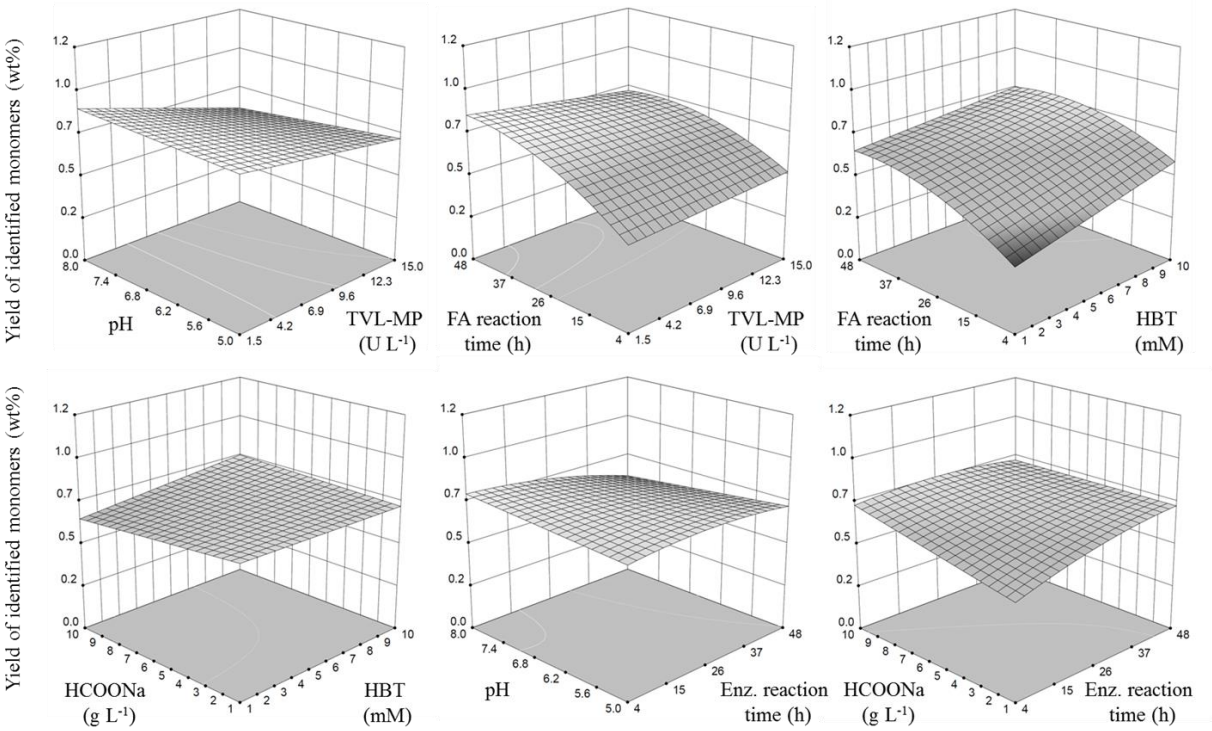

Figure 7.27 Effects of the different factors predicted by the response surface reduced second-degree polynomial model for yield of identified monomers after formic acid/formate treatment in wt% (based on lignin weight initially applied for the sequential treatment). Factors that are not shown were held constant at predicted optimal conditions concerning total lignin solubility (see text; adapted from Gasser et al. (2017)).

7.3.2.1.3. Combined biocatalytical and chemical processes

Evaluating the two-step process, most interesting process conditions for lignin treatment were selected based on overall lignin solubilization (solubilization either in aqueous solution after acidification after the enzymatic treatment or in EtAc after formic acid/formate treatment) since these conditions seemed most promising for the production of considerable amounts of low molecular weight oligomers from lignin. For this purpose, a model was fitted to the obtained results regarding overall lignin solubility. The predicted effects of the corresponding model are depicted in Figure 7.28. The exact effect of pH on the overall solubility is predicted to depend on several other factors, i.e., HBT concentration, enzymatic reaction time, reaction time of the formic acid/formate treatment, and sodium formate concentration. Lignin solubility decreases with increasing pH in all cases. This prediction corresponds well with the observed higher degree of lignin polymerization during enzymatic treatment at higher pH values. Since reaction conditions leading to high lignin solubilization were of interest the effects of all other factors on total lignin solubilization predicted by the model will be discussed in more detail leaving pH constant at 5. Furthermore, since results were transformed prior to fitting the model, factors that are not discussed were set constant at the predicted optimal conditions concerning lignin solubilization in order to give some quantitative measures. Increasing HBT concentration led to increasing lignin solubilization. The effect is more pronounced at lower enzymatic activities. Increasing HBT from 1.0 mM to 7.38 mM led

to an increase of 6.8 (3.8-9.6) and 3.3 (0.7-5.8) wt% at 1.5 kU L^{-1} and 15.0 kU L^{-1}, respectively. Further increasing HBT concentration did not lead to further substantial changes in lignin solubility. Increasing enzymatic activity also led to increased lignin solubilization. The effect is more considerable at lower HBT concentrations. Increasing enzymatic activity from 1.5 to 15.0 kU L^{-1} led to a solubility increase of 10.0 (7.0-12.8) and 5.8 (2.8-8.5) wt% at 1.0 and 10.0 mM HBT, respectively. Increasing reaction times had a moderate positive effect on lignin solubility. Increasing enzymatic reaction time from 4 to 48 h led to a solubility increase of 2.3 (-0.2-4.7) wt%. The effect of formic acid/formate reaction time depends on the enzymatic activity used during the first treatment step. By increasing reaction times from 4 to 48 h, solubility increased by 1.9 (-1.1-4.7) and 4.1 (1.8-6.3) wt% at 1.5 and 15 kU L^{-1}, respectively. Furthermore, increasing sodium formate concentration from 1.0 to 10.0 g L^{-1} led to increasing lignin solubility by 3.5 (1.0-5.8) wt%.

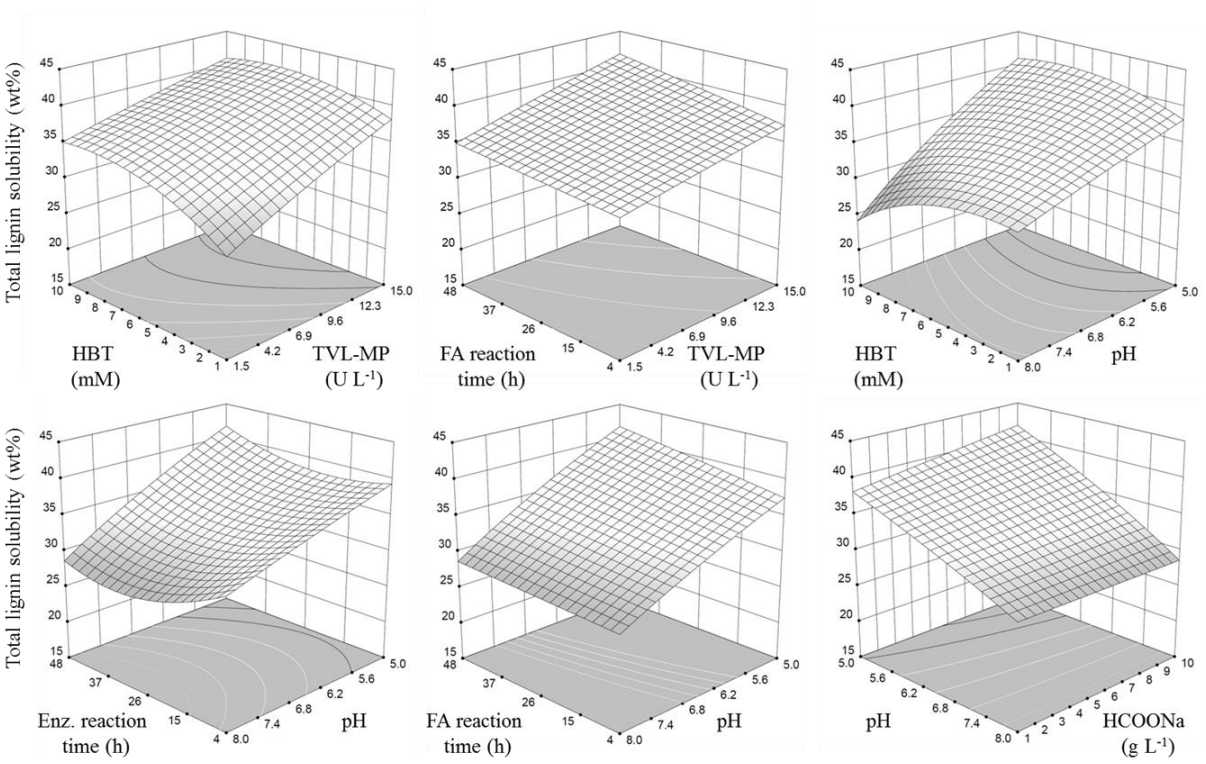

Figure 7.28 Interaction effects of the factors predicted by the response surface reduced second-degree polynomial model for total lignin solubility. Factors that are not shown were held constant at predicted optimal conditions (see text; adapted from Gasser et al. (2017)).

Optimal conditions regarding lignin solubilization are predicted to be 15.0 kU L^{-1} (enzymatic activity), 7.38 mM (HBT concentration), 47.75 h (enzymatic reaction time), 5.01 (initial pH of enzymatic reaction), 47.97 h (formic acid/formate reaction time), and 9.94 g L^{-1} (sodium formate concentration). An overall lignin solubilization of 41.7 wt% was predicted by the model for these conditions. In order to evaluate the validity of the different models, the experiments under these conditions were performed in triplicates; the results are discussed in paragraph 7.3.2.2.

7.3.2.2. Optimized lignin treatment regarding solubility for W-SL

Lignin was treated at predicted optimal conditions regarding total lignin solubility (either in aqueous solution at pH 2 after enzymatic treatment or in EtAc after formic acid/formate treatment). Experimental results are summarized in Table 7.3 and compared to the predictions of the different models derived from the RSM experiments. By and large the model predictions fit the experimental results well. With one exception all experimental results were within the 95 % confidence interval or 95 % prediction interval of the corresponding model. Only the total lignin solubility was slightly outside the prediction interval. However, taking into account the standard deviation of the experimental results (44.6±2.3 wt%), it was not considerably above the high value of the 95 % confidence interval (43.2 wt%) of the model.

Table 7.3 Comparison between experimental results of experiments conducted at predicted optimal conditions regarding total lignin solubility (errors show standard deviations, n=3) and model predictions (CI; confidence intervals of models, PI: prediction intervals of models; adapted from Gasser et al. 2017)

	Unit	Experimental results	Model prediction	95 % CI low	95 % CI high	95 % PI low	95 % PI high
Solubility after enzymatic treatment	wt%	36.7 ± 2.2	32.8	29.5	36.1	25.7	39.9
Mw of insoluble material after enzymatic treatment	Da	31,199 ± 1’283	28,328	24,680	32,228	20’129	37,925
EtAc solubility after formic acid/formate treatment	wt%	7.9 ± 0.2	9.8	8.2	11.3	6.8	12.7
Mw after formic acid/formate treatment	Da	22,763 ± 1’943	22,473	16,663	30,307	13,593	37,153
Mw of EtAc soluble fraction	Da	645 ± 9	872	705	1,105	595	1,396
Monomer yield after formic acid/formate treatment	wt‰	6.87 ± 0.21	7.03	6.34	7.71	5.93	8.12
Total lignin solubility	wt%	44.6 ± 2.3	41.7	40.0	43.2	39.1	44.1

The mass balance of the treated samples is depicted in Figure 7.29 and compared to an untreated control and a control in which the water insoluble lignin was treated by formic acid/formate treatment as well. Representative GPC chromatograms of the soluble fractions of the treated samples and controls are shown in Figure 7.30. Compared to the controls the enzymatic treatment led to increased lignin solubilization in aqueous solution at pH 2 by 16.5±3.0 wt%. Comparison of the GPC chromatograms of the aqueous soluble fractions of treated samples and controls (Fig. 4A) shows that mostly low molecular weight oligomeric lignin was solubilized during treatment. Since the lignin signal is superimposed by the HBT signal (HBT absorbance is high around 280 nm, ε_{280}=3,650 M^{-1} cm^{-1}), Mw of the soluble compounds was estimated based on the signal at 330 nm (HBT absorbance is considerably lower, ε_{330}=1,310 M^{-1} cm^{-1}). A Mw of 2,357±52 and 2,754±131 Da was calculated including and excluding the mediator peak, respectively. Consequently, the actual Mw of the soluble fraction lies between these two values. During the first treatment step DMBQ was again produced from lignin at a yield of 0.25±0.01 wt%, i.e., close to highest yields obtained during the first set of experiments (0.27 wt%). The enzymatic activity after treatment of the TVL-MP was 62.0±0.7 % of the initially applied activity. Furthermore, virtually all particles could be separated from the reaction suspension by application of a magnetic field, i.e., 100.1±2.8 % of the applied particle weight could be recovered after treatment.

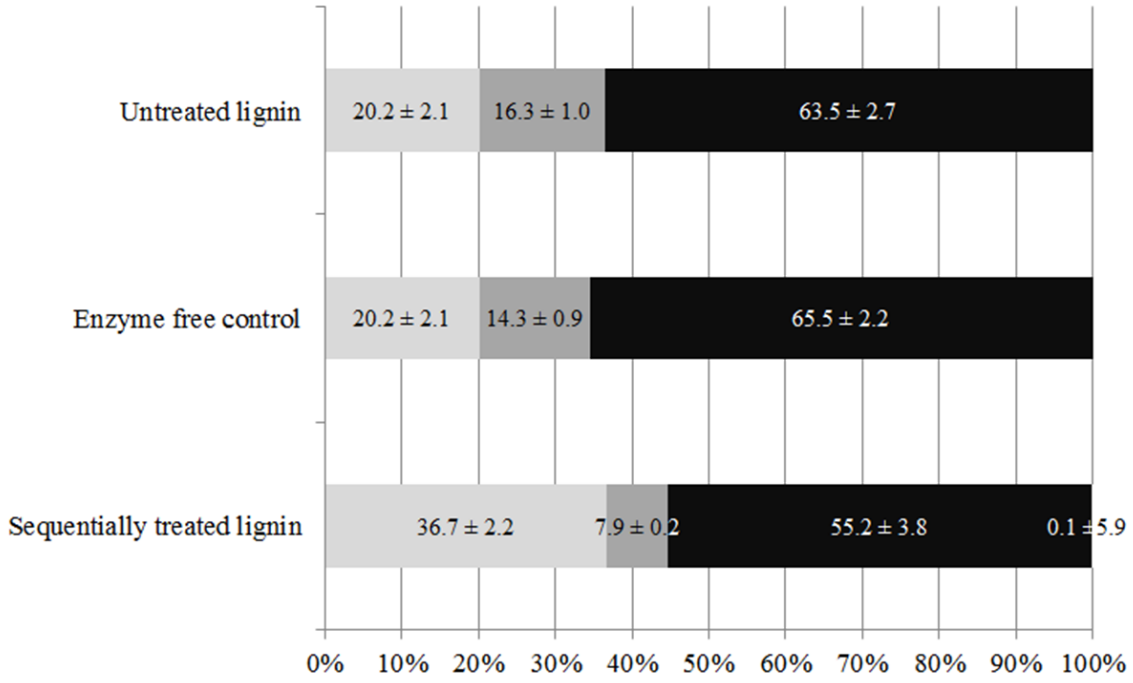

Figure 7.29 Mass balances of lignin sequentially treated at optimal conditions, of an untreated control, and a control only treated with formic acid/formate after separation of water (pH=2) soluble compounds. Values are given in wt% plus minus standard deviation (n=3). Light grey; aqueous soluble compounds (pH=2), dark grey; EtAc soluble compounds after formic acid/formate treatment (or in case of untreated controls after separation of water soluble (pH=2) compounds), black; residual material after treatment, white; material adsorbed on magnetite particles (adapted from Gasser et al. (2017)).

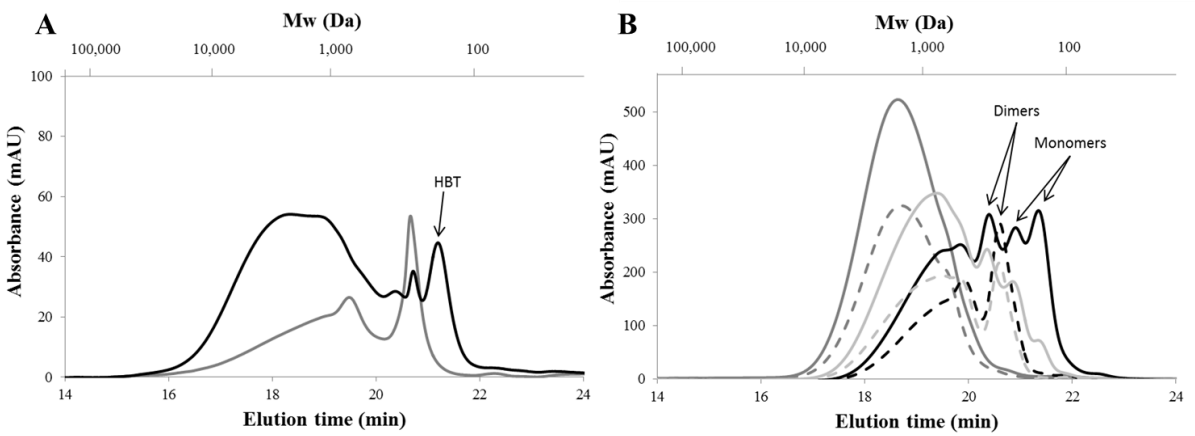

Figure 7.30 GPC chromatograms of soluble lignin products in aqueous solution after enzymatic treatment (A) and in EtAc after formic acid/formate treatment (B). Black lines: treated samples, dark grey lines; untreated controls, light grey lines; only formic acid/formate treated controls. A) Chromatograms are shown at 330 nm. B) Chromatograms are shown at 280 nm (solid lines) and 330 nm (dashed lines). Samples were treated using reaction conditions determined to be optimal regarding total lignin solubilization (see text; adapted from Gasser et al. (2017)).

Insoluble lignin residues after the first treatment were analyzed by FTIR and spectra were compared to insoluble lignin in aqueous solution at pH 2. The peak at 1510 cm^{-1} was used as lignin reference as described previously (Panday and Pitman 2003). Consequently, peak areas are given relative to the corresponding lignin peak area for quantitative comparison between samples. The different ratios are summarized in Table 7.4 and representative FTIR spectra are shown in Figure 7.31. Typical bands reported for lignin were observed and identified according to literature (Santos et al. 2015). Most identified bond types are listed in Table 7.4. Additionally, broad bands at 3360 cm^{-1} were observed which are due to O–H stretching vibration in aromatic and aliphatic structures (Santos et al. 2015). Furthermore, bands at 2937 and 2848 cm^{-1} are associated with a C–H vibration sketch in the CH_2 and CH_3 groups, respectively (Santos et al. 2015). There are little overall differences between treated samples and controls. Only between 1810 and 1539 cm^{-1} a clear increase in the bands due to the treatment was observed. Calculation of the shoulder at 1714-1725 and 1647 cm^{-1} which are associated with C=O bonds in lignin side-chains and on aromatic rings (Alriols et al. 2009), respectively and of the peak at 1595 cm^{-1} was difficult due to superposition of the peaks. Therefore, in contrast to the calculation of the other peak areas, these bands were calculated by constructing the baseline by connecting the lowest data points on either side of the whole peak (from 1810 to 1539 cm^{-1}). The results show a slight increase in those bands indicating lignin side-chain oxidation and formation of quinones by the HBT LMS corresponding well to the predicted reactions (Figure 7.16).

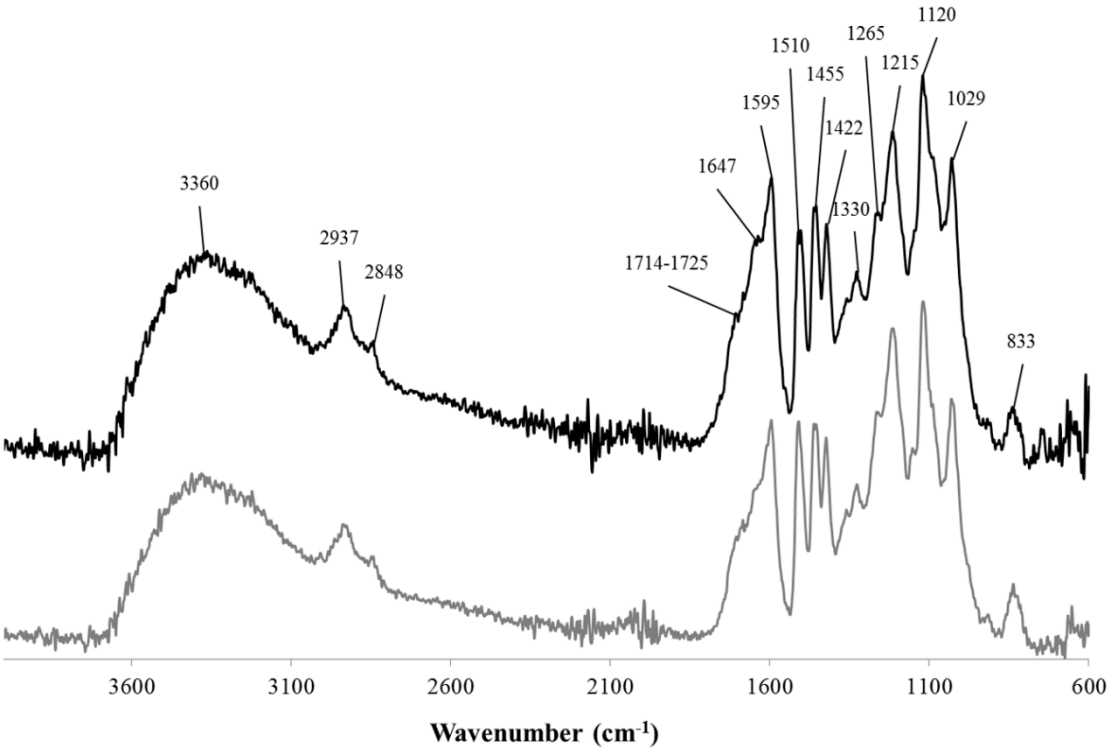

Figure 7.31 FTIR spectra, 4000–600 cm^{-1} region, of insoluble lignin after the first treatment step (black) and of water insoluble lignin (grey; adapted from Gasser et al. (2017)).

Table 7.4 Ratios of the intensities between different FTIR bands of water insoluble lignin after the first treatment step and for water insoluble untreated lignin (both at pH 2) and the corresponding lignin associated band. Errors show standard deviations (n=3; adapted from Gasser et al. 2017)

Type of bond	Wavenumber (cm^{-1})	Treated sample	Control
Stretching of C=O unconjugated to aromatic rings (oxidized side-chains)	1714 - 1725	1.99 ± 0.22	1.54 ± 0.06
Stretching of C=O conjugated to aromatic rings	1647	2.50 ± 0.11	2.03 ± 0.13
Aromatic skeletal vibrations	1595	2.88 ± 0.18	2.50 ± 0.15
C–H asymmetric vibrations and deformation (asymmetric in methyl and methylene)	1455	0.72 ± 0.03	0.70 ± 0.01
Aromatic skeleton vibrations	1422	0.48 ± 0.01	0.44 ± 0.02
Aromatic ring breathing, S and G condensed units	1330	0.19 ± 0.01	0.16 ± 0.01
Guaiacyl ring breathing with C=O stretching	1268	0.18 ± 0.03	0.18 ± 0.01
Ring breathing with C–C, C–O, and C=O stretching	1215	1.18 ± 0.04	1.32 ± 0.01
Aromatic in plane C–H bending deformation for S lignin	1120	1.92 ± 0.16	2.07 ± 0.05
Aromatic in plane C–H bending deformation for G lignin	1029	1.08 ± 0.13	1.25 ± 0.06
C–H out-of-plane bending in positions 2 and 6 of S units and all positions of H units	833	0.58 ± 0.06	0.62 ± 0.03

During formic acid/formate treatment further lignin depolymerization was observed. Low molecular weight compounds were extracted with EtAc and weighed after drying. 7.9±0.2 wt% of lignin could be extracted. This fraction consisted predominantly of low molecular weight lignin oligomers and of monomeric compounds and had a Mw of 645±9 Da (Figure 7.30B). Higher lignin amounts, i.e., 16.0±1.0 and 14.3 ± 0.9 wt% could be extracted with EtAc from untreated controls and controls only treated with formic acid/formate after separation of water soluble compounds, respectively. However, Mw of these fractions were considerably higher than Mw of the fraction obtained after sequential treatment, i.e., Mw was 1,872±39 and 1,047±44 Da for untreated controls and controls only treated with formic acid/formate after separation of water soluble compounds, respectively.

Table 7.5 Identified monomer yields in wt‰ of sequentially treated samples using reaction conditions determined to be optimal regarding total lignin solubilization (see text) and of untreated controls and controls only treated by formic acid/formate after removal of water soluble compounds. Errors are given as standard deviations of triplicates (adapted from Gasser et al. 2017).

	Sequentially treated sample	**Untreated control**	**Control treated by formic acid/formate**
DMBQ	2.49 ± 0.10	0.0 ± 0.0	0.00 ± 0.00
Vanillic acid	1.15 ± 0.03	0.38 ± 0.02	1.64 ± 0.06
Syringic acid	2.16 ± 0.07	0.14 ± 0.01	2.52 ± 0.08
Vanillin	1.20 ± 0.04	0.19 ± 0.03	1.14 ± 0.04
Syringaldehyde	1.26 ± 0.03	0.12 ± 0.00	1.30 ± 0.04
Acetovanillone	0.15 ± 0.01	0.00 ± 0.00	0.22 ± 0.01
Acetosyringone	0.78 ± 0.03	0.26 ± 0.00	1.19 ± 0.05
Hydroxybenzoic acid	0.17 ± 0.00	0.00 ± 0.00	0.20 ± 0.01

Obtained monomers during the sequential treatment are summarized in Table 7.5. DMBQ was formed during the first treatment and was not observed in controls showing that DMBQ formation was due to lignin oxidation by the biocatalytic treatment. Regarding identified low molecular weight phenolic compounds obtained after formic acid/formate treatment, yields of treated samples based on total lignin weight applied were slightly lower than yields of controls only treated by formic acid/formate treatment, i.e., they were 6.87±0.21 and 8.22±0.28 wt‰ for treated samples and controls, respectively. However, based on actually treated lignin, monomer yields were higher for enzymatically treated lignin than for controls, i.e., they were 11.23±0.11 and 10.30±0.09 wt‰ for treated samples and controls, respectively.

7.3.2.3. Discussion of optimization experiments

7.3.2.3.1. Enzymatic treatment

During the first treatment lignin was subjected to a LMS. Two different reaction processes occurred that are in competition, one progressing along phenoxy radical formation which can lead to polymerization through radical coupling, the other leading to lignin side-chain oxidation (Crestini et al. 2003). Side-chain oxidation can support lignin depolymerization by promoting Cα-Cβ breakdown (Camarero et al. 2014) which goes along with superoxide radical anion production (Crestini et al. 2003). The superoxide radical anions react further leading to the formation of additional lignin oxidation products like *o*-quinones, *p*-quinones, and ring-cleavage products (Crestini et al. 2003). While laccases in the absence of HBT only catalyze phenoxy radical formation, HBT also initiates side-chain oxidation. Side-chain oxidation even is suspected to be the main reaction pathway in presence of HBT (Crestini et al. 2003). This is supported by the observed negative effect on Mw of insoluble lignin as well as the positive effect on lignin solubility of higher HBT concentrations at lower pH values. The positive effect of higher enzyme activity on Mw of insoluble lignin might be partly ascribed to lignin polymerization by phenolic coupling reactions (Crestini et al. 2003). Furthermore, the increase in solubilization of lower molecular weight lignin due to increasing enzymatic activity also partly contributed to this increase in Mw.

Mw of insoluble lignin increased drastically at higher pH while solubility decreased. This indicated that lignin was polymerized considerably at high pH. Potentially more phenolic groups were accessible for oxidation by enzymes and/or mediators since lignin solubility increases with increasing pH. Additionally, increasing pH decreases the redox potential of phenolic substrates due to proton release (Xu et al. 2007). Therefore, the redox potential difference with the enzymes increases facilitating oxidation and, consequently, phenoxy radical formation (Xu et al. 2007). Furthermore, the oxidized lignin macromolecules might also more easily interact with each other if they are dissolved facilitating polymerization by phenolic oxidative coupling reactions.

Next to phenolic oxidative coupling reactions, phenoxy radical formation can also promote dis-proportionation leading either to side chain oxidation in the Cα position or to the formation of *p*-quinones (Kawai et al. 1988). This is supported by the observed production of DMBQ during the enzymatic treatment. The formation of DMBQ from dimeric phenolic β-1 lignin model compounds by laccase oxidation has been described previously (Kawai et al. 1988). Lignin degradation is initiated by oxidation of phenolic groups on lignin syringyl moieties leading to the formation of phenoxy radicals. Subsequently, a cation intermediate is formed before spontaneous reactions lead to alkyl-aryl cleavage and the formation of DMBQ (Kawai et al. 1988).

7.3.2.3.2. Formic acid/formate treatment

After the enzymatic treatment TVL-MPs were separated prior to acidification. Application of a magnetic field allowed separation and recovery of virtually all biocatalysts indicating their potential reusability.

Lignin precipitates formed after acidification. Subsequently, soluble compounds were separated from insoluble lignin which was treated further by formic acid/formate treatment. The reaction targets β-O-4 ether bonds within the lignin macromolecules. They are cleaved if they contain Cα ketones, i.e., if they have been oxidized during the first treatment step. The cleavage proceeds along an overall redox-neutral sequence of reaction steps leading to lignin depolymerization (Rahimi et al. 2014). However, with increasing reaction times Mw of lignin increased indicating that next to depolymerization reactions also some polymerization reactions occurred. It has been proposed that in acidic media, lignin carbocations are formed (Lundquist and Lundgren 1972). These carbocations undergo further reactions potentially forming enol ethers after β-proton elimination which subsequently leads to acid hydrolysis and lignin depolymerization (Lundquist and Lundgren 1972). However, re-polymerization of carbocations with other lignin macromolecules was also described (Sarkanen and Ludwig 1971). Occurrence of such lignin re-polymerization reactions might explain the increase in Mw with increasing formic acid/formate reaction time.

Mw after formic acid/formate treatment was also highly dependent on treatment conditions during the enzymatic treatment. Conditions leading to high Mw of insoluble residues after enzymatic treatment, i.e., high enzymatic activities, long reaction time, and high pH also induced higher Mw of lignin after the second treatment showing that more strongly polymerized lignin was more difficult to depolymerize during the second treatment step. This finding is also supported by the negative effect of increasing pH during enzymatic treatment on yields of EtAc soluble compounds after formic acid/formate treatment. Increasing sodium formate concentration on the other hand positively affected yields of EtAc soluble products indicating that formate promoted depolymerization reactions. This is in agreement with the proposed involvement of both an acid (to promote the loss of formate as leaving group) and a base (to take away a proton) during the rate limiting step of the cleavage reaction (Rahimi et al. 2014). Additionally, higher HBT concentrations and longer enzymatic reaction times seemed to promote depolymerization during formic acid/formate treatment as well since both led to a decrease of Mw of EtAc soluble products while increasing their yield. This could be due to increased side chain oxidation during the enzymatic reaction leading to the formation of more Cα ketones which were subsequently cleaved by the formic acid/formate reaction.

Highest monomer yields after formic acid/formate reaction were obtained if lignin was treated initially at pH 8 at low enzymatic activities, short enzymatic reaction times, and high HBT concentrations. This is reasonable since lower pH led to higher lignin solubilization during the first reaction step, thereby reducing lignin material for the formic acid/formate reaction. Furthermore, higher enzymatic activity and higher enzymatic reaction times led to higher lignin polymerization at high pH impeding subsequent lignin depolymerization to monomeric compounds. Additionally, higher HBT concentrations might have reduced phenoxy radical formation and therefore, decreased polymerization reactions facilitating

depolymerization during the second reaction. Increasing formic acid/formate reaction time positively affected monomer yields showing that lignin was depolymerized during the second treatment over time.

7.3.2.3.3. Optimized sequential treatment

Based on the RSM results, optimal treatment conditions regarding production of low molecular weight compounds were determined and proposed experiments conducted. Results corresponded well to model predictions and 44.6±2.3 wt% of lignin could be either solubilized in aqueous solution after the first treatment or EtAc after the second treatment. This constituted a considerable increase in comparison to untreated controls and controls only treated by formic acid/formate treatment (Figure 7.29). However, partial depolymerization of lignin only subjected to formic acid/formate treatment was observed as well indicating that some Cα ketones might already be present in lignin which is not uncommon (Rahimi et al. 2014) or that lignin depolymerization also occurred through other reactions like, e.g., acidic hydrolysis (Lundquist and Lundgren 1972).

Optimal reaction conditions during the enzymatic treatment were predicted to be at high enzymatic activity, medium HBT concentration, long enzymatic reaction times, and low pH. At these conditions high lignin solubilization was achieved during the first treatment while insoluble lignin was not polymerized strongly. Therefore, depolymerization to EtAc soluble compounds during the second treatment was not impaired as much as during treatments at higher pH and/or lower HBT concentrations. Optimal reaction conditions during formic acid/formate treatment were predicted to be at long treatment times and high sodium formate concentrations showing that the treatment led to lignin depolymerization over time and that sodium formate promoted depolymerization as discussed above.

7.3.3. Lignin treatment over several reaction cycles

Reuse of biocatalysts was investigated by applying TVL-MPs over five consecutive cycles for treatment of W-SL. HBT was applied as redox mediator at the beginning of each cycle. After each cycle biocatalysts were separated magnetically from the insoluble lignin products and reused in the next cycle. Insoluble lignin of each cycle was subjected to formic acid/formate treatment. Treatment conditions were the same as the conditions applied in subchapter 7.3.2.2.

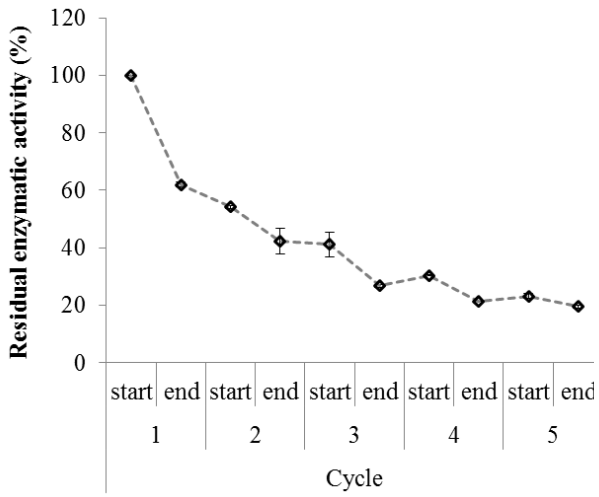

Figure 7.32 Residual enzymatic activity of the TVL-MP during the five reaction cycles. Every cycle lasted 47.97 h. Error bars show standard deviations (n=3).

Changes in the residual enzymatic activities during the treatment are shown in Figure 7.32. Considering particle weight, 81.9±0.5 % of the initially applied particle weight was removed magnetically after the last reaction cycle showing that around 20 % of the initially applied particles were lost during the different separation processes over all five cycles. Comparing enzymatic activities at the end and start of each cycle also indicated that only small amounts of TVL-MP were lost between the different cycles. TVL-MPs were considerably less stable during treatment of lignin than in stability tests conducted at pH 5 (see subchapter 6.2.4.1).

Particles retained 19.5±0.8 % and 62.0±0.2 % of their initial activity during the five cycles of lignin treatment (10 d of treatment in total) and after 10 d in stability tests at pH 5, respectively. Measuring pH after the reaction cycles showed that pH during the reactions decreased from 5.0 to ~4.5. Therefore, it might be that the stronger decrease in enzymatic activity during lignin treatment was due to a decrease in pH during the reaction. The decrease in pH might be due to the production of carboxylic acids through aromatic ring cleavage. Therefore, to decrease TVL-MP inactivation during treatment it might be necessary to control and adjust pH during the reaction, to start the treatment at higher pH, or to increase buffer capacity in order to prevent a pH decrease considerably below 5.

Mass balances during the consecutive cycles are summarized in Figure 7.33 A. Shown values are based on the overall lignin weight applied up to the corresponding cycle and consequently, give an overall mass balance up to the corresponding cycle. To prevent unnecessary particle losses and losses in enzymatic activity, particles were only washed repeatedly after the last reaction cycle but not between the different reaction cycles. Therefore, it is likely that considerable amounts of lignin were still associated with the TVL-MPs after lignin separation and transferred from one reaction cycle to the next. Consequently, the amounts of soluble compounds shown in Figure 7.33 A for cycles 1 to 4 also include

lignin not separated from TVL-MP. The effect can be expected to be highest after the first reaction cycle explaining the high amount of unseparated lignin after the first cycle, i.e., 64.8 wt%. Subsequently, the effect should reduce from one reaction cycle to the next since it can be assumed that similar total amounts of lignin could not be separated between the reaction cycles from the TVL-MP. Over all five cycles 40.9±0.6 wt% could be solubilized either in aqueous solution after enzymatic treatment or in EtAc after formic acid/formate treatment. Therefore, obtained low molecular weight product yields were only slightly below obtained yields after one cycle (see subchapter 7.3.2.2) in which 44.6±2.3 wt% of soluble products were obtained.

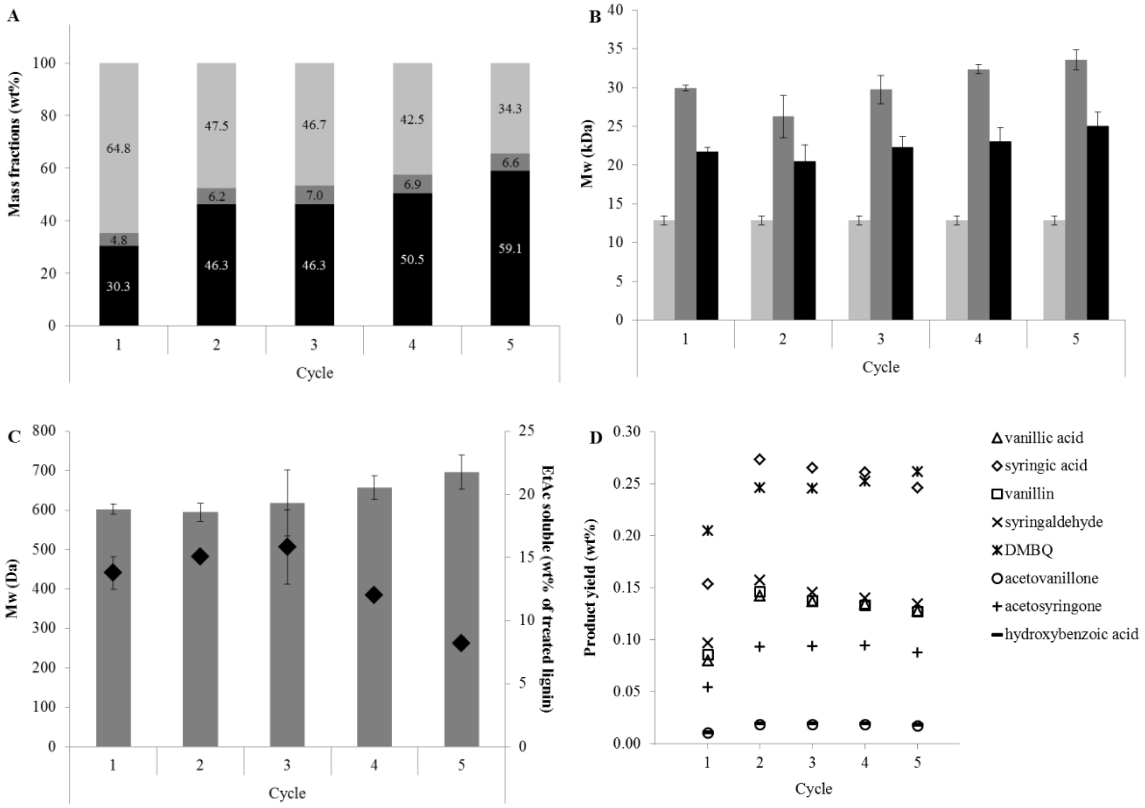

Figure 7.33 Summary of results of W-SL treatment over five consecutive reaction cycles with TVL-MP and subsequent formic acid/formate reaction step; A) mass balance after the different reaction cycles in wt% based on the total lignin weight subjected to treatment up to the corresponding cycle (soluble material or adsorbed on particles after first treatment (grey), EtAc soluble after second treatment (dark grey), insoluble residues (black)); B) Mw of starting material (grey), insoluble lignin after first treatment (dark grey), and of reaction products after second treatment (black); C) Mw (grey bars) and wt% (based on treated lignin, black diamonds) of EtAc soluble fractions after the second treatment; D) sum of yields of identified monomeric compounds over the different reaction cycles in wt% based on the total lignin weight subjected to treatment up to the corresponding cycle. Error bars show standard deviations (n=3).

No considerable differences between the different cycles could be observed concerning Mw after the different treatment steps (Figure 7.33 B). Mw of insoluble lignin after the biocatalytic treatment step was between 26.2±2.7 and 33.6±1.3 kDa. After formic acid/formate treatment the Mw decreased after all cycles and was between 20.5±2.1 and 25.0±1.8 kDa. Highest Mw was observed in both cases after the last treatment cycle. It can be speculated that lignin of highest molecular weight was only separated from the TVL-MP at the end of the experiment after extensive washing which might explain the slightly higher Mw after the last cycle.

Yields of EtAc soluble compounds based on the formic acid/formate treated lignin weight were similar during the first three cycles, i.e., they varied between 13.8±1.3 and 15.8±2.9 wt% (Figure 7.33 C). Subsequently, they slightly decreased during cycles four and five to 12.0±0.4 and 8.2±0.5 wt%, respectively. No considerable differences during the first three cycles were observed concerning Mw of the EtAc soluble fraction. Mw varied between 595±22 and 618±84 Da (Figure 7.33 C). Subsequently, Mw of EtAc soluble fractions increased to 658±30 and 696±43 Da after cycle four and five, respectively. The reduction in yield and increase in Mw of the EtAc soluble fraction in later reaction cycles might be due to less lignin oxidation by the biocatalytic treatment because of the considerably lower enzymatic activity in those later reaction cycles (Figure 7.32). Furthermore, results of the last reaction cycle might also be explained by the higher Mw of the insoluble lignin residues after the fifth reaction cycle which might have been more difficult to depolymerize.

Several monomeric reaction products could be identified during the lignin treatment. Product yields based on the total lignin weight applied up to the corresponding cycle are summarized in Figure 7.33 D. As in previous experiments DMBQ was the main monomeric product during the first reaction. A DMBQ yield of 2.62±0.02 wt‰ was obtained over the whole experiment. Hence, the yield was close to the yield obtained using TVL-MP only once (see subchapter 7.3.2.2), which yielded 2.49±0.10 wt‰ DMBQ. During the formic acid/formate treatment step several phenolic monomeric compounds were formed. Based on the total applied lignin weight yields of these compounds were stable during reaction cycle two to five and slightly lower during the first reaction cycle. The lower yields after the first cycle are due to the lower percentage of lignin that was treated by the formic acid/formate treatment after the first cycle (Figure 7.33 A). Yields of monomeric phenolic compounds after five cycles were generally slightly higher than yields obtained in the experiment using the TVL-MP only once (Table 7.5).

Overall results show that TVL-MP could be successfully reused over 10 days of lignin treatment. Monomer yields were slightly above and oligomer yields were slightly below yields obtained in the experiment using the TVL-MP only once. Furthermore, most particles could be successfully separated and only little losses in enzymatic activity between cycles were observed. However, enzymatic activities decreased more strongly compared to activity decreases in stability experiments indicating that controlling pH during the reaction might be necessary to prolong the utilization time of the biocatalysts.

7.3.4. Concluding remarks

In this subchapter a sequential treatment for partial lignin depolymerization was developed. The treatment allowed the production of considerable amounts of lignin oligomers as well as some phenolic monomeric compounds. Yields depended on the lignin material used and most promising results were obtained for lignins derived from wheat straw. Optimization of the process for the treatment of one selected lignin, i.e., W-SL allowed the production of up to 45 wt% of low molecular weight lignin mono-, and oligomers. While the process does not lead to the production of considerable amounts of directly marketable compounds (with the exception of DMBQ in case of OL), it might be used for the production of a stream of low molecular weight soluble aromatic products that can be upgraded further. They might be used in processes employing heterogeneous catalysts like hydrogenation, hydrogenolysis, decarbonylation, and decarboxylation since application of low molecular weight soluble compounds should reduce coking and char formation, while enhancing conversion, and facilitating product separation in such processes (Rahimi et al. 2014). Furthermore, they might be used as substitutes for aromatics in the production of resins, lacquer, or adhesives.

8. Conceptual process designs

Based on the results obtained in chapter 7 two strategies for lignin valorization applying the superparamagnetic biocatalysts seem promising. One strategy comprises a rather simple approach focusing on the production of DMBQ using immobilized laccases. For this approach OL would be the most promising feedstock of the tested lignins since obtained DMBQ yields were considerably higher than for other lignins. The other strategy would follow the sequential lignin treatment developed in subchapter 7.3 for the production of a mixture of low molecular weight aromatic mono-, and oligomers that could serve as feedstock for further upgrading. In the following conceptual process designs for both approaches are presented and different aspects of the processes are discussed. Furthermore, some preliminary cost estimates for the two processes were conducted.

8.1. Process focusing on DMBQ production

Simple treatment of lignin with laccases allows the production of DMBQ without necessitating the addition of redox mediators or co-factors as results of subchapter 7.1 have shown. Especially, treatment of OL seems interesting in this regard since yields of up to 2.20±0.05 wt% were achieved using this lignin. However, results also showed that producing DMBQ at such high yields necessitates application of a co-solvent like MeOH and that lignin has to be treated for several days. Still, DMBQ yields of close to 1 wt% were achieved after 15 min and 2 h using TVL and TVL-MP, respectively. Consequently, treatment times in the range of 1 to 2 h for the production of 1 wt% DMBQ from OL seem feasible if enough enzymatic activity is applied.

A possible process scheme for the production of DMBQ from lignin is shown in Figure 8.1. After treatment with TVL-MP the biocatalysts have to be separated magnetically from the reaction suspension. A possible strategy for efficient separation and recycling of the MPs is shown in Figure 8.2. The scheme is based on a reactor design that was used for the treatment of micropollutants with Titania-laccase biocatalysts (Hochstrat et al. 2015). Particles retained at magnet 1 placed at the outflow of the reactor can be washed back by flow reversal. The setup in principal allows continuous lignin treatment interrupted only by short time intervals necessary to return MPs to the reactor.

After separation of the biocatalysts MeOH has to be removed by e.g., evaporation (Werhan 2013) from the reaction suspension since it is completely miscible with many solvents, therefore, impeding subsequent extraction steps. MeOH obtained this way can be reused during the biocatalytic oxidation step. Subsequently, lower molecular weight compounds can be extracted by liquid-liquid extraction (LLE) using solvents like EtAc, diethyl ether, dichloromethane, 4-methyl furan, or toluene (Vigneault et al. 2007). Vigneault et al. (2007) tested the suitability of the above listed solvents for the extraction of monomers from a monomer rich fraction obtained from steam exploded aspen lignin. They found that only diethyl ether and EtAc totally extracted the monomers. However, both solvents have drawbacks. Diethyl ether forms unstable peroxides (Vigneault et al. 2007). Therefore, its use is associated with

considerable risks and costs in industrial processes. EtAc has rather high water solubility (up to 8.08 wt%, Riddick et al. 1986) and degrades to acetic acid and ethanol in aqueous solutions when it is heated making its recovery difficult (Vigneault et al. 2007). Therefore, Vigneault et al. (2007) suggests considering additional solvents like vinyl acetate, n-butyl acetate, or methyl isobutyl ketone which are less water soluble while potentially being good extracting agents for lignin monomers. After separation of the organic phase solid lignin reaction products can be separated from the aqueous phase by filtration. The liquid phase can potentially be recycled. However, if salts were added and/or the aqueous phase was acidified during LLE to increase separation effectiveness this might not be feasible or might necessitate an additional step of dilution and pH adjustment. Especially salts like NaCl or acids like HCl should be avoided if the aqueous phase is recycled since halides are known laccase inhibitors (Enaud et al. 2011). Therefore, other acids like H_3PO_4 should be used.

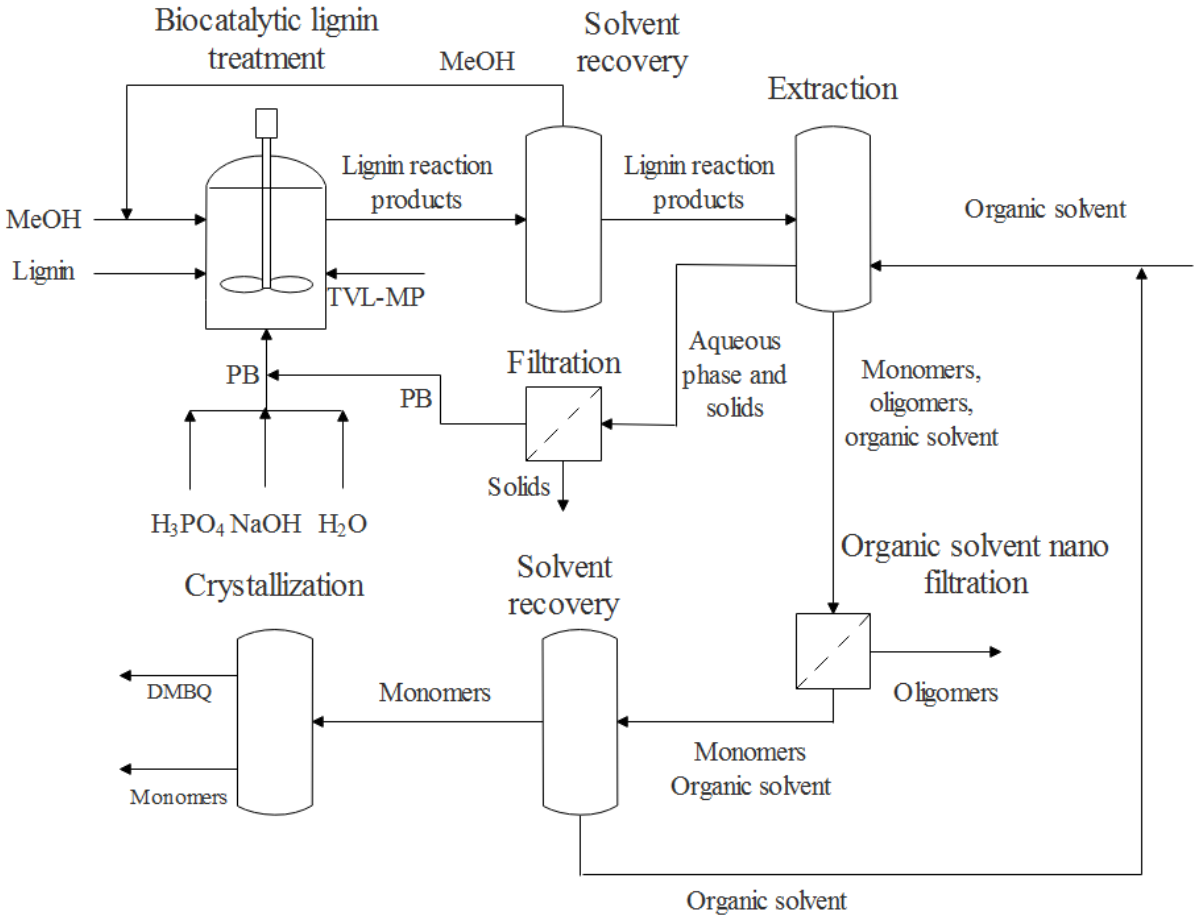

Figure 8.1 Conceptual flow diagram for the proposed lignin treatment for DMBQ production

During the next step monomers have to be separated from higher molecular weight oligomers. This might be achieved through organic solvent nanofiltration. Effective separation of monomers was achieved this way as demonstrated by the filtration of a lignin product mixture with an Mw of 1,150 Da testing different membranes with cut-offs between 250 and 900 Da (Werhan et al. 2012).

Subsequently, DMBQ has to be purified. As results from subchapter 7.1 suggests several low molecular weight compounds like vanillin and syringaldehyde are transformed during biocatalytic lignin treatment leaving a rather pure DMBQ fraction. Nevertheless, further purification after nanofiltration will be necessary. One possible approach might be crystallization. Most monomers usually found in lignins have melting points between 2 and 134 °C and boiling points between 180 and 330 °C (Vigneault et al. 2007). In comparison DMBQ has a rather high melting point between 253 and 257 °C. Therefore, crystallization should allow separation of most impurities. In general, a minimum difference in melting points of 10 °C seems necessary for effective separation by crystallization (Vigneault et al. 2007). For example, *p*-cresol was successfully separated by crystallization from 2,6-xylenol with *tert*-butyl alcohol as solvent (Jadhav et al. 1991). Furthermore, crystallization allowed separating phenol from *o*-cresol with 2-methyl-2-propanol as solvent (Jadhav et al. 1992). Melting points of the corresponding compounds differed by 16 °C and 10 °C in the first and second example, respectively.

Overall the process would yield four separate product fractions, i.e., DMBQ as purified monomeric compound which could be sold directly, a mixture of additional monomeric compounds (results indicate that this fraction would be obtained at very low yields), a fraction of oligomeric compounds which could be either upgraded further or used as substitute for aromatics in the production of resins, lacquer, or adhesives, and a fraction of higher molecular weight lignin which could be either treated further (e.g., by a chemical depolymerization step) or used for the production of heat and power.

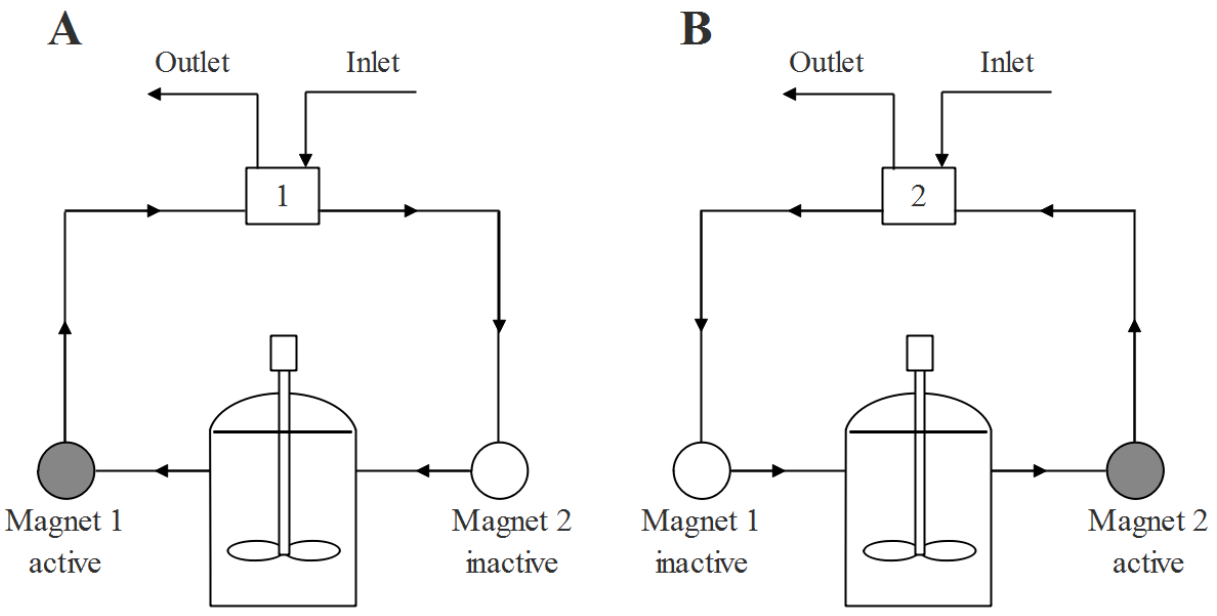

Figure 8.2 Scheme of possible reactor setup for separation of MPs from reaction suspension during lignin treatment. A) Valve is set to position 1 and MPs are retained at magnet 1. B) Valve is set to position 2. MPs previously retained at magnet 1 are washed back to the reactor while MPs are retained at magnet 2 (based on Hochstrat et al. 2015).

8.2. Sequential lignin treatment

Sequential treatment of lignin by LMS followed by a formic acid/formate treatment allows the production of low molecular weight aromatic oligomers at considerable yields as results of subchapter 7.3 have shown. A possible process scheme is shown in Figure 8.3. TVL-MP separation and reuse after the biocatalytic treatment step could be achieved as described in subchapter 8.1. Subsequently, reaction suspensions should be acidified to allow removal of high molecular weight products by filtration. As mentioned in subchapter 8.1 acids like HCl should be avoided if the aqueous phase is to be recycled since halides are laccase inhibitors. Thereafter, aromatic compounds and HBT are separated from the aqueous solution by LLE. The residual aqueous solution can potentially be reused during the biocatalytic treatment step. Monomers and HBT are subsequently separated from higher molecular weight compounds by organic solvent nanofiltration. After solvent recovery two fractions are obtained. One fraction consisting of aromatic oligomers and one fraction consisting mainly of HBT while also containing some monomeric compounds. The HBT containing monomeric fraction can either be directly reused in the biocatalytic treatment step or an additional purification step can be included separating monomers from HBT. As described in subchapter 8.1 separation might be achieved by crystallization since the melting point of HBT (155-158 °C) differs from the melting point of the main monomeric product, i.e., DMBQ (253-257 °C) and the potential other monomeric compounds present (2-134 °C). However, further study of such a process would be necessary and it would potentially require several stages in order to obtain high purity HBT and DMBQ. It might also be worth considering to only separate monomers from HBT after certain DMBQ concentrations are reached and to recycle HBT together with DMBQ and the other monomers as long as only small amounts of DMBQ could be obtained by purification.

After the first filtration step the separated solid material is subjected to the formic acid/formate treatment. Following treatment, formic acid can be removed by evaporation and recycled. Subsequently, LLE allows the separation in a mono- and oligomer containing fraction and a fraction of higher molecular weight lignin which could be either treated further (e.g., by a further depolymerization step) or used for the production of heat and power. Monomers can potentially be separated from the oligomers by organic solvent nanofiltration and further separation and purification might be considered. However, it seems questionable if product yields are high enough to justify the potentially laborious process. For example, Vigneault et al. (2007) investigated the separation of 12 monomers generated by lignin depolymerization. The proposed process consisted of a series of four vacuum distillation columns which produced five monomer streams. Three of these streams would have to be purified even further either by chromatography or crystallization. Consequently, this study highlights the challenging task of downstream processing of lignin products.

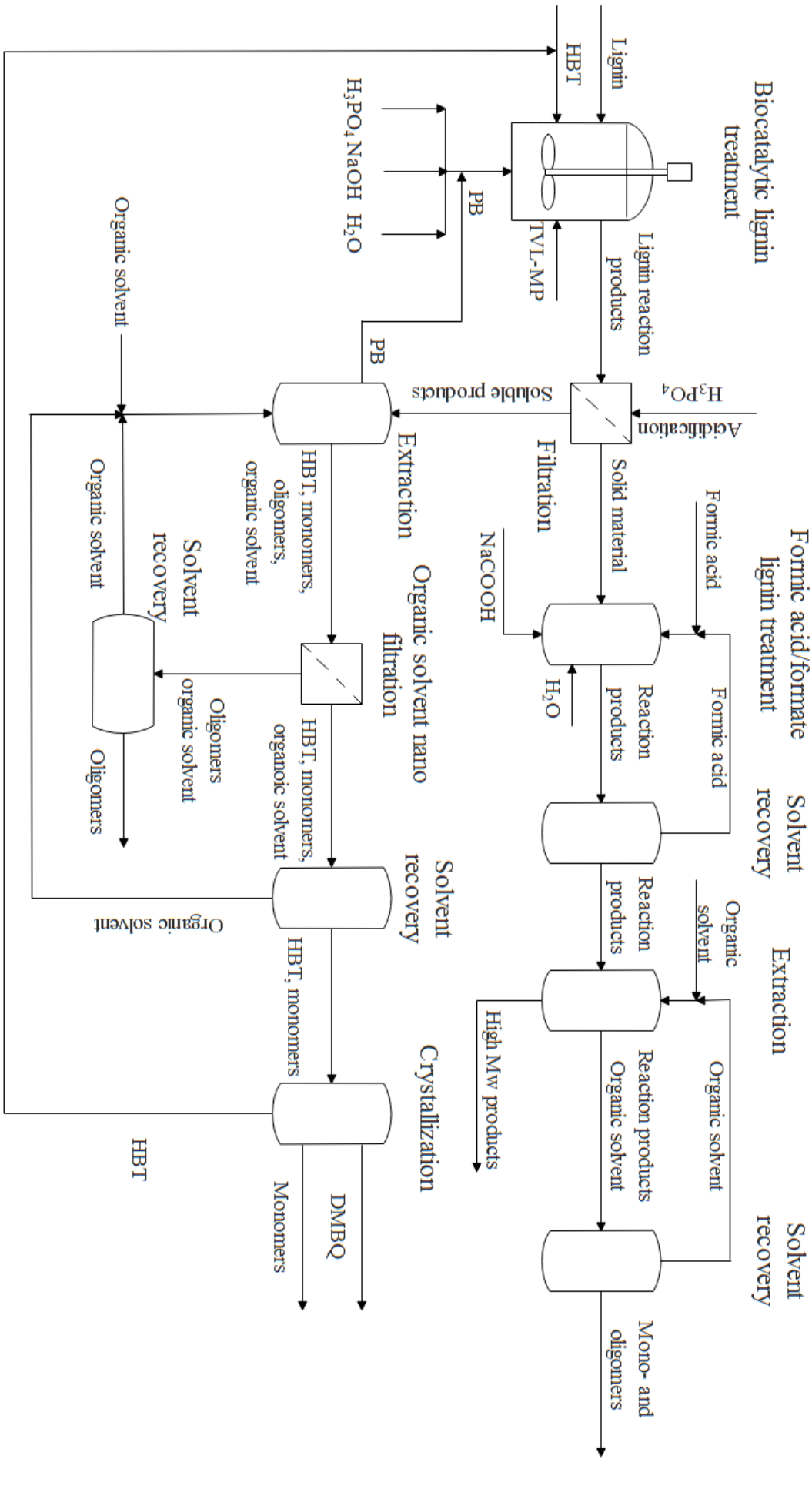

Figure 8.3 Conceptual flow diagram of the sequential lignin treatment process using the TVL-MP HBT LMS

8.3. Cost estimates

For further evaluation of the processes presented in subchapters 8.1 and 8.2 some preliminary cost estimates were performed. The cost-effectiveness of the treatments was evaluated by calculation of the benefit-cost ratio (BCR). In the present cases this gives the ratio between the total revenue and the total acquisition costs of chemicals, feedstock, consumables for TVL-MP production, and enzymes. Obviously cases yielding a BCR below one are of no further interest since consumable costs already outweigh revenues of products. In the present case a BCR of at least 2 should be achieved for a treatment option to be considered further, since no detailed data were available on all process steps and conditions and consequently not all costs could be included in the BCR calculation. Cost estimations were based on several assumptions. Assumptions that were made for all cases are listed below

- Only material streams that enter or exit the main process steps were considered.
- Costs for the production of TVL-MP only considered costs of consumables and enzymes. The cost estimate is presented in Table 8.1.
- Lignin revenue was assumed to be obtained from production of heat and power. The price of lignin was calculated based on the high heating value of lignin (21.5-23.5 MJ kg^{-1}, Blunk and Jenkins 2000) and it was assumed that lignin is used to replace crude oil. Crude oil price was based on the one-year projection of an online database and assumed to be 56 \$ $barrel^{-1}$ (Oil-Price 2016).
- High molecular weight products were assumed to be applicable in the same processes as lignin. Therefore, their revenue was assumed to be the same.
- Prices for consumables and monomeric products were based on market prices of online databases and are listed in Table 8.2.
- Recovery of monomeric products after separation and purification was assumed to be possible at a yield of 80 %.
- The price of lignin oligomers was set at the average price of phenol formaldehyde resins (1,670-2,000 \$ t^{-1} according to Van den Bosch et al. 2015), i.e., 1,800 \$ t^{-1}.
- Utility, equipment, labor, and energy costs were not considered.
- Costs for organic solvents for extraction were not considered, i.e., it was assumed that these solvents can be completely recycled.
- TVL-MP activity losses were calculated based on the results of the TVL-MP stability experiments.

Table 8.1 Costs for consumables used for production of TVL-MP. Consumable and enzyme costs were collected from an online database (Alibaba Group 2016). Costs for water were based on water tariffs from IWB (Industrielle Werke Basel 2016).

Consumable	Amount needed (t t^{-1} MP)	Consumable cost ($ t^{-1})	Specific consumable cost ($ t^{-1} MP)
TVL	0.0945	5,000	473
APTES	3.98	5,000	19,923
Glutaraldehyde (50 %)	1.04	2,000	2,086
$FeCl_2$	5.00	600	3,001
$FeCl_3$	12.81	400	5,122
NaOH	1.52	350	530
$NaNO_3$	3.35	350	1,174
H_2O	39.47	1.47	58
Total cost of consumables			**32,369**

Table 8.2 Prices of monomeric products and consumables used for calculations of cost and revenue of the different treatments

Product	**Price ($ t^{-1})**	**Reference**
DMBQ	800,000	Molbase 2016
Vanillin	11,694	Molbase 2016
Syringaldehyde	111,000	Molbase 2016
Syringic acid	12,903	Molbase 2016
Vanillic acid	80,000	Alibaba Group 2016
Acetovanillone	235,000	Alibaba Group 2016
Acetosyringone	50,000	Alibaba Group 2016
4-hydroxybenzoic acid	5,040	Molbase 2016
HBT	12,500	Alibaba Group 2016
H_2O	1.47	Industrielle Werke Basel 2016
NaOH	350	Alibaba Group 2016
H_3PO_4	500	Alibaba Group 2016
MeOH	300	Alibaba Group 2016
Formic acid (85 %)	400	Alibaba Group 2016
Sodium formate	300	Alibaba Group 2016

8.3.1. Cost estimates for DMBQ production from OL

The first two cases investigated were based on the production of DMBQ from OL described in subchapter 8.1. In both cases it was assumed that lignin will be treated for 2 h allowing the production of 1 wt% DMBQ. The first and second case differed regarding recycling of consumables. It was assumed that in the first and second case 0 and 90 % of consumables are reused, respectively. Results of the cost estimates are summarized in Table 8.3. In both cases MeOH costs clearly outweigh all other costs. Case 1 gave a BCR clearly below unity and is, therefore, not considered further. However, case 2 assuming reuse of 90 % of consumables gives a BCR of 2.27 indicating that this treatment option might be of economic interest. Results show that MeOH costs are of major importance and that, therefore, MeOH reuse is crucial to achieve an economical process.

Table 8.3 Cost estimate for the five discussed cases based on the conversion of one ton of lignin.

	Case 1		**Case 2**		**Case 3**		**Case 4**		**Case 5**	
	Cost/Revenue ($)		**Cost/Revenue ($)**		**Cost/Revenue ($)**		**Cost/Revenue ($)**		**Cost/Revenue ($)**	
Lignin	1	-211	1	-211	1	-211	1	-210	1	-210
Water	233	-344	23	-34	333	-491	33	-49	33	-49
H_3PO_4	2.3	-1,143	0.23	-114	3.3	-1,633	0.3	-163	0.3	-163
NaOH	0.67	-234	0.07	-23	0.95	-334	0.10	-33	0.10	-33
MeOH	79	-23,730	7.9	-2373						
Formic acid					90	-36,057	9	-3,605	1.26	-505
Sodium formate					0.9	-270	0.09	-27	0.01	-3.8
TVL-MP	0.007	-223	0.007	-223	0.083	-2,674	0.083	-2,674	0.083	-2,674
HBT					0.332	-4,155	0.033	-415	0.033	-415
High Mw product	0.867	183	0.867	183	0.55	116	0.55	116	0.55	116
Oligomers	0.098	177	0.098	177	0.43	783	0.43	783	0.43	783
DMBQ	0.008	6,400	0.008	6,400	0.002	1,676	0.002	1,676	0.002	1,676
Monomeric products					0.006	344	0.006	344	0.006	344
Balance		**-19,124**		**3,781**		**-42,904**		**-4,258**		**-1,133**
BCR		**0.26**		**2.27**		**0.06**		**0.41**		**0.72**

DMBQ production is the main revenue stream of the process. Therefore, the DMBQ price is critical for the whole process economics. In contrast to other monomeric products like vanillin no reliable market for bulk amounts of DMBQ exists. Consequently, the estimated price of 800 \$ kg^{-1} (Molbase 2016) might not be very reliable. For the process to yield a BCR of at least 2, DMBQ price should not be below 700 \$ kg^{-1}.

DMBQ is an anticancer agent (Rizzello et al. 2013) and a precursor for the production of several interesting chemicals. For example, DMBQ can be used for the production of pharmaceuticals like triaziquone or ladanein (Molbase 2016). Triaziquone is used in chemotherapy while ladanein has antiviral activity against the human immunodeficiency virus (HIV) and hepatitis C virus (HCV) and antileukemic activity (Alkhatib et al. 2010; Huang et al. 2009; Martin-Benlloch et al. 2014). Furthermore, several chemicals that can be used as precursors or building blocks can be produced from DMBQ (Molbase 2016). For example, DMBQ can be used to synthesize 3,4,5-trimethoxyphenol (Molbase 2016), a compound that can be used as precursor for the production of over 50 products including flavonoids, e.g., Wogonin used in cancer treatment (Li-Weber 2009). Consequently, especially pharmaceutical companies might be interested in the purchase of DMBQ.

8.3.2. Cost estimates for sequential treatment of W-SL

Cost estimates for the sequential treatment process described in subchapter 8.2 were made based on experimental results from subchapters 7.3.2, and 7.3.3. W-SL was chosen as feedstock for calculation of product amounts. Three different cases were considered initially based on the optimal treatment conditions regarding production of soluble compounds described in subchapter 7.3.2.2. In case three no recycling of consumables was assumed while in cases four and five 90 % recycling of consumable was assumed. Furthermore, in case five the lignin concentration during the formic acid/formate treatment was assumed to be 50 g L^{-1} instead of 7 g L^{-1}. Results of the cost estimates are summarized in Table 8.3.

All three cases gave a BCR below unity showing that they are of no economic interest. Main costs in case three arose from formic acid clearly outweighing all other costs showing that formic acid reuse is of major importance concerning process economics. In case four formic acid costs were still most considerable. However, also costs for TVL-MP amounted to 37 % of total costs. Further cost reductions for formic acid were achieved in case five by assuming an increase in lignin concentration during formic acid/formate treatment to 50 g L^{-1}. While this concentration might appear rather high, lignin treatments with such high loadings are described in literature (Van den Bosch et al. 2015). However, further experiments would be necessary to verify if effective lignin depolymerization is still achieved at such high loadings. In case five TVL-MP expenses became the main cost-factor showing that either an increase in TVL-MP stability or a decrease in the applied amount of TVL-MP might be crucial to achieve a BCR above one. TVL-MP stability might be increased by increasing and controlling pH during the biocatalytic treatment step. DMBQ was again the main source of revenue indicating that DMBQ

separation and purification might be worthwhile. However, also oligomers amounted to 27 % of the total revenue.

To see whether treatment conditions yielding BCR above unity might be established, BCR values were calculated for all experiments conducted for the optimization of the treatment of W-SL described in subchapter 7.3.2. For these calculations assumptions were the same as for case five, i.e., consumables were assumed to be recycled at 90 % and lignin concentration during the formic acid/formate treatment was assumed to be 50 g L^{-1}. RSM was used in order to study the effect of six influencing factors, i.e., enzymatic activity, HBT concentration, enzymatic treatment time, pH during enzymatic treatment, formic acid/formate reaction time, and sodium formate concentration on the lignin reaction products. A second-degree polynomial model was fitted to the BCR results using Design Expert 8.0.7.1 software. The model was subsequently reduced to only contain significant factors ($p \leq 0.05$) and factors necessary to maintain model hierarchy using the step-wise automatic model regression of the software. The ANOVA analysis and the resulting model are shown in the appendix (

Table A. 35). All six factors were predicted to have a significant effect on BCR. The predicted effects are shown in Figure 8.4. The effect of enzymatic treatment time on BCR was predicted to be dependent on enzymatic activity as well as HBT concentration. At low enzymatic activity BCR increased with increasing enzymatic treatment time. This might be explained by the increase in DMBQ and oligomer yields during longer enzymatic treatment times, outweighing the costs of TVL-MP inactivation. However, at higher enzymatic activities BCR clearly decreased with increasing enzymatic treatment times indicating that increasing costs due to TVL-MP inactivation with increasing reaction time outweighed the increasing revenues of DMBQ and oligomer production at higher enzymatic activities. BCR decreased with increasing HBT concentrations from 1 to 10 mM. This decrease was more substantial at lower enzymatic reaction times than at higher enzymatic reaction times, i.e., 0.52 and 0.35 at 4 and 48 h, respectively. This indicates that the added cost by applying higher HBT amounts were not outweighed by the higher revenues due to increased oligomer production. However, the smaller negative effect on BCR at longer enzymatic reaction times is explained by the increase in oligomer yields at higher enzymatic reaction times and HBT concentrations. The effect of pH on BCR is mostly explained by TVL-MP stability. TVL-MP were not very stable at pH 5 and 8 leading to increased costs for the biocatalysts at these more extreme pH values that could not be outweighed by higher product yields at pH 5. Finally, formic acid/formate treatment time and sodium formate concentration only have small effects on BCR. BCR increases by 0.31 and decreases by 0.18 by increasing sodium formate concentration from 1 to 10 g L^{-1} at 4 and 48 h of formic acid treatment time, respectively.

Optimal conditions for maximal BCR were determined to be 1.5 kU L^{-1} (enzymatic activity), 1.13 mM (HBT concentration), 40.9 h (enzymatic treatment time), 6.34 (pH during enzymatic treatment), 4 h (formic acid/formate reaction time), and 9.92 g L^{-1} (sodium formate concentration). BCR for these conditions was predicted to be 2.31. Consequently, next to minimizing formic acid amounts used, low

TVL-MP and HBT concentrations as well as a favorable pH regarding stability of the biocatalysts seem crucial to establish an economic process.

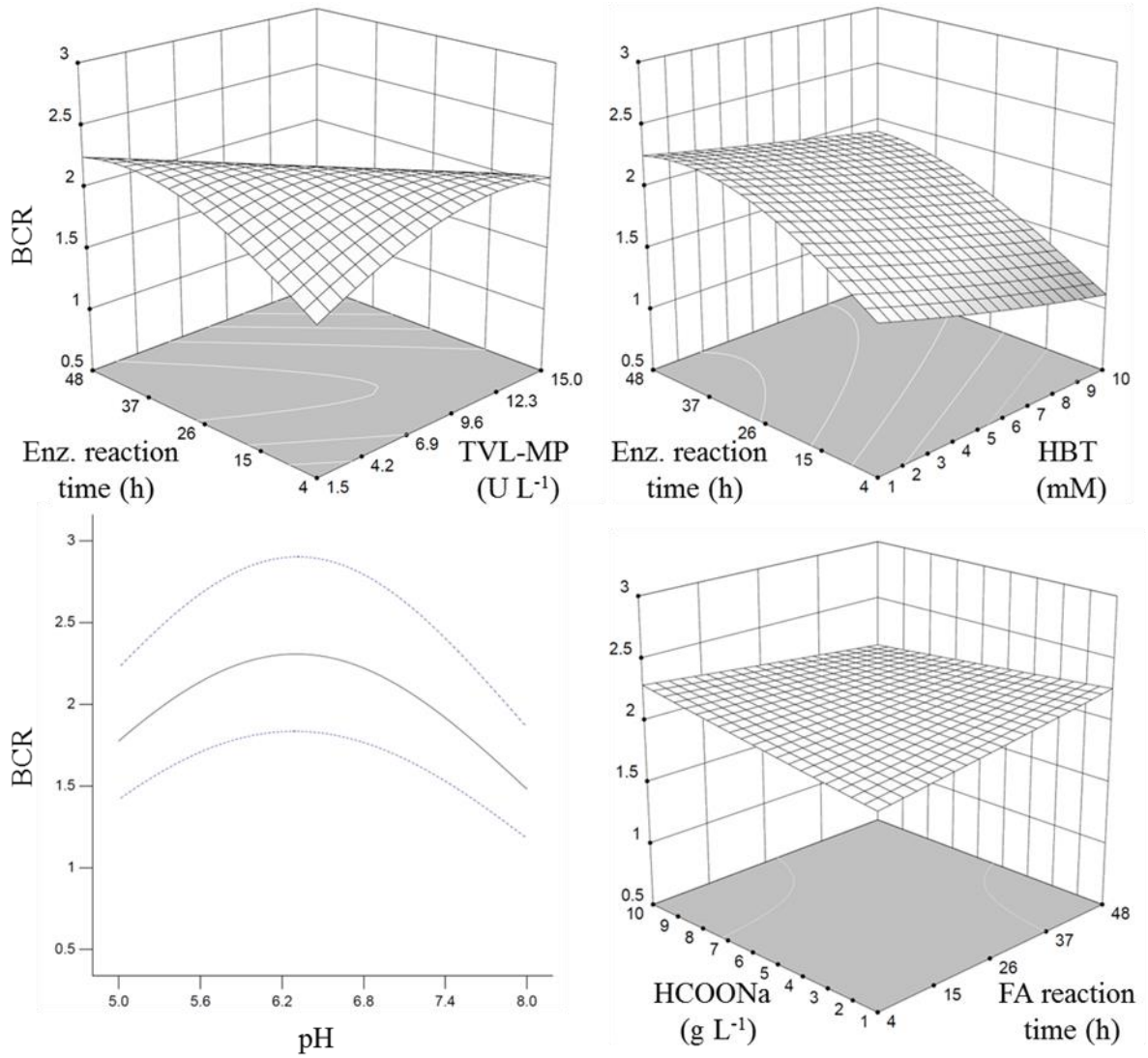

Figure 8.4 Effects of the different factors on the BCR predicted by the response surface second-degree polynomial model. Factors that are not shown were held constant at predicted optimal conditions (see text). Bands displayed show 95 % prediction intervals.

8.4. Concluding remarks

Conceptual process designs for two potential lignin valorization processes using biocatalytic nano-composites have been established. One process focuses on the production of a high value monomeric product, i.e., DMBQ by a single biocatalytic treatment step, the other on the production of DMBQ and oligomeric products from lignin by sequential treatment. A preliminary economic evaluation of the processes has been conducted and indicates that they might be operated profitable. However, several cost factors have not been included and some optimistic assumptions were made. Moreover, the profitability is highly dependent on the price of DMBQ in both cases. Therefore, more detailed study

especially including operation costs for down-stream processing as well as costs for utility, equipment, labor, and energy would be necessary for a more comprehensive assessment. Nevertheless, economic evaluation revealed that solvent reuse is of paramount importance in both cases to restrict consumable costs. Furthermore, treatment conditions should rather be established at conditions that allow prolonged use of the biocatalysts, i.e., conditions in which TVL-MP have high enzymatic stability. Moreover, rather low enzymatic activities and mediator concentrations should be applied in case of the sequential treatment even if this leads to lower product yields.

9. Conclusions

A valorization strategy for lignin employing oxidative enzymes immobilized on nanomaterials was developed in this thesis. The process focused on the production of value added mono- and oligomeric compounds from the heterogeneous biopolymer. Purification of the monomeric compounds allows their sale as fine chemicals while the oligomers can potentially be either further upgraded or used in the production of lacquers, adhesives, or resins.

Several commercially available enzymes were identified and used for lignin oxidation in the presence and absence of organic co-solvents. Organic solvents were employed in order to increase lignin solubility and, thereby, accessibility for the enzymes. Considerable oxidation of lignin by several of the tested enzymes was observed leading to lignin depolymerization as well as polymerization. Lignin polymerization most likely occurred through phenolic oxidative coupling reactions. Results also indicated that enzymes readily adsorbed on polymerized lignin. One main monomeric reaction product, i.e., DMBQ was identified after enzymatic lignin oxidation and could be produced at yields of up to 2.20±0.05 wt%. Results between the tested enzymes that induced DMBQ production did not differ considerably. Therefore, laccases were identified as the most promising biocatalysts for lignin treatment since they only need O_2 as co-factor and are produced at industrial scale making them much more affordable then some of the tested peroxidases.

Several redox-mediators were tested in combination with laccases to extend the reactivity of the enzymes beyond phenolic groups on lignin. Preliminary experiments indicated that artificial mediators like HBT or TEMPO might be more effective than natural phenolic mediators like *p*-coumaric acid, syringaldehyde, or acetosyringone since the natural mediators were partially polymerized during treatment, i.e., their oxidized forms were unstable and their redox conversion was not cyclic.

Enzymes were immobilized on solid carrier materials employing a sorption assisted immobilization method to facilitate separation from lignin, increase enzymatic stability, and allow their reuse. Two support materials were used, i.e., fsNP and MP. In a first step the particle surfaces were modified with an organosilane leading to particles displaying amino-groups on their surface. In a second steps enzymes were adsorbed on the particle surface before amino-groups of particles and enzymes were covalently connected by a cross-linking agent. Furthermore, internal cross-linking of enzymes and cross-linking between enzymes potentially occurred as well resulting in the formation of CLEAs on the particle surface. The immobilization process was optimized for fsNP regarding consumable consumption. Furthermore, up to five different enzymes were successfully immobilized on the same particles by successive immobilization. The versatility of the immobilization process was further demonstrated by successfully immobilizing several LMEs and LME combinations. Subsequently, the process was adapted for larger scale production of nanobiocatalysts and laccase-fsNP conjugates were produced at kilogram-scale. Increasing particle concentration to a degree at which mixing of the suspension was still

feasible represented the most crucial advancement allowing more efficient production of the biocatalysts.

Preliminary lignin treatment experiments applying fsNP-laccase conjugates showed that effective separation of the biocatalysts from the insoluble lignin material is not easily achieved. Therefore, a superparamagnetic nanomaterial, i.e., MP was evaluated as carrier material. The enzyme immobilization protocol was adapted and optimized for MP using RSM regarding enzymatic activity and stability of the biocatalysts. Subsequently, stability of the particles was evaluated at different pH values and in the presence of several chemical denaturants. Immobilized enzymes were considerably more stable than dissolved enzymes in all tested conditions and retained activity in all but one case (i.e., at pH 3) after nine weeks of incubation. Immobilization of DyP on MP revealed that one potential limitation of the immobilization procedure is the possible inactivation of certain enzymes through internal enzyme cross-linking by glutaraldehyde. However, pH adjustments during the cross-linking step can reduce or even prevent such unwanted effects as demonstrated for DyP indicating that process optimizations should be considered for each enzyme individually.

Preliminary lignin treatment experiments with laccase-MP conjugates showed that lignin was oxidized and partially depolymerized by the immobilized enzymes and that the particles could be effectively separated from the insoluble lignin material by application of a magnetic field demonstrating the reusability of the produced nanobiocatalytsts in the envisioned lignin treatment. Consequently, lignin treatments in presence of organic co-solvents or redox mediators with laccase-MP conjugates were conducted. Five different lignins were tested. Experimental results depended on the type of treatment and the used lignin. In treatments using MeOH, DMBQ was produced from all lignins with the exception of SW-SL. This was expected since softwood only contains traces of S. DMBQ most likely derives from those units since DMBQ and S both have methoxy groups on the aromatic ring in positions 3 and 5. DMBQ yields were similar for lignins derived from grasses, i.e., between 0.12 and 0.34 wt% and considerably higher for lignin from hardwood, i.e., 1.10 wt%. However, next to DMBQ production the treatment led to a decrease in soluble compounds and to an increase in Mw of insoluble compounds for all lignins indicating considerable lignin polymerization during treatment. This polymerization is most likely due to phenolic oxidative coupling reactions by phenoxy radicals produced by enzymatic lignin oxidation. Lignin polymerization was limited by employing a radical scavenger, i.e., Trolox. However, this also prevented the formation of DMBQ, i.e., depolymerization reactions were suppressed as well. Consequently, application of a radical scavenger seems unfit for application. Nonetheless, this experiment gave further evidence that the enzymatically catalyzed reactions involve radical formation. Application of laccase mediators HBT and TEMPO decreased Mw of insoluble lignin residues compared to treatments with MeOH. Furthermore, in case of lignins derived from grasses more lignin material was solubilized during treatment with HBT indicating lignin depolymerization. Lignin treatment using LMS enables lignin side-chain oxidation next to formation of phenoxy radicals. This

can lead to Cα-Cβ breakdown and, therefore, lignin depolymerization. Consequently, results indicate that such depolymerization reactions occurred to some extent and that phenoxy radical formation was reduced in presence of mediators.

Insoluble lignin obtained after the biocatalytic lignin treatment was subjected to a formic acid induced depolymerization step. This treatment was shown previously to cleave oxidized lignin β-O-4 side-chains in an overall redox-neutral sequence of reaction steps. The process led to further lignin depolymerization and the production of mono- and oligomers. Depending on the lignin and the type of biocatalytic treatment the Mw of the treated lignin either decreased or increased. Most notably Mw of lignins derived from wheat straw treated with HBT or MeOH decreased considerably during the formic acid/formate treatment. Therefore, one lignin from wheat straw, i.e., W-SL was selected for further optimization of the process. The HBT-LMS was used during the first reaction and the different reaction parameters were studied more in depth. The optimized process allowed production of 45 wt% mono- or oligomeric products. Yield of identified monomers was 0.94 wt%.

Subsequently, reusability of TVL-MP was shown in lignin treatment experiments using the HBT-LMS over five consecutive cycles lasting 10 d overall. Yields of low molecular weight products were only slightly below obtained yields at optimal conditions showing that TVL-MP could be successfully reused. However, TVL-MP only retained 19.5±0.8 % of their initial activity after the 10 d of treatment. Adjusting reaction conditions, e.g., increasing or controlling reaction pH might be expedient in order to increase TVL-MP stability and allow longer operating times of the biocatalysts.

Based on the obtained results from the lignin treatment experiments two approaches seem interesting for lignin valorization, one targeting DMBQ production from OL with TVL-MP using MeOH as co-solvent, the other comprising of the sequential treatment of lignins using TVL-MP and HBT targeting production of DMBQ as well as aromatic oligomers. The oligomers could either be further upgraded by other processes like hydrogenation, hydrogenolysis, decarbonylation, and decarboxylation or they might be used as substitutes for aromatics in the production of resins, lacquer, or adhesives. Preliminary evaluations of the benefits and costs of the different treatments showed that the main revenue in both processes is obtained from selling DMBQ. Therefore, results of the economic evaluation depended heavily on the DMBQ price. Since there is no reliable market for bulk amounts of DMBQ the results of the economic evaluation have to be interpreted with caution. Nonetheless, the evaluation has shown that recycling of solvents, HBT, and formic acid is essential to achieve a profitable process. Furthermore, results indicated that reaction conditions during the biocatalytic treatment should rather be optimized regarding higher stability of the biocatalysts even if this results in slightly lower product yields. Additionally, lignin concentrations during the formic acid/formate treatment step should be increased considerably.

10. Outlook

The presented process constitutes a promising first step towards a possible lignin valorization strategy. However, further improvements of the process as well as more detailed study of downstream processing and possible applications of reaction products are necessary before realization can be considered. Furthermore, the process yields different results depending on the lignin starting material. In this regard it can be expected to yield better results for lignins containing high contents of β-O-4 bonds. Lignins containing up to 93 % of substructures involved in β-O-4 bonds have been described (Martínez et al. 2008). Therefore, selecting suitable feedstocks and employing pretreatment methods preserving the native lignin structure might allow improving product yields. Processes to effectively separate the different components of lignocellulose into high purity sugars and native lignin streams like the γ-valerolactone-based process have been developed recently (Luterbacher et al. 2014) and might deliver lignins more suitable for depolymerization in the future.

One way to improve the biocatalytic process step would be to further reduce polymerization reactions. This might be achieved by limiting phenoxy radical formation. Therefore, preventing direct oxidation of lignin by the enzymes should be considered. One possibility might be shielding of the immobilized enzymes with a soft organosilica layer as described recently (Correro et al. 2016). This would prevent direct contact of the enzymes with lignin and only lower molecular weight compounds and redox-mediators would be oxidized by the biocatalysts. Moreover, shielding of the enzymes might further improve enzyme stability and thereby, potentially decrease process costs. However, applying such an approach most likely reduces or prevents DMBQ production and would rather be suitable if the production of lignin oligomers is targeted.

Regarding the chemical process for cleavage of oxidized β-O-4 side chains, alternatives to the formic acid/formate treatment should be considered as well. For example, in a recent study C-O cleavage of oxidized β-O-4 ether bonds was achieved by a zinc mediated depolymerization reaction in a 2-methoxyethanol water mixture (Lancefield et al. 2015). Replacement of formic acid would be desirable regarding consumable costs and corrosion caused by the acid which potentially increases equipment and maintenance costs. Furthermore, higher lignin loadings should be targeted in order to reduce consumable costs per lignin weight.

Separation and purification of low molecular weight products is a further topic needing additional research. LLE extraction followed by organic solvent nanofiltration seems a promising approach to obtain an oligomer and monomer fraction after lignin processing. In this regard suitable solvents should be identified. At present most studies use EtAc. However, as pointed out by Vigneault et al. (2007), EtAc might not be the ideal solvent since it has relatively high water solubility and degrades to acetic acid and ethanol in aqueous solutions when it is heated making its recovery difficult. Therefore, other solvents like vinyl acetate, n-butyl acetate, or methyl isobutyl ketone which allow easier separation and

reuse of the organic phase should be considered as well. Further purification of single monomers might be quite challenging and require several distillation, crystallization, and chromatography steps as shown for the separation of 12 monomeric compounds (Vigneault et al. 2007). Therefore, purification of single compounds might only be worthwhile if they have high added value and/or are produced at sufficiently high yields.

Oligomeric fractions obtained after lignin processing might be used directly as additives in the production of resins, adhesives, or lacquer. One potential application is the production of phenol formaldehyde like resins in which phenol is partly replaced by the oligomeric compounds. Furthermore, oligomers might be further upgraded by additional process steps like, e.g., hydrogenation, hydrogenolysis, decarbonylation, and decarboxylation. Applying low molecular weight compounds in such processes can be expected to lead to a reduction of coking and char formation and an increase in conversion yields compared to directly using lignin (Rahimi et al. 2014). Additionally, separation of products from heterogeneous catalysts should be facilitated as well (Rahimi et al. 2014).

Appendix

A1. Experimental matrices, response surface models, and results for the optimization of enzyme immobilization on superparamagnetic particles

A1.1. Optimization regarding specific enzymatic activity

A IV optimal design was chosen initially. IV optimal designs minimize the integral of the prediction variance across the design space, i.e., they are suitable for RSM where prediction is important. The levels chosen initially for the different factors were 10 and 90 mg protein g^{-1} MP, 0.5 and 4 mmol glutaraldehyde g^{-1} MP, 0.5 and 4 h protein adsorption time, 0.5 and 24 h glutaraldehyde reaction time, and pH 5 and 9 (Id 1-30 in Table A. 1). First results indicated that optimal conditions regarding specific enzymatic activity of the biocatalysts were outside the chosen design space regarding protein and glutaraldehyde amounts. Therefore, the design was augmented using Design Expert 8.0.7.1 software (again choosing IV optimality) to extend the design space to include protein amounts up to 200 mg protein g^{-1} MP and glutaraldehyde amounts up to 8 mmol glutaraldehyde g^{-1} MP (Id 31-54 in Table A. 1). To include all available information on the design space in the model fitting, experiments conducted between the augmentation of the design were included as well (Id 55-66 in Table A. 1). Protein amounts given in Table A. 1 correspond to the actually applied protein amounts (calculated based on activity measurements) and, therefore, deviate slightly from protein amounts suggested to be tested by the design.

Table A. 1 Experimental results used for development of the response surface reduced cubic model (adapted from Gasser et al. 2016)

Id	Factor 1 A:Protein amount	Factor 2 B:Glutaraldehyde amount	Factor 3 C:Protein adsorption time	Factor 4 D:Glutaraldehyde reaction time	Factor 5 E:pH	Response Specific activity
	mg g^{-1} MP	mmol g^{-1} MP	h	h		kU g^{-1} MP
1	72	0.50	2.50	24.0	5.90	2.27
2	71	2.40	0.50	15.5	7.30	3.56
3	21	0.50	1.00	0.5	9.00	0.51
4	25	0.50	0.50	22.2	5.00	1.81
5	49	2.18	2.50	22.5	9.00	2.82
6	75	3.25	0.50	22.1	5.00	4.27
7	9	4.00	0.50	24.0	9.00	0.84
8	76	4.00	1.20	24.0	8.90	3.67
9	86	4.00	3.30	0.5	5.00	4.10
10	11	0.50	4.00	24.0	7.70	0.61
11	10	4.00	3.10	24.0	5.00	1.15
12	10	4.00	4.00	7.6	9.00	0.87
13	64	1.88	4.00	14.1	5.00	3.67
14	97	4.00	4.00	24.0	7.80	5.17
15	58	2.39	4.00	0.5	7.10	2.43
16	52	4.00	1.70	12.5	7.00	3.68
17	73	0.50	0.50	19.2	8.80	1.58
18	45	4.00	1.70	12.5	7.00	3.21
19	67	1.88	4.00	14.1	5.00	3.76

Id	Factor 1 A:Protein amount	Factor 2 B:Glutaraldehyde amount	Factor 3 C:Protein adsorption time	Factor 4 D:Glutaraldehyde reaction time	Factor 5 E:pH	Response Specific activity
	mg g^{-1} MP	mmol g^{-1} MP	h	h		kU g^{-1} MP
20	87	0.89	0.80	2.0	5.80	2.40
21	57	2.18	2.50	22.5	9.00	2.69
22	13	2.09	1.70	12.7	7.00	0.78
23	10	3.96	0.50	23.9	5.80	1.15
24	90	0.50	3.80	7.8	9.00	1.16
25	55	2.39	4.00	0.5	7.10	2.45
26	10	0.76	2.80	11.7	9.00	0.42
27	86	1.36	2.80	7.9	6.70	2.82
28	87	3.35	1.00	0.5	9.00	3.19
29	13	0.50	3.20	0.5	5.00	0.48
30	13	2.09	1.70	12.7	7.00	1.19
31	132	0.50	2.58	17.1	5.00	0.40
32	120	3.77	0.50	13.7	9.00	3.57
33	121	7.92	4.00	15.1	7.00	2.39
34	121	7.92	4.00	15.1	7.00	2.57
35	97	6.99	0.50	24.0	9.00	2.41
36	114	6.99	0.50	24.0	8.00	3.14
37	157	6.99	0.50	24.0	9.00	3.31
38	179	8.00	0.50	24.0	8.00	2.79
39	210	4.44	2.30	10.3	6.97	3.19
40	198	0.50	4.00	24.0	9.00	1.99
41	203	0.50	4.00	0.5	5.00	0.64
42	191	0.50	0.50	0.5	8.22	1.20
43	209	8.00	3.13	0.5	9.00	3.81
44	44	8.00	1.68	18.6	5.00	2.21
45	213	4.44	2.30	10.3	6.97	2.71
46	16	8.00	4.00	0.5	5.00	1.38
47	98	8.00	2.15	0.6	6.70	2.62
48	13	8.00	4.00	24.0	9.00	0.90
49	12	8.00	0.50	0.5	8.60	1.02
50	181	2.00	1.38	24.0	5.48	2.22
51	189	8.00	0.50	0.5	5.00	2.86
52	196	8.00	4.00	24.0	5.00	3.36
53	179	3.70	0.50	22.7	7.29	3.59
54	37	8.00	1.68	18.6	5.00	2.16
55	129	6.21	4.00	24.0	9.00	4.78
56	136	6.21	4.00	24.0	9.00	4.52
57	141	6.21	4.00	24.0	9.00	4.45
58	77	5.51	4.00	24.0	5.00	3.16
59	71	5.51	4.00	24.0	5.00	3.24
60	75	5.51	4.00	24.0	5.00	3.01
61	97	4.71	0.50	24.0	9.00	4.22
62	102	4.71	0.50	24.0	9.00	4.00
63	102	4.71	0.50	24.0	9.00	4.00
64	103	4.90	0.50	24.0	9.00	4.44
65	107	4.90	0.50	24.0	9.00	4.33
66	105	4.90	0.50	24.0	9.00	4.63

Table A. 2 ANOVA for response surface reduced cubic model (adapted from Gasser et al. 2016)

Source	Sum of Squares	df	Mean Square	F Value	*p*-value Prob > F
Model	97.57	17	5.74	24.59	< 0.0001
A-Protein amount	1.28	1	1.28	5.5	0.0232
B-Glutaraldehyde amount	0.71	1	0.71	3.03	0.088
C-Protein adsorption time	0.13	1	0.13	0.54	0.4662
D-Glutaraldehyde reaction time	0.94	1	0.94	4.02	0.0505
E-pH	$3.78\ 10^{-3}$	1	$3.78\ 10^{-3}$	0.016	0.8992
AB	6.83	1	6.83	29.28	< 0.0001
BD	0.83	1	0.83	3.54	0.0661
BE	0.09	1	0.09	0.39	0.5367
CD	0.13	1	0.13	0.58	0.4513
CE	0.23	1	0.23	0.97	0.3294
DE	0.66	1	0.66	2.84	0.0986
A^2	6.45	1	6.45	27.65	< 0.0001
B^2	15.33	1	15.33	65.69	< 0.0001
E^2	0.68	1	0.68	2.93	0.0937
CDE	4.18	1	4.18	17.91	0.0001
BE^2	1.56	1	1.56	6.67	0.0129
A^3	4.33	1	4.33	18.55	< 0.0001
Residual	11.2	48	0.23		
Cor Total	108.77	65			

Table A. 3 Final equation in terms of actual factors (units for the different factors are mg g^{-1} MP, mmol g^{-1} MP, h, and h for protein amount, glutaraldehyde amount, protein adsorption time, and glutaraldehyde reaction time, respectively; adapted from Gasser et al. 2016)

Specific activity (kU g^{-1} MP)	=
-8.66272 (kU g^{-1} MP)	
+0.081542 (kU g^{-1} MP mg^{-1} protein g MP)	* Protein amount
+2.62092 (kU g^{-1} MP $mmol^{-1}$ g MP)	* Glutaraldehyde amount
+1.38662 (kU g^{-1} MP h^{-1})	* Protein adsorption time
+0.20448 (kU g^{-1} MP h^{-1})	* Glutaraldehyde reaction time
+1.84673 (kU g^{-1} MP)	* pH
+2.15423 10^{-3} (kU g^{-1} MP mg^{-1} protein g MP)	* Protein amount * Glutaraldehyde amount
-4.69*10^{3} (kU g^{-1} MP $mmol^{-1}$ g MP h^{-1})	* Glutaraldehyde amount * Glutaraldehyde reaction time
-0.5561 (kU g^{-1} MP $mmol^{-1}$ g MP)	* Glutaraldehyde amount * pH
-0.09799(kU g^{-1} MP h^{-2})	* Protein adsorption time * Glutaraldehyde reaction time
-0.21007 (kU g^{-1} MP h^{-1})	* Protein adsorption time * pH
-0.025393 (kU g^{-1} MP h^{-1})	* Glutaraldehyde reaction time * pH
-7.46114 10^{-4} (kU g^{-1} MP mg^{-2} protein g^{2} MP)	* (Protein amount)^{2}
-0.094961 (kU g^{-1} MP $mmol^{-2}$ g^{2} MP)	* (Glutaraldehyde amount)^{2}
-0.10783 (kU g^{-1} MP)	* pH^{2}
0.01455 (kU g^{-1} MP h^{-2})	* Protein adsorption time * Glutaraldehyde reaction time * pH
0.040394 (kU g^{-1} MP $mmol^{-1}$ g MP)	* Glutaraldehyde amount * pH^{2}
+1.82968 10^{-6} (kU g^{-1} MP mg^{-3} protein g^{3} MP)	* (Protein amount)^{3}

A1.2. Optimization regarding enzymatic stability

A second-degree polynomial model was fitted to each time point for every condition tested in the stability experiments shown in Table A. 4. The influence of five factors on the residual enzymatic stability was tested, i.e., protein amount, glutaraldehyde amount, protein adsorption time, glutaraldehyde reaction time, and pH. Transformation of the results was conducted prior to fitting whenever recommended by the software. Subsequently, all models were reduced to only contain significant ($p \leq 0.05$) factors and factors necessary to maintain model hierarchy using the step-wise automatic model regression of the software.

For every condition tested, i.e., for every pH value, every solvent, NaN_3, and H_2O_2 the F values of the models for the three time points tested, i.e., 1 day, 7 days, and 14 days were compared and the one with the highest F value, i.e., the model for which the effect of the five factors on the residual stability was predicted to be most relevant was selected for every condition. Selected time points were 1 day for pH 3, 7 days for MeOH and H_2O_2, and 14 days for pH 5, pH 7, pH 9 and NaN_3. ANOVA tables for all the selected models are shown in Table A. 5- Table A. 12 and the coefficients of the final equations in terms of actual factors are shown in Table A. 14.

Based on the selected time points, desirability (D) was calculated for every condition tested according to Eq. 3. For further explanation the reader is referred to 4.3.3.4.2. A second-degree polynomial model was fitted and the same five factors were tested. Subsequently, the model was reduced to only contain significant ($p \leq 0.05$) factors and factors necessary to maintain model hierarchy using the step-wise automatic model regression of the software. The ANOVA table is shown in Table A. 13 and the coefficients of the final equation in terms of the actual factors are shown in Table A. 14.

Table A. 4 Results of stability experiments conducted with biocatalysts produced using different formulations. The Id given in the first column corresponds to the Id given in Table A. 1, i.e., particles produced according to the formulation given in Table A. 1 were tested under the given conditions. Values are given as apparent residual enzymatic activity of starting activities in %. Samples were taken after 1, 7, and 14 days. Experiments with acetone, MeOH, NaN_3, and H_2O_2 were conducted at pH 7 (adapted from Gasser et al. 2016).

Id	pH 3			pH 5			pH 7			pH 9			Acetone (30%			MeOH (30% (v/v))			NaN_3 (100 µM)			H_2O_2 (1 mM)		
	1 d	7 d	14 d	1 d	7 d	14 d	1 d	7 d	14 d	1 d	7 d	14 d	1 d	7 d	14 d	1 d	7 d	14 d	1 d	7 d	14 d	1 d	7 d	14 d
1	29	1	0	82	75	51	95	90	76	29	10	4	40	14	22	60	31	6	68	60	51	73	54	54
2	49	7	0	102	76	69	98	92	89	60	35	14	64	29	35	85	53	21	93	64	89	82	70	50
3	30	4	1	86	54	61	69	67	56	33	11	7	39	13	18	56	23	5	83	52	51	72	53	47
4	25	1	0	86	68	43	81	69	59	34	10	4	49	15	21	66	30	6	74	52	50	65	37	42
5	71	7	1	86	71	56	102	85	88	74	32	17	55	21	22	73	39	15	96	71	92	78	66	59
6	72	7	0	104	87	69	108	107	103	52	-	-	53	28	36	77	54	20	79	87	86	80	66	60
7	55	9	3	92	76	71	76	67	68	70	46	25	48	30	28	67	34	14	78	82	80	73	76	74
8	50	9	1	75	78	52	94	103	103	91	51	38	84	44	33	77	45	33	84	76	84	106	79	65
9	57	5	1	101	83	59	95	95	91	65	37	26	72	33	38	77	53	27	91	84	100	78	64	59
10	24	1	0	90	72	42	104	69	72	33	10	5	36	11	14	56	24	4	61	44	49	71	36	31
11	50	6	2	82	65	48	87	85	74	70	23	13	54	25	20	65	28	13	85	90	65	66	70	45
12	56	9	2	83	68	66	96	78	70	55	29	17	47	23	18	63	29	13	82	82	71	77	69	59
13	45	4	0	98	73	59	89	82	78	59	21	14	57	22	25	57	34	11	76	65	60	75	61	63
14	48	7	0	106	90	81	109	104	99	92	54	37	71	43	42	81	55	30	81	77	81	85	79	74
15	41	4	0	96	73	57	95	94	84	51	26	11	55	23	23	63	34	12	78	66	67	65	45	58
16	67	6	1	87	68	62	94	99	93	80	28	22	66	31	26	73	44	22	81	70	73	89	75	66
17	31	2	0	114	85	54	74	69	63	50	16	6	41	16	19	55	36	6	78	80	62	58	55	48
18	43	5	1	105	80	66	97	90	82	65	33	25	55	32	34	78	42	22	83	95	75	83	70	67
19	41	4	0	97	77	68	96	92	78	52	22	13	50	23	28	65	45	13	77	69	65	66	60	68
20	30	2	0	91	75	55	91	95	85	44	15	7	47	20	24	53	34	8	64	57	60	75	63	55

Id	pH 3			pH 5			pH 7			pH 9			Acetone (30%			MeOH (30% (v/v))			NaN_3 (100 µM)			H_2O_2 (1 mM)		
	1 d	7 d	14 d	1 d	7 d	14 d	1 d	7 d	14 d	1 d	7 d	14 d	1 d	7 d	14 d	1 d	7 d	14 d	1 d	7 d	14 d	1 d	7 d	14 d
21	53	8	1	85	72	55	90	93	88	71	33	22	57	35	27	60	40	17	98	95	77	85	68	65
22	47	4	1	74	63	53	90	78	64	71	28	11	49	26	21	58	35	12	69	78	67	83	54	59
23	54	5	1	84	62	48	92	98	80	47	28	17	48	20	23	64	33	12	71	65	76	66	47	57
24	34	3	0	78	75	44	73	73	62	38	11	5	42	14	19	68	35	6	69	66	50	86	69	51
25	42	4	0	109	60	65	93	81	77	45	24	13	53	29	22	62	34	14	84	78	63	77	66	50
26	42	5	0	84	78	46	97	67	68	32	10	6	40	17	13	61	25	6	69	62	38	58	38	42
27	39	2	0	97	67	52	95	94	78	42	17	10	49	22	23	66	39	9	67	63	69	73	64	34
28	90	12	3	80	70	68	103	99	95	82	41	30	87	49	27	77	44	35	75	89	80	99	99	90
29	24	1	0	81	62	39	113	69	58	21	7	3	55	19	17	53	29	6	51	30	32	61	35	28
30	40	6	1	94	78	74	99	84	76	49	24	13	56	23	24	72	41	13	52	48	72	86	44	50
31	13	0	0	65	25	15	73	55	48	23	8	5	29	8	14	46	20	5	28	21	15	71	52	38
32	43	4	1	95	62	45	104	103	94	73	50	44	78	45	51	81	54	39	94	92	77	94	82	77
33	33	3	1	87	50	35	103	91	88	55	31	25	61	30	35	64	38	25	88	79	60	93	77	64
34	30	3	1	86	53	33	104	95	85	54	32	23	55	31	35	64	38	26	100	90	66	92	72	61
35	42	4	1	95	62	42	107	98	87	76	53	46	85	52	44	78	46	44	107	96	69	97	88	76
36	34	3	1	88	54	37	97	92	85	62	42	32	71	41	39	71	42	33	88	83	65	94	74	61
37	40	4	1	96	64	45	108	100	99	70	47	41	75	48	43	84	47	37	86	81	62	89	87	82
38	34	3	1	89	52	38	101	93	88	62	41	30	69	41	38	72	43	31	90	78	61	93	82	67
39	31	2	1	86	46	33	88	76	76	39	21	16	54	22	27	55	25	23	88	79	58	86	81	64
40	15	1	0	80	40	25	80	69	62	33	18	12	43	14	25	53	23	14	76	70	56	84	80	70
41	9	0	0	64	26	15	79	71	66	22	11	8	30	9	19	37	19	6	81	67	48	78	70	53
42	13	1	0	85	38	20	90	72	69	34	13	9	35	11	23	52	22	7	74	59	44	82	71	64
43	36	3	1	84	45	31	93	81	79	63	42	31	66	31	31	67	40	31	73	73	62	86	86	80

Id	pH 3			pH 5			pH 7			pH 9			Acetone (30%			MeOH (30% (v/v))			NaN_3 (100 µM)			H_2O_2 (1 mM)		
	1 d	7 d	14 d	1 d	7 d	14 d	1 d	7 d	14 d	1 d	7 d	14 d	1 d	7 d	14 d	1 d	7 d	14 d	1 d	7 d	14 d	1 d	7 d	14 d
44	31	2	1	95	50	29	96	79	77	45	25	20	47	19	26	55	26	16	86	75	59	91	80	66
45	25	2	0	88	46	32	88	72	72	45	21	21	50	21	24	59	24	17	80	63	49	83	68	58
46	24	1	1	85	43	28	109	79	74	36	20	14	38	15	15	45	19	12	83	70	58	86	72	59
47	37	2	1	86	54	31	88	75	77	43	24	18	55	23	25	60	27	20	77	66	57	92	82	73
48	26	2	1	80	49	30	100	75	72	54	35	35	54	24	26	62	28	23	76	74	74	69	49	42
49	26	2	0	91	55	38	98	78	77	55	24	22	47	20	31	61	24	22	79	71	60	86	68	65
50	22	1	0	77	42	29	94	82	71	37	17	16	45	16	23	53	24	16	72	64	55	76	69	55
51	35	2	1	88	49	35	103	79	82	40	21	17	48	21	29	64	29	21	73	63	53	80	68	53
52	25	2	1	78	43	28	88	71	70	39	20	21	46	19	24	55	24	18	68	63	47	78	76	66
53	34	2	1	77	45	30	96	79	74	49	27	23	55	28	40	66	39	26	71	66	50	84	88	73
54	30	2	0	84	45	28	95	80	78	45	25	23	46	19	23	53	23	17	75	67	56	90	76	66
67*	43	6	1	94	80	60	86	83	82	53	24	13	50	23	25	64	39	11	73	73	64	72	52	55

*) particles were produced with 9 mg g^{-1} protein, 4 mmol g^{-1} glutaraldehyde at pH 5 with 0.5 h protein adsorption time and 0.5 h glutaraldehyde reaction time.

Table A. 5 ANOVA for response surface reduced quadratic model for residual activities of biocatalysts after incubation at pH 3 for 1 d (adapted from Gasser et al. 2016).

Source	Sum of Squares	df	Mean Square	F Value	*p*-value Prob > F
Model	1.65	8	0.21	40.24	< 0.0001
A-Protein amount	0.3	1	0.3	57.54	< 0.0001
B-Glutaraldehyde amount	0.22	1	0.22	42.75	< 0.0001
E-pH	0.031	1	0.031	5.99	0.0182
AB	0.25	1	0.25	48.63	< 0.0001
BE	0.023	1	0.023	4.46	0.0402
A^2	0.17	1	0.17	32.57	< 0.0001
B^2	0.74	1	0.74	143.9	< 0.0001
E^2	0.024	1	0.024	4.69	0.0355
Residual	0.24	46	$5.14\ 10^{-3}$		
Cor Total	1.89	54			

Table A. 6 ANOVA for response surface reduced quadratic model for residual activities of biocatalysts after incubation at pH 5 for 14 d (adapted from Gasser et al. 2016).

Source	Sum of Squares	df	Mean Square	F Value	*p*-value Prob > F
Model	63.26	5	12.65	32.45	< 0.0001
A-Protein amount	18.85	1	18.85	48.36	< 0.0001
B-Glutaraldehyde amount	0.074	1	0.074	0.19	0.6645
AB	9.37	1	9.37	24.03	< 0.0001
A^2	5.21	1	5.21	13.37	0.0006
B^2	21.05	1	21.05	53.98	< 0.0001
Residual	19.1	49	0.39		
Cor Total	82.36	54			

Table A. 7 ANOVA for response surface reduced quadratic model for residual activities of biocatalysts after incubation at pH 7 for 14 d (adapted from Gasser et al. 2016).

Source	Sum of Squares	df	Mean Square	F Value	*p*-value Prob > F
Model	4902.4	4	1225.6	22.28	< 0.0001
A-Protein amount	42.59	1	42.59	0.77	0.3831
B-Glutaraldehyde amount	1438.9	1	1438.9	26.16	< 0.0001
A^2	1578.62	1	1578.62	28.7	< 0.0001
B^2	1920.84	1	1920.84	34.92	< 0.0001
Residual	2750.15	50	55		
Cor Total	7652.54	54			

Table A. 8 ANOVA for response surface reduced quadratic model for residual activities of biocatalysts after incubation at pH 9 for 14 d (adapted from Gasser et al. 2016)

Source	Sum of Squares	df	Mean Square	F Value	*p*-value Prob > F
Model	78.52	8	9.82	59.62	< 0.0001
A-Protein amount	0.95	1	0.95	5.78	0.0204
B-Glutaraldehyde amount	42.99	1	42.99	261.13	< 0.0001
D-Glutaraldehyde reaction time	1.03	1	1.03	6.27	0.0159
E-pH	8.01	1	8.01	48.67	< 0.0001
BE	1.34	1	1.34	8.13	0.0066
A^2	2.89	1	2.89	17.55	0.0001
B^2	15.57	1	15.57	94.57	< 0.0001
E^2	1.89	1	1.89	11.49	0.0015
Residual	7.41	45	0.16		
Cor Total	85.93	53			

Table A. 9 ANOVA for response surface reduced quadratic model for residual activities of biocatalysts after incubation in 30 % (v/v) acetone for 14 d (adapted from Gasser et al. 2016).

Source	Sum of Squares	df	Mean Square	F Value	*p*-value Prob > F
Model	3.45	6	0.58	71.57	< 0.0001
A-Protein amount	0.094	1	0.094	11.69	0.0013
B-Glutaraldehyde amount	1.96	1	1.96	244.1	< 0.0001
E-pH	0.19	1	0.19	23.92	< 0.0001
BE	0.036	1	0.036	4.48	0.0395
A^2	0.19	1	0.19	23.89	< 0.0001
B^2	0.81	1	0.81	100.66	< 0.0001
Residual	0.39	48	$8.04\ 10^{-3}$		
Cor Total	3.84	54			

Table A. 10 ANOVA for response surface reduced quadratic model for residual activities of biocatalysts after incubation in 30 % (v/v) MeOH for 7 d (adapted from Gasser et al. 2016).

Source	Sum of Squares	df	Mean Square	F Value	*p*-value Prob > F
Model	0.03	10	$2.99\ 10^{-3}$	22.52	< 0.0001
A-Protein amount	$1.35\ 10^{-3}$	1	$1.35\ 10^{-3}$	10.18	0.0026
B-Glutaraldehyde amount	$1.43\ 10^{-3}$	1	$1.43\ 10^{-3}$	10.78	0.002
C-Protein adsorption time	$1.45\ 10^{-4}$	1	$1.45\ 10^{-4}$	1.09	0.3016
E-pH	$2.20\ 10^{-3}$	1	$2.20\ 10^{-3}$	16.58	0.0002
AB	$4.46\ 10^{-3}$	1	$4.46\ 10^{-3}$	33.61	< 0.0001
AE	$1.37\ 10^{-3}$	1	$1.37\ 10^{-3}$	10.29	0.0025
BE	$6.83\ 10^{-4}$	1	$6.83\ 10^{-4}$	5.15	0.0282
A^2	$9.02\ 10^{-3}$	1	$9.02\ 10^{-3}$	67.95	< 0.0001
B^2	$7.66\ 10^{-3}$	1	$7.66\ 10^{-3}$	57.68	< 0.0001
C^2	$7.01\ 10^{-4}$	1	$7.01\ 10^{-4}$	5.28	0.0264
Residual	$5.84\ 10^{-3}$	44	$1.33\ 10^{-4}$		
Cor Total	0.036	54			

Table A. 11 ANOVA for response surface reduced quadratic model for residual activities of biocatalysts after incubation in 1 mM H_2O_2 for 7 d (adapted from Gasser et al. 2016).

Source	Sum of Squares	df	Mean Square	F Value	*p*-value Prob > F
Model	8492.1	6	1415.35	22.46	< 0.0001
A-Protein amount	1705.85	1	1705.85	27.07	< 0.0001
B-Glutaraldehyde amount	1799.07	1	1799.07	28.55	< 0.0001
E-pH	682.91	1	682.91	10.84	0.0019
AB	520.72	1	520.72	8.26	0.006
A^2	632.21	1	632.21	10.03	0.0027
B^2	802.7	1	802.7	12.74	0.0008
Residual	3024.36	48	63.01		
Cor Total	11516.5	54			

Table A. 12 ANOVA for response surface reduced quadratic model for residual activities of biocatalysts after incubation in 100 µM NaN_3 for 7 d (adapted from Gasser et al. 2016).

Source	Sum of Squares	df	Mean Square	F Value	*p*-value Prob > F
Model	7835.45	7	1119.35	11.86	< 0.0001
A-Protein amount	995.20	1	995.20	10.55	0.0022
B-Glutaraldehyde amount	1006.08	1	1006.08	10.66	0.002
D-Glutaraldehyde reaction time	33.97	1	33.97	0.36	0.5514
E-pH	483.19	1	483.19	5.12	0.0283
AD	445.05	1	445.05	4.72	0.035
A^2	1000.46	1	1000.46	10.60	0.0021
B^2	4048.65	1	4048.65	42.91	< 0.0001
Residual	4434.88	47	94.36		
Cor Total	12270.32	54			

Table A. 13 ANOVA for response surface reduced quadratic model for overall stability of the biocatalysts taking into account all the tested conditions (adapted from Gasser et al. 2016).

Source	Sum of Squares	df	Mean Square	F Value	*p*-value Prob > F
Model	0.54	7	0.077	51.69	< 0.0001
A-Protein amount	$3.36\ 10^{-3}$	1	$3.36\ 10^{-3}$	2.27	0.1388
B-Glutaraldehyde amount	0.16	1	0.16	109.3	< 0.0001
E-pH	0.048	1	0.048	32.34	< 0.0001
AB	$7.20\ 10^{-3}$	1	$7.20\ 10^{-3}$	4.86	0.0326
A^2	0.086	1	0.086	58.36	< 0.0001
B^2	0.23	1	0.23	156.53	< 0.0001
E^2	$8.19\ 10^{-3}$	1	$8.19\ 10^{-3}$	5.53	0.0231
Residual	0.068	46	$1.48\ 10^{-3}$		
Cor Total	0.6	53			

Table A. 14 Summary of the coefficients of the final equations in terms of actual factors of the different response surface reduced quadratic models for residual activities of biocatalysts. The factors are A- protein amount (mg g^{-1} MP), B- glutaraldehyde amount (mmol g^{-1} MP), C- protein adsorption time (h), D- glutaraldehyde reaction time (h), and E- pH (adapted from Gasser et al. 2016).

	Log(pH 3 1 d) =	**√(pH 5 14 d) =**	**pH 7 14 d =**	**√(pH 9 14 d) =**	**Log(Acetone 14d)=**	**1/√(MeOH 7d) =**	**NaN_3 14 d =**	**H_2O_2 7 d =**	**Overall stability**
	1.72727	6.80922	50.46417	5.4266	0.40883	0.16186	20.07045	13.85614	0.34549
A	6.1113 10^{-4}	-3.08426 10^{-4}	0.30836	0.016266	4.23598 10-3	-1.51605 10^{-4}	0.24558	0.36467	2.04409 10^{-3}
B	0.18668	0.62897	10.42592	0.89197	0.20648	-8.44388 10^{-3}	14.0763	9.58631	0.11156
C						0.013988			
D				0.015174			0.41033		
E	-0.13892			-1.44887	0.014054	4.22322 10^{-3}	1.89765	2.24507	-0.83305
AB	3.60098 10^{-4}	2.19323 10^{-3}				-4.81497 10^{-5}		-0.01637	6.11286 10^{-5}
AD							-4.40691 10^{-3}		
AE						-4.82237 10^{-5}			
BE	-4.52310 10^{-3}			0.034626	5.66690 10^{-3}	-7.87129 10^{-4}			
A^2	-1.46773 10^{-5}	-8.13977 10^{-5}	-1.4161 10^{-3}	-6.19298 10^{-5}	-1.56363 10^{-5}	3.39982 10^{-6}	-1.14461 10^{-3}	-8.97009 10^{-4}	-1.06736 10^{-5}
B^2	-0.02021	-0.10505	-1.00349	-0.094778	-0.02072	2.05458 10^{-3}	-1.46869	-0.65013	-0.011492
C^2						-2.84114 10^{-3}			7.32145 10^{-3}
E^2	0.012387			0.11107					

Table A. 15 Predicted optimal biocatalyst formulation and predicted specific activities and residual enzymatic activities by the different models to obtain biocatalysts with highest residual activity in corresponding conditions and prediction for biocatalyst formulation to obtain biocatalysts with overall optimal stability in all tested conditions (adapted from Gasser et al. 2016).

Model	Protein amount	Glutaraldehyde amount	Protein adsorption time	Glutaraldehyde reaction time	pH	Specific activity	pH 3 1d	pH 5 14d	pH 7 14d	pH 9 14d	Acetone 14d	MeOH 7d	NaN_3 14d	H_2O_2 7d
	mg g^{-1} MP	mmol g^{-1} MP	h	h		kU g^{-1} MP	%	%	%	%	%	%	%	%
pH 3	73	4.26	0.5*	24.0*	9	3.73	65.1	61	91.6	36.2	30.4	52.8	84.4	79.9
pH 5	45	3.46	0.5*	24.0*	9*	2.99	62.7	62.3	85.5	28.9	21.7	44.3	82.1	71.4
pH 7	109	5.19	0.5*	24.0*	9*	3.87	61.6	56	94.3	42	38.9	59	82.1	86.1
pH 9	131	6.35	0.5*	24	9	3.66	52.5	48.4	92.3	44	41.8	57.4	75.8	87.5
Acetone	135	6.21	0.5*	24.0*	9	3.66	52.9	48.6	92.3	44	41.9	57.8	75.7	87.7
MeOH	123	5.22	0.5	24.0*	9	3.78	59.7	54.3	94	42.4	39.8	59.6	80.3	87.2
NaN_3	61	4.79	0.5*	24	9	3.57	63.7	59.8	90.9	37.2	31.1	49.8	85	79.2
H_2O_2	154	5.44	0.5*	24.0*	9	3.55	53.1	48.8	91.4	42.6	40.2	56.9	74.6	88.1
Overall stability	111	5.15	0.5*	24.0*	9	3.86	61.6	56	94.3	41.9	38.8	59.1	82	86.2

*) Insignificant factors for the corresponding model; these factors were set to the specified value to predict the other residual activities and the specific activity.

A2. Experimental matrices, response surface models, and results for lignin experiments in organic solvent buffer mixtures

Table A. 16 ANOVA results of the two factor interaction model fitted to the results of the experiment testing the influence of different organic co-solvents and different enzyme mixtures on the AMF.

Source	Sum of Squares	df	Mean Square	F value	*p*-value
Model	$1.209\ 10^{8}$	30	$4.030\ 10^{6}$	2.50	0.0879
A-Solvent	$3.533\ 10^{7}$	4	$8.832\ 10^{6}$	5.49	0.0200
B-MnP	$1.537\ 10^{5}$	1	$1.537\ 10^{5}$	0.096	0.7651
C-LiP	$6.281\ 10^{6}$	1	$6.281\ 10^{6}$	3.90	0.0836
D-HRP	$1.465\ 10^{6}$	1	$1.465\ 10^{6}$	0.91	0.3680
E-Laccase	$2.820\ 10^{7}$	1	$2.820\ 10^{7}$	17.53	0.0031
AB	$5.582\ 10^{6}$	4	$1.396\ 10^{6}$	0.87	0.5230
AC	$4.678\ 10^{6}$	4	$1.170\ 10^{6}$	0.73	0.5979
AD	$5.338\ 10^{6}$	4	$1.334\ 10^{6}$	0.83	0.5424
AE	$1.393\ 10^{7}$	4	$3.481\ 10^{6}$	2.16	0.1639
BC	2338.20	1	2338.20	$1.453\ 10^{3}$	0.9705
BD	$1.684\ 10^{5}$	1	$1.684\ 10^{5}$	0.10	0.7546
BE	$1.649\ 10^{5}$	1	$1.649\ 10^{5}$	0.10	0.7570
CD	$3.965\ 10^{5}$	1	$3.965\ 10^{5}$	0.25	0.6329
CE	$5.682\ 10^{5}$	1	$5.682\ 10^{5}$	0.35	0.5687
DE	$6.577\ 10^{5}$	1	$6.577\ 10^{5}$	0.41	0.5404
Residual	$1.287\ 10^{7}$	8	$1.609\ 10^{6}$		
Lack of Fit	$8.132\ 10^{6}$	5	$1.626\ 10^{6}$	1.03	0.1196
Pure Error	$4.738\ 10^{6}$	3	$1.579\ 10^{6}$		

Table A. 17 ANOVA results of the reduced model fitted to the results of the experiment testing the influence of different organic co-solvents and different enzyme mixtures on the AMF.

Source	Sum of Squares	df	Mean Square	F value	*p*-value
Model	$9.102\ 10^{7}$	10	$9.102\ 10^{6}$	5.96	< 0.0001
A-Solvent	$4.478\ 10^{7}$	4	$1.120\ 10^{7}$	7.33	0.0004
C-LiP	$1.040\ 10^{7}$	1	$1.040\ 10^{7}$	6.81	0.0144
E-Laccase	$2.235\ 10^{7}$	1	$2.235\ 10^{7}$	14.64	0.0007
AE	$2.026\ 10^{7}$	4	$5.065\ 10^{6}$	3.32	0.0241
Residual	$4.275\ 10^{7}$	28	$1.527\ 10^{6}$		
Lack of Fit	$3.801\ 10^{7}$	25	$1.520\ 10^{6}$	0.96	0.6075

Table A. 18 Design matrix and results of experiments conducted to test the influence of different organic co-solvents and enzyme mixtures on the AMF after treatment of OL.

Factors					**Sum of areas of monomer fraction (AMF) (284 -308 nm) [mAU]**	
Co-solvent	LiP	HRP	MnP	TVL	Observed	Predicted
Experiments of D-optimal design						
No organic co-solvent	-	-	-	-	2,089	1,802
	+	-	+	-	3,254	2,873
	-	+	+	-	2,857	1,802
	+	+	-	-	1,149	2,873
	-	+	-	+	4,191	4,192
DMSO 30% (v/v)	-	-	-	-	2,712	4,764
	-	-	-	-	3,382	4,764
	+	-	+	-	5,498	5,835
	-	+	+	-	4,871	4,764
	+	+	-	-	6,215	5,835
	+	+	+	-	9,117	5,835
	-	-	-	+	10,346	10,346
2-Propanol 30% (v/v)	-	-	-	-	5,628	4,772
	-	-	-	-	2,797	4,772
	-	-	+	-	3,798	4,772
	+	-	-	-	6,347	5,843
	+	-	+	-	5,911	5,843
	-	+	-	-	7,181	4,772
	-	+	+	-	5,875	4,772
	+	+	-	-	5,420	5,843
	+	+	+	-	6,681	5,843
	-	-	+	+	6,098	5,200
	+	+	-	+	5,372	6,271
2-Methoxyethanol 30% (v/v)	-	-	-	-	5,114	4,106
	-	-	+	-	4,315	4,106
	+	-	+	-	4,383	5,177
	-	+	+	-	3,185	4,106
	+	+	-	-	5,675	5,177
	+	-	+	+	5,444	5,347
	-	+	+	+	4,178	4,276
MeOH 30% (v/v)	-	-	-	-	4,782	4,880
	-	-	-	-	3,775	4,880
	-	-	+	-	4,655	4,880
	+	-	-	-	6,411	5,950
	+	-	+	-	5,018	5,950
	-	+	-	-	7,090	4,880
	-	+	+	-	5,233	4,880
	+	+	+	-	5,282	5,950
	-	-	-	+	8,336	7,597
	+	+	+	+	7,927	8,667
Validation experiments						
DMSO 30% (v/v)	-	-	-	-	5,021	4,764
	-	+	-	+	9,711	10,346

(+) The corresponding enzyme is applied to the reaction mixture. Enzymes were applied at a concentration of, 50.0, 8.3, 16.7, and 16.7 mg protein per L^{-1} for LiP, HRP, MnP, and laccase respectively in the enzyme feed solution.

(-) The corresponding enzyme is not applied to the reaction mixture

Table A. 19 Design matrix and results of experiments conducted to test the influence of pH and enzyme mixtures on the AMF after treatment of OL.

Factors				**Sum of areas of monomer fraction (AMF) (276 -308 nm) [mAU]**		
pH	LiP [U per well]	HRP [U per well]	TVL [U per well]	Observed	Cubic model prediction	Reduced model prediction
Experiments conducted for model fitting						
3	0.21	6.00	0.75	5,627	4,874	4,664
3	0.00	6.00	0.00	3,563	4,092	4,154
3	0.11	3.00	0.38	5,957	5,724	5,731
3	0.00	2.55	0.75	7,143	6,144	5,969
3	0.21	0.00	0.75	5,877	6,687	7,086
3	0.21	2.52	0.00	5,911	6,313	5,903
3	0.00	6.00	0.00	4,358	4,092	4,154
3	0.00	0.00	6.00	6,950	7,280	6,851
3	0.50	3.00	0.00	6,697	6,512	5,791
3	0.25	0.00	0.00	6,633	6,381	7,122
3	0.00	3.00	0.00	3,355	5,262	5,587
3	0.50	0.00	6.00	6,519	6,280	7,056
3	0.50	6.00	6.00	6,788	6,772	7,745
3	0.00	6.00	6.00	8,038	8,001	7,540
3	0.50	6.00	3.00	6,810	7,171	6,052
3.32	0.00	1.90	0.33	7,592	5,805	6,309
4	0.13	1.50	3.00	6,597	7,222	6,533
4	0.00	0.80	0.50	7,770	7,004	7,396
4	0.00	3.00	0.15	7,662	7,000	6,956
4	0.00	0.80	0.15	7,234	6,960	7,430
4	0.00	3.00	0.50	6,100	7,131	6,960
4.1	0.00	3.87	6.00	7,477	7,400	7,174
4.1	0.00	0.00	6.00	7,484	7,124	6,908
4.5	0.00	0.00	0.45	8,145	8,130	8,142
4.5	0.21	2.59	0.52	8,012	7,387	6,737
5	0.21	6.00	0.28	5,476	5,756	7,493
5	0.08	6.00	0.75	6,632	6,615	8,244
5	0.25	6.00	3.00	6,441	6,261	7,055
5	0.50	0.00	0.00	6,327	6,480	5,627
5	0.25	3.00	6.00	6,938	7,166	6,720
5	0.25	3.00	0.00	8,139	8,339	7,202
5	0.13	1.50	1.50	6,909	7,284	7,744
5	0.00	3.75	0.33	8,960	9,079	8,678
5	0.00	1.90	0.33	8,390	8,718	8,619

Factors				Sum of areas of monomer fraction (AMF) (276 -308 nm) [mAU]		
pH	LiP [U per well]	HRP [U per well]	TVL [U per well]	Observed	Cubic model prediction	Reduced model prediction
5	0.00	1.90	0.33	7,475	8,718	8,619
5	0.00	1.90	0.33	8,731	8,718	8,619
5	0.00	1.90	0.03	9,146	8,848	8,643
5	0.00	0.05	0.33	7,906	8,787	8,560
5	0.00	1.90	0.33	8,623	8,718	8,619
5	0.00	1.90	0.33	8,364	8,718	8,619
5.5	0.13	0.00	0.75	8,313	7,069	7,804
6	0.00	2.61	0.00	10,516	9,072	8,406
6	0.00	2.61	0.00	9,837	9,072	8,406
6	0.10	3.69	0.37	7,940	7,995	8,255
6	0.13	1.50	1.50	6,284	6,646	7,637
6	0.13	3.00	1.50	8,122	7,384	7,955
6	0.00	0.80	0.15	7,775	8,244	7,902
6	0.00	3.00	0.15	8,200	9,131	8,517
6	0.00	0.80	0.50	7,790	7,976	7,939
6	0.00	3.00	0.50	9,622	8,887	8,515
6.68	0.00	1.90	0.33	5,294	5,926	5,751
7	0.21	0.00	0.00	2,247	2,661	2,722
7	0.21	3.42	0.75	4,418	4,988	4,719
7	0.07	0.00	0.28	1,808	1,789	2,782
7	0.14	6.00	0.00	4,330	4,900	5,929
7	0.00	0.00	0.75	2,456	2,404	2,992
7	0.00	6.00	0.50	4,864	6,109	5,810
7	0.21	3.42	0.75	4,716	4,988	4,719
7	0.21	0.00	0.00	3,227	2,661	2,722
7	0.00	0.00	6.00	5,871	5,818	5,785
7	0.50	0.00	6.00	5,745	5,960	6,089
7	0.25	3.00	3.00	6,033	5,391	5,073
7	0.50	6.00	6.00	5,799	5,715	5,770
7	0.00	6.00	0.00	8,283	6,616	5,841
7	0.50	6.00	0.00	6,606	6,486	6,145
7	0.50	0.00	3.00	4,748	4,681	4,492
7	0.00	6.00	6.00	5,544	5,627	5,466

Factors				Sum of areas of monomer fraction (AMF) (276 -308 nm) [mAU]		
pH	LiP [U per well]	HRP [U per well]	TVL [U per well]	Observed	Cubic model prediction	Reduced model prediction
Experiments conducted for verification						
3	0.39	3.48	4.28	8,073	12,314	6,867
3	0.39	3.48	4.28	7,415	12,314	6,867
3	0.39	3.48	4.28	7,542	12,314	6,867
3	0.39	0	4.28	8,091	9,605	7,059
3	0.39	0	4.28	8,824	9,605	7,059
3	0.39	0	4.28	8,685	9,605	7,059
3	0.37	0	3.88	9,314	9,702	7,062
3	0.37	0	3.88	8,911	9,702	7,062
3	0.37	0	3.88	9,017	9,702	7,062
3	0.5	0	6	7,217	6,280	7,056
3	0.5	0	6	8,442	6,280	7,056
3	0.5	0	6	9,002	6,280	7,056
5.62	0	0	6	8,369	8,776	8,610
5.62	0	0	6	8,441	8,776	8,610
5.62	0	0	6	7,785	8,776	8,610
5.71	0	6	0	9,648	9,418	9,530
5.71	0	6	0	9,107	9,418	9,530
5.71	0	6	0	9,853	9,418	9,530

Table A. 20 ANOVA results of the cubic model fitted to the results of the experiment testing the influence of pH and different enzyme mixtures on the AMF.

Source	Sum of Squares	df	Mean Square	F value	*p*-value
Model	$1.896\ 10^{8}$	34	$5.578\ 10^{6}$	6.13	< 0.0001
A-LiP	$7.469\ 10^{5}$	1	$7.469\ 10^{5}$	0.82	0.3718
B-HRP	$1.093\ 10^{5}$	1	$1.093\ 10^{5}$	0.12	0.7313
C-Laccase	$4.514\ 10^{4}$	1	$4.514\ 10^{4}$	0.050	0.8252
D-pH	$2.772\ 10^{5}$	1	$2.772\ 10^{5}$	0.30	0.5849
AB	$8.353\ 10^{5}$	1	$8.353\ 10^{5}$	0.92	0.3453
AC	$8.590\ 10^{4}$	1	$8.590\ 10^{4}$	0.094	0.7607
AD	$1.221\ 10^{6}$	1	$1.221\ 10^{6}$	1.34	0.2555
BC	$3.792\ 10^{4}$	1	$3.792\ 10^{4}$	0.042	0.8396
BD	$4.447\ 10^{6}$	1	$4.447\ 10^{6}$	4.88	0.0344
CD	$2.236\ 10^{6}$	1	$2.236\ 10^{6}$	2.46	0.1269
A^2	$1.785\ 10^{4}$	1	$1.785\ 10^{4}$	0.020	0.8895
B^2	$2.621\ 10^{6}$	1	$2.621\ 10^{6}$	2.88	0.0994
C^2	$1.040\ 10^{6}$	1	$1.040\ 10^{6}$	1.14	0.2933
D^2	$3.857\ 10^{5}$	1	$3.857\ 10^{5}$	0.42	0.5198
ABC	$5.482\ 10^{5}$	1	$5.482\ 10^{5}$	0.60	0.4435
ABD	4,329	1	4,329	$4.755\ 10^{-3}$	0.9455
ACD	$1.005\ 10^{5}$	1	$1.005\ 10^{5}$	0.11	0.7419
BCD	$7.871\ 10^{6}$	1	$7.871\ 10^{6}$	8.65	0.0060
A^2B	6,522	1	6,522	$7.164\ 10^{-3}$	0.9331
A^2C	1,762	1	1,762	$1.935\ 10^{-3}$	0.9652
A^2D	$2.024\ 10^{6}$	1	$2.024\ 10^{6}$	2.22	0.1458
AB^2	$1.187\ 10^{6}$	1	$1.187\ 10^{6}$	1.30	0.2620
AC^2	$8.392\ 10^{4}$	1	$8.392\ 10^{4}$	0.092	0.7634
AD^2	$4.634\ 10^{6}$	1	$4.634\ 10^{6}$	5.09	0.0310
B^2C	$2.878\ 10^{4}$	1	$2.878\ 10^{4}$	0.032	0.8600
B^2D	$1.741\ 10^{4}$	1	$1.741\ 10^{4}$	0.019	0.8909
BC^2	$2.073\ 10^{5}$	1	$2.073\ 10^{5}$	0.23	0.6365
BD^2	$2.243\ 10^{6}$	1	$2.243\ 10^{6}$	2.46	0.1263
C^2D	$2.448\ 10^{6}$	1	$2.448\ 10^{6}$	2.69	0.1108
CD^2	$3.817\ 10^{6}$	1	$3.817\ 10^{6}$	4.19	0.0489
A^3	$1.644\ 10^{6}$	1	$1.644\ 10^{6}$	1.81	0.1885
B^3	$6.171\ 10^{5}$	1	$6.171\ 10^{5}$	0.68	0.4164
C^3	$3.021\ 10^{5}$	1	$3.021\ 10^{5}$	0.33	0.5686
D^3	$9.274\ 10^{6}$	1	$9.274\ 10^{6}$	10.19	0.0032
Residual	$2.913\ 10^{7}$	32	$9.104\ 10^{5}$		
Lack of Fit	$2.708\ 10^{7}$	24	$1.128\ 10^{6}$	4.40	0.0179
Pure Error	$2.052\ 10^{6}$	8	$2.565\ 10^{5}$		

Table A. 21 ANOVA results of the reduced model fitted to the results of the experiment testing the influence of pH and different enzyme mixtures on the AMF.

Source	Sum of Squares	df	Mean Square	F value	*p*-value
Model	$1.672\ 10^{8}$	13	$1.286\ 10^{7}$	13.21	< 0.0001
A-LiP	$1.358\ 10^{7}$	1	$1.358\ 10^{7}$	13.95	0.0005
B-HRP	$2.545\ 10^{5}$	1	$2.545\ 10^{5}$	0.26	0.6113
C-Laccase	$4.038\ 10^{5}$	1	$4.038\ 10^{5}$	0.41	0.5223
D-pH	$9.640\ 10^{6}$	1	$9.640\ 10^{6}$	9.90	0.0027
AD	$1.109\ 10^{4}$	1	$1.109\ 10^{4}$	0.011	0.9154
BC	58.29	1	58.29	$5.988\ 10^{-5}$	0.9939
BD	$9.051\ 10^{6}$	1	$9.051\ 10^{6}$	9.30	0.0036
CD	$5.203\ 10^{4}$	1	$5.203\ 10^{4}$	0.053	0.8181
D^2	$7.374\ 10^{6}$	1	$7.374\ 10^{6}$	7.57	0.0081
BCD	$1.461\ 10^{7}$	1	$1.461\ 10^{7}$	15.00	0.0003
AD^2	$1.138\ 10^{7}$	1	$1.138\ 10^{7}$	11.69	0.0012
CD^2	$4.846\ 10^{6}$	1	$4.846\ 10^{6}$	4.98	0.0299
D^3	$1.575\ 10^{7}$	1	$1.575\ 10^{7}$	16.18	0.0002
Residual	$5.159\ 10^{7}$	53	$9.735\ 10^{5}$		
Lack of Fit	$4.954\ 10^{7}$	45	$1.101\ 10^{6}$	4.29	0.0174
Pure Error	$2.052\ 10^{6}$	8	$2.565\ 10^{5}$		

Table A. 22 Coefficients of the final equations in terms of the actual factors for the cubic and the reduced model

	Coefficient estimate	
Factor	**Cubic model**	**Reduced model**
Intercept	23,895	36,839
A-LiP	35,566	38,778
B-HRP	484	-1,042
C-Laccase	4,790	-418
D-pH	-16,814	-23,018
AB	2,290	-
AC	548	-490
AD	-20,963	-17,284
BC	307	213
BD	-548	250
CD	-1,730	160
A^2	71,128	-
B^2	228	-
C^2	-124	-
D^2	4,746	5,555
ABC	129	-
ABD	14	-
ACD	-89	-
BCD	-41	-49
A^2B	275	-
A^2C	239	-
A^2D	7,495	-
AB^2	-553	-
AC^2	-124	-
AD^2	1,832	1,732
B^2C	-5	-
B^2D	5	-
BC^2	-16	-
BD^2	73	-
C^2D	85	-
CD^2	126	-
A^3	-143,611	-
B^3	-33	-
C^3	-34	-
D^3	-396	-426

Table A. 23 Experimental setups conducted with LME immobilized on fsNP in 30 % (v/v) DMSO and 70 % PB buffer of the corresponding pH at an initial OL concentration of 0.263 g L^{-1} lasting 20 h.

pH	TVL-fsNP U L^{-1}	HRP-fsNP U L^{-1}	AMF (276 -308 nm) [mAU]
Central composite design			
5.00	0.33	1.90	9,745
5.00	0.62	1.90	9,400
5.00	0.33	3.75	9,135
4.00	0.50	0.80	9,185
5.00	0.33	1.90	10,582
6.00	0.15	0.80	10,109
6.00	0.15	3.00	9,717
6.00	0.50	0.80	9,262
5.00	0.33	1.90	10,518
4.00	0.15	3.00	9,816
4.00	0.15	0.80	10,288
3.32	0.33	1.90	10,073
5.00	0.33	1.90	10,282
5.00	0.03	1.90	9,663
4.00	0.50	3.00	9,064
5.00	0.33	0.05	9,885
6.68	0.33	1.90	7,071
5.00	0.33	1.90	9,625
6.00	0.50	3.00	9,833
5.00	0.33	1.90	9,959
Control experiments			
4.00	0.00	0.00	5,534
5.00	0.00	0.00	5,497
6.00	0.00	0.00	5,426
6.68	0.00	0.00	4,200

A3. Supplementary results for lignin treatments

Table A. 24 Yields of major low molecular weight compounds in wt‰ of initially applied lignin after different treatment steps of sequential treatments (± standard deviation, n=3). For details of different treatments see paragraph 7.3.1.

Lignin	Treatment	Compound	Yield (wt‰)		
			After 1st step	After 2nd step	Total
OL	Control	Vanillic acid		0.90±0.06	0.90±0.06
		Syringic acid	0.15±0.01	2.33±0.09	2.47±0.09
		Vanillin	0.47±0.06	1.56±0.15	2.03±0.16
		Syringaldehyde	1.40±0.02	5.73±0.51	7.13±0.54
		Acetovanillone		0.47±0.03	0.47±0.03
		Acetosyringone		0.17±0.01	0.17±0.01
	TVL-MP HBT	Vanillic acid		0.90±0.06	0.90±0.06
		Syringic acid		2.31±0.09	2.31±0.09
		Vanillin		1.64±0.15	1.64±0.15
		Syringaldehyde		5.78±0.51	5.78±0.51
		Acetovanillone		0.44±0.03	0.44±0.03
		Acetosyringone		0.17±0.01	0.17±0.01
		DMBQ	1.84±0.06		1.84±0.06
	TVL-MP TEMPO	Vanillic acid		1.06±0.06	1.06±0.06
		Syringic acid		2.76±0.09	2.76±0.09
		Vanillin	0.07±0.00	2.07±0.15	2.15±0.22
		Syringaldehyde	0.18±0.00	7.20±0.51	7.38±0.61
		Acetovanillone		0.47±0.03	0.47±0.03
		Acetosyringone		0.20±0.01	0.20±0.01
		DMBQ	1.00±0.19		1.00±0.19
	Control (30% (v/v) MeOH)	Vanillic acid		0.69±0.02	0.69±0.02
		Syringic acid	0.41±0.01	1.73±0.05	2.13±0.03
		Vanillin	1.29±0.03	0.67±0.00	1.96±0.03
		Syringaldehyde	4.64±0.10	2.55±0.06	7.19±0.11
		Acetosyringone		0.07±0.00	0.07±0.00
	TVL-MP (30% (v/v) MeOH)	Vanillic acid		0.56±0.02	0.56±0.02
		Syringic acid		2.11±0.05	2.11±0.05
		Vanillin	0.03±0.00	0.84±0.01	0.88±0.01
		Syringaldehyde	0.08±0.00	3.08±0.05	3.16±0.05
		DMBQ	10.99±0.18		10.99±0.18
W-SL	Control	Vanillic acid	0.19±0.01	1.05±0.04	1.24±0.04
		Syringic acid	0.07±0.00	1.45±0.05	1.52±0.05
		Vanillin	0.29±0.00	0.75±0.03	1.04±0.03
		Syringaldehyde	0.09±0.00	1.13±0.02	1.22±0.02
		Acetovanillone		0.26±0.01	0.26±0.01
		Acetosyringone	0.10±0.00	0.66±0.01	0.77±0.01
		4-hydroxybenzaldehyde	0.02±0.00	0.15±0.01	0.17±0.01
		Ferulic acid	0.09±0.01		0.09±0.01
		Guaiacol		0.61±0.02	0.61±0.02
		Hydroxybenzoic acid		0.13±0.01	0.13±0.01
	TVL-MP HBT	Vanillic acid		1.00±0.08	1.00±0.08
		Syringic acid		1.48±0.11	1.48±0.11
		Vanillin		1.02±0.10	1.02±0.10
		Syringaldehyde		1.37±0.11	1.37±0.11
		Acetovanillone		0.14±0.01	0.14±0.01
		Acetosyringone		0.64±0.04	0.64±0.04
		4-hydroxybenzaldehyde		0.16±0.01	0.16±0.01
		Guaiacol		0.24±0.01	0.24±0.01
		Hydroxybenzoic acid		0.14±0.01	0.14±0.01
		Hydroxyacetophenone	0.08±0.00		0.08±0.00
		DMBQ	2.41±0.04		2.41±0.04

Lignin	Treatment	Compound	Yield (wt‰) After 1st step	Yield (wt‰) After 2nd step	Yield (wt‰) Total
	TVL-MP TEMPO	Vanillic acid		1.39±0.06	1.39±0.06
		Syringic acid		1.84±0.09	1.84±0.09
		Vanillin	0.07±0.03	1.44±0.09	1.52±0.09
		Syringaldehyde		1.58±0.12	1.58±0.12
		Acetovanillone		0.14±0.01	0.14±0.01
		Acetosyringone		0.76±0.03	0.76±0.03
		4-hydroxybenzaldehyde	0.05±0.00	0.28±0.01	0.33±0.01
		Guaiacol		0.16±0.01	0.16±0.01
		Hydroxybenzoic acid		0.21±0.01	0.21±0.01
		Hydroxyacetophenone	0.09±0.00		0.09±0.00
		DMBQ	3.08±0.08		3.08±0.08
	Control (30% (v/v) MeOH)	Vanillic acid	0.16±0.01	1.03±0.10	1.19±0.10
		Syringic acid	0.06±0.01	1.38±0.09	1.45±0.09
		Vanillin	0.44±0.00	0.78±0.06	1.21±0.06
		Syringaldehyde	0.14±0.01	1.06±0.03	1.20±0.03
		Acetovanillone		0.14±0.01	0.14±0.01
		Acetosyringone	0.14±0.00	0.66±0.02	0.80±0.02
		4-hydroxybenzaldehyde	0.04±0.00	0.10±0.02	0.15±0.02
		Ferulic acid	0.16±0.01		0.16±0.01
		Guaiacol		0.39±0.05	0.39±0.05
		Hydroxybenzoic acid		0.11±0.02	0.11±0.02
	TVL-MP (30% (v/v) MeOH)	Vanillic acid		1.05±0.04	1.05±0.04
		Syringic acid		1.52±0.06	1.52±0.06
		Vanillin		0.84±0.06	0.84±0.06
		Syringaldehyde		1.05±0.04	1.05±0.04
		Acetovanillone		0.12±0.01	0.12±0.01
		Acetosyringone		0.64±0.02	0.64±0.02
		4-hydroxybenzaldehyde	0.09±0.00	0.11±0.01	0.20±0.01
		Hydroxybenzoic acid		0.13±0.00	0.13±0.00
		DMBQ	3.40±0.01		3.40±0.01
S-SL	Control	Vanillic acid	0.38±0.09	0.77±0.04	1.15±0.10
		Syringic acid	0.17±0.03	1.01±0.05	1.18±0.06
		Vanillin	0.47±0.10	0.56±0.03	1.03±0.10
		Syringaldehyde	0.30±0.05	0.60±0.03	0.90±0.05
		Acetovanillone	0.11±0.02	0.12±0.02	0.23±0.03
		Acetosyringone	0.90±0.15	0.31±0.03	1.22±0.15
		4-hydroxybenzaldehyde	0.04±0.01	0.12±0.02	0.16±0.02
		Coumaric acid	1.04±0.18		1.04±0.18
		Ferulic acid	0.39±0.06		0.39±0.06
		Guaiacol		0.40±0.04	0.40±0.04
		Hydroxybenzoic acid		0.14±0.00	0.14±0.00
		Hydroxyacetophenone	0.07±0.01	0.06±0.00	0.12±0.01
	TVL-MP HBT	Vanillic acid		0.69±0.07	0.69±0.07
		Syringic acid		1.03±0.12	1.03±0.12
		Vanillin		0.71±0.03	0.71±0.03
		Syringaldehyde		0.82±0.04	0.82±0.04
		Acetovanillone		0.10±0.00	0.10±0.00
		Acetosyringone		0.32±0.01	0.32±0.01
		4-hydroxybenzaldehyde		0.14±0.03	0.14±0.03
		Guaiacol		0.18±0.02	0.18±0.02
		Hydroxybenzoic acid	0.32±0.01	0.19±0.01	0.51±0.01
		Hydroxyacetophenone	0.17±0.00	0.05±0.01	0.22±0.01
		DMBQ	1.95±0.03		1.95±0.03

Lignin	Treatment	Compound	Yield (wt‰)		
			After 1st step	After 2nd step	Total
	TVL-MP TEMPO	Vanillic acid		0.95±0.01	0.95±0.01
		Syringic acid		1.21±0.01	1.21±0.01
		Vanillin	0.11±0.10	0.88±0.07	0.99±0.12
		Syringaldehyde		0.84±0.03	0.84±0.03
		Acetovanillone		0.11±0.01	0.11±0.01
		Acetosyringone		0.36±0.01	0.36±0.01
		4-hydroxybenzaldehyde	0.16±0.03	0.24±0.03	0.40±0.04
		Guaiacol		0.15±0.03	0.15±0.03
		Hydroxybenzoic acid	0.04±0.08	0.25±0.01	0.30±0.08
		Hydroxyacetophenone	0.20±0.01	0.06±0.01	0.25±0.01
		DMBQ	2.55±0.06		2.55±0.06
	Control (30% (v/v) MeOH)	Vanillic acid	0.17±0.00	0.91±0.03	1.07±0.03
		Syringic acid	0.17±0.00	1.16±0.08	1.32±0.08
		Vanillin	0.76±0.02	0.70±0.02	1.45±0.03
		Syringaldehyde	0.39±0.00	0.74±0.03	1.13±0.03
		Acetovanillone	0.12±0.00	0.14±0.01	0.26±0.01
		Acetosyringone	1.12±0.01	0.31±0.02	1.44±0.02
		4-hydroxybenzaldehyde	0.13±0.00	0.15±0.01	0.28±0.01
		Coumaric acid	1.36±0.00		1.36±0.00
		Ferulic acid	0.56±0.01		0.56±0.01
		Guaiacol		0.48±0.05	0.48±0.05
		Hydroxybenzoic acid		0.16±0.01	0.16±0.01
	TVL-MP (30% (v/v) MeOH)	Vanillic acid		1.02±0.06	1.02±0.06
		Syringic acid		1.27±0.09	1.27±0.09
		Vanillin		0.77±0.05	0.77±0.05
		Syringaldehyde		0.88±0.05	0.88±0.05
		Acetovanillone		0.13±0.00	0.13±0.00
		Acetosyringone		0.42±0.01	0.42±0.01
		4-hydroxybenzaldehyde	0.31±0.00	0.24±0.01	0.55±0.01
		Hydroxybenzoic acid		0.25±0.02	0.25±0.02
		DMBQ	3.06±0.01		3.06±0.01
SW-SL	Control	Vanillic acid	0.11±0.00	0.62±0.03	0.73±0.03
		Vanillin	0.24±0.00	0.54±0.02	0.78±0.02
		Acetovanillone	0.24±0.01	0.56±0.00	0.80±0.01
		4-hydroxybenzaldehyde		0.04±0.00	0.04±0.00
		Guaiacol		0.46±0.01	0.46±0.01
	TVL-MP HBT	Vanillic acid		0.96±0.08	0.96±0.08
		Vanillin	0.14±0.00	0.93±0.05	1.06±0.05
		Acetovanillone		0.26±0.01	0.26±0.01
		4-hydroxybenzaldehyde		0.08±0.00	0.08±0.00
	TVL-MP TEMPO	Vanillic acid		0.77±0.02	0.77±0.02
		Vanillin		0.79±0.03	0.79±0.03
		Acetovanillone		0.53±0.01	0.53±0.01
		4-hydroxybenzaldehyde		0.08±0.00	0.08±0.00
		Guaiacol		0.25±0.01	0.25±0.01
	Control (30% (v/v) MeOH)	Vanillic acid	0.06±0.00	0.25±0.02	0.31±0.02
		Vanillin	0.26±0.01	0.23±0.03	0.49±0.03
		Acetovanillone	0.28±0.02	0.13±0.02	0.40±0.03
		4-hydroxybenzaldehyde		0.02±0.01	0.02±0.01
		Guaiacol		0.08±0.00	0.08±0.00
	TVL-MP (30% (v/v) MeOH)	Vanillic acid		0.33±0.08	0.33±0.08
		Vanillin	0.32±0.01	0.30±0.07	0.62±0.07
		Acetovanillone	0.15±0.00	0.10±0.02	0.25±0.02
		4-hydroxybenzaldehyde	0.04±0.00	0.02±0.01	0.06±0.01
		Guaiacol		0.03±0.00	0.03±0.00

Lignin	Treatment	Compound	Yield (wt‰)		
			After 1st step	After 2nd step	Total
W-SE	Control	Vanillic acid	0.19±0.01	1.03±0.03	1.21±0.03
		Syringic acid	0.11±0.00	1.29±0.04	1.39±0.04
		Vanillin	0.10±0.00	1.19±0.02	1.29±0.02
		Syringaldehyde	0.25±0.04	1.20±0.04	1.45±0.05
		Acetovanillone	0.06±0.02	0.17±0.01	0.23±0.02
		Acetosyringone		0.38±0.02	0.38±0.02
		4-hydroxybenzaldehyde		0.09±0.01	0.09±0.01
		Coumaric acid	3.10±0.03		3.10±0.03
		Ferulic acid	4.00±0.07		4.00±0.07
		Hydroxybenzoic acid		0.12±0.00	0.12±0.00
	TVL-MP HBT	Vanillic acid		0.95±0.08	0.95±0.08
		Syringic acid		1.43±0.13	1.43±0.13
		Vanillin	0.25±0.00	1.37±0.14	1.62±0.14
		Syringaldehyde		1.30±0.14	1.30±0.14
		Acetovanillone		0.13±0.01	0.13±0.01
		Acetosyringone		0.31±0.01	0.31±0.01
		4-hydroxybenzaldehyde	0.16±0.00	0.11±0.01	0.27±0.01
		Hydroxybenzoic acid		0.15±0.01	0.15±0.01
		DMBQ	0.97±0.01		0.97±0.01
	TVL-MP TEMPO	Vanillic acid		1.35±0.05	1.35±0.05
		Syringic acid		1.91±0.07	1.91±0.07
		Vanillin		1.63±0.06	1.63±0.06
		Syringaldehyde		1.48±0.05	1.48±0.05
		Acetovanillone		0.14±0.00	0.14±0.00
		Acetosyringone		0.33±0.03	0.33±0.03
		4-hydroxybenzaldehyde		0.10±0.01	0.10±0.01
		Hydroxybenzoic acid		0.22±0.06	0.22±0.06
		DMBQ	1.43±0.05		1.43±0.05
	Control (30% (v/v) MeOH)	Vanillic acid		0.94±0.01	0.94±0.01
		Syringic acid	0.13±0.01	1.16±0.04	1.28±0.04
		Vanillin	0.49±0.01	1.03±0.01	1.52±0.02
		Syringaldehyde	0.32±0.01	1.01±0.01	1.33±0.02
		Acetovanillone		0.13±0.00	0.13±0.00
		Acetosyringone		0.32±0.01	0.32±0.01
		4-hydroxybenzaldehyde	0.06±0.00	0.06±0.01	0.12±0.01
		Coumaric acid	4.10±0.10		4.10±0.10
		Ferulic acid	5.66±0.14		5.66±0.14
		Hydroxybenzoic acid		0.11±0.00	0.11±0.00
	TVL-MP (30% (v/v) MeOH)	Vanillic acid		1.17±0.13	1.17±0.13
		Syringic acid		1.12±0.11	1.12±0.11
		Vanillin	0.41±0.01	1.35±0.16	1.76±0.16
		Syringaldehyde		1.27±0.20	1.27±0.20
		Acetovanillone		0.10±0.00	0.10±0.00
		Acetosyringone		0.19±0.01	0.19±0.01
		4-hydroxybenzaldehyde	0.49±0.00	0.22±0.02	0.71±0.02
		Coumaric acid	0.37±0.02		0.37±0.02
		Guaiacol		0.11±0.02	0.11±0.02
		Hydroxybenzoic acid		0.21±0.02	0.21±0.02
		DMBQ	1.15±0.01		1.15±0.01

A4. Experimental matrices, response surface models, and results for sequential lignin treatments

Table A. 25 Summary of the coefficients of the final equations in terms of actual factors of the different response surface reduced quadratic models. The factors are A- enzymatic activity (U L^{-1}), B- HBT concentration (mM), C- enzymatic reaction time (h), D- pH during enzymatic reaction, E- formic acid/formate reaction time (h), and F- HCOONa concentration (g L^{-1}). Yields and solubilities are given in wt% of lignin initially added to the reaction. Molecular weights are given in Da (adapted from Gasser et al. 2017).

	Response						
	Solubility after enz. =	**√(Mw of insoluble material after enz.) =**	**EtAc solubility after FA =**	**Monomer yield after FA=**	**Log(Mw after FA treatment) =**	**Mw of EtAc extract after FA =**	**(Total lignin solubility)$^{2.19}$ =**
	+9.65244	+100.00754	+0.77737	-0.31232	+4.13639	+0.018778	-2506.05245
A	+0.79651	+2.17860	-0.012634	+0.022040	-0.030939		+74.24300
B	+4.62006	-1.17494		+0.011212	-0.047695	+4.59129 10^{-4}	+515.72536
C	-0.42106	-3.57265		+0.014412	-8.57478 10^{-3}	+1.12677 10^{-4}	+4.45027
D	+0.74719	+5.54656	+0.25607	+0.077962	-0.015260	-3.24930 10^{-4}	+474.22353
E			+0.077642	+0.019748	+0.017261	-8.04278 10^{-5}	+27.72506
F			+1.45288	+0.012228	+0.016188	+2.50734 10^{-3}	+188.06947
AB							-3.82516
AC					+4.53465 10^{-4}		
AD				-3.51278 10^{-3}	+6.47272 10^{-3}		
AE			-4.47880 10^{-3}	-2.82821 10^{-4}			+0.73591
AF					-2.08920 10^{-3}		
BC							
BD	-0.37866						-48.04809
BE				-2.99664 10^{-4}			
BF				+1.41070 10^{-3}			
CD		+0.78210		-1.22910 10^{-3}	+1.36969 10^{-3}		-6.63466
CE							
CF				-4.86266 10^{-4}			
DE						+6.48922 10^{-5}	-4.48213
DF			-0.14148				-24.02246
EF						-2.83116 10^{-5}	
A^2							
B^2	-0.20017				+4.34912 10^{-3}		-15.03521
C^2	+8.05835 10^{-3}			-6.91463 10^{-5}			+0.73458
D^2							
E^2				-1.70989 10^{-4}			
F^2					-2.32899 10^{-4}	-1.53939 10^{-4}	

Table A. 26 Experimental matrix and results used for fitting of the second-degree polynomial models (enz: enzymatic treatment; FA: formic acid/formate treatment (adapted from Gasser et al. 2017).

	Factor 1	Factor 2	Factor 3	Factor 4	Factor 5	Factor 6	Response 1	Response 2	Response 3	Response 4	Response 5	Response 6	Response 7
Id	Enz. activity	HBT conc.	Enz. reaction time	pH during enz.	FA reaction time	HCOONa conc.	Solubility after enz.	Mw of insoluble material after enz.	EtAc solubility after FA	Monomer yield after FA	Mw after FA treatment	Mw of EtAc extract after FA	Total lignin solubility
	U L^{-1}	mM	h		h	g L^{-1}	wt%	Da	wt%	wt%	Da	Da	wt%
1	15	1	4	5	42.1	5.5	27.1	21157	6.1	0.6	19475	994	33.2
2	10.3	10	48	8	48	8.4	15.3	80646	6.2	0.73	56709	542	21.5
3	8.7	5.05	26.9	5	21.2	1	26.8	24688	1.7	0.61	18632	1460	28.5
4	1.5	10	4	5	4	1	22.3	17491	2.5	0.3	10624	1542	24.8
5	6.4	5.32	4	8	15.9	4.6	26.6	22509	5	0.6	15334	1032	31.6
6	1.5	8.83	25.6	8	4	10	9.6	34936	4.8	0.68	17844	1341	14.4
7	15	1	48	5	4	5.3	26.2	31273	5.1	0.36	16875	940	31.2
8	5.8	1.45	4	5	4	10	17.4	18046	9.7	0.4	11578	1260	27.1
9	1.5	1	48	8	4	1	18.9		3.9	0.42	12746	1535	22.8
10	2.2	6.99	48	5.5	6.9	4.9	22.7	20164	7.4	0.48	14102	862	30.1
11	8.7	5.05	26.9	5	21.2	1	25.4	24861	3.3	0.61	23567	1380	28.7
12	10.5	10	33.7	7.5	4	2.5	15.2	64473	2.8	0.5	36615	1015	18
13	2.3	9.1	26.9	5	47.1	8.2	19.9	20074	12	0.83	22039	848	31.8
14	1.5	1.54	48	5	48	7.9	19.2	20966	10.3	0.79	18825	968	29.5
15	15	1.9	30.8	6.5	22.3	6.3	26.7	42817	5	0.57	32025	704	31.7
16	1.5	1	21.4	6.5	20.5	5		30584	6.2	0.58	22239	1483	
17	15	1	22.5	8	7.1	10	25.2	62377	5.7	0.42	36211	932	30.9

	Factor 1	Factor 2	Factor 3	Factor 4	Factor 5	Factor 6	Response 1	Response 2	Response 3	Response 4	Response 5	Response 6	Response 7
Id	**Enz. activity**	**HBT conc.**	**Enz. reaction time**	**pH during enz.**	**FA reaction time**	**HCOONa conc.**	**Solubility after enz.**	**Mw of insoluble material after enz**	**EtAc solubility after FA**	**Monomer yield after FA**	**Mw after FA treatment**	**Mw of EtAc extract after FA**	**Total lignin solubility**
	U L^{-1}	**mM**	**h**		**h**	**g L^{-1}**	**wt%**	**Da**	**wt%**	**wt%**	**Da**	**Da**	**wt%**
18	5.4	1.54	48	6.5	30	10	19.8	52022	7.1	0.63	41655	782	26.8
19	15	1	4	7	4	1	28.7	31759	2.8	0.33	18538	2288	31.5
20	15	7.57	9.3	5.5	4.8	5.5	22.3	22543	7.9	0.46	13633	1039	30.2
21	15	5.15	48	8	27.8	2.1	27.4	82949	3	0.6	64602	507	30.4
22	1.5	1	4	8	48	10	12.2	20729	10.3	0.98	28186	771	22.5
23	1.5	10	36.6	7.5	37.2	1	7.7	45418	5.2	0.86	28483	592	12.9
24	15	5	29.3	6	48	10	25.5	32554	9.1	0.67	17034	899	34.6
25	7.8	10	30.8	6.5	29.7	5.3	20.2	32207	7.4	0.85	31116	508	27.6
26	1.5	1	48	5	48	1	15.9	21225	5.1	0.86	18017	710	20.9
27	13.4	10	48	5.5	48	1.4	29.1	30077	6	0.7	39469	561	35.1
28	1.5	1	21.4	6.5	20.5	5	7.1	32473	8.5	0.72	22874	862	15.6
29	15	10	48	5	11.7	10	28.6	30560	8.8	0.7	20078	672	37.4
30	4.1	5.77	4	6	48	1.7	20.2	20273	7.5	0.66	24464	759	27.8
31	9.6	10	4	6.5	29.5	9.6	21	24180	8.4	0.78	24321	828	29.5
32	6.4	5.32	4	8	15.9	4.6	21.9	28502	6.4	0.66	17226	872	28.3
33	15	9.96	39	7.5	15.9	10	18.6	62839	8.3	0.62	44359	771	27
34	9.5	1	28.4	7.5	48	3.3	19.7	61067	5.2	0.74	53806	686	25
35	13.3	10	4	6.5	19.4	1	26.8	25814	3	0.53	21679	897	29.8
36	15	10	4	8	48	1	27.1	33509	2.5	0.61	35537	570	29.6

Table A. 27 ANOVA for response surface reduced quadratic model for lignin solubility in aqueous solution (pH 2) after enzymatic treatment (adapted from Gasser et al. 2017).

Source	Sum of Squares	df	Mean Square	F Value	*p*-value Prob > F
Model	959.99	7	137.14	14.38	< 0.0001
A-TVL activity	646.22	1	646.22	67.76	< 0.0001
B-HBT concentration	0.9	1	0.9	0.095	0.7605
C-enz. reaction time	0.043	1	0.043	$4.49\ 10^{-3}$	0.9471
D-pH	87.3	1	87.3	9.15	0.0054
BD	97.26	1	97.26	10.2	0.0036
B^2	91.79	1	91.79	9.63	0.0045
C^2	103.92	1	103.92	10.9	0.0027
Residual	257.49	27	9.54		
Lack of Fit	245.94	25	9.84	1.7	0.4366
Pure Error	11.55	2	5.78		
Cor Total	1217.48	34			

Table A. 28 ANOVA for response surface reduced quadratic model for MW of insoluble material after enzymatic reaction (adapted from Gasser et al. 2017).

Source	Sum of Squares	df	Mean Square	F Value	*p*-value Prob > F
Model	59952.04	5	11990.41	87.53	< 0.0001
A-TVL activity	4800.18	1	4800.18	35.04	< 0.0001
B-HBT concentration	654.27	1	654.27	4.78	0.0371
C-enz. reaction time	22535.67	1	22535.67	164.51	< 0.0001
D-pH	30692.41	1	30692.41	224.05	< 0.0001
CD	9122.57	1	9122.57	66.59	< 0.0001
Residual	3972.64	29	136.99		
Lack of Fit	3781.72	26	145.45	2.29	0.272
Pure Error	190.92	3	63.64		
Cor Total	63924.68	34			

Table A. 29 ANOVA for response surface reduced quadratic model for EtAc solubility after formic acid/formate treatment (adapted from Gasser et al. 2017).

Source	Sum of Squares	df	Mean Square	F Value	*p*-value Prob > F
Model	189.2	6	31.53	21.35	< 0.0001
A-TVL activity	17.53	1	17.53	11.87	0.0018
D-pH	13.35	1	13.35	9.04	0.0054
E-Fa treatment time	17.16	1	17.16	11.62	0.0019
F-Sodium formate conc.	122.11	1	122.11	82.66	< 0.0001
AE	6.73	1	6.73	4.56	0.0414
DF	12.92	1	12.92	8.75	0.0061
Residual	42.84	29	1.48		
Lack of Fit	38.17	26	1.47	0.94	0.6172
Pure Error	4.67	3	1.56		
Cor Total	232.04	35			

Table A. 30 ANOVA for response surface reduced quadratic model for monomer yield after formic acid/formate treatment (adapted from Gasser et al. 2017).

Source	Sum of Squares	df	Mean Square	F Value	*p*-value Prob > F
Model	0.87	14	0.062	36.30	< 0.0001
A-TVL activity	0.062	1	0.062	36.25	< 0.0001
B-HBT concentration	0.057	1	0.057	33.13	< 0.0001
C-enz. reaction time	$2.216\ 10^{-4}$	1	$2.216\ 10^{-4}$	0.13	0.7227
D-pH	0.014	1	0.014	8.01	0.0100
E-Fa treatment time	0.45	1	0.45	265.18	< 0.0001
F-Sodium formate conc.	0.022	1	0.022	12.92	0.0017
AD	0.017	1	0.017	9.90	0.0049
AE	0.023	1	0.023	13.16	0.0016
BE	0.013	1	0.013	7.64	0.0116
BF	0.012	1	0.012	7.02	0.0150
CD	0.021	1	0.021	12.33	0.0021
CF	0.027	1	0.027	15.59	0.0007
C^2	$7.497\ 10^{-3}$	1	$7.497\ 10^{-3}$	4.38	0.0487
E^2	0.041	1	0.041	23.96	< 0.0001
Residual	0.036	21	$1.713\ 10^{-3}$		
Lack of Fit	0.025	18	$1.376\ 10^{-3}$	0.37	0.9245
Pure Error	0.011	3	$3.732\ 10^{-3}$		
Cor Total	0.91	35			

Table A. 31 ANOVA for response surface reduced quadratic model for Mw after formic acid/formate treatment (adapted from Gasser et al. 2017).

Source	Sum of Squares	df	Mean Square	F Value	*p*-value Prob > F
Model	1.2	12	0.1	13.84	< 0.0001
A-TVL activity	0.14	1	0.14	18.88	0.0002
B-HBT concentration	$1.02\ 10^{-5}$	1	$1.02\ 10^{-5}$	$1.42\ 10^{-3}$	0.9703
C-enz. reaction time	0.16	1	0.16	22.79	< 0.0001
D-pH	0.26	1	0.26	36.33	< 0.0001
E-Fa treatment time	0.26	1	0.26	35.51	< 0.0001
F-Sodium formate conc.	$4.38\ 10^{-4}$	1	$4.38\ 10^{-4}$	0.061	0.8073
AC	0.061	1	0.061	8.42	0.0081
AD	0.062	1	0.062	8.66	0.0073
AF	0.052	1	0.052	7.25	0.013
CD	0.029	1	0.029	4.05	0.0561
B^2	0.042	1	0.042	5.85	0.0239
E^2	0.077	1	0.077	10.73	0.0033
Residual	0.17	23	$7.20\ 10^{-3}$		
Lack of Fit	0.16	20	$7.95\ 10^{-3}$	3.64	0.1573
Pure Error	$6.56\ 10^{-3}$	3	$2.19\ 10^{-3}$		
Cor Total	1.36	35			

Table A. 32 ANOVA for response surface reduced quadratic model for Mw of EtAc soluble fraction after formic acid/formate treatment (adapted from Gasser et al. 2017).

Source	Sum of Squares	df	Mean Square	F Value	*p*-value Prob > F
Model	$9.34\ 10^{-4}$	8	$1.17\ 10^{-4}$	13.6	< 0.0001
B-HBT concentration	$1.02\ 10^{-4}$	1	$1.02\ 10^{-4}$	11.91	0.0019
C-enz. reaction time	$1.32\ 10^{-4}$	1	$1.32\ 10^{-4}$	15.38	0.0005
D-pH	$9.08\ 10^{-5}$	1	$9.08\ 10^{-5}$	10.58	0.0031
E-Fa treatment time	$3.53\ 10^{-4}$	1	$3.53\ 10^{-4}$	41.15	< 0.0001
F-Sodium formate conc.	$2.62\ 10^{-6}$	1	$2.62\ 10^{-6}$	0.31	0.5852
DE	$6.86\ 10^{-5}$	1	$6.86\ 10^{-5}$	7.99	0.0088
EF	$1.08\ 10^{-4}$	1	$1.08\ 10^{-4}$	12.6	0.0014
F^2	$6.14\ 10^{-5}$	1	$6.14\ 10^{-5}$	7.15	0.0126
Residual	$2.32\ 10^{-4}$	27	$8.59\ 10^{-6}$		
Lack of Fit	$1.95\ 10^{-4}$	24	$8.12\ 10^{-6}$	0.66	0.7632
Pure Error	$3.69\ 10^{-5}$	3	$1.23\ 10^{-5}$		
Cor Total	$1.17\ 10^{-3}$	35			

Table A. 33 ANOVA for response surface reduced quadratic model for overall lignin solubility, i.e., in aqueous solution (pH 2) after enzymatic treatment and EtAc solubility after formic acid/formate treatment (adapted from Gasser et al. 2017)

Source	Sum of Squares	df	Mean Square	F Value	*p*-value Prob > F
Model	$1.12\ 10^{7}$	14	$8.01\ 10^{5}$	28.21	< 0.0001
A-TVL activity	$5.00\ 10^{6}$	1	$5.00\ 10^{6}$	176.07	< 0.0001
B-HBT concentration	18790.01	1	18790.01	0.66	0.4255
C-enz. reaction time	2221.05	1	2221.05	0.078	0.7826
D-pH	$2.07\ 10^{6}$	1	$2.07\ 10^{6}$	73.08	< 0.0001
E-Fa treatment time	$2.06\ 10^{5}$	1	$2.06\ 10^{5}$	7.25	0.014
F-Sodium formate conc.	$4.24\ 10^{5}$	1	$4.24\ 10^{5}$	14.95	0.001
AB	$1.83\ 10^{5}$	1	$1.83\ 10^{5}$	6.45	0.0195
AE	$1.52\ 10^{5}$	1	$1.52\ 10^{5}$	5.35	0.0314
BD	$1.53\ 10^{6}$	1	$1.53\ 10^{6}$	53.74	< 0.0001
CD	$6.02\ 10^{5}$	1	$6.02\ 10^{5}$	21.2	0.0002
DE	$3.07\ 10^{5}$	1	$3.07\ 10^{5}$	10.81	0.0037
DF	$3.52\ 10^{5}$	1	$3.52\ 10^{5}$	12.38	0.0022
B^2	$4.91\ 10^{5}$	1	$4.91\ 10^{5}$	17.3	0.0005
C^2	$7.17\ 10^{5}$	1	$7.17\ 10^{5}$	25.25	< 0.0001
Residual	$5.68\ 10^{5}$	20	28385.96		
Lack of Fit	$4.83\ 10^{5}$	18	26830.89	0.63	0.7667
Pure Error	84763.19	2	42381.6		
Cor Total	$1.18\ 10^{7}$	34			

Table A. 34 Monomer yields obtained after formic acid/formate treatment. The Id given in the first column corresponds to the Id given in Table A. 26 to identify the different treatments. Values are given as wt‰ based on the applied lignin weight at the beginning of the first treatment step (adapted from Gasser et al. 2017).

Id	Vanillic acid	Syringic acid	Vanillin	Syring-aldehyde	Aceto-vanillone	Aceto-syringone	Hydroxy-benzoic acid
1	1.12	1.82	1.06	1.07	0.13	0.73	0.11
2	1.16	2.35	1.30	1.36	0.16	0.82	0.15
3	0.81	1.98	1.08	1.25	0.12	0.78	0.09
4	0.32	0.94	0.47	0.67	0.14	0.49	0.00
5	1.08	1.90	1.04	1.13	0.11	0.66	0.09
6	1.12	1.97	1.08	1.39	0.19	1.10	0.00
7	0.47	1.02	0.69	0.88	0.09	0.48	0.00
8	0.52	1.09	0.64	0.91	0.14	0.68	0.00
9	0.61	1.29	0.64	0.89	0.16	0.66	0.00
10	0.55	1.64	0.87	1.03	0.08	0.62	0.00
11	0.80	2.04	1.08	1.22	0.12	0.79	0.08
12	0.75	1.45	0.90	1.23	0.11	0.60	0.00
13	1.18	2.78	1.37	1.39	0.22	1.19	0.13
14	1.21	2.59	1.38	1.47	0.19	0.97	0.14
15	0.93	1.70	1.07	1.20	0.10	0.56	0.09
16	1.01	1.86	0.94	1.07	0.11	0.70	0.10
17	0.92	1.20	0.67	0.85	0.09	0.48	0.00
18	0.97	2.01	1.14	1.20	0.13	0.71	0.12
19	0.51	0.97	0.56	0.79	0.00	0.49	0.00
20	0.70	1.35	0.79	1.03	0.10	0.59	0.00
21	1.00	1.85	1.04	1.20	0.11	0.64	0.11
22	1.65	2.94	1.77	1.86	0.23	1.11	0.22
23	1.53	2.66	1.32	1.55	0.17	1.18	0.17
24	1.32	2.04	1.08	1.08	0.16	0.84	0.15
25	1.30	2.67	1.54	1.74	0.17	0.92	0.18
26	1.35	2.81	1.43	1.57	0.19	1.09	0.17
27	1.14	2.29	1.03	1.18	0.16	1.10	0.16
28	1.29	2.24	1.12	1.34	0.14	0.88	0.15
29	1.14	2.26	1.24	1.35	0.12	0.74	0.11
30	1.16	2.19	0.92	1.16	0.14	0.87	0.16
31	1.41	2.39	1.42	1.48	0.15	0.79	0.17
32	1.05	2.10	1.02	1.18	0.14	1.00	0.12
33	1.14	1.92	1.10	1.21	0.11	0.63	0.13
34	1.45	2.29	1.26	1.31	0.14	0.82	0.15
35	0.89	1.64	0.89	0.99	0.11	0.68	0.08
36	1.09	1.87	0.99	1.12	0.13	0.73	0.13

Table A. 35 Coefficients of the final equations in terms of actual factors and ANOVA results of the two factor interaction model fitted to the results of the experiment testing the influence of different sequential treatments on BCR.

Source	**Coefficients Ln(BCR) =**	**Sum of Squares**	**df**	**Mean Square**	**F value**	***p*-value**
Model		3.09	12	0.26	30.99	< 0.0001
Intercept	-5.91796					
A-TVL activity	+0.062541	0.27	1	0.27	32.98	< 0.0001
B-HBT concentration	-0.04405	0.43	1	0.43	51.87	< 0.0001
C-enz. reaction time	+0.022492	0.012	1	0.012	1.41	0.2479
D-pH	+1.94477	0.18	1	0.18	21.64	0.0001
E-Fa treatment time	$+3.61\ 10^{-3}$	$2.114\ 10^{-3}$	1	$2.114\ 10^{-3}$	0.25	0.6189
F-Sodium formate conc.	+0.018456	$4.973\ 10^{-3}$	1	$4.973\ 10^{-3}$	0.60	0.4472
AC	$-1.56\ 10^{-3}$	0.68	1	0.68	82.00	< 0.0001
BC	$+5.30\ 10^{-4}$	0.038	1	0.038	4.61	0.0426
EF	$-5.73\ 10^{-4}$	0.044	1	0.044	5.24	0.0317
A^2	$-2.34\ 10^{-3}$	0.066	1	0.066	7.91	0.0099
C^2	$-2.62\ 10^{-4}$	0.11	1	0.11	12.79	0.0016
D^2	-0.15425	0.68	1	0.68	81.93	< 0.0001
Residual		0.19	23	$8.313\ 10^{-3}$		
Lack of Fit		0.18	20	$9.209\ 10^{-3}$	3.94	0.1423
Pure Error		$7.014\ 10^{-3}$	3	$2.338\ 10^{-3}$		

References

Abächerli, A., Doppenberg, F. 1998. Method for preparing alkaline solutions containing aromatic polymers. World Intellectual Property Organization. WO1998042912 A1.

Achyuthan, K.E., Achyuthan, A.M., Adams, P.D., Dirk, S.M., Harper, J.C., Simmons, B.A., Singh, A.K. 2010. Supramolecular self-assembled chaos: Polyphenolic lignin's barrier to cost-effective lignocellulosic biofuels. Molecules, 15(12), 8641-8688.

Adler E (1977) Lignin chemistry – past, present and future. Wood Science and Technology, 11(3): 169–218.

Ahmad, M., Roberts, J.N., Hardiman, E.M., Singh, R., Eltis, L.D., Bugg, T.D.H. 2011. Identification of DypB from *Rhodococcus jostii* RHA1 as a lignin peroxidase. Biochemistry, 50(23), 5096-5107.

Aitken, M.D., Irvine, R.L. 1989. Stability testing of ligninase and Mn-peroxidase from *Phanerochaete chrysosporium*. Biotechnology and Bioengineering, 34(10), 1251-1260.

Akamatsu, Y., Shimada, M. 1994. Partial purification and characterization of glyoxylate oxidase from the brown-rot basidiomycete *Tyromyces palustris*. Phytochemistry, 37(3), 649-653.

Alam, M.Z., Mansor, M.F., Jalal, K.C.A. 2009. Optimization of decolorization of methylene blue by lignin peroxidase enzyme produced from sewage sludge with *Phanerocheate chrysosporium*. Journal of Hazardous Materials, 162(2–3), 708-715.

Alberton, D., Silva de Oliveira, L., Peralta, R.M., Barbosa-Tessmann, I.P. 2007. Production, purification, and characterization of a novel galactose oxidase from *Fusarium acuminatum*. Journal of Basic Microbiology, 47(3), 203-212.

Alibaba Group 2016. www.alibaba.com, accessed on 27.5.2016.

Alkhatib, R., Joha, S., Cheok, M., Roumy, V., Idziorek, T., Preudhomme, C., Quesnel, B., Sahpaz, S., Bailleul, F., Hennebelle, T. 2010. Activity of ladanein on leukemia cell lines and its occurrence in *Marrubium vulgare*. Planta medica, 76(1), 86-87.

Alriols, M.G., Tejado, A., Blanco, M., Mondragon, I., Labidi, J. 2009. Agricultural palm oil tree residues as raw material for cellulose, lignin and hemicelluloses production by ethylene glycol pulping process. Chemical Engineering Journal, 148(1), 106-114.

Altikatoglu, M., Basaran, Y., Arioz, C., Ogan, A., Kuzu, H. 2010. Glucose oxidase-dextran conjugates with enhanced stabilities against temperature and pH. Applied Biochemistry and Biotechnology, 160(8), 2187-2197.

Ammann, E.M., Gasser, C.A., Hommes, G., Corvini, P.F.X. 2014. Immobilization of defined laccase combinations for enhanced oxidation of phenolic contaminants. Applied Microbiology and Biotechnology, 98(3), 1397-1406.

Ando S, Kakimoto T, Itoh K, Arai I, Kiyoto K, Hanai S. (1988) Increased digestibility of cedar by pretreatment with peracetic acid and steam explosion. Biotechnology and Bioengeneering 31:802–804

Ardao, I., Magnin, D., Agathos, S.N. 2015. Bioinspired production of magnetic laccase-biotitania particles for the removal of endocrine disrupting chemicals. Biotechnology and Bioengineering, 112(10), 1986-1996.

Arends, I.W.C.E., Li, Y.-X., Sheldon, R.A. 2006. Stabilities and rates in the laccase/TEMPO-catalyzed oxidation of alcohols. Biocatalysis and Biotransformation, 24(6), 443-448.

Arnold, F.H. 1990. Engineering enzymes for non-aqueous solvents. Trends in Biotechnology, 8(0), 244-249.

Artolozaga, M.J., Kubátová, E., Volc, J., Kalisz, H.M. 1997. Pyranose 2-oxidase from *Phanerochaete chrysosporium* – further biochemical characterisation. Applied Microbiology and Biotechnology, 47(5), 508-514.

Auhorn, W.J., Niemela, K. 2007. Process chemicals for the production of chemical pulp. Professional Papermaking, 2, 10-20.

Aurilia, V., Parracino, A., Saviano, M., Rossi, M., D'Auria, S. 2007. The psychrophilic bacterium *Pseudoalteromonas halosplanktis* TAC125 possesses a gene coding for a cold-adapted feruloyl esterase activity that shares homology with esterase enzymes from γ-proteobacteria and yeast. Gene, 397(1–2), 51-57.

Ba, S., Arsenault, A., Hassani, T., Jones, J.P., Cabana, H. 2013. Laccase immobilization and insolubilization: from fundamentals to applications for the elimination of emerging contaminants in wastewater treatment. Critical Reviews in Biotechnology, 33(4), 404-418.

Backa, S., Gierer, J., Reitberger, T., Nilsson, T. 1992. Hydroxyl radical activity in brown-rot fungi studied by a new chemiluminescence method. Holzforschung, 46(1), 61-67.

Badamali, S.K., Luque, R., Clark, J.H., Breeden, S.W. 2009. Microwave assisted oxidation of a lignin model phenolic monomer using Co(salen)/SBA-15. Catalysis Communications, 10(6), 1010-1013.

Baldrian, P. 2004. Purification and characterization of laccase from the white-rot fungus *Daedalea quercina* and decolorization of synthetic dyes by the enzyme. Applied Microbiology and Biotechnology, 63(5), 560-563.

Baldrian, P. 2006. Fungal laccases – occurrence and properties. FEMS Microbiology Reviews, 30(2), 215-242.

Ball, A.S., Betts, W.B., McCarthy, A.J. 1989. Degradation of lignin-related compounds by actinomycetes. Applied and Environmental Microbiology, 55(6), 1642-1644.

Baminger, U., Subramaniam, S.S., Renganathan, V., Haltrich, D. 2001. Purification and characterization of cellobiose dehydrogenase from the plant pathogen *Sclerotium(Athelia) rolfsii*. Applied and Environmental Microbiology, 67(4), 1766-1774.

Barbosa, O., Ortiz, C., Berenguer-Murcia, A., Torres, R., Rodrigues, R.C., Fernandez-Lafuente, R. 2014. Glutaraldehyde in bio-catalysts design: a useful crosslinker and a versatile tool in enzyme immobilization. RSC Advances, 4(4), 1583-1600.

Battistuzzi, G., Di Rocco, G., Leonardi, A., Sola, M. 2003. 1H NMR of native and azide-inhibited laccase from *Rhus vernicifera*. Journal of Inorganic Biochemistry, 96(4), 503-506.

Baumgartner, J., Bertinetti, L., Widdrat, M., Hirt, A.M., Faivre, D. 2013. Formation of magnetite nanoparticles at low temperature: From superparamagnetic to stable single domain particles. PLoS ONE, 8(3), e57070.

Bayramoğlu, G., Kiralp, S., Yilmaz, M., Toppare, L., Arıca, M.Y. 2008. Covalent immobilization of chloroperoxidase onto magnetic beads: Catalytic properties and stability. Biochemical Engineering Journal, 38(2), 180-188.

Berlin, A., Balakshin, M., Gilkes, N., Kadla, J., Maximenko, V., Kubo, S., Saddler, J. 2006. Inhibition of cellulase, xylanase and β-glucosidase activities by softwood lignin preparations. Journal of Biotechnology, 125(2), 198-209.

Berlin, A., Gilkes, N., Kilburn, D., Bura, R., Markov, A., Skomarovsky, A., Okunev, O., Gusakov, A., Maximenko, V., Gregg, D., Sinitsyn, A., Saddler, J. 2005a. Evaluation of novel fungal cellulase preparations for ability to hydrolyze softwood substrates – evidence for the role of accessory enzymes. Enzyme and Microbial Technology, 37(2), 175-184.

Berlin, A., Gilkes, N., Kurabi, A., Bura, R., Tu, M., Kilburn, D., Saddler, J. 2005b. Weak lignin-binding enzymes. Applied Biochemistry and Biotechnology, 121-124, 163-170.

Bertrand, T., Jolivalt, C., Briozzo, P., Caminade, E., Joly, N., Madzak, C., Mougin, C. 2002. Crystal structure of a four-copper laccase complexed with an arylamine: Insights into substrate recognition and correlation with kinetics. Biochemistry, 41(23), 7325-7333.

Bhat, R.R., Genzer, J. 2007. Tuning the number density of nanoparticles by multivariant tailoring of attachment points on flat substrates. Nanotechnology, 18(2), 025301.

Bloom, J.D., Arnold, F.H. 2009. In the light of directed evolution: Pathways of adaptive protein evolution. Proceedings of the National Academy of Sciences, 106(Supplement 1), 9995-10000.

Blunk, S.L., Jenkins, B.M. 2000. Combustion properties of lignin residue from lignocellulose fermentation. National Renewable Energy Laboratory, NREL Subcontract ACG-8-18021-01, Davis, California.

Bommarius, A., Riebel-Bommarius, B. 2004. Biocatalysis: Fundamentals and applications. Wiley, New York.

Borges da Silva, E.A., Zabkova, M., Araújo, J.D., Cateto, C.A., Barreiro, M.F., Belgacem, M.N., Rodrigues, A.E. 2009. An integrated process to produce vanillin and lignin-based polyurethanes from kraft lignin. Chemical Engineering Research and Design, 87(9), 1276-1292.

Borthakur N 2007. World Intellectual Property Organization. WO 2007/094013 A1

Bourbonnais, R., Paice, M.G., Reid, I.D., Lanthier, P., Yaguchi, M. 1995. Lignin oxidation by laccase isozymes from *Trametes versicolor* and role of the mediator 2,2'-azinobis(3-ethylbenzthiazoline-6-sulfonate) in kraft lignin depolymerization. Applied and Environmental Microbiology, 61(5), 1876-80.

Bozell, J. J.; Holladay, J. E.; Johnson, D.; White, J. F. 2007. Top Value added candidates from biomass, Volume II: Results of screening for potential candidates from biorefinery lignin; Pacific Northwest National Laboratory: Richland, WA.

Brady, D., Jordaan, J. 2009. Advances in enzyme immobilisation. Biotechnology Letters, 31(11), 1639-1650.

Brunow, G. 2001. Methods to reveal the structure of lignin. In: Lignin, humic substances and coal (Biopolymers, vol. 1), (Eds.) Hofrichter, M., Steinbuchel, A., Wiley-VCH, Weinheim, Germany, pp. 89-107.

Brunow G., Lundquist K., Gellerstedt G. 1999. Lignin. In: Analytical methods in wood chemistry pulping, and papermaking, (Eds.) Sjöström, E., Alén, R., Springer, Berlin Heidelberg, Germany, pp. 77–124.

Bugg, T.D.H., Ahmad, M., Hardiman, E.M., Singh, R. 2011. The emerging role for bacteria in lignin degradation and bio-product formation. Current Opinion in Biotechnology, 22(3), 394-400.

Buswell, J.A., Odier, E. 1987. Lignin biodegradation. Critical Reviews in Biotechnology, 6(1), 1-60.

Cabana, H., Alexandre, C., Agathos, S.N., Jones, J.P. 2009. Immobilization of laccase from the white rot fungus *Coriolopsis polyzona* and use of the immobilized biocatalyst for the continuous elimination of endocrine disrupting chemicals. Bioresource Technology, 100(14), 3447-3458.

Cadenas, E., Merényi, G., Lind, J. 1989. Pulse radiolysis study on the reactivity of Trolox C phenoxyl radical with superoxide anion. FEBS Letters, 253(1-2), 235-238.

Camarero, S., Ibarra, D., Martínez, Á.T., Romero, J., Gutiérrez, A., del Río, J.C. 2007. Paper pulp delignification using laccase and natural mediators. Enzyme and Microbial Technology, 40(5), 1264-1271.

Camarero, S., Martínez, M.J., Martínez, A.T. 2014. Understanding lignin biodegradation for the improved utilization of plant biomass in modern biorefineries. Biofuels, Bioproducts and Biorefining, 8(5), 615-625.

Camarero, S., Sarkar, S., Ruiz-Dueñas, F.J., Martínez, M.J., Martínez, Á.T. 1999. Description of a versatile peroxidase involved in the natural degradation of lignin that has both manganese peroxidase and lignin peroxidase substrate interaction sites. Journal of Biological Chemistry, 274(15), 10324-10330.

Cañas, A.I., Camarero, S. 2010. Laccases and their natural mediators: Biotechnological tools for sustainable eco-friendly processes. Biotechnology Advances, 28(6), 694-705.

Canevali, C., Orlandi, M., Pardi, L., Rindone, B., Scotti, R., Sipila, J., Morazzoni, F. 2002. Oxidative degradation of monomeric and dimeric phenylpropanoids: reactivity and mechanistic investigation. Journal of the Chemical Society Dalton Transactions, 15, 3007-3014.

Cantarella, G., Galli, C., Gentili, P. 2003. Free radical versus electron-transfer routes of oxidation of hydrocarbons by laccase/mediator systems: Catalytic or stoichiometric procedures. Journal of Molecular Catalysis B: Enzymatic, 22(3-4), 135-144.

Cantone, S., Hanefeld, U., Basso, A. 2007. Biocatalysis in non-conventional media-ionic liquids, supercritical fluids and the gas phase. Green Chemistry, 9(9), 954-971.

Castellanos, I.J., Cruz, G., Crespo, R., Griebenow, K. 2002. Encapsulation-induced aggregation and loss in activity of γ-chymotrypsin and their prevention. Journal of Controlled Release, 81(3), 307-319.

Chakar, F.S., Ragauskas, A.J. 2004. Review of current and future softwood kraft lignin process chemistry. Industrial Crops and Products, 20(2), 131-141.

Cheng, X., Jia, R., Li, P., Tu, S., Zhu, Q., Tang, W., Li, X. 2007. Purification of a new manganese peroxidase of the white-rot fungus *Schizophyllum* sp. F17, and decolorization of azo dyes by the enzyme. Enzyme and Microbial Technology, 41(3), 258-264.

Childs, R.E., Bardsley, W.G. 1975. The steady-state kinetics of peroxidase with 2,2'-azino-di-(3-ethyl-benzthiazoline-6-sulphonic acid) as chromogen. Biochemical Journal, 145(1), 93-103.

Chum, H.L., Douglas, L.J., Feinberg, D.A., Schroeder, H.A. 1985. Evaluation of pretreatments of biomass for enzymatic hydrolysis of cellulose. Solar Energy Research Institute. Available from http://www.nrel.gov/docs/legosti/old/2183.pdf

Cohen, R., Suzuki, M.R., Hammel, K.E. 2005. Processive endoglucanase active in crystalline cellulose hydrolysis by the brown rot basidiomycete *Gloeophyllum trabeum*. Applied and Environmental Microbiology, 71(5), 2412-2417.

Collins, P.J., Kotterman, M., Field, J.A., Dobson, A. 1996. Oxidation of anthracene and benzo[a]pyrene by laccases from *Trametes versicolor*. Applied and Environmental Microbiology, 62(12), 4563-4567.

Collinson, S.R., Thielemans, W. 2010. The catalytic oxidation of biomass to new materials focusing on starch, cellulose and lignin. Coordination Chemistry Reviews, 254(15-16), 1854-1870.

Correro, M.R., Moridi, N., Schützinger, H., Sykora, S., Ammann, E.M., Peters, E.H., Dudal, Y., Corvini, P.F.X., Shahgaldian, P. 2016. Enzyme shielding in an enzyme-thin and soft organosilica layer. Angewandte Chemie International Edition, 55(21), 6285-6289.

Corvini, P.F.X., Shahgaldian, P. 2010. LANCE: Laccase-nanoparticle conjugates for the elimination of micropollutants (endocrine disrupting chemicals) from wastewater in bioreactors. Reviews in Environmental Science and Biotechnology, 9(1), 23-27.

Couderc, R., Baratti, J. 1980. Oxidation of methanol by the yeast, *Pichia pastoris*. Purification and properties of the alcohol oxidase. Agricultural and Biological Chemistry, 44(10), 2279-2289.

Courjean, O., Mano, N. 2011. Recombinant glucose oxidase from Penicillium amagasakiense for efficient bioelectrochemical applications in physiological conditions. Journal of Biotechnology, 151(1), 122-129.

Crestini, C., Caponi, M.C., Argyropoulos, D.S., Saladino, R. 2006. Immobilized methyltrioxo rhenium (MTO)/H_2O_2 systems for the oxidation of lignin and lignin model compounds. Bioorganic & Medicinal Chemistry, 14(15), 5292-5302.

Crestini, C., Jurasek, L., Argyropoulos, D.S. 2003. On the mechanism of the laccase–mediator system in the oxidation of lignin. Chemistry – A European Journal, 9(21), 5371-5378.

Crestini, C., Melone, F., Saladino, R. 2011. Novel multienzyme oxidative biocatalyst for lignin bioprocessing. Bioorganic & Medicinal Chemistry, 19(16), 5071-5078.

Crestini, C., Pro, P., Neri, V., Saladino, R. 2005. Methyltrioxorhenium: a new catalyst for the activation of hydrogen peroxide to the oxidation of lignin and lignin model compounds. Bioorganic & Medicinal Chemistry, 13(7), 2569-2578.

Cullity, B.D., Graham, C.D. 2008. Introduction to magnetic materials. 2nd ed. John Wiley & Sons, Hoboken, New Jersey.

Crognale, S., Pulci, V., Brozzoli, V., Petruccioli, M., Federici, F. 2006. Expression of penicillium variabile P16 glucose oxidase gene in *Pichia pastoris* and characterization of the recombinant enzyme. Enzyme and Microbial Technology, 39(6), 1230-1235.

Cyr, A., Chiltz, F., Jeanson, P., Martel, A., Brossard, L., Lessard, J., Ménard, H. 2000. Electrocatalytic hydrogenation of lignin models at Raney nickel and palladium-based electrodes. Canadian Journal of Chemistry, 78(3), 307-315.

da Costa Sousa, L., Chundawat, S.P.S., Balan, V., Dale, B.E. 2009. `Cradle-to-grave' assessment of existing lignocellulose pretreatment technologies. Current Opinion in Biotechnology, 20(3), 339-347.

Dabo, P., Cyr, A., Lessard, J., Brossard, L., Ménard, H. 1999. Electrocatalytic hydrogenation of 4-phenoxyphenol on active powders highly dispersed in a reticulated vitreous carbon electrode. Canadian Journal of Chemistry, 77(7), 1225-1229.

Dai, L., Klibanov, A.M. 1999. Striking activation of oxidative enzymes suspended in nonaqueous media. Proceedings of the National Academy of Sciences, 96(17), 9475-9478.

Davin, L.B., Lewis, N.G. 2005. Lignin primary structures and dirigent sites. Current Opinion in Biotechnology, 16(4), 407-415.

de Jong, E., van Berkel, W.J.H., van der Zwan, R.P., de Bont, J.A.M. 1992. Purification and characterization of vanillyl-alcohol oxidase from *Penicillium simplicissimum*. European Journal of Biochemistry, 208(3), 651-657.

Deere, J., Magner, E., Wall, J.G., Hodnett, B.K. 2002. Mechanistic and structural features of protein adsorption onto mesoporous silicates. The Journal of Physical Chemistry B, 106(29), 7340-7347.

Delwiche, C.F., Graham, L.E., Thomson, N. 1989. Lignin-like compounds and sporopollenin coleochaete, an algal model for land plant ancestry. Science, 245(4916), 399-401.

Demarche, P., Junghanns, C., Mazy, N., Agathos, S.N. 2012. Design-of-experiment strategy for the formulation of laccase biocatalysts and their application to degrade bisphenol A. New Biotechnology, 30(1), 96-103.

De Maio, A., El-Masry, M.M., Portaccio, M., Diano, N., Di Martino, S., Mattei, A., Bencivenga, U., Mita, D.G. 2003. Influence of the spacer length on the activity of enzymes immobilised on nylon/polyGMA membranes: Part 1. Isothermal conditions. Journal of Molecular Catalysis B: Enzymatic, 21(4–6), 239-252.

Doğan, S., Turan, P., Doğan, M., Arslan, O., Alkan, M. 2005. Purification and characterization of *Ocimum basilicum* L. Polyphenol oxidase. Journal of Agricultural and Food Chemistry, 53(26), 10224-10230.

Doherty, W.O.S., Mousavioun, P., Fellows, C.M. 2011. Value-adding to cellulosic ethanol: Lignin polymers. Industrial Crops and Products, 33(2), 259-276.

Dominguez-Ramos, A., Aldaco, R., Irabien, A. 2008. Electrochemical oxidation of lignosulfonate: Total organic carbon oxidation kinetics. Industrial & Engineering Chemistry Research, 47(24), 9848-9853.

Dominguez-Ramos, A., Aldaco, R., Irabien, A. 2010a. Photovoltaic solar electrochemical oxidation (PSEO) for lignosulphonate waste water treatment. Chemical Engineering Transactions, 21, 379-384.

Dominguez-Ramos, A., Aldaco, R., Irabien, A. 2010b. Photovoltaic solar electrochemical oxidation (PSEO) for treatment of lignosulfonate wastewater. Journal of Chemical Technology and Biotechnology, 85(6), 821-830.

Doukyu, N., Ogino, H. 2010. Organic solvent-tolerant enzymes. Biochemical Engineering Journal, 48(3), 270-282.

Dubé, E., Shareck, F., Hurtubise, Y., Daneault, C., Beauregard, M. 2008. Homologous cloning, expression, and characterisation of a laccase from *Streptomyces coelicolor* and enzymatic decolourisation of an indigo dye. Applied Microbiology and Biotechnology, 79(4), 597-603.

Duff, S.J.B., Murray, W.D. 1996. Bioconversion of forest products industry waste cellulosics to fuel ethanol: A review. Bioresource Technology, 55(1), 1-33.

Durán, N., Rosa, M.A., D'Annibale, A., Gianfreda, L. 2002. Applications of laccases and tyrosinases (phenoloxidases) immobilized on different supports: A review. Enzyme and Microbial Technology, 31(7), 907-931.

Eijsink, V.G.H., Gåseidnes, S., Borchert, T.V., van den Burg, B. 2005. Directed evolution of enzyme stability. Biomolecular Engineering, 22(1-3), 21-30.

El-Ashtoukhy, E.S.Z., Amin, N.K., Abdelwahab, O. 2009. Treatment of paper mill effluents in a batch-stirred electrochemical tank reactor. Chemical Engineering Journal, 146(2), 205-210.

Enaud, E., Trovaslet, M., Naveau, F., Decristoforo, A., Bizet, S., Vanhulle, S., Jolivalt, C. 2011. Laccase chloride inhibition reduction by an anthraquinonic substrate. Enzyme and Microbial Technology, 49(6–7), 517-525.

Enoki, M., Watanabe, T., Nakagame, S., Koller, K., Messner, K., Honda, Y., Kuwahara, M. 1999. Extracellular lipid peroxidation of selective white-rot fungus, *Ceriporiopsis subvermispora*. Fems Microbiology Letters, 180(2), 205-211.

Eriksson, T., Börjesson, J., Tjerneld, F. 2002. Mechanism of surfactant effect in enzymatic hydrolysis of lignocellulose. Enzyme and Microbial Technology, 31(3), 353-364.

Evans, C.S., Dutton, M.V., Guillén, F., Veness, R.G. 1994. Enzymes and small molecular mass agents involved with lignocellulose degradation. FEMS Microbiology Reviews, 13(2-3), 235-239.

Fabbrini, M., Galli, C., Gentili, P. 2002. Radical or electron-transfer mechanism of oxidation with some laccase/mediator systems. Journal of Molecular Catalysis B: Enzymatic, 18(1–3), 169-171.

Faith, W.L., Keyes, D.B., Clark, D.S. 1965. Industrial Chemicals. John Wiley & Sons, New York.

Faulds, C. 2010. What can feruloyl esterases do for us? Phytochemistry Reviews, 9(1), 121-132.

Ferreira, P., Medina, M., Guillen, F., Martinez, M.J., Van Berkel, W.J., Martinez, A.T. 2005. Spectral and catalytic properties of aryl-alcohol oxidase, a fungal flavoenzyme acting on polyunsaturated alcohols. Biochemical Journal, 389(3), 731-8.

Festa, G., Autore, F., Fraternali, F., Giardina, P., Sannia, G. 2008. Development of new laccases by directed evolution: Functional and computational analyses. Proteins, 72(1), 25-34.

Forney, L.J., Reddy, C.A., Tien, M., Aust, S.D. 1982. The involvement of hydroxyl radical derived from hydrogen peroxide in lignin degradation by the white rot fungus Phanerochaete chrysosporium. The Journal of Biological Chemistry, 257(19), 11455-62.

Freudenberg, K. 1965. Lignin: Its constitution and formation from *p*-hydroxycinnamyl alcohols: Lignin is duplicated by dehydrogenation of these alcohols; intermediates explain formation and structure. Science, 148(3670), 595-600.

Freudenberg K, Neish AC (1968) Constitution and biosynthesis of lignin. Springer, Berlin-Heidelberg-New York.

Fukushima, K. 2001. Regulation of syringyl to guaiacyl ratio in lignin biosynthesis. Journal of Plant Research, 114(4), 499-508.

Gajzago I., Rose P., Vamos-Vigyazo L. 1973. Possibilities of enzymic hydrolysis of cellulose-containing wastes. II. Chemical pretreatment of poplar sawdust and of corn cob to improve the efficiency of enzymic hydrolysis. Acta Alimentaria Academiae Scientiarum Hungaricae, 2, 55–67.

Galli, C., Gentili, P. 2004. Chemical messengers: Mediated oxidations with the enzyme laccase. Journal of Physical Organic Chemistry, 17(11), 973-977.

Gamelas, J.A.F., Pontes, A.S.N., Evtuguin, D.V., Xavier, A.M.R.B., Esculcas, A.P. 2007. New polyoxometalate–laccase integrated system for kraft pulp delignification. Biochemical Engineering Journal, 33(2), 141-147.

Garcia-Conesa, M.T., Crepin, V.F., Goldson, A.J., Williamson, G., Cummings, N.J., Connerton, I.F., Faulds, C.B., Kroon, P.A. 2004. The feruloyl esterase system of *Talaromyces stipitatus*: Production of three discrete feruloyl esterases, including a novel enzyme, TsFaeC, with a broad substrate specificity. Journal of Biotechnology, 108(3), 227-241.

García-Ruiz, E., Maté, D., Ballesteros, A., Martinez, A., Alcalde, M. 2010. Evolving thermostability in mutant libraries of ligninolytic oxidoreductases expressed in yeast. Microbial Cell Factories, 9(1), 1-13.

Gaspar, A.R., Gamelas, J.A.F., Evtuguin, D.V., Pascoal Neto, C. 2007. Alternatives for lignocellulosic pulp delignification using polyoxometalates and oxygen: a review. Green Chemistry, 9(7), 717-730.

Gasser, C.A., Ammann, E.M., Schäffer, A., Shahgaldian, P., Corvini, P.F.X. 2016. Production of superparamagnetic nanobiocatalysts for green chemistry applications. Applied Microbiology and Biotechnology, 100(16), 7281-7296.

Gasser, C.A., Ammann, E.M., Shahgaldian, P., Corvini, P.F.X. 2014a. Laccases to take on the challenge of emerging organic contaminants in wastewater. Applied Microbiology and Biotechnology, 98(24), 9931-9952.

Gasser, C.A., Čvančarová, M., Ammann, E.M., Schäffer, A., Shahgaldian, P., Corvini, P.F.X. 2017. Sequential lignin depolymerization by combination of biocatalytic and formic acid/formate treatment steps. Applied Microbiology and Biotechnology, 101(6), 2575-2588.

Gasser, C.A., Hommes, G., Schäffer, A., Corvini, P.F.X. 2012. Multi-catalysis reactions: New prospects and challenges of biotechnology to valorize lignin. Applied Microbiology and Biotechnology, 95(5), 1115-1134.

Gasser, C.A., Yu, L., Svojitka, J., Wintgens, T., Ammann, E.M., Shahgaldian, P., Corvini, P.F.X., Hommes G. 2014b. Advanced enzymatic elimination of phenolic contaminants in wastewater: a nano approach at field scale. Applied Microbiology and Biotechnology, 98(7), 3305-3316.

Gerencser, A.A., Neilson, A., Choi, S.W., Edman, U., Yadava, N., Oh, R.J., Ferrick, D.A., Nicholls, D.G., Brand, M.D. 2009. Quantitative microplate-based respirometry with correction for oxygen diffusion. Analytical Chemistry, 81(16), 6868-6878.

Ghodake, G., Kalme, S., Jadhav, J., Govindwar, S. 2009. Purification and partial characterization of lignin peroxidase from acinetobacter calcoaceticus NCIM 2890 and its application in decolorization of textile dyes. Applied Biochemistry and Biotechnology, 152(1), 6-14.

Giardina, P., Faraco, V., Pezzella, C., Piscitelli, A., Vanhulle, S., Sannia, G. 2010. Laccases: A never-ending story. Cellular and Molecular Life Sciences, 67(3), 369-385.

Giardina, P., Palmieri, G., Fontanella, B., Rivieccio, V., Sannia, G. 2000. Manganese peroxidase isoenzymes produced by *Pleurotus ostreatus* grown on wood sawdust. Archives of Biochemistry and Biophysics, 376(1), 171-179.

Gierer, J. 1980. Chemical aspects of kraft pulping. Wood Science and Technology, 14(4), 241-266.

Gil-Rodríguez, P., Ferreira-Batista, C., Vázquez-Duhalt, R., Valderrama, B. 2008. A novel heme peroxidase from *Raphanus sativus* intrinsically resistant to hydrogen peroxide. Engineering in Life Sciences, 8(3), 286-296.

Glenn, J.K., Gold, M.H. 1985. Purification and characterization of an extracellular Mn(II)-dependent peroxidase from the lignin-degrading basidiomycete, *Phanerochaete chrysosporium*. Archives of Biochemistry and Biophysics, 242(2), 329-341.

Gluckstein, J., Hu, M., Kidder, M., McFarlane, J., Narula, C., Sturgeon, M. 2010. Final report: Investigation of catalytic pathways for lignin breakdown into monomers and fuels. Oak Ridge National Laboratory. ORNL/TM-2010/281.

Godden, B., Ball, A.S., Helvenstein, P., Mccarthy, A.J., Penninckx, M.J. 1992. Towards elucidation of the lignin degradation pathway in actinomycetes. Journal of General Microbiology, 138(11), 2441-2448.

Gold, M.H., Kuwahara, M., Chiu, A.A., Glenn, J.K. 1984. Purification and characterization of an extracellular H_2O_2-requiring diarylpropane oxygenase from the white rot basidiomycete, *Phanerochaete chrysosporium*. Archives of Biochemistry and Biophysics, 234(2), 353-362.

Gold, M.H., Youngs, H.L., Gelpke, M.D. 2000. Manganese peroxidase. Metal Ions in Biological systems, 37, 559-86.

Gomes, E., Aguiar, A.P., Carvalho, C.C., Bonfá, M.R.B., Silva, R.d., Boscolo, M. 2009. Ligninases production by basidiomycetes strains on lignocellulosic agricultural residues and their application in the decolorization of synthetic dyes. Brazilian Journal of Microbiology, 40, 31-39.

Gómez-Toribio, V., Martínez, A.T., Martínez, M.J., Guillén, F. 2001. Oxidation of hydroquinones by the versatile ligninolytic peroxidase from *Pleurotus eryngii*. European Journal of Biochemistry, 268(17), 4787-4793.

Gómez-Toribio, V., Garcia-Martin, A.B., Martinez, M.J., Martinez, A.T., Guillen, F. 2009. Induction of extracellular hydroxyl radical production by white-rot fungi through quinone redox cycling. Applied and Environmental Microbiology, 75(12), 3944-3953.

González-García, S., Teresa Moreira, M., Artal, G., Maldonado, L., Feijoo, G. 2010. Environmental impact assessment of non-wood based pulp production by soda-anthraquinone pulping process. Journal of Cleaner Production, 18(2), 137-145.

Gorke, J., Srienc, F., Kazlauskas, R. 2010. Toward advanced ionic liquids. Polar, enzyme-friendly solvents for biocatalysis. Biotechnology and Bioprocess Engineering, 15(1), 40-53.

Gosselink R.J.A. 2011. Lignin as a renewable aromatic resource for the chemical industry. Dissertation – Proefschrift, Wageningen.

Grous, W.R., Converse, A.O., Grethlein, H.E. 1986. Effect of steam explosion pretreatment on pore size and enzymatic hydrolysis of poplar. Enzyme and Microbial Technology, 8(5), 274-280.

Gross, G.G., Zenk, M.H. 1969. Reduktion aromatischer Säuren zu Aldehyden und Alkoholen im zellfreien System. European Journal of Biochemistry, 8(3), 420-425.

Guillén, F., Gómez-Toribio, V., Martínez, M.J., Martínez, A.T. 2000. Production of hydroxyl radical by the synergistic action of fungal laccase and aryl alcohol oxidase. Archives of Biochemistry and Biophysics, 383(1), 142-147.

Guillén, F., Martínez, A.T., Martínez, M.J. 1992. Substrate specificity and properties of the aryl-alcohol oxidase from the ligninolytic fungus *Pleurotus eryngii*. European Journal of Biochemistry, 209(2), 603-611.

Guillén, F., Martínez, M.J., Muñoz, C., Martínez, A.T. 1997. Quinone redox cycling in the ligninolytic fungus *Pleurotus eryngii* leading to extracellular production of superoxide anion radical. Archives of Biochemistry and Biophysics, 339(1), 190-199.

Gülçİn, İ., İrfan Küfrevİoğlu, Ö., Oktay, M. 2005. Purification and characterization of polyphenol oxidase from nettle (*Urtica dioica* L.) and inhibitory effects of some chemicals on enzyme activity. Journal of Enzyme Inhibition and Medicinal Chemistry, 20(3), 297-302.

Guo, Q., Packer, L. 2000. Ascorbate-dependent recycling of the vitamin E homologue Trolox by dihydrolipoate and glutathione in murine skin homogenates. Free Radical Biology and Medicine, 29(3–4), 368-374.

Gvozdev, A., Tukhvatullin, I., Gvozdev, R. 2010. Purification and properties of alcohol oxidase from *Pichia putida*. Biochemistry (Moscow), 75(2), 242-248.

Haibo, Z., Yinglong, Z., Feng, H., Peiji, G., Jiachuan, C. 2009. Purification and characterization of a thermostable laccase with unique oxidative characteristics from *Trametes hirsuta*. Biotechnology Letters, 31(6), 837-843.

Hailes, H.C., Dalby, P.A., Woodley, J.M. 2007. Integration of biocatalytic conversions into chemical syntheses. Journal of Chemical Technology and Biotechnology, 82(12), 1063-1066.

Hammel, K.E., Cullen, D. 2008. Role of fungal peroxidases in biological ligninolysis. Current Opinion in Plant Biology, 11(3), 349-355.

Hammel, K.E., Jensen, K.A., Mozuch, M.D., Landucci, L.L., Tien, M., Pease, E.A. 1993. Ligninolysis by a purified lignin peroxidase. Journal of Biological Chemistry, 268(17), 12274-81.

Hammel, K.E., Kapich, A.N., Jensen Jr, K.A., Ryan, Z.C. 2002. Reactive oxygen species as agents of wood decay by fungi. Enzyme and Microbial Technology, 30(4), 445-453.

Harkin, J., Obst, J. 1973. Syringaldazine, an effective reagent for detecting laccase and peroxidase in fungi. Experientia, 29(4), 381-387.

Harreither, W., Sygmund, C., Augustin, M., Narciso, M., Rabinovich, M.L., Gorton, L., Haltrich, D., Ludwig, R. 2011. Catalytic properties and classification of cellobiose dehydrogenases from ascomycetes. Applied and Environmental Microbiology, 77(5), 1804-1815.

Hartmann, M., Jung, D. 2010. Biocatalysis with enzymes immobilized on mesoporous hosts: the status quo and future trends. Journal of Materials Chemistry, 20(5), 844-857.

Hashemifard, N., Mohsenifar, A., Ranjbar, B., Allameh, A., Lotfi, A.S., Etemadikia, B. 2010. Fabrication and kinetic studies of a novel silver nanoparticles–glucose oxidase bioconjugate. Analytica Chimica Acta, 675(2), 181-184.

Hatakka, A. 1994. Lignin-modifying enzymes from selected white-rot fungi: Production and role from in lignin degradation. FEMS Microbiology Reviews, 13(2–3), 125-135.

Hatakka, A., Hammel, K.E. 2010. Fungal biodegradation of lignocelluloses. In: The mycota, a comprehensive treatise on fungi as experimental systems for basic and applied research, industrial applications (vol. 10), (Ed.) Hofrichter, M., Springer, Berlin Heidelberg, pp. 319-340.

Hegde, S., Muralikrishna, G. 2009. Isolation and partial characterization of alkaline feruloyl esterases from *Aspergillus niger* CFR 1105 grown on wheat bran. World Journal of Microbiology and Biotechnology, 25(11), 1963-1969.

Henriksson, G., Johansson, G., Pettersson, G. 2000. A critical review of cellobiose dehydrogenases. Journal of Biotechnology, 78(2), 93-113.

Heremans, K. 1982. High pressure effects on proteins and other biomolecules. Annual Review of Biophysics and Bioengineering, 11(1), 1-21.

Herrmann, W.A., Weskamp, T., Zoller, J.P., Fischer, R.W. 2000. Methyltrioxorhenium: oxidative cleavage of CC-double bonds and its application in a highly efficient synthesis of vanillin from biological waste. Journal of Molecular Catalysis A: Chemical, 153(1-2), 49-52.

Higuchi, T. 2006. Look back over the studies of lignin biochemistry. Journal of Wood Science, 52(1), 2-8.

Hochstrat, R., Wintgens, T., Corvini, P.F.X. 2015. Immobilised biocatalysts for bioremediation of groundwater and wastewater. IWA Publishing, London.

Hocking, M.B. 1997. Vanillin: Synthetic flavoring from spent sulfite liquor. Journal of Chemical Education, 74(9), 1055.

Hofrichter, M., Ziegenhagen, D., Vares, T., Friedrich, M., Jäger, M.G., Fritsche, W., Hatakka, A. 1998. Oxidative decomposition of malonic acid as basis for the action of manganese peroxidase in the absence of hydrogen peroxide. FEBS Letters, 434(3), 362-366.

Hofrichter, M., Lundell, T., Hatakka, A. 2001. Conversion of milled pine wood by manganese peroxidase from *Phlebia radiata*. Applied and Environmental Microbiology, 67(10), 4588-4593.

Hofrichter, M., Ullrich, R., Pecyna, M., Liers, C., Lundell, T. 2010. New and classic families of secreted fungal heme peroxidases. Applied Microbiology and Biotechnology, 87(3), 871-897.

Holladay J.E., White J.F., Bozell J.J., Johnson D. 2007. Top value-added chemicals from biomass, volume II—results of screening for potential candidates from biorefinery lignin. Pacific Northwest National Laboratory, DOE.

Holtman, K.M., Chang, H.M., Kadla, J.F. 2007. An NMR comparison of the whole lignin from milled wood, MWL, and REL dissolved by the DMSO/NMI procedure. Journal of Wood Chemistry and Technology, 27(3-4), 179-200.

Hommes, G., Gasser, C.A., Ammann, E.M., Corvini, P.F.X. 2013. Determination of oxidoreductase activity using a high-throughput microplate respiratory measurement. Analytical Chemistry, 85(1), 283-291.

Hommes, G., Gasser, C.A., Howald, C.B.C., Goers, R., Schlosser, D., Shahgaldian, P., Corvini, P.F.X. 2012. Production of a robust nanobiocatalyst for municipal wastewater treatment. Bioresource Technology, 115(0), 8-15.

Hou, H., Zhou, J., Wang, J., Du, C., Yan, B. 2004. Enhancement of laccase production by *Pleurotus ostreatus* and its use for the decolorization of anthraquinone dye. Process Biochemistry, 39(11), 1415-1419.

Hu, T.Q., Lee, C.L., James, B.R., Rettig, S.J. 1997. Stereoselective hydrogenation of lignin degradation model compounds. Canadian Journal of Chemistry, 75(9), 1234-1239.

Hu, X., Wang, P., Hwang, H.-m. 2009. Oxidation of anthracene by immobilized laccase from *Trametes versicolor*. Bioresource Technology, 100(21), 4963-4968.

Huang, C.H., Kuo, H.S., Liu, J.W., Lin, Y.L. 2009. Synthesis and antitumor evaluation of novel bis-triaziquone derivatives. Molecules, 14(7), 2306-2316.

Hüner, P. 2007. MSc. Thesis, Istanbul Technical University, Institute of Science and Technology, Istanbul, Turkey.

Industrielle Werke Basel 2016. www.iwb.ch, accessed on 27.5.2016.

Isobe, K., Kato, A., Sasaki, Y., Suzuki, S., Kataoka, M., Ogawa, J., Iwasaki, A., Hasegawa, J., Shimizu, S. 2007. Purification and characterization of a novel alcohol oxidase from *Paenibacillus* sp. AIU 311. Journal of Bioscience and Bioengineering, 104(2), 124-128.

Isroi, Millati, R., Syamsiah, S., Niklasson, C., Cahyanto, M.N., Lundquist, K., Taherzadeh, M.J. 2011. Biological pretreatment of lignocelluloses with white-rot fungi and its applications: A review. BioResources, 6(4), 5224-5259.

Jadhav, U., Dawkar, V., Tamboli, D., Govindwar, S. 2009. Purification and characterization of veratryl alcohol oxidase from *Comamonas* sp. UVS and its role in decolorization of textile dyes. Biotechnology and Bioprocess Engineering, 14(3), 369-376.

Jadhav, V.K., Chivate, M.R., Tavare, N.S. 1991. Separation of *p*-cresol from its mixture with 2,6-xylenol by adductive crystallization. Journal of Chemical & Engineering Data, 36(2), 249-251.

Jadhav, V.K., Chivate, M.R., Tavare, N.S. 1992. Separation of phenol from its mixture with *o*-cresol by adductive crystallization. Journal of Chemical & Engineering Data, 37(2), 232-235.

Jeoung, J.H., Pippig, D.A., Martins, B.M., Wagener, N., Dobbek, H. 2007. HTHP: A novel class of hexameric, tyrosine-coordinated heme proteins. Journal of Molecular Biology, 368(4), 1122-1131.

Jin, L., Schultz, T.P., Nicholas, D.D. 1990. Structural characterization of brown-rotted lignin. Holzforschung, 44(2), 133-138.

Jochems, P., Satyawali, Y., Diels, L., Dejonghe, W. 2011. Enzyme immobilization on/in polymeric membranes: status, challenges and perspectives in biocatalytic membrane reactors (BMRs). Green Chemistry, 13(7), 1609-1623.

Johannes, C., Majcherczyk, A. 2000a. Natural mediators in the oxidation of polycyclic aromatic hydrocarbons by laccase mediator systems. Applied Environmental Microbiology, 66(2), 524-528.

Johannes, C., Majcherczyk, A. 2000b. Laccase activity tests and laccase inhibitors. Journal of Biotechnology, 78(2), 193-199.

Johansson, T., Nyman, P.O. 1993. Isozymes of lignin peroxidase and manganese(II) peroxidase from the white-rot basidiomycete *Trametes versicolor*: I. Isolation of enzyme forms and characterization of physical and catalytic properties. Archives of Biochemistry and Biophysics, 300(1), 49-56.

Joosten, V., van Berkel, W.J.H. 2007. Flavoenzymes. Current Opinion in Chemical Biology, 11(2), 195-202.

Joseleau, J.-P., Gharibian, S., Comtat, J., Lefebvre, A., Ruel, K. 1994. Indirect involvement of ligninolytic enzyme systems in cell wall degradation. FEMS Microbiology Reviews, 13(2-3), 255-263.

Junghanns, C., Parra, R., Keshavarz, T., Schlosser, D. 2008. Towards higher laccase activities produced by aquatic ascomycetous fungi through combination of elicitors and an alternative substrate. Engineering in Life Sciences, 8(3), 277-285.

Kamm, B., Gruber, P.R., Kamm, M. 2007. Biorefineries – industrial processes and products. In: Ullmann's encyclopedia of industrial chemistry, Wiley-VCH., Weinheim, Germany.

Kapich, A., Hofrichter, M., Vares, T., Hatakka, A. 1999a. Coupling of manganese peroxidase-mediated lipid peroxidation with destruction of nonphenolic lignin model compounds and 14C-Labeled Lignins. Biochemical and Biophysical Research Communications, 259(1), 212-219.

Kapich, A.N., Jensen, K.A., Hammel, K.E. 1999b. Peroxyl radicals are potential agents of lignin biodegradation. FEBS Letters, 461(1–2), 115-119.

Karhunen, P., Rummakko, P., Sipilä, J., Brunow, G., Kilpeläinen, I. 1995a. The formation of dibenzodioxocin structures by oxidative coupling. A model reaction for lignin biosynthesis. Tetrahedron Letters, 36(25), 4501–4504.

Karhunen, P., Rummakko, P., Sipilä, J., Brunow, G., Kilpeläinen, I. 1995b. Dibenzodioxocins; a novel type of linkage in softwood lignins. Tetrahedron Letters, 36(1), 169–170.

Kashima, K., Maeda, Y., Oshima, M. 1964. Method for liquefying lignin. Canadian Patent 700210

Katrib, F.A., Chambat, G., Joseleau, J.P. 1988. Organic solvent pretreatment to enhance enzymic saccharification of straw. Journal of the Science of Food and Agriculture, 43(4), 309–317.

Kawai, S., Umezawa, T., Higuchi, T. 1988. Degradation mechanisms of phenolic β-1 lignin substructure model compounds by laccase of *Coriolus versicolor*. Archives of Biochemistry and Biophysics, 262(1), 99-110.

Kellner, H., Luis, P., Zimdars, B., Kiesel, B., Buscot, F. 2008. Diversity of bacterial laccase-like multicopper oxidase genes in forest and grassland Cambisol soil samples. Soil Biology and Biochemistry, 40(3), 638-648.

Kersten, P., Cullen, D. 2007. Extracellular oxidative systems of the lignin-degrading basidiomycete *Phanerochaete chrysosporium*. Fungal Genetics and Biology, 44(2), 77-87.

Kim, J., Clark, D.S., Dordick, J.S. 2000. Intrinsic effects of solvent polarity on enzymic activation energies. Biotechnology and Bioengineering, 67(1), 112-116.

Kim, S.G., Jung, B.W., Kim, H. 2011. Hemocyanin-derived phenoloxidase activity with broad temperature stability extending into the cold environment in hemocytes of the hair crab *Erimacrus isenbeckii*. Comparative Biochemistry and Physiology Part B: Biochemistry and Molecular Biology, 159(2), 103-108.

Kinne, M., Poraj-Kobielska, M., Ullrich, R., Nousiainen, P., Sipilä, J., Scheibner, K., Hammel, K.E., Hofrichter, M. 2011. Oxidative cleavage of non-phenolic β-O-4 lignin model dimers by an extracellular aromatic peroxygenase. Holzforschung, 65(5), 673-679.

Koseki, T., Fushinobu, S., Ardiansyah, A., Shirakawa, H., Komai, M. 2009. Occurrence, properties, and applications of feruloyl esterases. Applied Microbiology and Biotechnology, 84(5), 803-810.

Kromidas, S. 2011. Validierung in der Analytik, 2nd ed.; Wiley-VCH, Weinheim, Germany.

Kudanga, T., Nyanhongo, G.S., Guebitz, G.M., Burton, S. 2011. Potential applications of laccase-mediated coupling and grafting reactions: A review. Enzyme and Microbial Technology, 48(3), 195-208.

Kukkola, E.M., Koutaniemi, S., Gustafsson, M., Karhunen, P., Ruel, K., Lundell, T.K., Saranpaa, P., Brunow, G., Teeri, T.H., Fagerstedt, K.V. 2003. Localization of dibenzodioxocin substructures in lignifying Norway spruce xylem by transmission electron microscopy-immunogold labeling. Planta, 217(2), 229-37.

Kulak, A.N., Semsarilar, M., Kim, Y.-Y., Ihli, J., Fielding, L.A., Cespedes, O., Armes, S.P., Meldrum, F.C. 2014. One-pot synthesis of an inorganic heterostructure: uniform occlusion of magnetite nanoparticles within calcite single crystals. Chemical Science, 5(2), 738-743.

Kumar, A., Goswami, P. 2006. Functional characterization of alcohol oxidases from *Aspergillus terreus* MTCC 6324. Applied Microbiology and Biotechnology, 72(5), 906-911.

Kumar, V.V., Cabana, H. 2016. Towards high potential magnetic biocatalysts for on-demand elimination of pharmaceuticals. Bioresource Technology, 200, 81-89.

Kumar, V.V., Sivanesan, S., Cabana, H. 2014. Magnetic cross-linked laccase aggregates — bioremediation tool for decolorization of distinct classes of recalcitrant dyes. Science of the Total Environment, 487, 830-839.

Kurniawati, S., Nicell, J.A. 2009. A comprehensive kinetic model of laccase-catalyzed oxidation of aqueous phenol. Biotechnology Progress, 25(3), 763-773.

Kunamneni, A., Ballesteros, A., Plou, F.J., Alcalde, M. 2007. Fungal laccase – a versatile enzyme for biotechnological applications. In: Communicating current research and educational topics and trends in applied microbiology, (Ed.) Méndez-Vilas, A., Formex, Badajoz, pp. 233-245.

Laemmli, U.K. 1970. Cleavage of structural proteins during the assembly of the head of bacteriophage T4. Nature, 227(5259), 680-685.

Lan, J., Huang, X., Hu, M., Li, Y., Qu, Y., Gao, P., Wu, D. 2006. High efficient degradation of dyes with lignin peroxidase coupled with glucose oxidase. Journal of Biotechnology, 123(4), 483-490.

Lancefield, C.S., Ojo, O.S., Tran, F., Westwood, N.J. 2015. Isolation of functionalized phenolic monomers through selective oxidation and C-O Bond cleavage of the β-O-4 linkages in lignin. Angewandte Chemie, 127(1), 260-264.

Leatham, G.F. 1986. The ligninolytic activities of *Lentinus edodes* and *Phanerochaete chrysosporium*. Applied Microbiology and Biotechnology, 24(1), 51-58.

Lee, K., Moon, S.H. 2003. Electroenzymatic oxidation of veratryl alcohol by lignin peroxidase. Journal of Biotechnology, 102(3), 261-268.

Lee, S.H., Doherty, T.V., Linhardt, R.J., Dordick, J.S. 2009. Ionic liquid-mediated selective extraction of lignin from wood leading to enhanced enzymatic cellulose hydrolysis. Biotechnology and Bioengineering, 102(5), 1368-1376.

Leitner, C., Volc, J., Haltrich, D. 2001. Purification and characterization of pyranose oxidase from the white rot fungus *Trametes multicolor*. Applied and Environmental Microbiology, 67(8), 3636-3644.

Leonowicz, A., Cho, N., Luterek, J., Wilkolazka, A., Wojtas-Wasilewska, M., Matuszewska, A., Hofrichter, M., Wesenberg, D., Rogalski, J. 2001. Fungal laccase: properties and activity on lignin. Journal of Basic Microbiology, 41(3-4), 185-227.

Leonowicz, A., Rogalski, J., Jaszek, M., Luterek, J., Wojtas-Wasilewska, M., Malarczyk, E., Ginalska, G., Fink-Boots, M., Cho, N.S. 1999. Cooperation of fungal laccase and glucose 1-oxidase in transformation of Björkman lignin and some phenolic compounds. Holzforschung, 53(4), 376-380.

Levasseur, A., Piumi, F., Coutinho, P.M., Rancurel, C., Asther, M., Delattre, M., Henrissat, B., Pontarotti, P., Asther, M., Record, E. 2008. FOLy: An integrated database for the classification and functional annotation of fungal oxidoreductases potentially involved in the degradation of lignin and related aromatic compounds. Fungal Genetics and Biology, 45(5), 638-645.

Li, J., Gellerstedt, G., Toven, K. 2009. Steam explosion lignins; their extraction, structure and potential as feedstock for biodiesel and chemicals. Bioresource Technology, 100(9), 2556-2561.

Li, J., Henriksson, G., Gellerstedt, G. 2007. Lignin depolymerization/repolymerization and its critical role for delignification of aspen wood by steam explosion. Bioresource Technology, 98(16), 3061-3068.

Liers, C., Bobeth, C., Pecyna, M., Ullrich, R., Hofrichter, M. 2010. DyP-like peroxidases of the jelly fungus *Auricularia auricula-judae* oxidize nonphenolic lignin model compounds and high-redox potential dyes. Applied Microbiology and Biotechnology, 85(6), 1869-1879.

Liitiä, T.M., Maunu, S.L., Hortling, B., Toikka, M., Kilpeläinen, I. 2003. Analysis of technical lignins by two- and three-dimensional NMR spectroscopy. Journal of Agricultural and Food Chemistry, 51(8), 2136-2143.

Lin, D., Nunes, A.C., Majkrzak, C.F., Berkowitz, A.E. 1995. Polarized neutron study of the magnetization density distribution within a $CoFe_2O_4$ colloidal particle II. Journal of Magnetism and Magnetic Materials, 145(3), 343-348.

Lin, S.Y., Dence, C.W. 1992. Methods in lignin chemistry, first ed., Springer, Berlin Heidelberg, Germany.

Liu, C., Zhang, Z.J. 2001. Size-dependent superparamagnetic properties of Mn spinel ferrite nanoparticles synthesized from reverse micelles. Chemistry of Materials, 13(6), 2092-2096.

Liu, J.Z., Wang, T.L., Huang, M.T., Song, H.Y., Weng, L.P., Ji, L.N. 2006. Increased thermal and organic solvent tolerance of modified horseradish peroxidase. Protein Engineering, Design & Selection, 19(4), 169-173.

Li-Weber, M. 2009. New therapeutic aspects of flavones: The anticancer properties of *Scutellaria* and its main active constituents Wogonin, Baicalein and Baicalin. Cancer Treatment Reviews, 35(1), 57-68.

Lloret, L., Eibes, G., Feijoo, G., Moreira, M.T., Lema, J.M., Hollmann, F. 2011. Immobilization of laccase by encapsulation in a sol–gel matrix and its characterization and use for the removal of estrogens. Biotechnology Progress, 27(6), 1570-1579.

Lobos, S., Larraín, J., Salas, L., Cullen, D., Vicuña, R. 1994. Isoenzymes of manganese-dependent peroxidase and laccase produced by the lignin-degrading basidiomycete *Ceriporiopsis subvermispora*. Microbiology, 140(10), 2691-2698.

Lora. J.H. 2008. Industrial commercial lignins: Sources, properties and applications. In: Monomers, polymers and composites from renewable resources, (Eds.) Belgacem, M.N., Gandini, A., Elsevier, Amsterdam, Netherlands, pp. 225–241.

Lora, J.H., Glasser, W.G. 2002. Recent industrial applications of lignin: A sustainable alternative to nonrenewable materials. Journal of Polymers and the Environment, 10(1), 39-48.

Lu, F., Ralph, J. 2010. Lignin. In: Cereal straw as a resource for sustainable biomaterials and biofuels, (Ed.) Sun, R.C., Elsevier, Amsterdam, Netherlands, pp. 169-198.

Ludwig, R., Harreither, W., Tasca, F., Gorton, L. 2010. Cellobiose dehydrogenase: A versatile catalyst for electrochemical applications. ChemPhysChem, 11(13), 2674-2697.

Lundell, T.K., Mäkelä, M.R., Hildén, K. 2010. Lignin-modifying enzymes in filamentous basidiomycetes – ecological, functional and phylogenetic review. Journal of Basic Microbiology, 50(1), 5-20.

Lundquist, K., Lundgren, R. 1972. Acid degradation of lignin. Acta Chemica Scandinavica, 26, 2005-2023.

Luterbacher, J.S., Azarpira, A., Motagamwala, A.H., Lu, F., Ralph, J., Dumesic, J.A. 2015. Lignin monomer production integrated into the γ-valerolactone sugar platform. Energy & Environmental Science, 8, 2657-2663.

Luterbacher, J.S., Rand, J.M., Alonso, D.M., Han, J., Youngquist, J.T., Maravelias, C.T., Pfleger, B.F., Dumesic, J.A. 2014. Nonenzymatic sugar production from biomass using biomass-derived γ-valerolactone. Science, 343(6168), 277-280.

Luterek, J., Gianfreda, L., Wojtaś-Wasilewska, M., Cho, N.S., Rogalski, J., Jaszek, M., Malarczyk, E., Staszczak, M., Fink-Boots, M., Leonowicz, A. 1998. Activity of free and immobilized extracellular *Cerrena unicolor* laccase in water miscible organic solvents. Holzforschung, 52(6), 589-595.

Ma, M., Zhang, Y., Yu, W., Shen, H.Y., Zhang, H.Q., Gu, N. 2003. Preparation and characterization of magnetite nanoparticles coated by amino silane. Colloids and Surfaces A: Physicochemical and Engineering Aspects, 212(2–3), 219-226.

Ma, Y.S., Chang, C.N., Chiang, Y.P., Sung, H.F., Chao, A.C. 2008. Photocatalytic degradation of lignin using Pt/TiO_2 as the catalyst. Chemosphere, 71(5), 998-1004

Mahdavi, B., Lafrance, A., Martel, A., Lessard, J., Méard, H., Brossard, L. 1997. Electrocatalytic hydrogenolysis of lignin model dimers at Raney nickel electrodes. Journal of Applied Electrochemistry, 27(5), 605-611.

Mansfield, S.D., Mooney, C., Saddler, J.N. 1999. Substrate and enzyme characteristics that limit cellulose hydrolysis. Biotechnology Progress, 15(5), 804-816.

Marco-Urrea, E., Pérez-Trujillo, M., Cruz-Morató, C., Caminal, G., Vicent, T. 2010. Degradation of the drug sodium diclofenac by *Trametes versicolor* pellets and identification of some intermediates by NMR. Journal of Hazardous Materials, 176(1–3), 836-842.

Marquardt, W., Harwardt, A., Hechinger, M., Kraemer, K., Viell, J., Voll, A. 2010. The biorenewables opportunity - toward next generation process and product systems. AIChE Journal, 56(9), 2228-2235.

Marr, A.C., Liu, S. 2011. Combining bio- and chemo-catalysis: from enzymes to cells, from petroleum to biomass. Trends in Biotechnology, 29(5), 199-204.

Martin-Benlloch, X., Elhabiri, M., Lanfranchi, D.A., Davioud-Charvet, E. 2014. A practical and economical high-yielding, six-step sequence synthesis of a flavone: Application to the multigram-scale synthesis of Ladanein. Organic Process Research & Development, 18(5), 613-617.

Martínez, Á.T., Rencoret, J., Marques, G., Gutiérrez, A., Ibarra, D., Jiménez-Barbero, J., del Río, J.C. 2008. Monolignol acylation and lignin structure in some nonwoody plants: A 2D NMR study. Phytochemistry, 69(16), 2831-2843.

Martínez, Á.T., Speranza, M., Ruiz-Dueñas, F.J., Ferreira, P., Camarero, S., Guillén, F., Martínez, M.J., Gutiérrez, A., Río, J.C.d. 2005. Biodegradation of lignocellulosics: microbial, chemical, and enzymatic aspects of the fungal attack of lignin. International Microbiology, 8(3), 195-204.

Martinez, D., Larrondo, L.F., Putnam, N., Gelpke, M.D.S., Huang, K., Chapman, J., Helfenbein, K.G., Ramaiya, P., Detter, J.C., Larimer, F., Coutinho, P.M., Henrissat, B., Berka, R., Cullen, D., Rokhsar, D. 2004. Genome sequence of the lignocellulose degrading fungus *Phanerochaete chrysosporium* strain RP78. Nature Biotechnology, 22(6), 695-700.

Marzullo, L., Cannio, R., Giardina, P., Santini, M.T., Sannia, G. 1995. Veratryl alcohol oxidase from *Pleurotus ostreatus* participates in lignin biodegradation and prevents polymerization of laccase-oxidized substrates. The Journal of Biological Chemistry, 270(8), 3823-3827.

Mateo, C., Palomo, J.M., Fernandez-Lorente, G., Guisan, J.M., Fernandez-Lafuente, R. 2007. Improvement of enzyme activity, stability and selectivity via immobilization techniques. Enzyme and Microbial Technology, 40(6), 1451-1463.

Mayer, A.M. 2006. Polyphenol oxidases in plants and fungi: Going places? A review. Phytochemistry, 67(21), 2318-2331.

McCarthy, S.A., Davies, G.L., Gun'ko, Y.K. 2012. Preparation of multifunctional nanoparticles and their assemblies. Nature Protocols, 7(9), 1677-1693.

McIlvaine, T.C. 1921. A buffer solution for colorimetric comparison. The Journal of Biological Chemistry, 49(1), 183-186.

Meier, D., Berns, J., Faix, O., Balfanz, U., Baldauf, W. 1994. Hydrocracking of organocell lignin for phenol production. Biomass and Bioenergy, 7(1–6), 99-105.

Mester, T., Field, J.A. 1998. Characterization of a novel manganese peroxidase-lignin peroxidase hybrid isozyme produced by *Bjerkandera* Species Strain BOS55 in the absence of manganese. Journal of Biological Chemistry, 273(25), 15412-15417.

Michalowicz, G., Toussaint, B., Vignon, M.R. 1991. Ultrastructural changes in poplar cell wall during steam explosion treatment. Holzforschung, 45(3), 175-179.

Michels, J., Wagemann, K. 2010. The German lignocellulose feedstock biorefinery project. Biofuels, Bioproducts and Biorefining, 4(3), 263-267.

Michniewicz, A., Ullrich, R., Ledakowicz, S., Hofrichter, M. 2006. The white-rot fungus *Cerrena unicolor* strain 137 produces two laccase isoforms with different physico-chemical and catalytic properties. Applied Microbiology and Biotechnology, 69(6), 682-688.

Mielgo, I., López, C., Moreira, M.T., Feijoo, G., Lema, J.M. 2003. Oxidative degradation of azo dyes by manganese peroxidase under optimized conditions. Biotechnology Progress, 19(2), 325-331.

Migneault, I., Dartiguenave, C., Bertrand, M.J., Waldron, K.C. 2004. Glutaraldehyde: behavior in aqueous solution, reaction with proteins, and application to enzyme crosslinking. BioTechniques, 37(5), 790-6, 798-802.

Miyazaki, K. 2005. A hyperthermophilic laccase from *Thermus thermophilus* HB27. Extremophiles, 9(6), 415-425.

Miyazaki-Imamura, C., Oohira, K., Kitagawa, R., Nakano, H., Yamane, T., Takahashi, H. 2003. Improvement of H_2O_2 stability of manganese peroxidase by combinatorial mutagenesis and high throughput screening using in vitro expression with protein disulfide isomerase. Protein Engineering, 16(6), 423-428.

Mohamed, A.F., Hossam, M.S., Ahmed, I.E. 1983. Effect of peracetic acid, sodium hydroxide and phosphoric acid on cellulosic materials as pretreatment for enzymatic hydrolysis. Enzyme and Microbial Technology, 5(6),421–424.

Molbase 2016. www.molbase.com, accessed on 27.5.2016.

Molter, T.W., McQuaide, S.C., Suchorolski, M.T., Strovas, T.J., Burgess, L.W., Meldrum, D.R., Lidstrom, M.E. 2009. A microwell array device capable of measuring single-cell oxygen consumption rates. Sensors and Actuators B: Chemical, 135(2), 678-686.

Morawski, B., Quan, S., Arnold, F.H. 2001. Functional expression and stabilization of horseradish peroxidase by directed evolution in *Saccharomyces cerevisiae*. Biotechnology and Bioengineering, 76(2), 99-107.

Morozova, O., Shumakovich, G., Shleev, S., Yaropolov, Y. 2007. Laccase-mediator systems and their applications: A review. Applied Biochemistry and Microbiology, 43(5), 523-535.

Moukouli, M., Topakas, E., Christakopoulos, P. 2008. Cloning, characterization and functional expression of an alkalitolerant type C feruloyl esterase from *Fusarium oxysporum*. Applied Microbiology and Biotechnology, 79(2), 245-254.

Muheim, A., Waldner, R., Sanglard, D., Reiser, J., Schoemaker, H.E., Leisola, M.S.A. 1991. Purification and properties of an aryl-alcohol dehydrogenase from the white-rot fungus *Phanerochaete chrysosporium*. European Journal of Biochemistry, 195(2), 369-375.

Murzin, D.Y., Leino, R. 2008. Sustainable chemical technology through catalytic multistep reactions. Chemical Engineering Research and Design, 86(9), 1002-1010.

Muurinen, E. 2000. Organosolv pulping—a review and distillation study related to peroxyacid pulping. Dissertation, University of Oulu, Oulu, Finland.

Myers, R.H., Montgomery, D.C., Anderson-Cook, C.M. 2009. Response surface methodology: Process and product optimization using designed experiments. 3rd ed. John Wiley & Sons, New Jersey.

Nadif, A., Hunkeler, D., Käuper, P. 2002. Sulfur-free lignins from alkaline pulping tested in mortar for use as mortar additives. Bioresource Technology, 84(1), 49-55.

Nair, R.R., Demarche, P., Agathos, S.N. 2013. Formulation and characterization of an immobilized laccase biocatalyst and its application to eliminate organic micropollutants in wastewater. New Biotechnology, 30(6), 814-823.

Nakanishi, K., Sakiyama, T., Imamura, K. 2001. On the adsorption of proteins on solid surfaces, a common but very complicated phenomenon. Journal of Bioscience and Bioengineering, 91(3), 233-244.

Niladevi, K.N., Jacob, N., Prema, P. 2008. Evidence for a halotolerant-alkaline laccase in *Streptomyces psammoticus*: Purification and characterization. Process Biochemistry, 43(6), 654-660.

Odaci, D., Telefoncu, A., Timur, S. 2010. Maltose biosensing based on co-immobilization of α-glucosidase and pyranose oxidase. Bioelectrochemistry, 79(1), 108-113.

Ogino, H., Ishikawa, H. 2001. Enzymes which are stable in the presence of organic solvents. Journal of Bioscience and Bioengineering, 91(2), 109-116.

Öhman, F. 2006. Precipitation and separation of lignin from kraft black liquor. Dissertation, Chalmers University of Technology, Sweden.

Oil Price 2016. www.oil-price.net, Accessed on 27.5.2016.

Okamoto, K., Yanase, H. 2002. Aryl alcohol oxidases from the white-rot basidiomycete *Pleurotus ostreatus*. Mycoscience, 43(5), 391-395.

Ostwald W (1925) Ueber die Geschwindigkeitsfunktion der Viskosität disperser Systeme. I. Colloid and Polymer Science, 36(2), 99–117.

Ortiz-Bermúdez, P., Srebotnik, E., Hammel, K.E. 2003. Chlorination and cleavage of lignin structures by fungal chloroperoxidases. Applied and Environmental Microbiology, 69(8), 5015-5018.

Ozawa, S., Klibanov, A.M. 2000. Myoglobin-catalyzed epoxidation of styrene in organic solvents accelerated by bioimprinting. Biotechnology Letters, 22(16), 1269-1272.

Ozimek, P., Veenhuis, M., van der Klei, I.J. 2005. Alcohol oxidase: A complex peroxisomal, oligomeric flavoprotein. FEMS Yeast Research, 5(11), 975-983.

Pakhadnia, Y., Malinouski, N., Lapko, A. 2009. Purification and characteristics of an enzyme with both bilirubin oxidase and laccase activities from mycelium of the basidiomycete *Pleurotus ostreatus*. Biochemistry (Moscow), 74(9), 1027-1034.

Paloheimo, M., Valtakari, L., Puranen, T., Kruus, K., Kallio, J., Mantyla, A., Fagerstrom, R., Ojapalo, P., Vehmaanpera, J. 2006. Novel laccase enzyme and use thereof. European Patent WO/2006/032723.

Palonen, H., Tjerneld, F., Zacchi, G., Tenkanen, M. 2004. Adsorption of *Trichoderma reesei* CBH I and EG II and their catalytic domains on steam pretreated softwood and isolated lignin. Journal of Biotechnology, 107(1), 65-72.

Pandey, K.K., Pitman, A.J. 2003. FTIR studies of the changes in wood chemistry following decay by brown-rot and white-rot fungi. International Biodeterioration & Biodegradation, 52(3), 151-160.

Pandey, M.P., Kim, C.S. 2011. Lignin depolymerization and conversion: A review of thermochemical methods. Chemical Engineering & Technology, 34(1), 29-41.

Pardini, V.L., Vargas, R.R., Viertler, H., Utley, J.H.P. 1992. Anodic cleavage of lignin model dimers in methanol. Tetrahedron, 48(35), 7221-7228.

Parpot, P., Bettencourt, A.P., Carvalho, A.M., Belgsir, E.M. 2000. Biomass conversion: Attempted electrooxidation of lignin for vanillin production. Journal of Applied Electrochemistry, 30(6), 727-731.

Partenheimer, W. 2009. The aerobic oxidative cleavage of lignin to produce hydroxyaromatic benzaldehydes and carboxylic acids via metal/bromide catalysts in acetic acid/water mixtures. Advanced Synthesis & Catalysis, 351(3), 456-466.

Paszczyński, A., Crawford, R.L., Huynh, V.B. 1988. Manganese peroxidase of *Phanerochaete chrysosporium*: Purification. Methods in Enzymology, 161, 264-270.

Patel, R.N., Hou, C.T., Laskin, A.I., Derelanko, P. 1981. Microbial oxidation of methanol: Properties of crystallized alcohol oxidase from a yeast, *Pichia* sp. Archives of Biochemistry and Biophysics, 210(2), 481-488.

Pazur, J.H., Kleppe, K. 1964. The oxidation of glucose and related compounds by glucose oxidase from *Aspergillus niger*. Biochemistry, 3(4), 578-583.

Périé, F.H., Sheng, D., Gold, M.H. 1996. Purification and characterization of two manganese peroxidase isozymes from the white-rot basidiomycete *Dichomitus squalens*. Biochimica et Biophysica Acta (BBA) - Protein Structure and Molecular Enzymology, 1297(2), 139-148.

Petri, A., Gambicorti, T., Salvadori, P. 2004. Covalent immobilization of chloroperoxidase on silica gel and properties of the immobilized biocatalyst. Journal of Molecular Catalysis B: Enzymatic, 27(2–3), 103-106.

Pielhop, T., Larrazabal, G.O., Studer, M.H., Brethauer, S., Seidel, C.M., Rudolf von Rohr, P. 2015. Lignin repolymerisation in spruce autohydrolysis pretreatment increases cellulase deactivation. Green Chemistry, 17(6), 3521-3532.

Pierre, A.C. 2004. The sol-gel encapsulation of enzymes. Biocatalysis and Biotransformation, 22(3), 145-170.

Piontek, K., Antorini, M., Choinowski, T. 2002. Crystal structure of a laccase from the fungus *Trametes versicolor* at 1.90-Å resolution containing a full complement of coppers. Journal of Biological Chemistry, 277(40), 37663-37669.

Phillis, J.W., Estevez, A.Y., O'Regan, M.H. 1998. Protective effects of the free radical scavengers, dimethyl sulfoxide and ethanol, in cerebral ischemia in gerbils. Neuroscience Letters, 244(2), 109-111.

Plasseraud, L., Süss-Fink, G. 1997. Catalytic hydrogenation of benzene derivatives under biphasic conditions. Journal of Organometallic Chemistry, 539(1-2), 163-170.

Polizzi, K.M., Bommarius, A.S., Broering, J.M., Chaparro-Riggers, J.F. 2007. Stability of biocatalysts. Current Opinion in Chemical Biology, 11(2), 220-225.

Portjanskaja, E., Preis, S. 2007. Aqueous photocatalytic oxidation of lignin: The influence of mineral admixtures. International Journal of Photoenergy, 2007, Article ID 76730.

Portjanskaja, E., Stepanova, K., Klauson, D., Preis, S. 2009. The influence of titanium dioxide modifications on photocatalytic oxidation of lignin and humic acids. Catalysis Today, 144(1-2), 26-30.

Prillinger, H., Esser, K. 1977. The phenoloxidases of the ascomycete *Podospora anserina*. Molecular and General Genetics MGG, 156(3), 333-345.

Qiu, H., Li, Y., Ji, G., Zhou, G., Huang, X., Qu, Y., Gao, P. 2009. Immobilization of lignin peroxidase on nanoporous gold: Enzymatic properties and in situ release of H_2O_2 by co-immobilized glucose oxidase. Bioresource Technology, 100(17), 3837-3842.

Rahimi, A., Azarpira, A., Kim, H., Ralph, J., Stahl, S.S. 2013. Chemoselective metal-free aerobic alcohol oxidation in lignin. Journal of the American Chemical Society, 135(17), 6415-6418.

Rahimi, A., Ulbrich, A., Coon, J.J., Stahl, S.S. 2014. Formic-acid-induced depolymerization of oxidized lignin to aromatics. Nature, 515(7526), 249-252.

Ralph, J., Brunow, G., Harris, P.J., Dixon, R.A., Schatz, P.F., Boerjan, W. 2009. Lignification: Are lignins biosynthesized via simple combinatorial chemistry or via proteinaceous control and template replication? In: Recent Advances in Polyphenol Research (vol. 1), (Eds.) Daayf, F., Lattanzio, V., Wiley-Blackwell, New Jersey, pp. 36-66.

Ralph, J., Lundquist, K., Brunow, G., Lu, F., Kim, H., Schatz, P., Marita, J., Hatfield, R., Ralph, S., Christensen, J., Boerjan, W. 2004. Lignins: Natural polymers from oxidative coupling of 4-hydroxyphenyl-propanoids. Phytochemistry Reviews, 3(1-2), 29-60.

Ralph, J., Marita, J.M., Ralph, S.A., Hatfield, R.D., Lu, F., Ede, R.M., Peng, J., Quideau, S., Helm, R.F., Grabber, J.H., Kim, H., Jimenez-Monteon, G., Zhang, Y., Jung, H.J.G., Landucci, L.L., MacKay, J.J., Sederoff, R.R., Chapple, C., Boudet, A.M. 1999. Solution-state NMR of lignins. In: Advances in lignocellulosics characterization, (Eds.) Argyropoulos, D.S., Rials, T., TAPPI Press, Atlanta, pp. 55–108.

Ramachandra, M., Crawford, D.L., Hertel, G. 1988. Characterization of an extracellular lignin peroxidase of the lignocellulolytic actinomycete *Streptomyces viridosporus*. Applied and Environmental Microbiology, 54(12), 3057-3063.

Ramachandra Rao, S., Ravishankar, G.A. 2000. Vanilla flavour: production by conventional and biotechnological routes. Journal of the Science of Food and Agriculture, 80(3), 289-304.

Reading, N.S., Aust, S.D. 2000. Engineering a disulfide bond in recombinant manganese peroxidase results in increased thermostability. Biotechnology Progress, 16(3), 326-333.

Reetz, M.T., Carballeira, J.D., Vogel, A. 2006. Iterative saturation mutagenesis on the basis of B factors as a strategy for increasing protein thermostability. Angewandte Chemie International Edition, 45(46), 7745-7751.

Riddick, J.A., Bunger, W.B., Sakano, T.K. 1986. Organic solvents: Physical properties and methods of purification. 4th edition. John Wiley and Sons, New York.

Rittstieg, K., Suurnakki, A., Suortti, T., Kruus, K., Guebitz, G., Buchert, J. 2002. Investigations on the laccase-catalyzed polymerization of lignin model compounds using size-exclusion HPLC. Enzyme and Microbial Technology, 31(4), 403-410.

Rizzello, C.G., Mueller, T., Coda, R., Reipsch, F., Nionelli, L., Curiel, J.A., Gobbetti, M. 2013. Synthesis of 2-methoxy benzoquinone and 2,6-dimethoxybenzoquinone by selected lactic acid bacteria during sourdough fermentation of wheat germ. Microbial Cell Factories, 12, 105-105.

Roach, P., Farrar, D., Perry, C.C. 2005. Interpretation of protein adsorption: Surface-induced conformational changes. Journal of the American Chemical Society, 127(22), 8168-8173.

Rochefort, D., Leech, D., Bourbonnais, R. 2004. Electron transfer mediator systems for bleaching of paper pulp. Green Chemistry, 6(1), 14-24.

Rodrigues, R.C., Ortiz, C., Berenguer-Murcia, A., Torres, R., Fernandez-Lafuente, R. 2013. Modifying enzyme activity and selectivity by immobilization. Chemical Society Reviews, 42(15), 6290-6307.

Rodríguez, A., Sánchez, R., Requejo, A., Ferrer, A. 2010. Feasibility of rice straw as a raw material for the production of soda cellulose pulp. Journal of Cleaner Production, 18(10–11), 1084-1091.

Roy, J.J., Abraham, T.E. 2006. Preparation and characterization of cross-linked enzyme crystals of laccase. Journal of Molecular Catalysis B: Enzymatic, 38(1), 31-36.

Ruiz-Dueñas, F.J., Martínez, Á.T. 2009. Microbial degradation of lignin: How a bulky recalcitrant polymer is efficiently recycled in nature and how we can take advantage of this. Microbial Biotechnology, 2(2), 164-177.

Ruiz-Dueñas, F.J., Morales, M., García, E., Miki, Y., Martínez, M.J., Martínez, A.T. 2009. Substrate oxidation sites in versatile peroxidase and other basidiomycete peroxidases. Journal of Experimental Botany, 60(2), 441-452.

Rüttimann-Johnson, C., Cullen, D., Lamar, R.T. 1994. Manganese peroxidases of the white rot fungus *Phanerochaete sordida*. Applied and Environmental Microbiology, 60(2), 599-605.

Ryan, B.J., Ó'Fágáin, C. 2007. Effects of single mutations on the stability of horseradish peroxidase to hydrogen peroxide. Biochimie, 89(8), 1029-1032.

Saake, B., Lehnen, R. 2000. Lignin. In: Ullmann's Encyclopedia of Industrial Chemistry (vol. 21), Wiley-VCH, Weinheim, Germany, pp. 21-36.

Sánchez, C. 2009. Lignocellulosic residues: Biodegradation and bioconversion by fungi. Biotechnology Advances, 27(2), 185-194.

Sanchez-Amat, A., Solano, F. 1997. A pluripotent polyphenol oxidase from the melanogenic marine *Alteromonas sp* Shares catalytic capabilities of tyrosinases and laccases. Biochemical and Biophysical Research Communications, 240(3), 787-792.

Sandborn, L.R.; Salvesen, J.R.; Howard, G.C. U.S. Patent 2 057 117, Oct. 13, 1936.

Sanderson, K. 2011. Lignocellulose: A chewy problem. Nature, 474(7352), 12-14.

Santhanam, N., Badri, D.V., Decker, S.R., Manter, D.K., Reardon, K.F., Vivanco, J.M. 2012. Lignocellulose decomposition by microbial secretions. In: Secretions and exudates in biological systems (vol. 12), (Eds.) Vivanco, J.M., Baluška, F., Springer, Berlin Heidelberg, Germany, pp. 125-153.

Santos, J.I., Martín-Sampedro, R., Fillat, Ú., Oliva, J.M., Negro, M.J., Ballesteros, M., Eugenio, M.E., Ibarra, D. 2015. Evaluating lignin-rich residues from biochemical ethanol production of wheat straw and olive tree pruning by FTIR and 2D-NMR. International Journal of Polymer Science, Article ID 314891.

Sarkanen, K.V., Ludwig, C.H. 1971. Lignins: Occurrence, formation, structure and reactions. Wiley-Interscience, New York.

Sasaki, Y., Kataoka, M., Urano, N., Ogawa, J., Iwasaki, A., Hasegawa, J., Isobe, K., Shimizu, S. 2010. Cloning, sequencing and expression analysis of a gene encoding alcohol oxidase in *Paenibacillus sp.* AIU 311. Journal of Bioscience and Bioengineering, 110(2), 147-151.

Schäfer, A., Bieg, S., Huwig, A., Kohring, G., Giffhorn, F. 1996. Purification by immunoaffinity chromatography, characterization, and structural Analysis of a thermostable pyranose oxidase from the white rot fungus *Phlebiopsis gigantea*. Applied and Environmental Microbiology, 62(7), 2586-2592.

Schröder, C.R., Polerecky, L., Klimant, I. 2007. Time-resolved pH/pO_2 mapping with luminescent hybrid sensors. Analytical Chemistry, 79(1), 60-70.

Schlosser, D., Höfer, C. 2002. Laccase-catalyzed oxidation of Mn^{2+} in the presence of natural Mn^{3+} chelators as a novel source of extracellular H_2O_2 Production and its impact on manganese peroxidase. Applied and Environmental Microbiology, 68(7), 3514-3521.

Schou, C., Christensen, M.H., Schulein, M. 1998. Characterization of a cellobiose dehydrogenase from *Humicola insolens*. The Biochemical journal, 330(1), 565-571.

Schulz, J., Roucoux, A., Patin, H. 2000. Stabilized rhodium(0) nanoparticles: A reusable hydrogenation catalyst for arene derivatives in a biphasic water-liquid system. Chemistry - A European Journal, 6(4), 618-624.

Selinheimo, E., Saloheimo, M., Ahola, E., Westerholm-Parvinen, A., Kalkkinen, N., Buchert, J., Kruus, K. 2006. Production and characterization of a secreted, C-terminally processed tyrosinase from the filamentous fungus *Trichoderma reesei*. Febs Journal, 273(18), 4322-4335.

Sellés-Marchart, S., Casado-Vela, J., Bru-Martínez, R. 2006. Isolation of a latent polyphenol oxidase from loquat fruit (*Eriobotrya japonica* Lindl.): Kinetic characterization and comparison with the active form. Archives of Biochemistry and Biophysics, 446(2), 175-185.

Senczuk, A.M., Machwe, A., Kapoor, M. 2003. High constitutive peroxidase activity and constitutive thermotolerance in *Neurospora crassa*. Mycoscience, 44(2), 0129-0137.

Serdakowski, A.L., Dordick, J.S. 2008. Enzyme activation for organic solvents made easy. Trends in Biotechnology, 26(1), 48-54.

Sergeev, A.G., Hartwig, J.F. 2011. Selective, Nickel-catalyzed hydrogenolysis of aryl ethers. Science, 332(6028), 439-443.

Shah, V., Nerud, F. 2002. Lignin degrading system of white-rot fungi and its exploitation for dye decolorization. Canadian Journal of Microbiology, 48(10), 857-870.

Shao, X., Gao, Y., Jiang, M., Li, L. 2009. Deletion and site-directed mutagenesis of laccase from *Shigella dysenteriae* results in enhanced enzymatic activity and thermostability. Enzyme and Microbial Technology, 44(5), 274-280.

Sheldon, R.A. 2007. Enzyme immobilization: The quest for optimum performance. Advanced Synthesis & Catalysis, 349(8-9), 1289-1307.

Sheldon, R.A. 2008. E factors, green chemistry and catalysis: an odyssey. Chemical Communications, 29, 3352-3365.

Shin, K., Oh, I., Kim, C. 1997. Production and purification of remazol brilliant blue R decolorizing peroxidase from the culture filtrate of *Pleurotus ostreatus*. Applied and Environmental Microbiology, 63(5), 1744-1748.

Shindler, J.S., Childs, R.E., Bardsley, W.G. 1976. Peroxidase from human cervical mucus. European Journal of Biochemistry, 65(2), 325-331.

Shimizu, S., Hattori, S., Hata, H., Yamada, H. 1988. A novel fungal enzyme, NADPH-dependent carbonyl reductase, showing high specificity to conjugated polyketones. European Journal of Biochemistry, 174(1), 37-44.

Sigoillot, C., Lomascolo, A., Record, E., Robert, J.L., Asther, M., Sigoillot, J.C. 2002. Lignocellulolytic and hemicellulolytic system of *Pycnoporus cinnabarinus*: Isolation and characterization of a cellobiose dehydrogenase and a new xylanase. Enzyme and Microbial Technology, 31(6), 876-883.

Singer, S.J. 1963. The properties of proteins in nonaqueous solvents (vol. 17). In: Advances in protein chemistry, (Eds.) Anfinsen, C.B., Kenneth Bailey, M.L., Anson, J., Edsall, T., Academic Press, pp. 1-68.

Singh Arora, D., Kumar Sharma, R. 2010. Ligninolytic fungal laccases and their biotechnological applications. Applied Biochemistry and Biotechnology, 160(6), 1760-1788.

Singh, D., Zeng, J., Chen, S. 2011. Increasing manganese peroxidase productivity of *Phanerochaete chrysosporium* by optimizing carbon sources and supplementing small molecules. Letters in Applied Microbiology, 53(1), 120-123.

Simpson, C., Jordaan, J., Gardiner, N.S., Whiteley, C. 2007. Isolation, purification and characterization of a novel glucose oxidase from *Penicillium sp.* CBS 120262 optimally active at neutral pH. Protein Expression and Purification, 51(2), 260-266.

Silva, J.L., Weber, G. 1993. Pressure stability of proteins. Annual Review of Physical Chemistry, 44, 89-113.

Sixta, H. 2006. Handbook of Pulp. Wiley-VCH, Weinheim, Germany.

Slomczynski, D., Nakas, J.P., Tanenbaum, S.W. 1995. Production and characterization of laccase from *Botrytis cinerea* 61-34. Applied and Environmental Microbiology, 61(3), 907-12.

Smith, P.K., Krohn, R.I., Hermanson, G.T., Mallia, A.K., Gartner, F.H., Provenzano, M.D., Fujimoto, E.K., Goeke, N.M., Olson, B.J., Klenk, D.C. 1985. Measurement of protein using bicinchoninic acid. Analytical Biochemistry, 150(1), 76-85.

Sun, L., Bulter, T., Alcalde, M., Petrounia, I.P., Arnold, F.H. 2002. Modification of galactose oxidase to introduce glucose 6-oxidase activity. ChemBioChem, 3(8), 781-783.

Sun, N., Rodriguez, H., Rahman, M., Rogers, R.D. 2011. Where are ionic liquid strategies most suited in the pursuit of chemicals and energy from lignocellulosic biomass? Chemical Communications, 47(5), 1405-1421.

Sun, S.W., Lin, Y.C., Weng, Y.M., Chen, M.J. 2006. Efficiency improvements on ninhydrin method for amino acid quantification. Journal of Food Composition and Analysis, 19(2-3), 112-117.

Sun, Y., Cheng, J. 2002. Hydrolysis of lignocellulosic materials for ethanol production: A review. Bioresource Technology, 83(1), 1-11.

Suzuki, T., Honda, Y., Mukasa, Y., Kim, S.J. 2006. Characterization of peroxidase in buckwheat seed. Phytochemistry, 67(3), 219-224.

Taboada-Puig, R., Junghanns, C., Demarche, P., Moreira, M.T., Feijoo, G., Lema, J.M., Agathos, S.N. 2011. Combined cross-linked enzyme aggregates from versatile peroxidase and glucose oxidase: Production, partial characterization and application for the elimination of endocrine disruptors. Bioresource Technology, 102(11), 6593-6599.

Takakura, Y., Kuwata, S. 2003. Purification, characterization, and molecular cloning of a pyranose oxidase from the fruit body of the basidiomycete, *Tricholoma matsutake*. Bioscience, Biotechnology, and Biochemistry, 67(12), 2598-2607.

Taniguchi, M., Tanaka, M., Matsuno., R, Kamikubo, T. 1982. Evaluation of chemical pretreatment for enzymatic solubilization of rice straw. European Journal of Applied Microbiology and Biotechnology, 14(1), 35-39.

Teixeira, L.C., Linden, J.C., Schroeder, H.A. 1999a. Alkaline and peracetic acid pretreatments of biomass for ethanol production. Applied Biochemistry and Biotechnology, 77(1), 19-34.

Teixeira, L.C., Linden, J.C., Schroeder, H.A. 1999b. Optimizing peracetic acid pretreatment conditions for improved simultaneous saccharification and co-fermentation (SSCF) of sugar cane bagasse to ethanol fuel. Renewable Energy, 16(1-4), 1070-1073.

ten Have, R., Teunissen, P.J.M. 2001. Oxidative mechanisms involved in lignin degradation by white-rot fungi. Chemical Reviews, 101(11), 3397-3413.

Thring, R.W., Breau, J. 1996. Hydrocracking of solvolysis lignin in a batch reactor. Fuel, 75(7), 795-800.

Thompson, D.N., Chen, H.C., Grethlein, H.E. 1992. Comparison of pretreatment methods on the basis of available surface area. Bioresource Technology, 39(2),155-163.

Tien, M., Kirk, T.K. 1988. Lignin peroxidase of *Phanerochaete-Chrysosporium*. Methods in Enzymology, 161, 238-249.

Tolba, R., Tian, M., Wen, J., Jiang, Z.H., Chen, A. 2010. Electrochemical oxidation of lignin at IrO_2-based oxide electrodes. Journal of Electroanalytical Chemistry, 649(1-2), 9-15.

Topakas, E., Vafiadi, C., Christakopoulos, P. 2007. Microbial production, characterization and applications of feruloyl esterases. Process Biochemistry, 42(4), 497-509.

Toven, K., Gellerstedt, G. 1999. Structural changes of softwood kraft lignin in oxygen delignification and prebleaching. In: 10th international symposium on wood and pulping chemistry (vol. 2), pp. 340–345.

Tsuge, H., Natsuaki, O., Ohashi, K. 1975. Purification, properties, and molecular features of glucose oxidase from *Aspergillus niger*. Journal of Biochemistry, 78(4), 835-843.

Turner, N.J. 2009. Directed evolution drives the next generation of biocatalysts. Nature Chemical Biology, 5(8), 567-573.

Uzan, E., Nousiainen, P., Balland, V., Sipila, J., Piumi, F., Navarro, D., Asther, M., Record, E., Lomascolo, A. 2010. High redox potential laccases from the ligninolytic fungi *Pycnoporus coccineus* and *Pycnoporus sanguineus* suitable for white biotechnology: From gene cloning to enzyme characterization and applications. Journal of Applied Microbiology, 108(6), 2199-2213.

Valderrama, B., Ayala, M., Vazquez-Duhalt, R. 2002. Suicide inactivation of peroxidases and the challenge of engineering more robust enzymes. Chemistry & Biology, 9(5), 555-565.

van de Velde, F., Bakker, M., van Rantwijk, F., Rai, G.P., Hager, L.P., Sheldon, R.A. 2001. Engineering chloroperoxidase for activity and stability. Journal of Molecular Catalysis B: Enzymatic, 11(4-6), 765-769.

Van den Bosch, S., Schutyser, W., Vanholme, R., Driessen, T., Koelewijn, S.F., Renders, T., De Meester, B., Huijgen, W.J.J., Dehaen, W., Courtin, C.M., Lagrain, B., Boerjan, W., Sels, B.F. 2015. Reductive lignocellulose fractionation into soluble lignin-derived phenolic monomers and dimers and processable carbohydrate pulps. Energy & Environmental Science, 8(6), 1748-1763.

van den Heuvel, R.H.H., Fraaije, M.W., Laane, C., van Berkel, W.J.H. 2001. Enzymatic synthesis of vanillin. Journal of Agricultural and Food Chemistry, 49(6), 2954-2958.

van Haveren, J., Scott, E.L., Sanders, J. 2008. Bulk chemicals from biomass. Biofuels, Bioproducts and Biorefining, 2(1), 41-57.

van Rantwijk, F., Sheldon, R.A. 2007. Biocatalysis in ionic liquids. Chemical Reviews, 107(6), 2757-2785.

Vanholme, R., Morreel, K., Ralph, J., Boerjan, W. 2008. Lignin engineering. Current Opinion in Plant Biology, 11(3), 278-285.

Vares, T., Kalsi, M., Hatakka, A. 1995. Lignin peroxidases, manganese peroxidases, and other ligninolytic enzymes produced by *Phlebia radiata* during solid-state fermentation of wheat straw. Applied and Environmental Microbiology, 61(10), 3515-20.

Vayssières, L., Chanéac, C., Tronc, E., Jolivet, J.P. 1998. Size tailoring of magnetite particles formed by aqueous precipitation: An example of thermodynamic stability of nanometric oxide particles. Journal of Colloid and Interface Science, 205(2), 205-212.

Vennestrøm, P.N.R., Christensen, C.H., Pedersen, S., Grunwaldt, J.-D., Woodley, J.M. 2010a. Next-Generation Catalysis for Renewables: Combining Enzymatic with Inorganic Heterogeneous Catalysis for Bulk Chemical Production. ChemCatChem, 2(3), 249-258.

Vennestrøm, P.N.R., Taarning, E., Christensen, C.H., Pedersen, S., Grunwaldt, J.D., Woodley, J.M. 2010b. Chemoenzymatic combination of glucose oxidase with titanium silicalite-1. ChemCatChem 2(8), 943–945.

Vernwal, S.K., Yadav, R.S.S., Yadav, K.D.S. 2006. Purification of a peroxidase from *Solanum melongena* fruit juice. Indian Journal of Biochemistry & Biophysics, 43(4), 239-243.

Vigneault, A., Johnson, D.K., Chornet, E. 2007. Base-catalyzed depolymerization of lignin: Separation of monomers. The Canadian Journal of Chemical Engineering, 85(6), 906-916.

Voitl, T., Nagel, M.V., von Rohr, P.R. 2010. Analysis of products from the oxidation of technical lignins by oxygen and $H_3PMo_{12}O_{40}$ in water and aqueous methanol by size-exclusion chromatography. Holzforschung, 64(1), 13-19.

Voitl, T., Rudolf von Rohr, P. 2010. Demonstration of a process for the conversion of kraft lignin into vanillin and methyl vanillate by acidic oxidation in aqueous methanol. Industrial & Engineering Chemistry Research, 49(2), 520-525.

Voitl, T., Rudolf von Rohr, P. 2008. Oxidation of lignin using aqueous polyoxometalates in the presence of alcohols. ChemSusChem, 1(8-9), 763-769.

Wan, Y.Y., Du, Y.M., Miyakoshi, T. 2008a. Enzymatic catalysis of 2,6-dimethoxyphenol by laccases and products characterization in organic solutions. Science in China Series B: Chemistry, 51(7), 669-676.

Wan, Y.Y., Du, Y.M., Miyakoshi, T. 2008b. *Rhus* laccase catalysis and product characterization of 1,2-dimethoxyphenol in organic solutions. Chinese Chemical Letters, 19(3), 333-336.

Wang, Y., Vazquez-Duhalt, R., Pickard, M.A. 2002. Purification, characterization, and chemical modification of manganese peroxidase from *Bjerkandera adusta* UAMH 8258. Current Microbiology, 45(2), 77-87.

Wang, Z., Cai, Y., Liao, X., Zhang, F., Zhang, D., Li, Z. 2010. Production and characterization of a novel laccase with cold adaptation and high thermal stability from an isolated fungus. Applied Biochemistry and Biotechnology, 162(1), 280-294.

Webster, R., Pacey, M., Winchester, T., Johnson, P., Jezequel, S. 1998. Microbial oxidative metabolism of diclofenac: Production of 4′-hydroxydiclofenac using *Epiccocum nigrum* IMI354292. Applied Microbiology and Biotechnology, 49(4), 371-376.

Weetall, H.H. 1974. Immobilized enzymes. Analytical applications. Analytical Chemistry, 46(7), 602A-615A.

Werhan, H. 2013. A process for the complete valorization of lignin into aromatic chemicals based on acidic oxidation. Dissertation, ETH Zürich, Zürich.

Werhan, H., Farshori, A., Rudolf von Rohr, P. 2012. Separation of lignin oxidation products by organic solvent nanofiltration. Journal of Membrane Science, 423-424, 404-412.

Werhan, H., Mir, J.M., Voitl, T., Rudolf von Rohr, P. 2011. Acidic oxidation of kraft lignin into aromatic monomers catalyzed by transition metal salts. Holzforschung, 65(5), 703-709.

Werz, J.L., Bédué, O. 2013. Lignocellulosic Biorefineries. EPFL Press, Lausanne.

Whittaker, J.W. 2005. The radical chemistry of galactose oxidase. Archives of Biochemistry and Biophysics, 433(1), 227-239.

Wong, D. 2006. Feruloyl esterase. Applied Biochemistry and Biotechnology, 133(2), 87-112.

Wong, D. 2009. Structure and action mechanism of ligninolytic enzymes. Applied Biochemistry and Biotechnology, 157(2), 174-209.

Wörmeyer, K., Ingram, T., Saake, B., Brunner, G., Smirnova, I. 2011. Comparison of different pretreatment methods for lignocellulosic materials. Part II: Influence of pretreatment on the properties of rye straw lignin. Bioresource Technology, 102(5), 4157-4164.

Wu, M., Neilson, A., Swift, A.L., Moran, R., Tamagnine, J., Parslow, D., Armistead, S., Lemire, K., Orrell, J., Teich, J., Chomicz, S., Ferrick, D.A. 2007. Multiparameter metabolic analysis reveals a close link between attenuated mitochondrial bioenergetic function and enhanced glycolysis dependency in human tumor cells. American Journal of Physiology - Cell Physiology, 292(1), C125-C136.

Wu, Y.R., Luo, Z.H., Kwok-Kei Chow, R., Vrijmoed, L.L.P. 2010. Purification and characterization of an extracellular laccase from the anthracene-degrading fungus *Fusarium solani* MAS2. Bioresource Technology, 101(24), 9772-9777.

Wyman, C., Goodman, B. 1993. Biotechnology for production of fuels, chemicals, and materials from biomass. Applied Biochemistry and Biotechnology, 39-40(1), 41-59.

Xu, C., Arancon, R.A.D., Labidi, J., Luque, R. 2014. Lignin depolymerisation strategies: Towards valuable chemicals and fuels. Chemical Society Reviews, 43, 7485-7500.

Xu, F. 1996. Oxidation of phenols, anilines, and benzenethiols by fungal laccases: Correlation between activity and redox potentials as well as halide inhibition. Biochemistry, 35(23), 7608-7614.

Xu, F., Damhus, T., Danielsen, S., Østergaard, L.H. 2007. Catalytic applications of laccase. In: Modern biooxidation, (Eds.) Schmid, R.D., Urlacher, V.B., 1st edn., Wiley-VCH. Weinheim, pp. 43-75.

Yadav, P., Sharma, J.K., K. Singh, V., Yadav, K.D.S. 2010. N-oxidation of arylamines to nitrosobenzenes using chloroperoxidase purified from *Musa paradisiaca* stem juice. Biocatalysis and Biotransformation, 28(3), 222-226.

Yang, W.Y., Min, D.Y., Wen, S.X., Jin, L., Rong, L., Tetsuo, M., Bo, C. 2006. Immobilization and characterization of laccase from Chinese *Rhus vernicifera* on modified chitosan. Process Biochemistry, 41(6), 1378-1382.

Yamaura, M., Camilo, R.L., Sampaio, L.C., Macêdo, M.A., Nakamura, M., Toma, H.E. 2004. Preparation and characterization of (3-aminopropyl)triethoxysilane-coated magnetite nanoparticles. Journal of Magnetism and Magnetic Materials, 279(2-3), 210-217.

Yelle, D.J., Ralph, J., Lu, F., Hammel, K.E. 2008. Evidence for cleavage of lignin by a brown rot basidiomycete. Environmental Microbiology, 10(7), 1844-1849.

Young, R.A., Davis, J.L. 1986. Organic acid pulping of wood, part II, acetic acid pulping of aspen. Holzforschung, 40(2), 99-108

Zacchi, G., Skoog, K., Hahn-Hagerdal, B. 1988. Economic evaluation of enzymatic hydrolysis of phenol-pretreated wheat straw. Biotechnology and Bioengineering, 32(4), 460-466.

Zamocky, M., Ludwig, R., Peterbauer, C., Hallberg, B.M., Divne, C., Nicholls, P., Haltrich, D. 2006. Cellobiose dehydrogenase - a flavocytochrome from wood-degrading, phytopathogenic and saprotropic fungi. Current Protein and Peptide Science, 7(3), 255-80.

Zakrzewska, M.E., Bogel-Łukasik, E., Bogel-Łukasik, R. 2010. Solubility of carbohydrates in ionic liquids. Energy Fuels, 24(2), 737-745.

Zakzeski, J., Bruijnincx, P.C.A., Jongerius, A.L., Weckhuysen, B.M. 2010a. The catalytic valorization of lignin for the production of renewable chemicals. Chemical Reviews, 110(6), 3552-3599.

Zakzeski, J., Bruijnincx, P.C.A., Weckhuysen, B.M. 2011. In situ spectroscopic investigation of the cobalt-catalyzed oxidation of lignin model compounds in ionic liquids. Green Chemistry, 13(3), 671-680.

Zakzeski, J., Jongerius, A.L., Weckhuysen, B.M. 2010b. Transition metal catalyzed oxidation of Alcell lignin, soda lignin, and lignin model compounds in ionic liquids. Green Chemistry, 12(7), 1225-1236.

Zeng, J., Yoo, C.G., Wang, F., Pan, X., Vermerris, W., Tong, Z. 2015. Biomimetic Fenton-catalyzed lignin depolymerization to high-value aromatics and dicarboxylic acids. ChemSusChem, 8(5), 861-871.

Zhang, X., Eigendorf, G., Stebbing, D.W., Mansfield, S.D., Saddler, J.N. 2002. Degradation of trilinolein by laccase enzymes. Archives of Biochemistry and Biophysics, 405(1), 44-54.

Zhang, L., Gellerstedt, G. 2001. NMR observation of a new lignin structure, a spiro-dienone. Chemical Communications, 2001, 2744-2745.

Zhang, L., Henriksson, G., Gellerstedt, G. 2003. The formation of β–β structures in lignin biosynthesis – are there two different pathways? Organic & Biomolecular Chemistry, 1(20),3621-3624.

Zhang, Y.H. 2008. Reviving the carbohydrate economy via multi-product lignocellulose biorefineries. Journal of Industrial Microbiology and Biotechnology, 35(5), 367-375.

Zhao, H. 2010. Methods for stabilizing and activating enzymes in ionic liquids—a review. Journal of Chemical Technology and Biotechnology, 85(7), 891-907.

Zhao, X., Cheng, K., Liu, D. 2009. Organosolv pretreatment of lignocellulosic biomass for enzymatic hydrolysis. Applied Microbiology and Biotechnology, 82(5), 815-827.

Zheng, Y., Zhongli, P., Zhang, R. 2009. Overview of biomass pretreatment for cellulosic ethanol production. International Journal of Agricultural and Biological Engineering, 2(3), 51-68.

Zhou, H., Yang, D., Qiu, X., Wu, X., Li, Y. 2013. A novel and efficient polymerization of lignosulfonates by horseradish peroxidase/H_2O_2 incubation. Applied Microbiology and Biotechnology, 97(24), 10309-10320.

Zimmermann, Y.S., Shahgaldian, P., Corvini, P., Hommes, G. 2011. Sorption-assisted surface conjugation: a way to stabilize laccase enzyme. Applied Microbiology and Biotechnology, 92(1), 169-178.

Zumárraga, M., Bulter, T., Shleev, S., Polaina, J., Martínez-Arias, A., Plou, F.J., Ballesteros, A., Alcalde, M. 2007. In vitro evolution of a fungal laccase in high concentrations of organic cosolvents. Chemistry & Biology, 14(9), 1052-1064.

List of publications

Journal publications

Gasser, C.A., Čvančarová, M., Ammann, E.M., Schäffer, A., Shahgaldian, P., Corvini P.F.X. 2017. Sequential lignin depolymerization by combination of biocatalytic and formic acid/formate treatment steps. Applied Microbiology and Biotechnology, 101(6), 2575-2588.

Gasser, C.A., Ammann, E.M., Schäffer, A., Shahgaldian, P., Corvini, P.F.X. 2016. Production of superparamagnetic nanobiocatalysts for green chemistry applications. Applied Microbiology and Biotechnology, 100(16), 7281-7296.

Arca-Ramos, A., Ammann, E.M., Gasser, C.A., Nastold, P., Eibes, G., Feijoo, G., Lema, J.M., Moreira, M.T., Corvini, P.F.X. 2015. Assessing the use of nanoimmobilized laccases to remove micropollutants from wastewater. Environmental Science and Pollution Research, 23(4), 3217–3228.

Gasser, C.A., Ammann, E.M., Shahgaldian, P., Corvini, P.F.X. 2014. Laccases to take on the challenge of emerging organic contaminants in wastewater. Applied Microbiology and Biotechnology, 98(24), 9931-9952.

Gasser, C.A., Yu, L., Svojitka, J., Wintgens, T., Ammann, E.M., Shahgaldian, P., Corvini, P.F.X., Hommes G. 2014. Advanced enzymatic elimination of phenolic contaminants in wastewater: a nano approach at field scale. Applied Microbiology and Biotechnology, 98(7), 3305-3316.

Ammann, E.M., Gasser, C.A., Hommes, G., Corvini, P.F.X. 2014. Immobilization of defined laccase combinations for enhanced oxidation of phenolic contaminants. Applied Microbiology and Biotechnology, 98(3), 1397-1406.

Hommes, G., Gasser, C.A., Ammann, E.M., Corvini, P.F.X. 2013. Determination of oxidoreductase activity using a high-throughput microplate respiratory measurement. Analytical Chemistry, 85(1), 283-291.

Gasser, C.A., Hommes, G., Schäffer, A., Corvini, P.F.X. 2012. Multi-catalysis reactions: new prospects and challenges of biotechnology to valorize lignin. Applied Microbiology and Biotechnology, 95(5), 1115-1134.

Hommes, G., Gasser, C.A., Howald, C.B.C., Goers, R., Schlosser, D., Shahgaldian, P., Corvini, P.F.X. 2012. Production of a robust nanobiocatalyst for municipal wastewater treatment. Bioresource Technology, 115(0), 8-15.

Madliger, M., Gasser, C.A., Schwarzenbach, R.P., Sander, M. 2011. Adsorption of transgenic insecticidal Cry1Ab protein to silica particles. Effects on transport and bioactivity. Environmental Science & Technology, 45(10), 4377-4384.

Conference contributions

Gasser, C.A., Mucha M., Ammann, E.M., Nastold, P., Corvini, P.F.X. Fourth International Conference on Lignocellulosic Ethanol, Landshut, September 2014.

Gasser, C.A., Mucha M., Ammann, E.M., Nastold, P., Corvini, P.F.X. 16th International Biotechnology Symposium and Exhibition, Fortaleza, September 2014.

Gasser, C.A., Mucha M., Ammann, E.M., Nastold, P., Corvini, P.F.X. Lignin 2014 - biosynthesis and utilization, Umeå, August 2014.

Gasser, C.A., Corvini, P.F.X., Wintgens, T. ecochem, Basel, November 2013.

Gasser, C.A., Ammann, E.M., Hommes, G., Ma, Y., Yu, L., Wintgens, T. 8th IWA Micropol and Ecohazard Conference, Zürich, June 2013.

Gasser, C.A., Hommes, G., Corvini, P.F.X. Environmental Microbiology and Biotechnology in the frame of the Knowledge-Based Bio and Green Economy, Bologna, April 2012.

Curriculum Vitae

Name:	Christoph Andreas Gasser
Date of birth:	6.3.1983
Place of birth:	Zürich, Switzerland
Nationality:	Swiss

2011-2016	PhD Student at the Faculty of Mathematics, Computer Science and Natural Science, RWTH Aachen, Germany
2011-2016	Research Associate at University of Applied Sciences and Arts Northwestern Switzerland, Muttenz, Switzerland
July – December 2010	Civil service at University of Applied Sciences and Arts Northwestern Switzerland, Muttenz, Switzerland.
2009-2011	Project work as freelancer for Rytec AG and Textor Engineering AG, Münsingen, Switzerland
August 2009	Receipt of the degree Master of Science ETH
2008	Project work as freelancer for Textor Engineering AG, Münsingen, Switzerland
2008	Internship at Rytec AG, Münsingen, Switzerland
2003-2009	Study of environmental sciences at ETH Zürich
	Major in Biogeochemistry and Pollutant Dynamics
2002	Receipt of the general qualification for university entrance (Matura)
1998-2002	Attendance at the Mathematisch-Naturwissenschaftliches Gymnasium Rämibühl, Zürich, Switzerland

Basel, October 2016